Closed-Loop Neural Engineering Approaches to Motor Rehabilitation

Brian Joseph Mogen

A dissertation

submitted in partial fulfillment of the

requirements for the degree of

Doctor of Philosophy

University of Washington

2018

Reading Committee:

Eberhard Fetz, Chair

Steve Perlmutter

Eric Chudler

Program Authorized to Offer Degree:

BioEngineering

University of Washington

Abstract

Closed-Loop Neural Engineering Approaches to Motor Rehabilitation

Brian Joseph Mogen

Chair of the Supervisory Committee:
Prof. Eberhard Fetz
Physiology and Biophysics

Here I present several approaches to applying engineering design principles to the central nervous system with the goal of using closed-loop approaches to enhance rehabilitative processes. These approaches cover invasive access to the brain and spinal cord, as well as physical rehabilitation techniques that employ closed loop principles for direct clinical utility. Targeted plasticity in the motor cortex was induced in a nonhuman primate model using paired electrical stimulation. This stimulation produced robust changes in a subset of tested sites and conformed to the predicted changes following Hebb's framework of spike-timing dependent plasticity. Novel electrode access to the cervical spinal cord allows for targeting of hand and arm motor pools. I designed, fabricated, tested, and iterated on two approaches to access the ventral aspect of the spinal cord to directly stimulate arm movement using targeted electrical stimulation with the goal of creating robust, de-fatiguing motor outputs from a stable stimulation site. Finally, I architected a closed-loop rehabilitation platform that directly measures hand and arm function, uses those measurements to control engaging gameplay in a digital environment, and quantify the quality of movement created by the user with the goal of making long term rehabilitation fun, accurate, and engaging for the end user. These approaches taken together represent a comprehensive approach to closed-loop motor rehabilitation.

Contents

LIST OF FIGURES

LIST OF TABLES

ACKNOWLEDGEMENTS

This thesis represents years of work, and more importantly, years of learning and growth. There is no doubt that I would not have succeeded without the incredible network of support, encouragement, and collaboration here at UW.

My adviser, Eb Fetz, is the foremost person who enabled my learning. He provided an environment where non-traditional projects and thinking were encouraged, preliminary results were thoughtfully analyzed, and my wandering interests were guided and refined. Eb supported and pushed me to think deeply about the problems I was facing in neuroscience and engineering, as well as the freedom to explore uncharted territories in. His generosity with my time allowed me to explore and understand many areas beyond the work presented in this thesis.

Thank you to my committee members, Eb, Steve Perlmutter, Eric Chudler, Colin Studholme, and Emily Cox Pahnke. I appreciate the probing questions, encouragement, and advice you have provided me over the course of my graduate career.

The Fetz/Perlmutter lab group was an amazing place to grow. Tyler Libey, my labmate and friend who accompanied me on the great vHAB adventure as well as troubleshooting all of my work and projects. Steve Perlmutter who shared and nurtured years' worth of neuroscience, surgical, and hardware expertise. Steph Seeman who waded through an incredibly challenging 3 years of co-project work. Bethany Kondiles, who helped find answers to all of my neuroscience questions. Olivia Robinson who made all of my early experiments possible, Larry Shupe, who could always help find the problem in my recording setup or analysis code.

Becky Shaefer and Rob Robinson, thank you for the patience and kindness you brought to the primate handling process. Your excellent teaching allowed me to come out the other side of grad school unscathed by monkeys. Other individuals who have built my foundation include

Dimi Gklezakos, Lars Crawford, Dev Sarma, Andrew Bogaard, Stavros Zanos, Samira Moorjani, Andrew Richardson, and the rest of the Fetz/Perlmutter lab group as well as Jared Olson, Tim Rich, and Ryan Buckmaster.

I would be remiss to forget the Center for Sensorimotor Neural Engineering (CSNE). Most of you reading this document will see the themes of CSNE embedded across all disparate parts of this thesis. CSNE funded almost my entire graduate career and connected me with an amazing network of people across the neural engineering field who shaped my learning, perspective, and network. CSNE allowed me to work on ethics of neural implants, research issues in virtual reality, novel stimulation and recording hardware for brain-computer interfaces, and new electrode materials with the most amazing people in the world. May your legacy live on so that other students can have the same opportunities that I did.

Personally I must first thank my family. My parents, Brad and Kim, have been through the PhD path and understood the highs and lows that come with the territory. Along with my brother Kevin, they have shared my moments of despair and celebrated my moments of triumph. Thank you for being such rocks to stand on.

BJM

Seattle, 2018

Chapter 1. Introduction

1.1 The many loops of the central nervous system

There are many scales of space and time in which the nervous system operates to keep organisms moving around in the world. The entire process can be imagined as tiers of multi-layered closed loops that interact to produce changes at the molecular, cellular, system, and organism levels. Much work has gone into studying the mechanisms by which these loops can be modified or changed at various levels and timecourses. Traditional models for monitoring these changes are often very unnatural, whether that entails studying cellular mechanisms in a culture dish, or constraining the behavior of a mouse or rat so electrophysiological measures can be taken. There is much less work available on modifying these loops in whole and freely-behaving animals (Fetz 2015). In Chapter 2 we present work showing that a measure of cortical connectivity, the Cortico-Cortico Evoked Potential, can be modulated via Spike Timing-Dependent mechanisms in freely behaving primates. This result helps color the understanding of the impact of long-term Brain Machine Interfaces (BMIs) that deliver cortical stimulation at sub-second timescales. The subsequent chapters contain explorations around larger-scale loops in the motor system.

1.2 Opportunities for innovation

True BMI technology has many barriers to being implemented in humans. First, I would argue, is a lack of reasonable interventions that can justify the surgical, financial, and social risks that come with the bleeding edge of new technology. Current work on restoring and augmenting function does not have a clear solution for reanimating the movement and function of a patient's own hand. (McCrimmon 2016). In Chapter 3 we present a series of novel electrode designs for

reanimating the hand and arm through an approach that can place electrodes on the ventral aspect of the spinal cord, a novel and more easily approached location than current Intra Spinal Micro Stimulation techniques.

If we expand the scope of our BMI definition to include all technologies that rely on feedback to effect a change in an organism's behavior we can bring more reasonably applied solutions into the picture. In many cases the motor system can recover lost function through a variety of methodologies and clinical interventions that benefit from repetitive motions and positive feedback through the visual and auditory systems (Lang 2015). In Chapter 4 we describe a new closed loop rehabilitation platform that can augment traditional physical therapy treatments in the immediate term by sensing an impaired user's movement and remaining muscle activity, using those signals to control a series of rehabilitative exercises, and providing goal-oriented feedback to the user. We believe this early type of intervention is the closest broadly-categorized BMI to clinical utility at the present time.

1.3 References

Fetz, E. E. (2015). Restoring motor function with bidirectional neural interfaces. In Progress in Brain Research (Vol. 218, pp. 241-252). Elsevier.

Lang, C. E., Lohse, K. R., & Birkenmeier, R. L. (2015). Dose and timing in neurorehabilitation: prescribing motor therapy after stroke. Current opinion in Neurology, 28(6), 549.

McCrimmon, C. M., Wang, P. T., Nenadic, Z., & Do, A. H. (2016). BCI-Based Neuroprostheses and Physiotherapies for Stroke Motor Rehabilitation. In Neurorehabilitation Technology (pp. 617-627). Springer, Cham.

Chapter 2. Cortico-Cortico Plasticity in Nonhuman Primates using Paired Electrical Stimulation

In this chapter we explore whether the use of paired stimulation produces plastic changes in primate sensorimotor cortex following spike-timing-dependent rules.

2.1 Summary of Contributions

This chapter was published as Paired Stimulation for Spike-Timing-Dependent Plasticity in Primate Sensorimotor Cortex in the February 2017 volume of the Journal of Neuroscience.

This work was a natural offshoot of my original thesis goal of modifying cortico-spinal plasticity in primates. While pursuing both the new design of spinal implants and approaching cortico spinal evoked potentials there was time between design revisions that was amenable to this exploration. After the initial tests Stephanie Seeman joined the project to help manage the long experiments and massive amounts of data collected.

I designed the study and exclusively debugged the first tests and troubleshooting of timecourses and animal handling. I designed the dual electrodes used and the surgical techniques for implanting them in primates. I performed all primate surgeries. I trained the animals, handled daily care, and performed the experiments. I also analyzed data, edited the publication, and responded to reviewer comments. A section on data collected not included in publication is also added.

The full citation of the work follows:

Stephanie C. Seeman, Brian J. Mogen, Eberhard E. Fetz, Steve I. Perlmutter

Paired Stimulation for Spike-Timing-Dependent Plasticity in Primate Sensorimotor Cortex, Journal of Neuroscience, Volume 37, Issue 7, February 2017, Pages 1935-1949.

DOI:10.1523/JNEUROSCI.2046-16.2017.

2.2 PUBLICATION

2.2.A Introduction

Neuroplasticity underlies many brain functions from learning and memory to recovery from injury (Sanes and Donoghue, 2000; Stuchlik, 2014). Hebb postulated that the repeated association of presynaptic and postsynaptic spiking modifies neuronal connections and forms the basis of learning (Hebb, 1949). The tenet of Hebbian plasticity as a basic mechanism of neuroplasticity has motivated an extensive field of research (Brown et al., 1990; Bi and Poo, 2001; Caporale and Dan, 2008).

Seminal in vitro studies by Markram et al. (1997) and Bi and Poo (1998) elucidated the activity-dependent nature by which a synapse is modified. If postsynaptic neuron B consistently generates an action potential within a short time window after receiving input from presynaptic neuron A, then the connection from A»B is strengthened. If B fires an action potential consistently before the input from A, then the connection from A»B is weakened (Bi and Poo, 1998). Further studies have demonstrated the time course of this spike-timing-dependent plasticity (STDP) in many brain regions and organisms, including humans (Arai et al., 2011; Koch et al., 2013). However, intricacies of the precise temporal window and symmetry of the effect vary between type of synapse, brain areas, and species (Caporale and Dan, 2008; Feldman, 2012). Additional studies have shown that, although timing is important, other factors such as dendritic location (Froemke et al., 2005) and convergence of inputs (Sjöström et al., 2001), the relative timing of spike trains (Froemke and Dan, 2002), and background firing rate (Sjöström et al., 2001) all play a role on the effects of plasticity.

In vivo studies have demonstrated circuit and behavioral effects consistent with STDP using protocols such as pairing of sensory stimuli with electrical stimulation of central neurons

or pairing of two different sensory stimuli (Feldman, 2012). Pairing of neural activity with electrical stimulation in primary motor cortex has also produced STDP-like changes in cortical connections in nonhuman primates (Jackson et al., 2006; Lucas and Fetz, 2013; Nishimura et al., 2013; Zanos, 2013) and rodents (Rebesco et al., 2010). In these studies, recorded spikes, muscle activity, or cortical field potentials were used to trigger stimulation repeatedly at a distant, but connected site. Varying the interval between the triggering event and stimulation produced an STDP time course remarkably similar to in vitro results.

These findings, coupled with recent advances in brain–computer interface technology, suggest that directed STDP could strengthen or reorganize spared connections preferentially and produce lasting, functional recovery after neural damage such as stroke or spinal cord injury (SCI). Functional motor recovery facilitated by STDP paradigms has been demonstrated in animal models of stroke (Guggenmos et al., 2013) and SCI (McPherson et al., 2015), as well as in stroke (Buetefisch et al., 2011) and SCI (Bunday and Perez, 2012) patients.

We sought to investigate the efficacy of open-loop, paired stimulation between sites in the sensorimotor cortex of awake, behaving monkeys to induce STDP. Although closed-loop stimulation has many advantages, one limitation is the need to record a strong and relevant trigger signal. This requirement is challenging for clinical applications that need to be effective over a patient's lifetime. Paired stimulation bypasses the need for recording a neural signal for activity-dependent stimulation. Rebesco and Miller (2011) showed that paired stimulation in awake, behaving rats can produce increased functional connectivity in cortex. We used paired stimulation at a fixed interval, which can be applied for any connected sites at any time, to control the timing of presynaptic and postsynaptic activity. In addition, previous findings have largely focused on changes in behavioral outputs in response to STDP protocols and the extent of

cortical reorganization due to these protocols remains unclear. By recording LFPs from many sites in the hand area of sensorimotor cortex, we were able to measure direct changes in connectivity.

2.2.B Materials and Methods

Implant

Dual electrodes. Two male monkeys (*Macaca nemestrina*), Q and U, were implanted bilaterally with custom-made dual electrodes (Fig. 2.2.1a) arranged in two 3 5 grids over sensorimotor cortex (Fig. 2.2.1b). Dual electrodes were constructed using two 0.005-inch bare platinum-iridium (PtIr) wire rods cut to 3mm(surface electrode) and 5mm(intracortical electrode) and each soldered to 32 gauge, insulated lead wires (Fig. 2.2.1a). The connection between the PtIr rod and lead wire was further insulated with 10 um parylene by the University of Washington Microfabrication Facility to insulate the solder joint and PtIr rod. The tips of each rod were then deinsulated by hand using a scalpel to an impedance of 22–160 kΩ (Monkey Q) and 4–60 kΩ (Monkey U). For each dual electrode, a 3 and

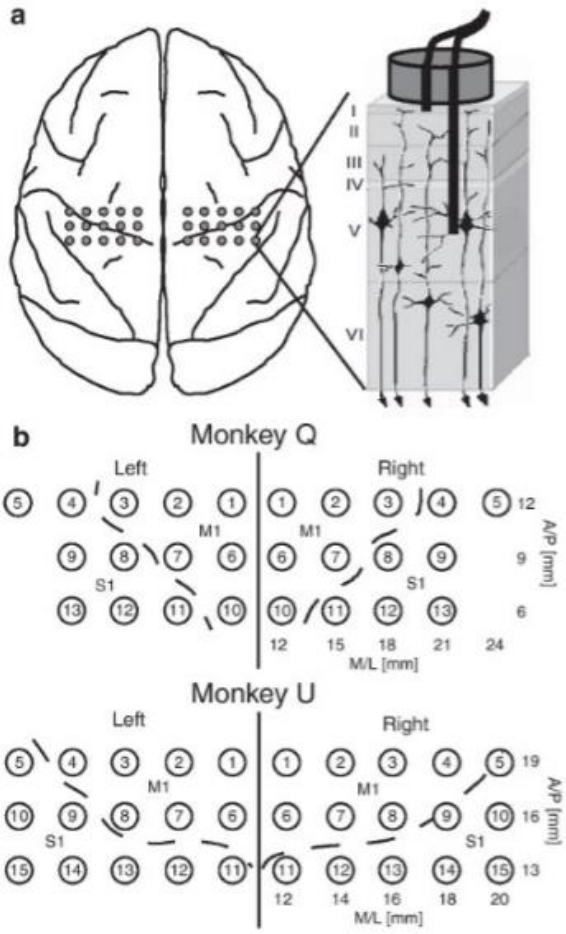

Figure 2.2.1. Implant Schematic. **a**, Top-down view of macaque brain showing the approximate position of each dual electrode with respect to midline and the central and arcuate sulci (gray circles). Expansion shows side view schematic of dual electrode leads with respect to cortical layers. **b**, Numbered electrode sites for each monkey relative to the central sulcus (dotted line), as determined by median nerve stimulation.

a 5mm PtIr rod were secured in a small piece of polytetrafluoroethylene (PTFE) tubing with silicon glue. The tips of the 3 and 5 mm rods were placed 0.5 and 2–2.5 mm from the edge of the PTFE tube (Fig. 2.2.1a). In this way, the 5 mm rod penetrated to layer 5 of motor cortex containing corticofugal pyramidal cell somas, whereas the 3 mm rod rested on the surface of the brain. After each dual array was constructed, the back ends of the lead wires were soldered to connectors, one per hemisphere.

Implant surgery. All surgeries were performed under isoflurane anesthesia and aseptic conditions. An incision was made along the midline of the scalp and muscle and connective tissue were resected to expose enough skull to place a 2.5-inch-diameter titanium casing. Four to eight screws were placed in the skull around the edge of the exposure. At least four of the skull screws were T-screws used as grounds for the electrode implant. Holes were drilled with a 1.1 mm bit in a 3 x 5 grid with 2–3 mm center-to-center spacing using stereotaxic coordinates (Fig. 2.2.1b). After all of the holes were drilled, one dual electrode was placed with forceps into each hole until resistance was felt between the longer rod and the dura. The dual electrode was then pushed through the dura and into the brain until a second resistance was felt between the shorter rod and the dura. We use the term "surface" instead of epidural or subdural to describe the location of the shorter rod because it was impossible to know whether the dura was punctured by the shorter rod. Once all of the dual electrodes for one hemisphere were implanted, a thin coat of dental acrylic (methyl methacrylate) was used to seal the holes and hold them in place. This process was repeated for the other hemisphere. The casing was then placed over the implant and secured to the skull screws with acrylic. The connectors for the dual electrodes were cemented to the skull within the casing. Animals received postoperative courses of analgesics and antibiotics.

Behavior

Monkey U performed a center-out target acquisition wrist task in a sound-attenuating recording booth. Monkey U's right hand was restrained in a manipulandum measuring torque about the wrist in the radial/ulnar (RU) and flexion/ extension (FE) axes. The torque produced in the FE–RU plane was displayed as the *x*–*y* coordinates of a tracking cursor on a video monitor in front of the animal. A trial began when a center target appeared on the monitor, representing the "zero force" or neutral position of the cursor. Monkey U was required to hold the cursor in the center target for 2 s before a peripheral target at one of eight cardinal positions was presented. Monkey U then moved the cursor by exerting isometric force on the manipulandum to the intended target and held it there for 2 s before returning to a second center target. The center-out-center sequence was considered one trial. Applesauce reward was dispensed on a variable 1:2 ratio for every peripheral target presented and at the end of each trial. Monkey Q merely sat quietly in the recording booth.

Recordings

General acquisition. Local field potentials (LFPs) were recorded using amplifiers from Guger Technologies in Monkey Q (4800 Hz sampling rate) and the Grapevine Neural Interface System from Ripple in Monkey U (30,000 Hz downsampled to 5000 Hz post hoc). Single-ended recordings from the intracortical and surface electrodes of one hemisphere, referenced to a skull screw, were made simultaneously on up to 26 channels (13 dual electrodes) in Monkey Q and up to 30 channels in Monkey U (15 dual electrodes). Post hoc recordings were re-referenced as a bipolar signal for each dual electrode (intracortical – surface) to acquire a more localized recording and high-pass filtered over 10 Hz. Wrist torques in the RU and FE axes were sampled for Monkey U by the Grapevine system at 1000 Hz.

Estimate of electrode location relative to the central sulcus. The stereotaxic coordinates at which the electrodes were implanted were determined using an atlas to target the hand area of motor cortex. Because the atlas is only an approximate guide, coordinates were sometimes amended in surgery such that the middle of the grid was ~18 mm lateral to bregma, which is the approximate location of hand motor area (Fetz and Cheney, 1980). To determine the location of each dual electrode more accurately relative to primary motor (M1) or somatosensory (S1) cortex, monopolar responses to stimulation of the contralateral median nerve were recorded with the monkey under ketamine sedation. The waveshape of the evoked potentials in stimulus-triggered averages (StTAs) of single-ended, surface recordings indicated the position of the recoding site relative to the central sulcus (McCarthy et al., 1991). Evoked potentials with a positive phase followed by a negative phase were generated in precentral cortex, whereas a negative phase followed by a positive phase occurred in postcentral cortex. Based on these recordings, a putative position of the central sulcus was drawn onto the grid (Fig. 2.2.1b).

Stimulation

Assessment of corticocortical connectivity. To identify connectivity between recording sites, monkeys were seated in a primate chair in a recording booth while electrical stimulation was delivered to each dual electrode. Stimulation was biphasic, with the negative phase leading on the intracortical wire and the positive phase leading on the surface wire of the dual electrode. Stimuli were delivered in a series of increasing current intensities, termed stimulus ramps, ranging from 0 to 2.25mA with 7–10 increments in the ramp and interstimulus intervals of 300–

500 ms; each ramp was repeated continuously 100 times (Fig. 2.2.2b). Stimulus-evoked potentials (EPs) were measured at all ipsilateral sites in response to stimulation at one site during testing. A stimulus–response curve was produced for each site (Fig. 2.2.3c), building a map of connectivity across the grid. Single pulse stimulation of some sites elicited wrist and hand movement. For paired-stimulation conditioning experiments, ramp stimulation was performed in the booth for the two sites involved in conditioning (sites A and B) as well as a third control site (site C) not involved in conditioning. The order of test stimulation was randomized among the three sites. Testing stimulation was delivered at various time points relative to conditioning, as shown in Figure 2a. However, not all time points were recorded for each session to minimize the amount of time that an animal was handled because a complete session spanned several days.

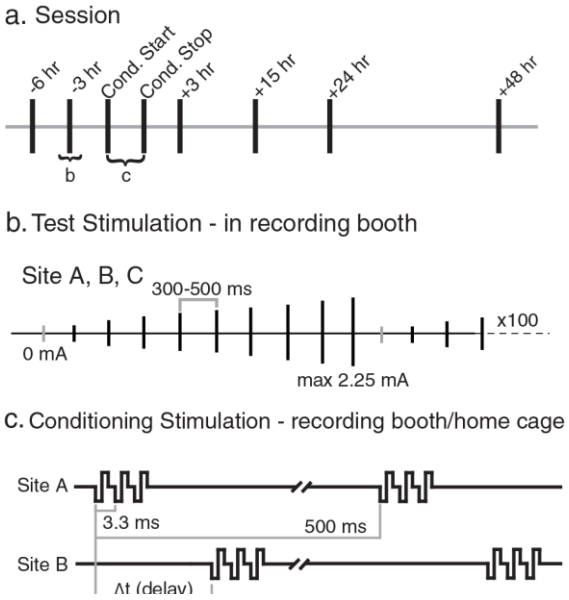

Figure 2.2.2. Experimental timeline. **a**, Session timeline with all possible time points for testing and conditioning stimulation (not all time points were measured for every session). **b**, Schematic of ramped test stimulation applied to sites A–C during each testing time point (e.g., "b" in a). The exact number and magnitude of current steps varied across sessions, but was consistent within a session. **c**, Schematic of conditioning stimulation applied at sites A and B during conditioning period (e.g., "c" in a).

Conditioning. Three reciprocally connected sites were identified via EPs and selected for paired-stimulation conditioning. The "presynaptic" site was termed A, the "postsynaptic site" B, and the third site, C, was used as a control. For Monkey Q, conditioning stimulation was performed with the Neurochip2 (Zanos et al., 2011) in the home cage to assess the efficacy of

STDP while the animal was freely behaving, similar to previous monkey and rodent studies (Jackson et al., 2006; Rebesco et al., 2010; Rebesco and Miller, 2011; Lucas and Fetz, 2013; Nishimura et al., 2013). Stimulation pulses were bipolar and biphasic as described during testing. Conditioning stimulation was delivered first to site A and then to site B with a fixed delay (Fig. 2.2.2c). For Monkey U, conditioning stimulation was performed in the recording booth, using rack-mounted equipment. Similar to Monkey Q, site A received stimulation first, followed by site B.

The paired-stimulation protocol during conditioning was as follows: three pulses at 330 Hz were delivered to site A and to

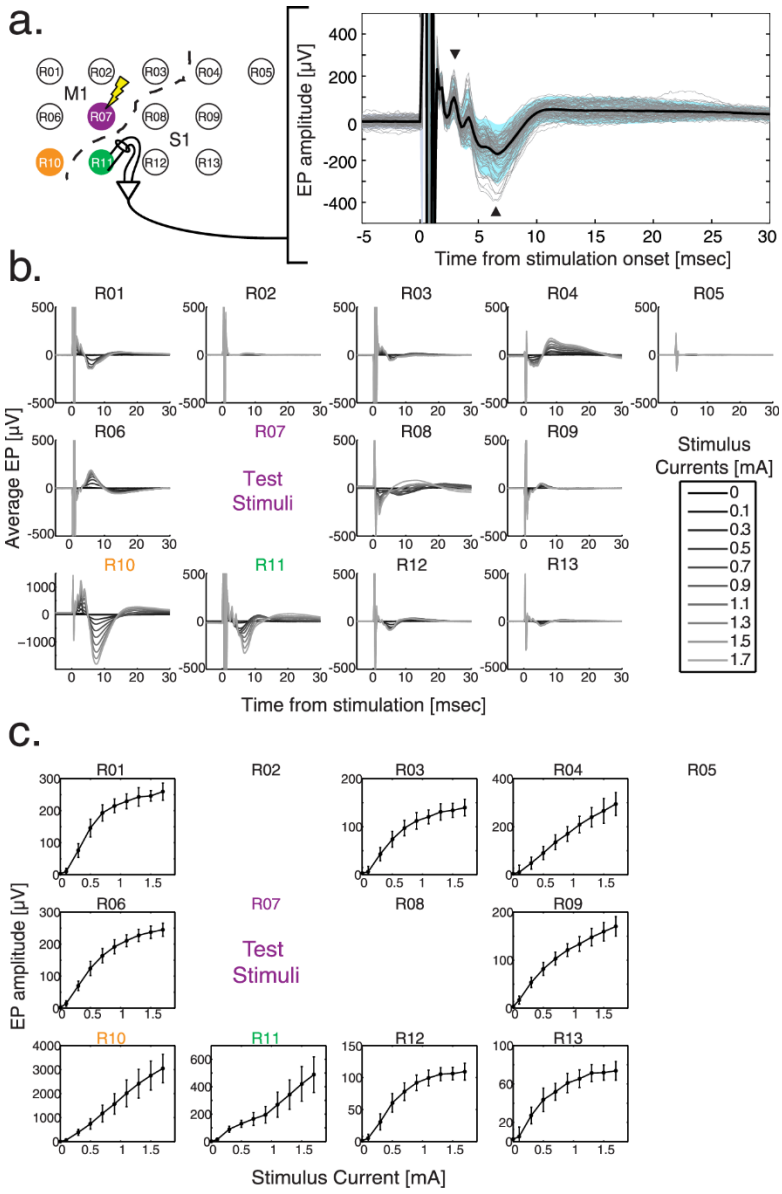

Figure 2.2.3. Cortical connectivity from stimulus-evoked potentials. **a,** Example test stimulation (1.1mA)applied to purple site and recorded at green site in monkey Q (orange site is control, C, site used in Fig. 2.2.6). StTA shows average EP in black, individual trials (n=97) are shown in gray, and the light-blue shadow is the 95% confidence interval. Black arrowheads denote the max peak and trough used to calculate EP amplitude. **b**, Overlaid StTAs at each recording site for all current intensities of test stimuli delivered to R7. **c**, Stimulus–response curves for each recording site for stimulation at R7 (mean±SEM). Blank panels indicate no response as judged from b.

site B separated by a specified delay (t) as measured between the first pulse in each train. This sequence was repeated at 2Hz for 1–3 h (Fig. 2.2.2c). Other stimulation protocols were also tested including 2 Hz single pulses, trains of 5 pulses at 1 kHz, trains of 10 pulses at 500 Hz, as well as longer duration conditioning sessions from 24 up to 72 h. We saw no consistent differences under these protocols and thus used three pulses at 330 Hz for the remainder of the study. A previous study also found that stimulus trains promote better plasticity in vivo than single pulses (Rebesco and Miller, 2011). The stimulus current selected for conditioning was one-third of the current in the middle of the dynamic range of the stimulus–response curve during testing (because condition stimulation was a three-pulse train instead of a single pulse during testing). The selected amplitudes were sufficient to activate neurons at site A and B without adverse effects such as disturbing the animal, causing cortical depression (due to prolonged stimulation with high currents; McCreery et al., 1986), or causing seizures. The current was further adjusted to be just at or below motor threshold if the one-third criterion evoked clear movements.

Analysis

EPs. The peak–trough amplitude of EPs was measured and analyzed to document the strength of corticocortical connectivity. Trials were aligned on stimulus onset and grouped for a given current intensity. All trials were inspected by eye and those with movement artifacts were removed. From the remaining trials, StTAs were calculated from 50 ms before to 30 ms after the time of stimulation for each current intensity (Fig. 2.2.3a). To separate a physiological response from electrical artifact, a biphasic stimulation pulse was delivered directly into the Guger Technologies amplifiers to visualize the artifact. The artifact returned to baseline by 1 ms after stimulation, so any waveform within the first millisecond was ignored. The Grapevine system

has built-in artifact suppression, which grounded the recording channels for 1 ms at the time of stimulation. Each stimulus-aligned trial was also examined by eye for evidence of a clean separation between the stimulus artifact and the physiological response. Trials in which there was possible contamination by the artifact were discarded. The amplitude of the average EP was quantified by subtracting the largest trough from the largest peak in a window 1.5 to 30 ms after stimulation for all current intensities (Fig. 2.2.3a, arrowheads). Latency of the EP features could vary slightly, so care was taken to ensure that the same peak and trough for a given EP were measured across time points. This metric was chosen as a simple, unbiased way to capture the complicated, often multiphasic shape of the EP. Conditioning effects were measured as the percentage change in average EP amplitude from before to after conditioning, similar to other studies measuring changes in field potential recordings (Hess et al., 1996). For some conditioning experiments, testing was performed at regular intervals before and/or after the conditioning window to assess diurnal trends and wash-out of the effect. Preconditioning EP amplitudes were then quantified as the mean of all testing sessions before the start of conditioning. A subset of EPs were also quantified in Monkey U by the slope and amplitude of the first phase of the response because this was the response component most likely to be due to a monosynaptic connection between sites A and B. Only EPs from Monkey U were analyzed in this way because the artifact suppression feature of the Ripple amplifiers, and their ability to record up to 30 kHz, allowed consistent identification of the rising edge of the first phase of the response.

Statistics. All EP amplitudes were quantified as a mean +/- SEM and p-values were calculated with a two-sample z test, except where noted. ANOVAs were used to determine the significance of differences between group means, followed by post hoc Kolmogorov–Smirnov

(K–S) or t tests. Results from the z test indicated that many connections outside of the A»B pair changed strength after conditioning stimulation. To quantify this network-wide change and to determine whether the A»B connection showed greater effects, we created cumulative density curves for the A, B, and C sites. Cumulative distributions have been used in in vitro STDP studies to assess effects between different experimental conditions (Lu et al., 2007). A control distribution for the outputs of site A (Acont) was compiled from the percentage change after conditioning of the evoked responses at all sites except B and C. Similar distributions were calculated for sites B (Bcont) and C (Ccont). One-sample K–S tests were used to determine whether the mean EP changes in the control distributions were significantly different from zero. The p-values for these tests are shown in the diagonal elements of matrices (termed "significance matrices") at the bottom of Figures 2.2.10 and 2.2.13.

The Acont, Bcont, and Ccont distributions were compared with the distributions of EP amplitude changes between two of the A, B, and C sites (e.g., distribution of the A»B effects). The K–S test was used to assess the significance of differences between a control and a site-pair-specific distribution. The p-values for these tests are shown in the off-diagonal elements of the significance matrices in Figures 2.2.10 and 2.2.13. For instance, in Figure 2.2.10, the upper right quadrant is the p-value of a K–S test between the A»B distribution and the Acont distribution. Two-sided significance of $p < 0.05$ for EP changes was based on the lower 2.5th and upper 97.5th percentile of control distributions.

2.2.C Results

Paired-stimulation conditioning was delivered between pairs of sites in sensorimotor cortex of awake, behaving monkeys to induce STDP. Results were obtained from two M. nemestrina monkeys for 15 different pairs of functionally connected sites, two of which showed

delay-dependent effects consistent with STDP as measured by the peak–trough amplitude of EPs.

Selection of conditioning pairs from EPs

We used EPs to identify and quantify the strength of connections between cortical sites. Changes in EP amplitude due to paired stimulation conditioning were interpreted as a change of connection strength. Stimulus ramps (see Materials and Methods) were delivered at each site individually while responses at all other sites on the electrode grid were recorded. StTAs of EPs revealed high connectivity across the grid, as indicated by short-latency, multiphase potentials. Figure 3a shows an example EP at site R11 in response to stimulation at site R7 at 1.1 mA. The first phase usually began within 2 ms, followed by broad, longer-latency phases that usually returned to baseline by ~50 ms after stimulation. After distinguishing the physiological response from the stimulation artifact (see Materials and Methods), a peak–trough measure quantified the amplitude of EPs between 1.5–30 ms after stimulation (EP amp = largest peak - largest trough; Fig. 2.2.3a, arrowheads). The stimulus ramps used a range of current amplitudes to describe the stimulus–response relationship (Fig. 2.2.3b,c). We chose a current range and step resolution that identified a threshold, linear range, and saturation point for a wide range of connected sites (see Materials and Methods). As can be seen in Figure 2.2.3b, stimulation at a single site elicited responses at many other sites, though not all. EP latency, shape, number of phases, and amplitude varied greatly from site to site, likely due to multiple factors, both technical (e.g., the relative positioning of the electrodes) and physiological (e.g., underlying monosynaptic and polysynaptic connectivity between sites). The polarity of EPs varied from site to site as well (Fig. 2.2.3b), likely due to the location of the electrodes with respect to the current dipoles both in cortical depth and across the central sulcus (Buzsáki et al., 2012). The median latency to the

first EP phase for all responses in both monkeys was 2.7 ms, although this varied over a large range (1.6– 12.7 ms, n= 187 EPs; Fig. 2.2.4a). The number of phases in a given EP ranged from one to eight with a median of three (Fig. 2.2.4b). Because EPs were highly variable from site to site, coupled with the conflation of technical and physiological mechanisms underlying EP shape, we hesitate to infer too much about the precise connectivity between sites solely based on EP characteristics (e.g., which EP phases correspond to monosynaptic vs polysynaptic connections). Because both could be affected by the conditioning paradigm, we used the peak–trough amplitude to quantify the strength of connections between sites and how this changed with paired stimulation.

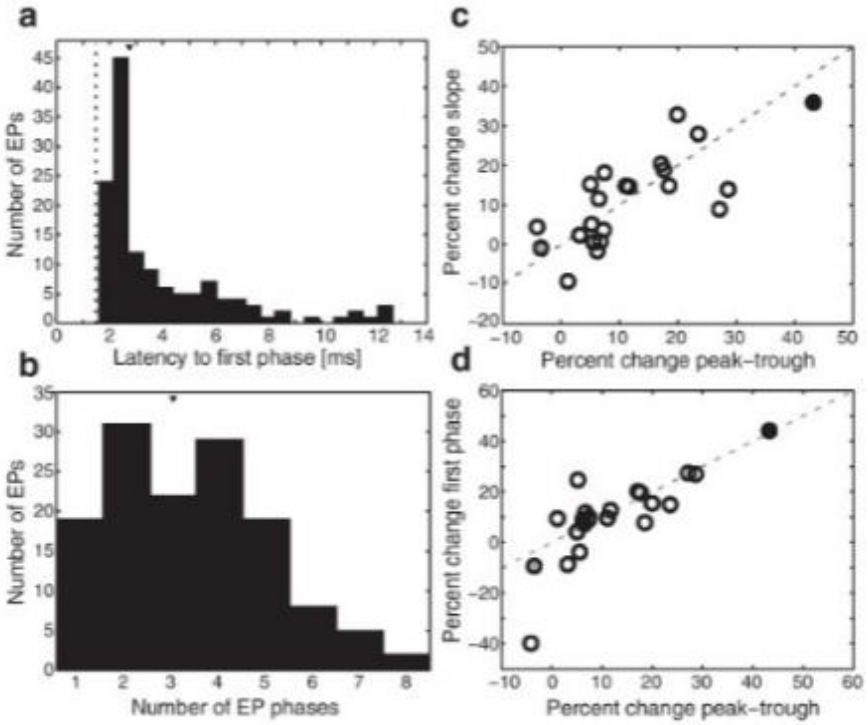

Figure 2.2.4. Characterization and comparison of EP measures. **a,** Histogram of latency to first phase of EP for all responses in both monkeys. Dotted line denotes minimum cutoff due to electrical artifact (1.5 ms) and arrowhead denotes median (2.7 ms). **b**, Histogram of number of phases in each EP. Arrowhead denotes median (3.0). **c,** Percentage change in A»B EP amplitude after conditioning compared with percentage change in slope of the first A»B EP phase for responses in Monkey U, for which we could record at a higher sampling rate and separate the first EP phase reliably from recording artifact (see Materials and Methods). **d,** Percentage change in A»B EP amplitude after conditioning compared with percentage change in amplitude of first A»B EP phase. Dotted line denotes unity; filled black point shows result from a successful conditioning session (Fig. 2.2.8); filled gray point shows result from an unsuccessful conditioning session (Fig. 2.2.14).

Furthermore, conditioning effects on the slope and amplitude of the first response phase, which may be more susceptible to STDP effects (Diesmann et al., 1999), were highly correlated with the effects on the peak–trough amplitude (Fig. 2.2.4c,d, peak–trough vs slope $p = 0.66$, peak–trough vs first phase $p = 0.38$, paired t test).

To assess the specificity of changes in connectivity due to the paired stimulation, we compared the effects of conditioning on the A»B connection with those from A»C and C»B. Changes in EP amplitudes from A»C reveal nonspecific, presynaptic effects at site A, whereas changes in the C»B connection reveal nonspecific, postsynaptic effects at the B site. It is important to note that, although we selected a C site that was recurrently connected to both A and B, many other sites on the grid showed EPs from A and/or B (Fig. 2.2.3b) and could also be used to detect changes in global excitability due to the stimulation.

Table 2.2.1. Conditioning sessions for Monkey Q

Experiment	Session	A Site	B Site	C Site	Pulses	Current [uA]	Frequency [Hz]	Delay [ms]	Duration [h]	A»B [% change]	B»A [% change]	A»C [% change]	C»B [% change]
1	20140917	R7	R11	R10	3@330Hz	330	2	20	3	87.41*	3.13	3.91	1.70
	20141006							10		-42.13*	-62.80	2.43	-1.13
	20141027							30		70.79*	13.78	14.30	9.59
	20150119							20		34.70*	-53.50*	-25.0	-8.08
	20150316							200		-20.96	2.21	-.21	6.88
	20150330							50		-45.07*	-1.42	15.24	23.53*
	20150403							20		250.65*	7.50	8.45	No EP
	20150403†							20		-3.45	-10.66	9.37	No EP
	20150406							100		-10.39	-1.45	22.6	23.0
	20140422							30		-17.77	6.94	31.43*	15.35*
	20140427							10		52.96*	-10.30	19.74	31.48*
	20150720					-	-	-		-7.92	29.42*	9.10	-0.032
2	20150216	L7	L11	L10	3@330Hz	330	2	20	3	34.18*	-34.70*	-44.49*	-24.76*
	20150608							20		-1.93	52.24*	-16.66	0.35
	20150804							20		-19.18	28.47*	-25.7	6.70
3	20150128	R11	R7	R10	3@330Hz	330	2	20	3	-14.14	19.97	6.68	-21.34
4	20150126	L3	L4	L8	3@330Hz	330	2	20	3	-17.82	-13.14	3.71	-20.49
5	20150615	L4	L3	L2	3@330Hz	330	2	20	3	5.22	-29.65*	-10.61	-9.02
6	20150706	L8	L4	L6	3@330Hz	330	2	20	3	-17.51	8.86	12.77	-6.03

Experiments are grouped by sites and sessions and are listed chronologically. Percentage change in EP amplitude was measured immediately after paired stimulation ended. In session 20150403 two conditioning blocks were performed with a 3 h gap in between. The first entry is the result of the first conditioning block and 20150403† is the second conditioning block (see Results). *$p<0.05$ based on control distributions from Figure 2.2.13.

Paired stimulation increases EP amplitude

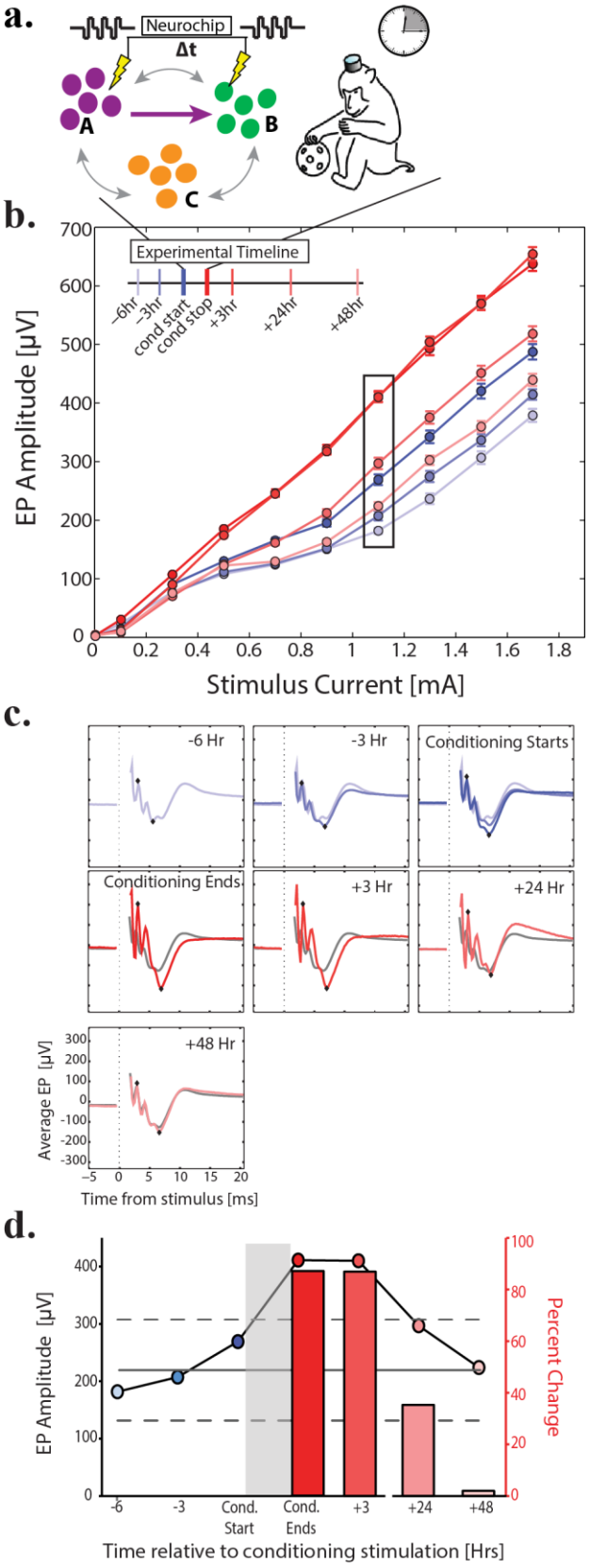

A representative paired-stimulation conditioning session (Table 2.2.1, session 20140917) with a 20ms delay between stimuli is shown in Figure 2.2.5. Three hours of conditioning stimulation (3-pulse trains at 330 Hz every 500 ms, 330 A) were delivered at sites R7 (A site) and R11 (B site) (Fig. 2.2.3a) while Monkey Q was in the home cage. Although stimulus ramps were used to probe the connectivity between sites (Fig. 2.2.3), a

Figure 2.2.5. Three-hour paired-stimulation conditioning session at 20 ms delay. ***a***, Schematic of conditioning between site A and site B using the Neurochip while Monkey Q was in the home cage for 3 h. Sites A, B, and C were the same as in Figure 2.2.3*a*. ***b***, Preconditioning (blue) and postconditioning (red) stimulus–response curves at time points relative to conditioning as denoted by timeline. ***c***, Average EP from A»B at current denoted by black box in ***b***; diamonds denote peak and trough used to measure amplitude in ***b***. Blue EPs in top three panels are averaged into a composite baseline (gray trace) in subsequent panels. ***d***, Circles and left axis showing EP amplitude at times relative to conditioning at current denoted by black box in **b**. Horizontal gray line is mean of three preconditioning points; dashed line is 95% confidence interval. Bars and right axis show percentage increase in EP amplitude above composite baseline. Conditioning occurred during gray bar. Delay between stimuli was 20 ms.

(e.g., 0.34 CV; Fig. 2.2.3a), there was more variability over the course of 3 h before conditioning, consistent with previous observations (Richardson and Fetz, 2012). To account for this variability, we used the mean of all preconditioning EPs as a baseline (Fig. 2.2.5c,d). Immediately after conditioning, the EP amplitude from A»B increased 87.4% (from 219.3 ± 83.6 μV to 411.0 ± 9.0 μV, mean ± SD, n = 295; $p < 0.001$). This increase in connection strength from A»B was maintained 3 h later (410.0 ± 9.0 μV, 86.9%, $p < 0.001$). Twenty-four hours after conditioning ceased, the amplitude fell back within the SD of the preconditioning baseline, but still remained significantly elevated (297.0 ± 10.0 μV, $p < 0.001$) and, by 48 h after conditioning, had fully returned to baseline (224.0 ± 7.0μV, $p = 0.56$; Fig. 2.2.5d.). Changes in the slope of the stimulus–response curve, another measure of connection strength (Hess et al., 1996), follow those of the EP amplitude at the chosen current (Fig. 2.2.6, $p = 0.54$, paired t test, n = 41 sessions), suggesting that these results are consistent over the range of stimulus currents tested.

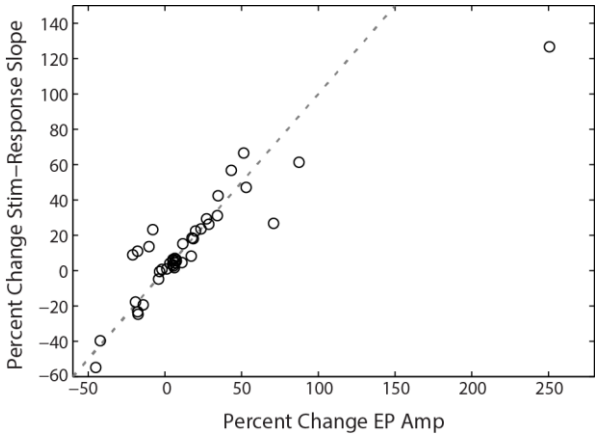

Figure 2.2.6. Comparison of conditioning effects with two different EP measures. Shown is the percentage change in A»B EP amplitude after conditioning compared with percentage change in A»B slope of stimulus–response curve after conditioning for all conditioning sessions in both monkeys. The stimulus–response curve was fit with a linear function to good approximation ($r^2 \geq 0.82$).

Because potentiation of the A»B connection was maintained for at least 3 h in the absence of continued paired stimulation, we ran a second conditioning block to determine whether the A»B connection could be potentiated further. We tested this during one session (Table 1, session 20150403†) in which a 3 h block of paired stimulation was followed by 3 h of no stimulation and then an additional 3 h of paired

stimulation. During the first conditioning block, the A»B EP increased from 123.1 ± 25.0 µV to 431.6 ±56.2µV (250.7%, $p < 0.05$). After 3 h of no stimulation the A»B amplitude fell to 261.6 ± 44.6 µV, which was still significantly larger than the preconditioning amplitude (112.5%, $p < 0.05$). However, after a second 3 h block of paired stimulation, the A»B EP amplitude did not increase further and was maintained at 256.6 ± 36.0 µV (3.45% compared with the previous testing period, $p > 0.05$).

Although paired stimulation was delivered between specific A»B sites, the widespread connections across the electrode grid allowed us to see effects throughout the network. A summary of the post conditioning responses at all sites to stimulation at A, B, or C during the session illustrated in Figure 2.2.5 is shown in Figure 2.2.7 (white tiles indicate no EP recorded). Many connections showed small increases or decreases in response to paired stimulation, but an ANOVA revealed a significant difference between the mean A»B, A»C (3.9%), and C»B (1.7%) responses immediately after conditioning ($p < 0.001$). Post hoc analyses demonstrated that the change in EP amplitude from A»B was significantly larger than that between A»C ($p < 0.001$, 2-sample t test) and C»B ($p < 0.001$). Two other sites showed a significant amplitude increase in EPs elicited from site A immediately after

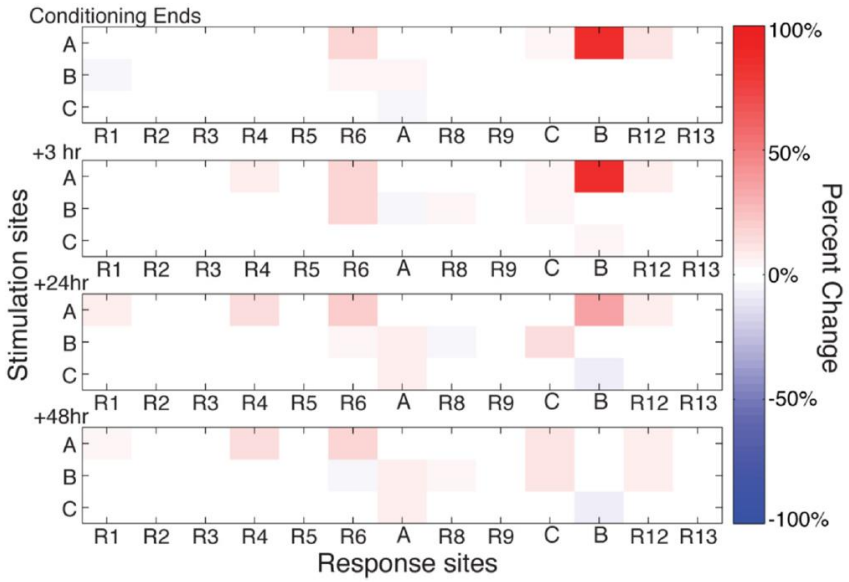

Figure 2.2.7. Network-wide effects of conditioning. Percentage change in EPs (color map shown to right) from A, B, and C to all other sites where there was a response. Panels show time points after conditioning (top to bottom). Data are from the same conditioning session shown in Figure 2.2.5.

conditioning (R6:17.6%, $p < 0.001$; and R12: 11.7%, $p < 0.001$; Fig. 2.2.7). Stimulation protocols producing changes in cortical connectivity that are unrelated to the stimulus pairing have been reported previously (Rebesco and Miller, 2011). These effects could result from global changes in cortical excitability due to the repetitive stimulation, which will be discussed in further detail below. The bottom three panels of Figure 2.2.7 show network-wide changes at testing periods 3, 24, and 48 h after conditioning.

A second example conditioning session in Monkey U (Table 2.2.2, session 20150603) is shown in Figure 2.2.8. Because Monkey U was engaged in a behavioral task, testing and conditioning periods were obtained in the booth during one session. Conditioning stimulation was delivered for 1 h at a delay of 20 ms between site L3 (A site) and L7 (B site), with site L2

Table 2.2.2. Conditioning sessions for Monkey U

Session	A Site	B Site	C Site	Pulses	Current [uA]	Frequency [Hz]	Delay [ms]	Duration [h]	A»B [% change]	B»A [% change]	A»C [% change]	C»B [% change]
20150528	L3	L7	L2	3@330Hz	80	2	20	1	51.37*	8.41	-12.41	-0.97
20150529							B stim only		17.65	157.22*	2.54	-3.18
20150603							20		43.27*	7.14	-16.05	-2.09
20150604					-	-	-		19.96	0.54	0.29	2.74
20150608							10		27.15*	5.41	-0.47	0.68
20150609							30		23.53	4.07	4.80	1.17
20150611							100		6.20	1.50	4.52	-1.59
20150612							200		7.46	-3.82	0.88	0.72
20150806							20		28.64*	5.419	12.24	6.04
20150807							20		6.70	-1.14	8.30	0.96
20150928							20		18.52	2.92	36.19*	4.27
20151001				1	200		6		11.70	5.28	13.85	-1.14
20160108				3@330Hz	80		50		11.11	17.25	29.10*	2.88
20150707	L13	L12	L9	3@330Hz	100	2	20	1	5.23	-1.07	0.23	4.33
20150708					200		20		-3.46	-.45	-3.32	-3.75
20150922	L4	L8	L12	3@330Hz	80	2	20	1	5.04	3.30	-9.17	-3.38
20150924							20		6.46	8.97	11.07	2.40
20150521	L7	L3	L2	3@330Hz	80	2	20	1	5.57	53.75*	-11.60	6.28
20150522	L8	L6	L12	3@330Hz	100	2	20	1	3.20	3.40	3.76	-5.91
20150527	L10	L15	L14	3@330Hz	120	2	20	1	17.16	-7.31	27.45*	-40.74
20150702	L8	L9	L3	3@330Hz	120	2	20	1	7.29	4.14	6.64	1.11
20150709	L6	L2	L7	3@330Hz	140	2	20	1	-4.10	2.90	4.70	3.46
20150710	L12	L8	L13	3@330Hz	140	2	20	1	1.16	4.82	-1.78	2.64

Experiments are grouped by sites and sessions and are listed chronologically. Percentage change in EP amplitude was measured immediately after paired stimulation ended. *$p < 0.05$ based on control distributions from Figure 2.2.13.

serving as the control (C site) (Fig. 2.2.8a). Figure 2.2.8b shows the average EP for 400 µA stimuli before and after conditioning, with the peak and trough denoted by the black diamonds and the corresponding stimulus–response relationship shown in in Figure 2.2.8c. The insets show similar results obtained using the rising slope of the first component of the evoked potential as the measured variable, as has been used in in vitro paired-stimulation plasticity experiments (Froemke and Dan, 2002). Both metrics show a similar effect of conditioning (Fig. 2.2.4c, black filled circle). Again, we saw a large increase in EP amplitude from A»B (43.3%, $p < 0.001$) and variable increases and decreases among other connections. An ANOVA comparing mean responses among A»B, A»C (16%), and C»B (2.1%) was significant ($p < 0.001$) and post hoc t tests showed significant differences between the A»B and A»C and the A»B and C»B effects (both $p < 0.001$). As in the previous example, conditioning led to significant changes of EP amplitude at several other sites across the electrode grid (Fig. 2.2.8d). In summary, these two conditioning sessions exhibited a significant increase in EP amplitude between the targeted site pair that was accompanied by weaker, nonspecific effects at both the presynaptic and postsynaptic sites.

STDP and global changes result from paired stimulation

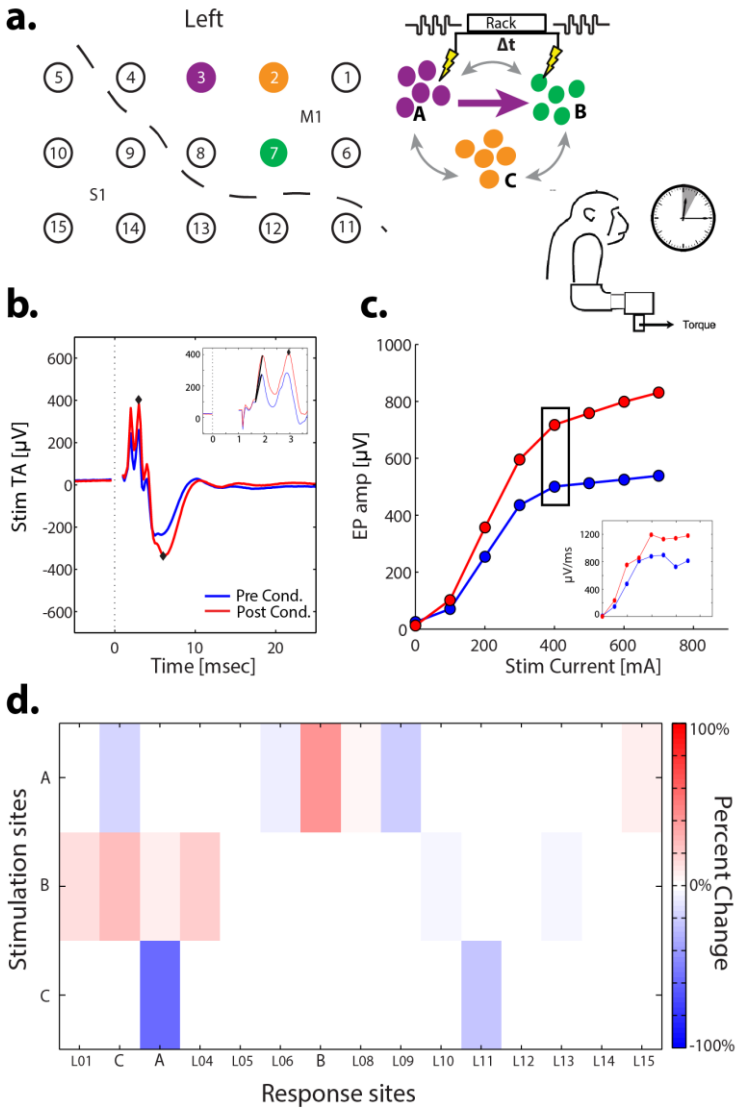

Figure 2.2.8. One-hour paired-stimulation conditioning session at 20 ms delay. ***a***, Schematic of conditioning session with 20 ms delay using rack-mounted equipment while Monkey U was in the booth for 1 h. Left, Cortical positions of A (purple), B (green), and C (orange) sites relative to the central sulcus (dotted line). ***b***, StTA of A»B EP before (blue) and after (red) conditioning at current amplitude denoted by black box in ***c***. Diamonds indicate peak and trough used to calculate amplitude plotted in ***c***. Inset shows magnified view of the early part of the EP; black lines and arrows indicate the slope of the first response phase. ***c***, Stimulus–response curve of A»B EP before (blue) and after (red) conditioning. Black box is current amplitude, 400μA depicted in ***b***. Inset, Stimulus–response curve for slope of the first phase with the same color scheme. ***d***, Percentage change in EPs from A, B, and C to all other sites where there was a response, as in Figure 2.2.7. Fifteen EP sites showed statistically significant changes, either increases or decreases, although none was as large as for the A»B EP. Significant EPs were A»C, A»L6, A»L8, A»L9, A»L15, B»L1, B»C, B»A, B»L4, B»L10, B»L13, C»A, C»L6, C»B, and C»L11.

STDP is characterized by a specific relationship between the change in synaptic strength and the delay between presynaptic and postsynaptic firing. Short delays, such as the 20 ms interstimulus interval highlighted in the above examples, are optimal for inducing potentiation in the A»B direction, whereas longer delays, typically 50 ms, lie outside of the potentiation window (Bi and Poo, 1998). We tested a range of delays (6, 10, 20, 30, 50, 100, and 200 ms; Tables 2.2.1, 2.2.2) for the R7»R11 (Monkey Q) and L3»L7 (Monkey U) site pairs to determine whether the paired stimulation conditioning effects were consistent with an STDP rule. Figure 2.2.9 shows that, at delays < 50 ms, the A»B connection is potentiated preferentially in accordance with a pre-before-post rule (Bi and Poo, 2001). The reverse B»A connection serves as a proxy for post-before-pre conditioning, for which the STDP rule predicts synaptic depression (Bi and

Poo, 1998). Although most B»A responses showed little change with conditioning, two cases in Monkey Q (Fig. 2.2.9, circles, lower left quadrant) showed the expected decrease.

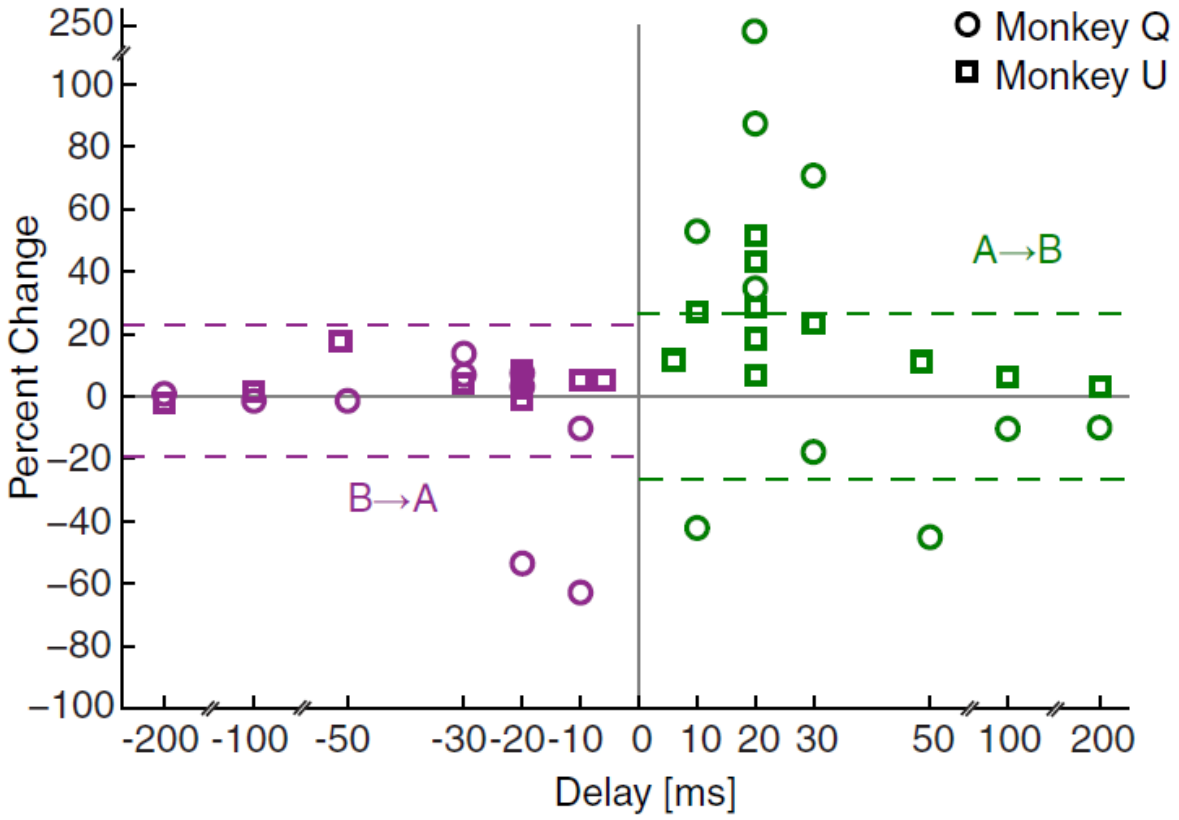

Figure 2.2.9. Conditioning effect as a function of paired-stimulation delay. Conditioning delay versus percentage change in EP amplitude immediately after paired stimulation ended between sites shown in Figure 2.2.5 (Monkey Q, circles) and Figure 2.2.8 (Monkey U, squares). Positive delays indicate pre»post (A»B) stimulation and negative delays indicate post»pre (B»A) stimulation. Dotted lines show 2.5th and 97.5th percentiles for the A distribution (green) or the B distribution (purple) from Figure 2.2.10*a* and *c*, respectively.

To confirm that the STDP effects were robust, we repeated conditioning sessions with the optimal 20 ms interstimulus delay for these two site pairs. Conditioning produced significant increases in EP amplitude from A»B in many, although not all, sessions (Fig. 2.2.9, Tables 2.2.1, 2.2.2). On average, the change in A»B EP amplitude for 20 ms delays at these two site pairs was significantly different from zero (median change = + 39%; $p < 0.01$, one-sample sign test; the small number of data points were not normally distributed). A Kruskal–Wallis test showed a

significant difference ($p = 0.002$) between the A»B, A»C (median = 6.1%), and C»B (1.0%) distributions for all 20-ms-delay sessions. Post hoc analyses indicated a significant difference between the A»B and C»B distributions ($p = 0.007$, Mann–Whitney test) and between the A»B and A»C distributions ($p < 0.001$).

The effect of interstimulus interval on changes in the strength of the A»B connection strongly suggests a role for Hebbian STDP. However, as in the example conditioning sessions described above (Figs. 2.2.7, 2.2.8d), we observed EP changes outside of the target A»B connection that were not predicted by STDP. This result led us to question whether the A»B effects could be accounted for by global changes in excitability. To separate global from targeted, paired-stimulation effects on EP amplitude, we created a distribution of postconditioning effects for all outputs from site A (except B and C) and site B (except A and C) for the two site pairs (Q:R7»R11, U:L3»L7) across all delays (n = 23 sessions; Fig. 2.2.10 a, c). These two distributions were termed Acont and Bcont (see Materials and Methods) and are shown as histograms (Fig. 2.2.10a, c) and cumulative densities (Fig. 2.2.10b, d) in Figure 10. The Acont distribution showed a significant increase in EP amplitude compared with zero ($4.0 \pm 1.0\%$, $p < 0.001$, 1-sample t test, upper left quadrant of significance matrix at the bottom right of Fig. 2.2.10), highlighting the nonspecific effects of repetitive stimulation.

Comparison of the cumulative density curve of the Acont distribution to that compiled from just the A»B effects (Fig. 2.2.10b) shows a significant separation ($p < 0.001$, K–S test, upper right quadrant of significance matrix; Fig. 2.2.10). Therefore, the increase in connectivity strength from A to B due to the targeted conditioning surpasses that of the global effects on the network. Furthermore, increases in A»B EPs at short delays (10–30 ms) drive this difference because A»B effects at long delays (50–200 ms) were not significantly different from Acont (n =

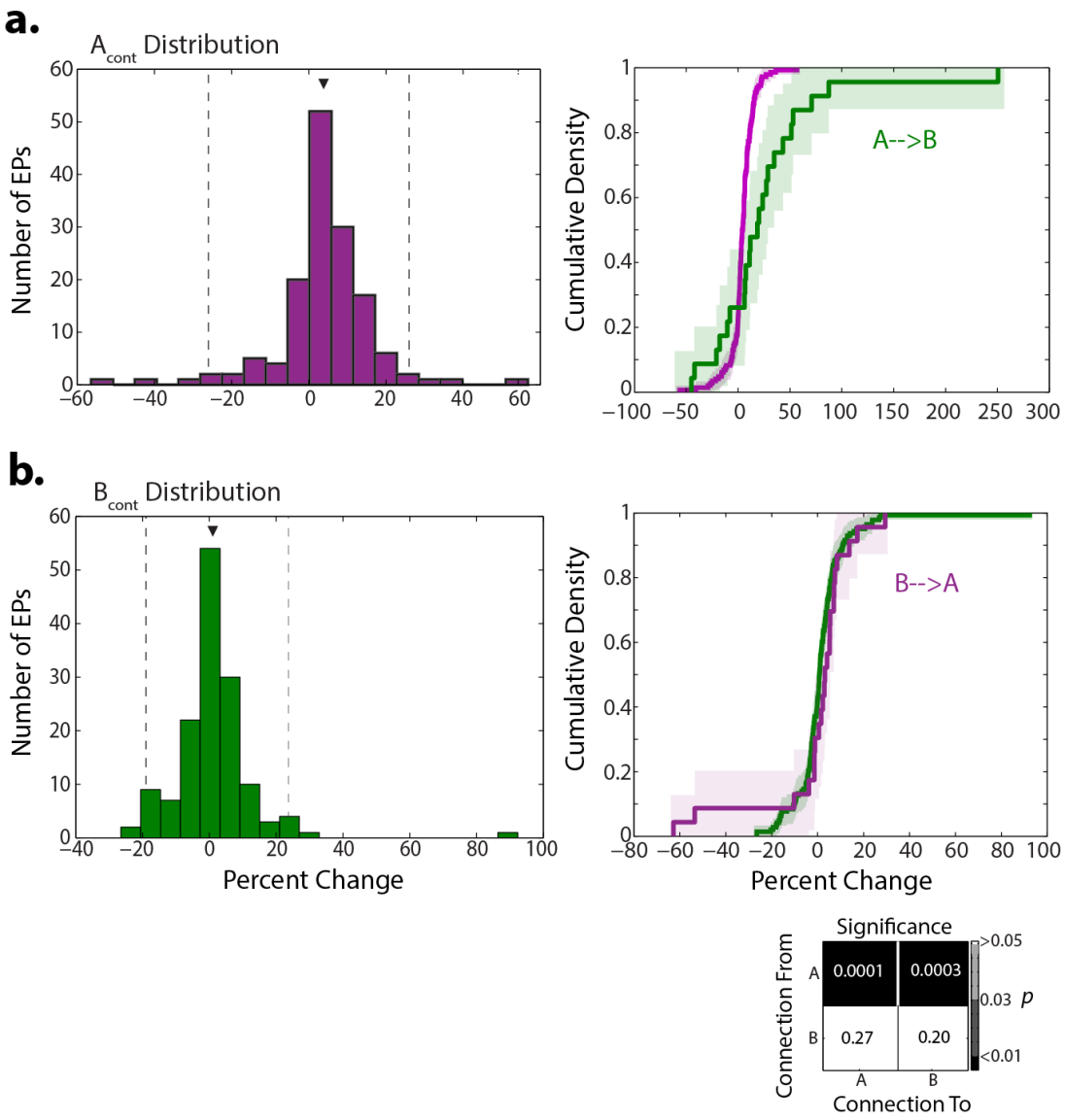

Figure 2.2.10. Cumulative density curves describe network-wide effects of conditioning. ***a***, A_{cont} distribution for all conditioning sessions for the two site pairs depicted in Figures 2.2.7 and 2.2.8 showing the percentage change in EP amplitude from all sites except B and C for which stimulation at site A evokes a response; arrowhead denotes mean (+4.0%, n=146 EPs, $p < 0.001$) and dotted lines indicated the 2.5th and 97.5th percentiles, which are recapitulated in Figure 2.2.9. ***b***, A_{cont} distribution depicted as a cumulative density (purple) superimposed with the cumulative density of percentage change in A»B EPs (green) from all delays depicted in Figure 2.2.9. Light-colored shadows indicate the 95% confidence interval. ***c***, B_{cont} distribution(mean = +1.3%, n = 143 EPs, p = 0.2), as in ***a***. ***d***, B_{cont} distribution cumulative density (green) compared with cumulative density of percentage change in B»A EPs (purple), as in ***b***. Bottom right, Significance matrix for all effects: on-diagonal quadrants indicate p-value of A_{cont} and B_{cont} means compared with zero (one-sample t test); off-diagonal quadrants indicate comparison of the directed connection with the control distribution in the same row (two-sample K–S test).

6 sessions, p = 0.175, K–S test). Conversely, conditioning effects on the B»A EPs were not

different from those in the Bcont distribution (Fig. 2.2.10d; p=0.27, K–S test, lower left quadrant of significance matrix; Fig. 2.2.10) regardless of paired-stimulation delay (50–200 ms delays: n = 6 sessions, p = 0.26, K–S test).

Paired stimulation produces inconsistent STDP effects at most site pairs

The results from the two site pairs discussed above demonstrated that STDP-like effects could be induced between cortical neurons after paired stimulation. We sought to extend these results to multiple sites and tested 13 other pairs in the hand area of primary motor and somatosensory cortex across both monkeys (Fig. 2.2.11) using a 20 ms interstimulus delay. These sites encompassed both M1 and S1. However, we did not see any significant difference in effects on EP amplitude when considering connections within a particular region (M1»M1, S1»S1) or those that crossed the central sulcus (M1»S1, S1»M1) (one-way ANOVA, p = 0.18). The changes in the A»B, B»A, and A»C connections at 20 ms delay for all site pairs tested are shown in Figure 2.2.12 and Tables 2.2.1 and 2.2.2 summarize all conditioning experiment parameters. The two site pairs discussed above (Q:R7»R11 and U:L3»L7, leftmost in Fig. 2.2.12) highlight a pattern that is consistent with an STDP time course: an increased A»B connection and minimal changes in B»A

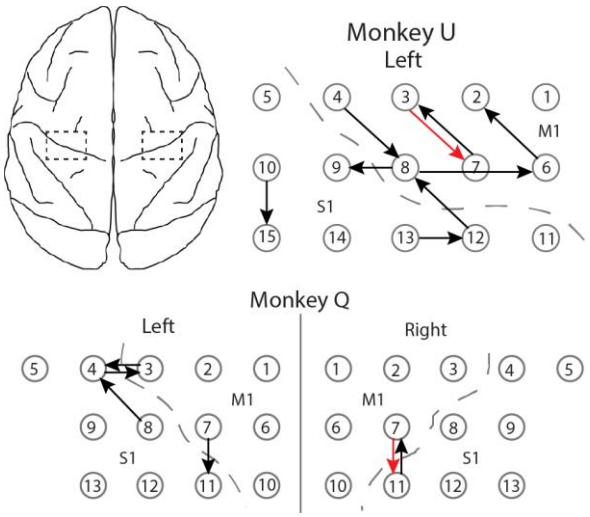

Figure 2.2.11. Schematic of all conditioning pairs. Top left, Top-down view of macaque brain; dashed boxes outline positions of implant area bilaterally. Top right, Left electrode grid in Monkey U with A»B pairs used for conditioning sessions indicated by arrows; arrow points from A to B. Only the left hemisphere was used in Monkey U, which performed a behavioral task using the right hand. Bottom, Bilateral electrode grids for Monkey Q with A»B pairs used for conditioning sessions indicated. Dashed lines in Monkeys U and Q mark the central sulcus.

and A»C. Across all 13 site pairs tested, only one other pair (monkey Q:L7»L11) showed this pattern, but it was unrepeatable in two other sessions (Fig. 2.2.12).

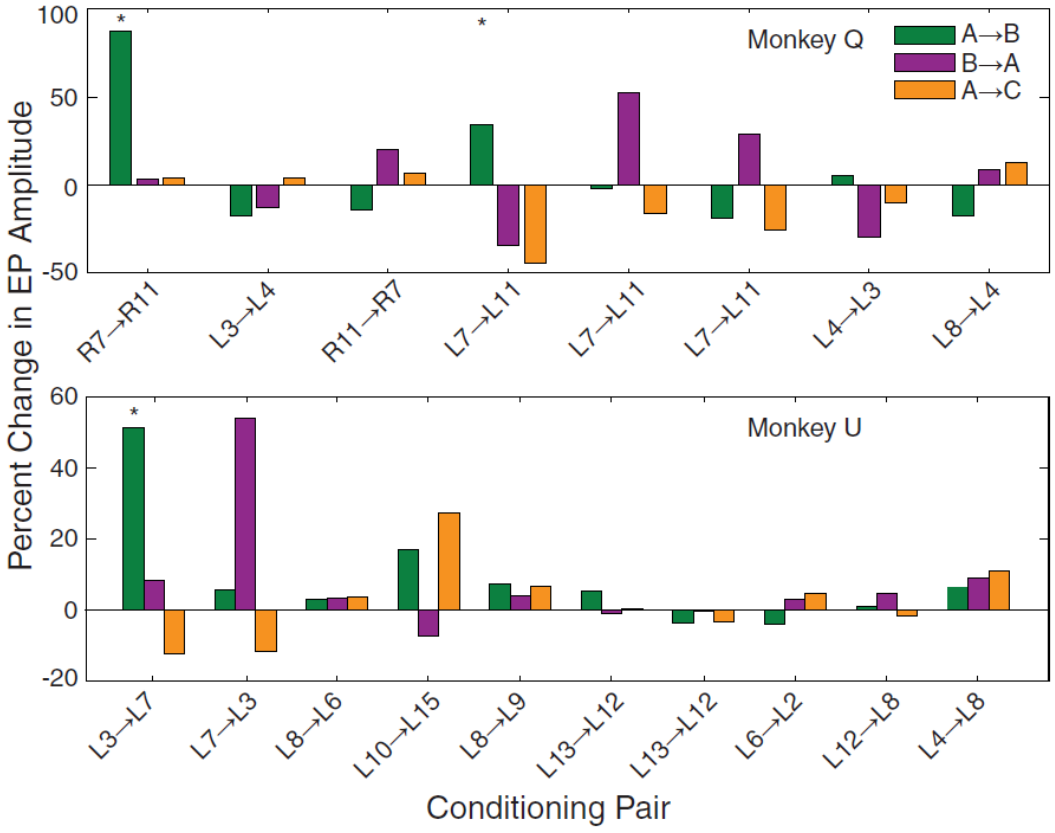

Figure 2.2.12. Summary of conditioning results for all conditioning sessions. Shown is the percentage change in A»B, B»A, and A»C EPs after conditioning at 20 ms delay for all site pairs tested in Monkey Q (top) and Monkey U (bottom). For the far left pair in each panel (*t*op, R7»R11; bottom, L3»L7), multiple sessions at a 20 ms delay were conducted and these data are representative examples depicted in Figures 5 and 8. *$p < 0.05$ as determined by control distributions in Figure 2.2.13.

To examine the significance of the paired stimulation effects compared with the global effects for all site pairs, we again calculated cumulative distributions. Figure 2.2.13a summarizes the results for sessions with a 20ms delay for all 15 site pairs as the Acont distribution compared with the cumulative density of A»B and A»C effects. Similar distributions are shown for the B and C sites (Fig. 2.2.13b,c). There was a small, but significant, shift in the mean of Acont (2.5 ± 0.9%, 1-sample t test, p = 0.01, n = 251, Fig. 13a, inset) and Bcont (2.7 ± 1.0%, p = 0.01, n =

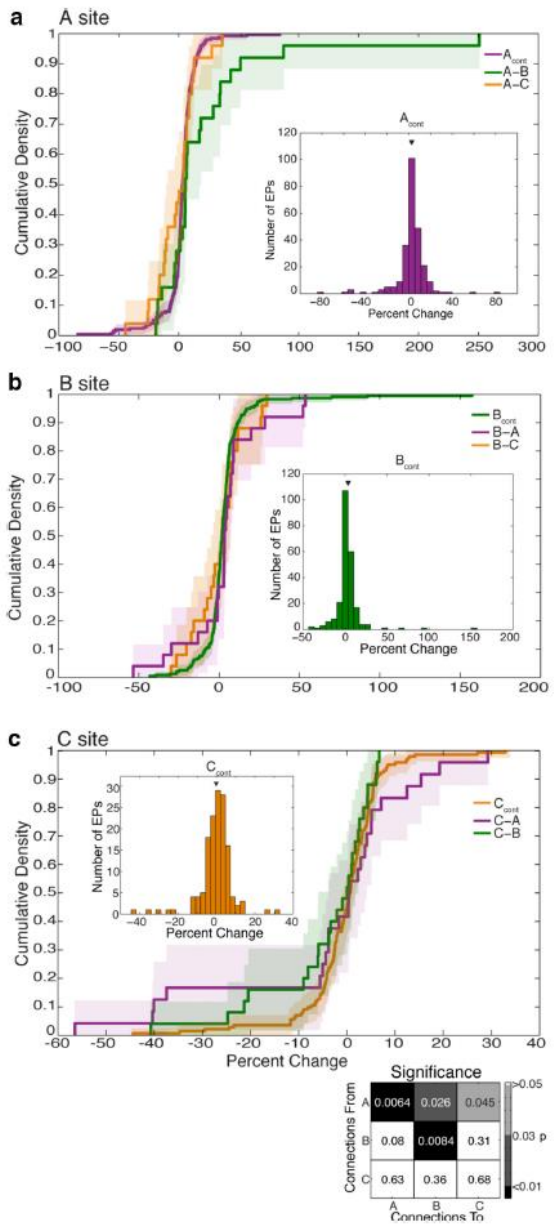

237, Fig. 2.2.13b, inset) away from zero after conditioning at a 20 ms delay, demonstrating the global changes in connections from stimulated sites. The mean of the Ccont distribution was not significantly different from zero (0.23 ± 0.28%, p = 0.68, Fig. 2.2.13c, inset), suggesting that the connections from unstimulated sites were not globally affected by conditioning. The p-values for these tests are shown in the diagonal elements of the significance matrix shown at the bottom of Figure 2.2.13.

The A»B distribution showed significant separation from the Acont distribution (p= 0.03, K–S test, upper middle element of the significance matrix; Fig. 2.2.13a), particularly at large percentage increases (the upper right

Figure 2.2.13. Network-wide effects of paired stimulation across all sessions. ***a***, Cumulative densities for the Acont distribution (purple) from all site pairs at a conditioning delay of 20 ms overlaid with the A»B (green) and A»C (orange) distributions. ***b***, Cumulative densities for the Bcont (green curve), B»A (purple), and B»C (orange) distributions. ***c***, Cumulative densities for the Ccont (orange curve), C»A (purple), and C»B (green) distributions. For all panels, light-colored shadow indicates 95% confidence interval; insets show histograms for the appropriate control distribution and arrowheads mark the mean. Cumulative densities were calculated similarly to those in Figure 10. Bottom right, Significance matrix for all combinations: on-diagonal quadrants indicate *p*-value of Acont, Bcont , and Ccont means compared with zero (one-sample *t* test); off-diagonal quadrants indicate comparison of the directed connection with the control distribution in the same row (two-sample K–S test).

tail of the A»B curve), again indicating an effect of targeted conditioning beyond the global effects on the network. Only three of the 15 site pairs tested (Monkey U: L3»L7; Monkey Q: R7»R11 and L7»L11; Fig. 2.2.12), including the two pairs described in Figures 2.2.7 and 2.2.8, drive this separation and lie outside of the 95th percentile of the Acont distribution. In contrast, there were no significant differences in the distributions for the B»A connection ($p = 0.08$, middle left element of the significance matrix) and the B»C connection ($p = 0.31$) compared with Bcont (Fig. 2.2.13b) or for the C»A connection ($p = 0.63$) and the C»B connection ($p = 0.36$) compared with the Ccont distribution (Fig. 2.2.13c). The A»C distribution was marginally significantly different from Acont ($p = 0.05$).

An example site pair that did not exhibit a significant conditioning effect (Table 2.2.2, session 20150708) is shown in Figure 2.2.14. The A»B EP amplitude was 722.6 ± 6.6 µV before conditioning and 697.6 ± 6.0 µV after conditioning (3.5%, $p > 0.05$, Fig. 2.2.14b–d). Again, we measured the slope of the rising phase of the EP to confirm that the absence of an effect was not due to the peak–trough measure. As can be seen in the insets of Figure 2.2.14, b and c, the changes in slope before and after conditioning closely follow those of the peak–trough amplitude (Fig. 2.2.4c, gray filled circle). This was seen consistently across many experiments. There was no significant difference between the percentage change seen in A»B after conditioning using the

peak–trough amplitude compared with the slope of the first rising phase (p=0.66, paired t test;

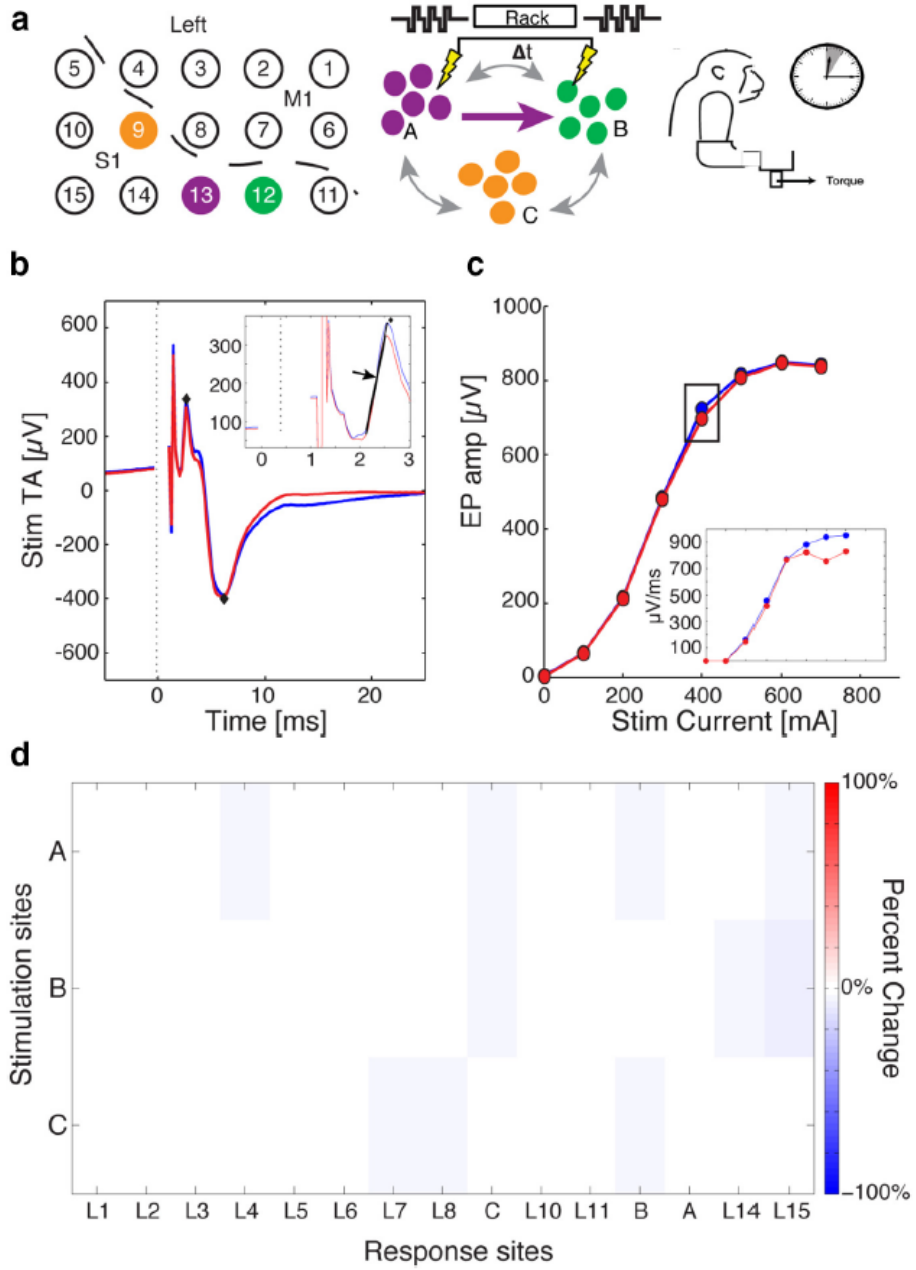

Figure 2.2.14. Paired stimulation does not produce a conditioning effect at all sites. ***a***, Schematic of recording grid with A (purple), B (green), and C (orange) sites denoted for a conditioning session at a 20ms delay in Monkey U while in the recording booth for 1 h. ***b***, StTA of A»B EP before (blue) and after (red) conditioning. Inset, Expansion of StTA showing the slope (black line and arrow) of the first EP phase. Black diamonds denote peak and trough used to calculate amplitude in ***c***. ***c***, A»B stimulus–response curve before (blue) and after (red) conditioning. Black box denotes current depicted in ***b***. Inset, Stimulus–response curve before and after conditioning for slope of first EP phase. ***d***, Percentage change in EP amplitude from A–C to all other recording sites after conditioning.

Fig. 2.2.4c) or the absolute amplitude of the first phase (p=0.38, paired t test; Fig. 2.2.4d).

2.2.D Discussion

This study aimed to induce synaptic plasticity in sensorimotor cortex in awake, behaving nonhuman primates using a pairedstimulation protocol. Sites in precentral and/or postcentral cortex were deemed functionally connected if stimulation of one site evoked an LFP response at the other site. Prolonged paired stimulation of some connected sites at a fixed delay resulted in STDP, as evidenced by increased EP amplitude when conditioning with short delays but not long ones (Fig. 2.2.9). Plasticity effects in the targeted A»B connection surpassed global increases in connectivity throughout the network (Fig. 2.2.13). Surprisingly, this effect was only produced in two of 15 site pairs (13%). Effects in the other 13 site pairs predominantly showed global increases in connectivity (50% of pairs) or depression of the targeted site pair (44% of pairs), likely resulting from changes in excitability or generalized plasticity (Pascual-Leone et al., 1998). These results are consistent with other studies, both in vitro (Bi and Poo, 1998) and in vivo (Jackson et al., 2006), showing that the expected effects of STDP were variable and occurred only in a subset of cases. The effects that we observed raise questions about the mechanisms underlying STDP between cortical populations induced with paired electrical stimulation in vivo.

STDP between cortical populations may be induced via paired stimulation

Typical in vitro STDP studies document connectivity changes using a direct measure of EPSPs (Markram et al., 1997; Bi and Poo, 1998; Sjöström et al., 2001; Froemke and Dan, 2002). Evidence of STDP has also been obtained with indirect measures such as evoked movements (Jackson et al., 2006; Lucas and Fetz, 2013), postspike electromyographic responses (Nishimura

et al., 2013), motor evoked potentials (Wolters et al., 2003), network modeling (Rebesco et al., 2010; Rebesco and Miller, 2011), and others (Feldman, 2012). This study is one of the first to show long-lasting STDP in evoked LFPs mediated by cortical connections. The corticocortical EPs typically showed multiple phases, probably mediated by monosynaptic and polysynaptic connections between the sites. In two of the site pairs, STDP effects were robust, repeatable, and displayed a classic STDP time course (Fig. 2.2.9). The changes were evident in multiple EP phases (Fig. 2.2.5c), suggesting that many pathways between the two sites were similarly enhanced by paired stimulation. These results indicate that paired stimulation can induce targeted plasticity under the appropriate circumstances. Surprisingly, a majority of sites did not show STDP, which could be explained by several factors, as discussed below.

STDP is a multifaceted phenomenon

Paired stimulation of a source population at A and a target population at B could be considered comparable to the pre-post pairing in in vitro studies (Bi and Poo, 1998; Feldman, 2000; Froemke and Dan, 2002). In principle, paired electrical stimulation in vivo will similarly induce activity at the presynaptic and postsynaptic sites in an appropriately timed manner to induce plasticity. However, as has been demonstrated in vitro, timing is only one of many factors governing plasticity at a given synapse (Feldman, 2012). We found that pairs of single pulses were insufficient, but trains of three pulses produced results consistent with observations in rodents (Rebesco and Miller, 2011). Sjöström et al. (2001) demonstrated the influences of background firing rate and cooperativity of multiple inputs on STDP effects in V1 with fixed pre-post delays. Spatiotemporal integration is critical for sufficient depolarization in the postsynaptic neuron such that a well-timed back-propagating action potential will promote STDP (Lisman and Spruston, 2005).

The intrinsic connectivity of cortical networks, comprising the number, strength, and location of connections, is another key factor governing synaptic plasticity (Sjöström et al., 2001; Froemke et al., 2005). Recordings of EPs from large populations provide only a gross measure of network connectivity that cannot resolve the specific synapses that might be conditioned. Of the many possible connections between cells at sites A and B, Figure 2.2.15 illustrates key pathways that could help to explain our mixed results. Long-range pyramidal cell collaterals identified in neuroanatomical studies (DeFelipe et al., 1986) likely provide the major excitatory pathway giving rise to EPs; these would be modified by conditioning and are probably the site of plastic effects observed in other in vivo STDP studies (Jackson et al., 2006; Rebesco et al., 2010; Rebesco and Miller, 2011). Because LFPs incorporate many nearby current sources (Buzsáki et al., 2012), the EPs cannot differentiate those pathways that may be more

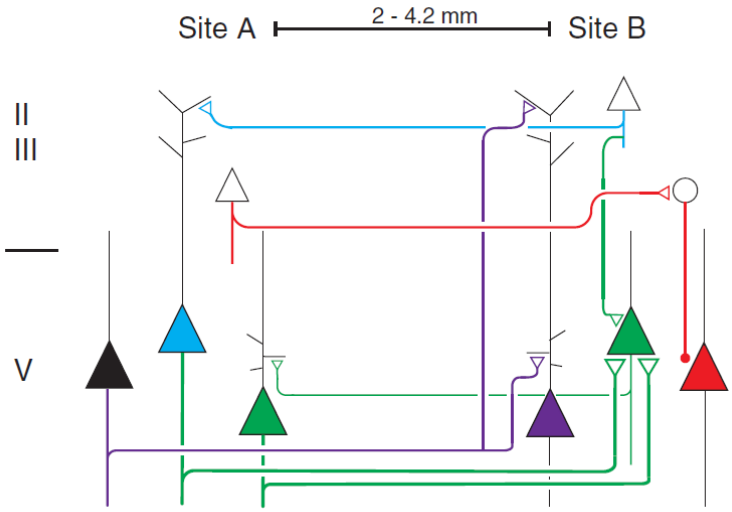

Figure 2.2.15. Proposed diagram of interareal connections and STDP effects. Four of many potential pathways connecting an A and B site in sensorimotor cortex are shown to illustrate differential STDP effects produced in these networks and how they may interact. Upper layer 2/3 and layer 5 are the likely targets of the dual electrodes for each site, so only these layers are shown. The green pathway from A»B highlights successful potentiation due to convergent excitatory input between layer 5 pyramidal cells, as well as collaterals within the B site. Similarly, the green pathway from B»A shows successful depression. The other three pathways do not promote STDP for various reasons. The red pathway results in inhibition between A and B via inhibitory interneurons (circles). In the purple pathway, whereas inputs to the proximal dendrites would promote potentiation, inputs on the distal dendrites would not. Similarly, depression in the blue pathway is unsuccessful because the primary connection from B»A is in the distal dendrites.

amenable to STDP. Because spatial integration is one of the factors contributing to STDP (Sjo¨stro¨m et al., 2001), pathways having high convergence would be more likely to show plasticity (Fig. 2.2.15, green pathway).

There are also multiple forms of STDP that occur in a regional and synapse-specific fashion (Feldman, 2012). In traditional Hebbian STDP, positive delays (pre before post) produce LTP, whereas negative delays (post before pre) promote LTD. Conversely, in anti-Hebbian STDP, LTD is produced at positive delays and moderate LTP at negative delays. Anti-Hebbian STDP occurs at a variety of synapses, particularly those of layer 2/3 neuron axons on the distal dendrites of layer 5 neurons, likely due to attenuation of the back-propagating action potential (Sjöström and Häusser, 2006). Because our paired stimulation probably invoked STDP at both proximal and distal dendrites, the resulting mixture of Hebbian and anti-Hebbian effects could have prevented net LTP from occurring at site B (Fig. 2.2.15, purple pathway). Connections between excitatory and inhibitory neurons (Fig. 2.2.15, red pathway) show a variety of STDP time courses (Caporale and Dan, 2008), further obscuring the net effects produced among a heterogeneous population. It should also be noted that fields from antidromically activated cells at B would presumably not be changed by the conditioning protocol and thus would dilute the measure of any actual A»B conditioning.

Traditional Hebbian STDP also predicts depression in the B»A connections because this involves a negative delay. To the extent that the B»A connections from distal layer 2/3 at B to layer 5 cells at A exhibit anti-Hebbian STDP this would be consistent with the lack of B»A depression that we observed (Fig. 2.2.15, blue pathway). In addition, STDP effects incorporating multiple spike times do not add linearly (Froemke and Dan, 2002) and therefore, whereas B»A

connections may have experienced a negative delay between the initial paired-stimulation pulses, continued activation via recurrence may have interfered with the simplest Hebbian mechanism.

Timing of presynaptic and postsynaptic activation is one of the few parameters that we could control experimentally, along with rate of stimulation. For two of our site pairs, a sufficient combination of these factors aligned such that the rate and timing of paired stimulation promoted STDP. We tested other protocols varying the rate, number of pulses, or duration of stimulation to optimize the parameter space (see Materials and Methods), but these did not produce conditioning effects for the other 13 site pairs. However, it seems likely that the synaptic connections mediating the EPs between these other pairs would be modifiable and that other, untested stimulation protocols would have activated the appropriate circuit elements for inducing STDP at these sites.

Artificial effects of electrical stimulation

Electrical stimulation is an excellent way to activate neurons rapidly, yet it is inherently artificial and nonspecific because it can activate axons and recruit neurons transynaptically (Gustafsson and Jankowska, 1976; Histed et al., 2009) in nonphysiological spatiotemporal patterns. Many studies using electrical stimulation to induce STDP record a neural signal from the presynaptic and postsynaptic site (Markram et al., 1997; Bi and Poo, 1998) or trigger postsynaptic stimulation from a neural event (Jackson et al., 2006; Rebesco et al., 2010; Nishimura et al., 2013; Zanos, 2013) to ensure proper timing of action potentials and postsynaptic depolarization. We hypothesized that paired stimulation would be sufficient to induce well-timed spiking both presynaptically and postsynaptically with fixed delays appropriate to promote plasticity. This hypothesis is substantiated by in vivo evidence that paired stimulation can change the inferred connectivity of neural networks (Rebesco and Miller, 2011). Furthermore, studies in humans

using transcranial magnetic stimulation to pair stimulation of the median nerve with associated cortical areas demonstrate classic Hebbian STDP (Wolters et al., 2003). Therefore paired-stimulation protocols should be able to promote targeted plasticity, as we observed for a subset of site pairs. However, it is possible that the artificial pattern of neural activation with electrical stimulation was not permissive for STDP at the other sites.

Conditioning with spike-triggered stimulation (Jackson et al., 2006) produced a larger proportion of positive plasticity effects than paired electrical stimulation, which could be due to several significant experimental differences. Stimulating at site A rather than using recorded trigger spikes would have activated a larger population of more diverse cell types synchronously and consequently recruited a broader range of plasticity mechanisms, such as Hebbian and anti-Hebbian effects. The net result of this broader recruitment may have been less facilitation of excitatory connections, producing fewer cases of significant changes in EPs in the present study. Second, the triggering spikes in the Jackson et al. (2006) study occurred in association with normal behavior, whereas we delivered paired stimulation in a preprogrammed manner independently of the modulation of local activity with movements or sleep spindles. Third, documenting the conditioning effects with peripheral responses to trains of cortical microstimuli rather than with cortical potentials evoked by single test stimuli would have involved different circuit mechanisms and potential loci of plasticity. These issues could be investigated in future experiments by direct comparison of results with spike- and stimulus-triggered conditioning.

The complexity of different STDP mechanisms for different cell pairs (Sjöström et al., 2001; Feldman, 2012) could be addressed with more specific stimulation techniques. For example, optogenetic stimulation can be used to activate only local excitatory pyramidal neurons, rather than the diverse, more widely distributed, excitatory and inhibitory population

recruited by electrical stimuli (Yazdan-Shahmorad et al., 2016). In a paired-stimulation protocol, optogenetic stimulation could begin to elucidate how different circuit elements contribute to STDP in cortical networks.

In conclusion, our results indicate that conditioning in monkey sensorimotor cortex with paired electrical stimulation produced results consistent with STDP, but in a surprisingly small proportion of sites. The neural mechanisms explaining these results remain to be further elucidated. Future experiments could compare the results of conditioning with electrical stimulation and results with optogenetic or spike-triggered stimulation at the same cortical sites.

2.2.E Additional Datasets Generated

This project encompassed almost three years' worth of experiments, troubleshooting, and experimental tangents. Alongside each session of stimulation data we also collected 10 minutes of spontaneous recording, also at 4800 or 5000 Hz. A coherence analysis was conducted on the spontaneous data and can be found in Stephanie Seeman's PhD thesis (UW Neuroscience Program) but the results did not conclusively show any reliable metric of change in the conditioning paradigms we tested. Our initial tests followed the experimental timing set forth by Jackson et al. (2006). We attempted 24 hours of stimulation in a paired configuration using single and triplicate pulses as well as theta-burst stimulation protocols. The results of those early tests were incredibly varied. In most cases we saw global depression of outputs and inputs in response to stimulation. The net amount of current we were injecting was several orders of magnitude larger than that of Jackson which may have contributed to the sporadic. All together there is a compendium of over 100 10-minute spontaneous recordings across two animals and the corresponding stimulation data available for further study.

2.2.F References

Arai N, Muller-Dahlhaus F, Murakami T, Bliem B, Lu MK, Ugawa Y, Ziemann U (2011) State-dependent and timing-dependent bidirectional associative plasticity in the human SMA-M1 network. J Neurosci 31:
15376–15383.

Bi GQ, Poo MM (1998) Synaptic modifications in cultured hippocampal neurons: dependence on spike timing, synaptic strength, and postsynaptic cell type. J Neurosci 18:10464 –10472.

Bi G, Poo M (2001) Synaptic modification by correlated activity: Hebb's postulate revisited. Annu Rev Neurosci 24:139 –166.

Brown TH, Kairiss EW, Keenan CL (1990) Hebbian synapses: Biophysical mechanisms and algorithms. Annu Rev Neurosci 13:475–511.

Buetefisch C, Heger R, Schicks W, Seitz R, Netz J (2011) Hebbian-type stimulation during robot-assisted training in patients with stroke. Neurorehabil Neural Repair 25:645– 655.

Bunday KL, Perez MA (2012) Motor recovery after spinal cord injury enhanced by strengthening corticospinal synaptic transmission. Curr Biol 22:2355–2361.

Buzsáki G, Anastassiou CA, Koch C (2012) The origin of extracellular fields and currents–EEG, ECoG, LFP and spikes. Nat Rev Neurosci 13:407– 420.

Caporale N, Dan Y (2008) Spike timing-dependent plasticity: a Hebbian learning rule. Annu Rev Neurosci 31:25– 46.

DeFelipe J, Conley M, Jones EG (1986) Long-range focal collateralization of axons arising from corticocortical cells in monkey sensory-motor cortex. J Neurosci 6:3749 –3766.

Diesmann M, Gewaltig MO, Aertsen A (1999) Stable propagation of synchronous spiking in cortical neural networks. Nature 402:529 – 533.

Feldman DE (2000) Timing-based LTP and LTD at vertical inputs to layer II/III pyramidal cells in rat barrel cortex. Neuron 27:45–56.

Feldman DE (2012) The spike-timing dependence of plasticity. Neuron 75:556–571.

Fetz EE, Cheney PD (1980) Postspike facilitation of forelimb muscle activity by primate corticomotoneuronal cells. J Neurophysiol 44:751–772.

Froemke RC, Dan Y (2002) Spike-timing-dependent synaptic modification induced by natural spike trains. Nature 416:433– 438.

Froemke RC, Poo MM, Dan Y (2005) Spike-timing-dependent synaptic plasticity depends on dendritic location. Nature 434:221–225.

Guggenmos DJ, Azin M, Barbay S, Mahnken JD, Dunham C, Mohseni P, Nudo RJ (2013) Restoration of function after brain damage using a neural prosthesis. Proc Natl Acad Sci U S A 110:21177–21182.

Gustafsson B, Jankowska E (1976) Direct and indirect activation of nerve cells by electrical pulses applied extracellularly. J Physiol 258:33– 61.

Hebb DO (1949) The organization of behavior: a neuropsychological theory.
New York: Wiley.

Hess G, Aizenman CD, Donoghue JP (1996) Conditions for the induction of long-term potentiation in layer II/III horizontal connections of the rat motor cortex. J Neurophysiol 75:1765–1778.

Histed MH, Bonin V, Reid RC (2009) Direct activation of sparse, distributed populations of cortical neurons by electrical microstimulation. Neuron 63:508 –522.

Jackson A, Mavoori J, Fetz EE (2006) Long-term motor cortex plasticity induced by an electronic neural implant. Nature 444:56–60.

Koch G, Ponzo V, Di Lorenzo F, Caltagirone C, Veniero D (2013) Hebbian and anti-Hebbian spike-timing-dependent plasticity of human corticocortical connections. J Neurosci 33:9725–9733.

Lisman J, Spruston N (2005) Postsynaptic depolarization requirements for LTP and LTD: a critique of spike timing-dependent plasticity. Nat Neurosci 8:839–841.

Lu JT, Li CY, Zhao JP, Poo MM, Zhang XH (2007) Spike-timing dependent plasticity of neocortical excitatory synapses on inhibitory interneurons depends on target cell type. J Neurosci 27:9711–9720.

Lucas TH, Fetz EE (2013) Myo-cortical crossed feedback reorganizes primate motor cortex output. J Neurosci 33:5261–5274.

Markram H, Lu¨bke J, Frotscher M, Sakmann B (1997) Regulation of synaptic efficacy by coincidence of postsynaptic APs and EPSPs. Science 275: 213–215.

McCarthy G, Wood CC, Allison T (1991) Cortical somatosensory evoked potentials. I. Recordings in the monkey Macaca fascicularis. J Neurophysiol 66:53– 63.

McCreery DB, Bullara LA, Agnew WF (1986) Neuronal activity evoked by chronically implanted intracortical microelectrodes. Exp Neurol 92:147– 161.

McPherson JG, Miller RR, Perlmutter SI (2015) Targeted, activity-dependent spinal stimulation produces long-lasting motor recovery in chronic cervical spinal cord injury. Proc Natl Acad Sci U S A 112:12193–12198.

Nishimura Y, Perlmutter SI, Eaton RW, Fetz EE (2013) Spike-timingdependent plasticity in primate corticospinal connections induced during free behavior. Neuron 80:1301–1309.

Pascual-Leone A, Tormos JM, Keenan J, Tarazona F, Can˜ete C, Catala´ MD (1998) Study and modulation of human cortical excitability with transcranial magnetic stimulation. J Clin Neurophysiol 15:333–343.

Rebesco JM, Miller LE (2011) Enhanced detection threshold for in vivo cortical stimulation produced by Hebbian conditioning. J Neural Eng 8:016011.

Rebesco JM, Stevenson IH, Ko¨rding KP, Solla SA, Miller LE (2010) Rewiring neural interactions by micro-stimulation. Front Syst Neurosci 4: pii: 39.

Richardson AG, Fetz EE (2012) Brain state-dependence of electrically evoked potentials monitored with head-mounted electronics. IEEE Trans Neural Syst Rehabil Eng 20:756 –761.

Sanes JN, Donoghue JP (2000) Plasticity and primary motor cortex. Annu Rev Neurosci 23:393–415.

Sjöström PJ, Häusser M (2006) A cooperative switch determines the sign of synaptic plasticity in distal dendrites of neocortical pyramidal neurons. Neuron 51:227–238.

Sjöström PJ, Turrigiano GG, Nelson SB (2001) Rate, timing, and cooperativity jointly determine cortical synaptic plasticity. Neuron 32:1149– 1164.

Stuchlik A (2014) Dynamic learning and memory, synaptic plasticity and neurogenesis: an update. Front Behav Neurosci 8:106.

Wolters A, Sandbrink F, Schlottmann A, Kunesch E, Stefan K, Cohen LG, Benecke R, Classen J (2003) A temporally asymmetric Hebbian rule governing plasticity in the human motor cortex. J Neurophysiol 89:2339– 2345.

Yazdan-Shahmorad A, Diaz-Botia C, Hanson TL, Kharazia V, Ledochowitsch P, Maharbiz MM, Sabes PN (2016) A large-scale interface for optogenetic stimulation and recording in nonhuman primates. Neuron 89:927– 939.

Zanos S (2013) Cortical surface recurrent brain-computer interfaces. Doctoral dissertation. University of Washington, Seattle, WA.

Zanos S, Richardson AG, Shupe L, Miles FP, Fetz EE (2011) The Neurochip-2: an autonomous head-fixed computer for recording and stimulating in freely behaving monkeys. IEEE Trans Neural Syst Rehabil Eng 19:427– 435.

Chapter 3. Novel Cervical Spinal Implant Designs and Tests for Motor Reanimation in Primates

Design and evaluation of a new technique for electrical stimulation of the cervical spinal cord to control hand and arm movement in the nonhuman primate.

3.1 INTRODUCTION

The spinal cord has been a clinical target for accessing the central nervous system since the mid 1960s when Shealy and colleagues first used an implanted pulse generator to stimulate the dorsal columns to alleviate pain based on Wall and Melzack's Gate Theory of Pain. (Shealy 1967, Melzack and Wall 1965). Since then, electrical stimulation has become a tool for a variety of sensory and motor recovery paradigms, and a promising area of exploration whose clinical applications have been limited by technology and methodological difficulty in all animal models, including higher order animals like humans and non-human primates.

EPIDEMIOLOGY

There are more than 282,000 people with spinal cord injury and associated paralysis in the United States (NSCIS 2016). These people face a variety of challenges depending on the anatomical level and severity of their injury. Injuries range from slight compression of the spinal cord in conditions like cervical myelopathy to complete transection of the spinal cord stemming from severe trauma. The range of symptoms these patients face is similarly expansive, from tingling and numbness in the extremities, to incontinence, or even complete loss of motor control, sensory perception, and autonomic function below the level of injury. Patients who have lost function in all four limbs (tetraplegia) report that recovering hand and arm function is more important than regaining walking and leads to the greatest increase in quality of life (French et al. 2010).

Damage to the spinal cord itself can be functionally addressed by restorative methods. Restorative techniques and research into the problem fall mainly in two areas: regenerative, and augmentative. Regenerative techniques in this context include interventions designed to natively regrow and reconnect disconnected spinal areas above and below injuries and include pharmacological and biological approaches. These advances employ small-molecule therapies, and stem cell therapies designed to either enhance native healing mechanisms post-injury or deliver novel neural outgrowth and cellular precursors (Silva, et al. 2014). These therapies are promising and outside the scope of this thesis work. Detailed reviews on stem cell therapies (Vismara, et al.2017), small molecules (Varma, et al. 2013), and combination therapies (Fong, et al. 2009) can be found elsewhere.

Augmentative techniques have focused on restoring motor function using a variety of stimulation techniques targeting various levels of the motor system from muscles to peripheral nerves, and the spinal cord directly. These techniques involve electrically stimulating the motor system in a variety of established methods that induce movement via activating neural tissue either directly or by modulating the excitability of a neuronal population, or activating fibers of passage. These augmentative techniques provide a direct method for reanimating lost function key for improving quality of life for patients.

ANATOMICAL CONSIDERATIONS

The spinal cord is a critical passage carrying vital control information which influences voluntary limb movements as well respiratory, digestive, and bowel functions. Many of the descending tracts present in the cord to handle control of these activities have been highly conserved across vertebrate evolution, including both spinothalamic and spinocerebellar tracts (Watson, et al. 2009). The evolution of fine motor control in humans and non-human primates

has also created evolutionary disparities in relative tract sizes that carry descending fine motor commands (Lemon 2008). The dorsolateral corticospinal tract present in humans and old world monkeys (including macaques used throughout this experiment) is anatomically greater in number of fibers present per tract and lateral placement than in new world monkeys and rats and other small mammals. This anatomical difference is also mirrored electrophysiologically in the amplitude of cortico-motoneuronal EPSPs as well as functionally in the hand dexterity across species (Courtine, et al. 2007). The differences across species here indicate that the scientific community needs to pay attention to appropriate models for human functions, like fine motor control, that do not have appropriate analogs in all preclinical animal models.

ELECTRODE TECHNOLOGY

Current electrode technology is limited in the spinal stimulation field; however technology parallels to cortical electrical stimulation in the BCI field can be drawn. In cortical BCI there is a tradeoff in signal/stimulation output specificity and invasiveness. This has separated cortical modalities into electroencephalography, electrocorticography, and intracortical recording and stimulation. These modalities allow access to most aspects of the brain due to the relatively uniform and shallow anatomy of the brain across animal models. The spinal cord is much more difficult to access both surgically and non-invasively based on its position and asymmetric dorsal-ventral geometry. Therefore, the analogs to cortical stimulation techniques are imperfect. So far the field has adapted EEG technology for non-invasive stimulation, and dorsal-only epidural techniques for pain management in most animal models. Intra-spinal recordings and stimulation are also common in small animal models but become much rarer in a few studies using chronic intra-spinal electrodes in primates (Zimmerman and Jackson 2014, Nishimura, et al. 2013b).

These technologies have seen limited application to primate motor stimulation paradigms and upper extremity motor outputs. Transcutaneous stimulation of the lumbo-sacral cord has shown promise in restoring some volitional motor function in standing, rhythmic activity, and assisted stepping (Grahn, et al. 2017); however results from the cervical cord have not been realized yet. Epidural stimulation offers a seemingly more targeted stimulation by placing electrodes closer to the spinal cord. Commercially available spinal stimulation electrodes come in two configurations, paddle, and longitudinal (Figure 3.3.0). Both are designed with pain management in mind and neither is optimized for motor outputs in large animal models. Epidural stimulation has shown great promise in pain management (Bendersky, et al. 2014) but has failed to provide the electrode coverage required to provide therapeutic motor recovery at the cervical level in patients with Parkinson's Disease (Thevathasan, et al. 2010). Earlier work in rodents did produce reliable motor recovery in a Parkinson's Model, indicating that differences in electrode technology may play a key factor in efficacy (Fuentes, et al. 2009), especially considering that epidural cervical stimulation has been able to reduce spasticity due to spinal cord injury in humans (Barola, et al. 1995).

Figure 3.3.0. Boston Scientific Spinal Cord Lead Portfolio. Current lead designs include paddles (left) and longitudinal electrodes with varying electrode density and size. (Boston Scientific, Marlborough, MA)

Over the past decade intraspinal stimulation has been explored as a technique to bring more targeted control to the upper limb. These studies have been carried out with high impedance microwire electrodes mostly made by hand. Moritz et al (2007) conducted a seminal mapping study throughout the cervical region of the sedated primate cord and showed that the outputs

from intraspinal stimulation sites do not follow clean, distinct somatotopic organization within the cord, and can elicit several simultaneous muscle activations. Follow-up work showed that the movements from intraspinal stimulation were synergistic, and realistic reaching and grasping behaviors could be recreated using only two stimulation sites (Zimmerman, et al. 2011), selected from many tested sites. This stimulation paradigm has also been used to demonstrate restorative possibility (Mushahwar and Horch, 2000) and explore fundamental neural principles in the corticospinal pathway (Jankowska and Edgely, 2006). Evidence of spike-timing dependent plasticity mechanisms in corticospinal motor pathways has been seen in experiments coupling cortical neural activity to intraspinal stimulation in freely behaving animals (Nishimura, et al. 2013a). Additional work showed an awake animal with a spinal cord injury could learn to control spinal stimulation via both cortical activity and remaining muscle activity to perform a torque tracking task (Nishimura, et al. 2013b). Animals with a temporary disruption to the cortico-spinal path are able to control intraspinal stimulation using unaffected cortical signals to accomplish complex reaching and grasping behaviors as well (Zimmerman and Jackson 2014).

In a comparison of epidural, subdural, and intraspinal stimulation from a variety of locations along the cord Sharpe 2014 tested an acute, sedated primate preparation with limited ventral spinal cord stimulation using large silver ball electrodes. The resulting low stimulation thresholds and varied motor outputs showed that the ventral cord could be an interesting target for further study. Of all the previous work only two studies of note have managed to maintain intraspinal electrodes in the primate spinal cord for chronic applications (Nishimura, et al. 2013b, Zimmerman and Jackson 2014).

RATIONALE

Early stimulation experiments provide significant evidence and hope for reanimation applications in higher-order animals; however very few restorative stimulation paradigms have been actualized in humans and non-human primates thus far. One of the challenges, as highlighted by the comparative lack of human and NHP studies, is the lack of suitable long-term targeted stimulation paradigms. Personal communications with researchers using spinal stimulation in primates highlighted the difficulty of obtaining stable, long-term recordings and stimulation paradigms for use in non-human primates and a recent review by Giszter (2015) highlights the challenges facing long-term motor recovery at the spinal cord:

> *"Data in spinal cord of primate from Nishimura (2013b) and in cat from Mushahwar. (2000) suggest that current electrodes cannot exceed about 3 month survival times in spinal implantations. The ideal type and design of electrode to record and stimulate spinal cord for long-term neuroprostheses use remains an unsolved problem."*

From a translational research perspective, the lack of a safe, long term electrode paradigm for specific motor stimulation in primates has limited the ability of the clinical community to provide restorative therapies for patients suffering from all varieties and severities of spinal cord injury. This lack of options prompts the need for designing new approaches to accessing the spinal column for a variety of restorative procedures in primates.

3.2 System Summary and Design Principles

In this engineered system we describe a series of electrode designs and surgical approaches that aim to improve functionality of augmentative spinal stimulation techniques by accessing the circumference of the spinal cord for targeted electrical stimulation. The working hypothesis that the ventral aspect of the spinal cord offers unique access to motor pools, ventral spinal roots, and fibers of passage that may be amenable to fine motor control paradigms based on the stimulation

results previously seen with intraspinal stimulation was explored in three iterations. Mechanical considerations of microelectrodes and the rostral-caudal movement of the spinal cord in the spinal column (Danner, et al. 2016) affect the robustness of long-term implanted electrodes. The goal of the platform is an ECoG-like surface electrode paradigm that can be used to access the entire circumference of the spinal cord at any spinal segment in the primate to allow for the most versatile therapeutic outputs. Based on a seminal mapping by Moritz et al. (2007), we focus work on the cervical spinal cord where the anatomy is fairly uniform and stimulation is known to produce a variety of hand and arm movements that are highly relevant to the patient goals of independence and motor function recovery (Anderson, et al. 2004).

3.3 Design 1.0

The first design of our novel spinal stimulation system was created for acute testing of surgical protocols and motor responses to stimulation under sedation in a proof-of-concept setting in nonhuman primates. The original design was based on the hypothesis that flexible electrode technology could be used to fit into the subdural space surrounding the spinal cord and stimulate neural tissue to elicit robust motor activity without penetrating electrodes. Figure 3.3.1 shows an idealized version of the electrode system overlaid on a fixed spinal cord, highlighting the unique stimulation combinations provided by novel electrode placement. We hoped to directly stimulate ventral motor pools and fibers of passage projecting to motor control areas of the cervical spine.

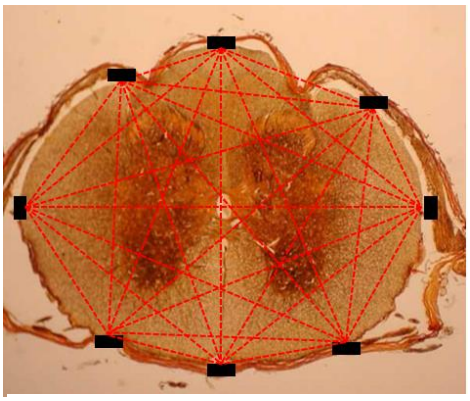

Figure 3.3.1. Cross section of spinal cord with theoretical electrode placement (black) possible bipolar current stimulation paths (red).

3.3.A Design

There were several key factors in the original design of the subdural spinal array. Length, width, and radius of curvature all had to be matched to the specific anatomy of the animals undergoing surgery to ensure that the array would fit around the cord without damaging the dorsal or ventral roots. The manufacturing design and electrode materials are based on flexible electrode fabrication techniques adapted from microfluidic fabrication techniques. Schematics for the electrodes were created to scale in Adobe Illustrator (Adobe Systems, San Jose, CA) and sent to a contract manufacturer for fabrication (CorTec Neuro, GmbH, Freiburg, Germany). CorTec used the design schematics to manufacture a multilayer electrode array using proprietary bonding techniques. The array has a poly-dimethyl-siloxane (PDMS) base layer that was chemically treated to bond a metal base layer using photolithographic techniques. The metallic base layer then was treated to be able to hold platinum traces containing the flexible electrode leads and electrode contact pads. The traces were designed as alternating zig zags to allow movement and flexion of the array without breaking the continuity of the electrode connections in the array. Another layer of PDMS was deposited on top of the leads and cured, creating an electrically-insulated flexible electrode array. The features and final shape of the array was then exposed by laser cutting the outline of the array, through-holes, and electrode contacts from the PDMS. A catheter containing insulated guide wires was attached to the electrode leads on one end and a labeled connector on the other to allow connection of the electrode array to the

recording and stimulation hardware used in the experiments. Figure 3.3.2 shows the final seven-electrode array, catheter, and dimensions used for testing Design 1.0.

3.3.A.1 Physical Constraints

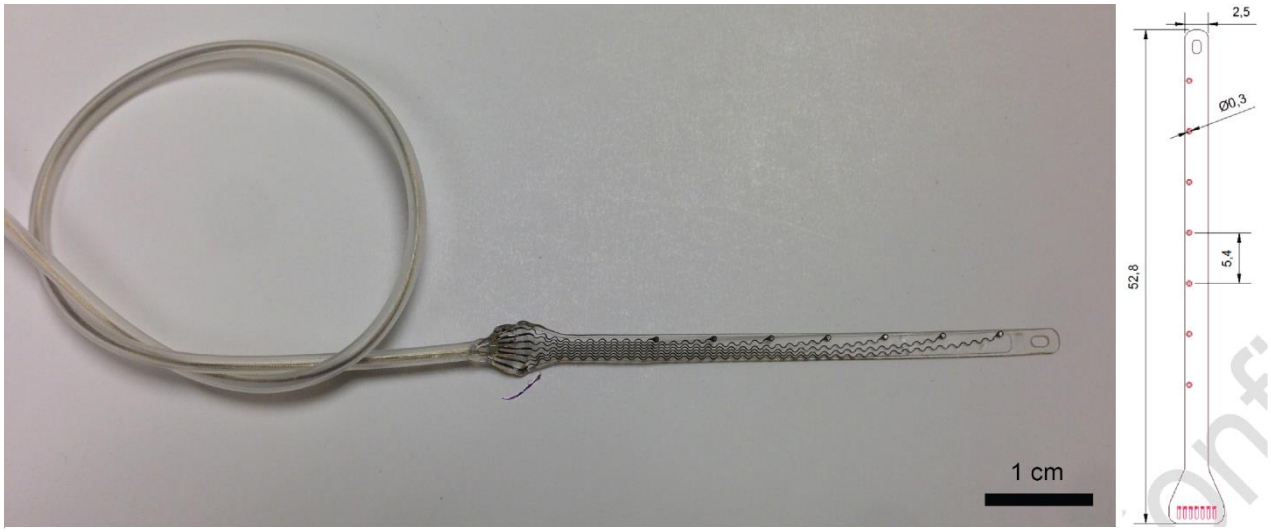

Figure 3.3.2. Custom Cor Tec array fabricated for encircling the spinal cord in the cervical enlargement. The flexible array has seven 300µm platinum/iridium contacts encased in silicon rubber (PDMS) for flexibility and strength. These electrodes arose from discussions at the 2013 CSNE Microelectrode Conference.

There are several factors at play in designing for the spinal cord that were considered during the design process. The factors fell into two areas of concern, the sizing of the array and the curvature needed to wrap the small primate spinal cord. Based on previous experience, it was estimated that ~1.5mm of subdural space exists surrounding the spinal cord, making the depth the least important factor as compared to length and width. The length of the array was based on historical data from imaging and skeleton reconstructions. We modeled the spinal cord as an ellipse with major and minor axes of 0.7 and 0.5 cm respectively to arrive at an approximate circumference of 3.8cm using Ramanujan's approximation:

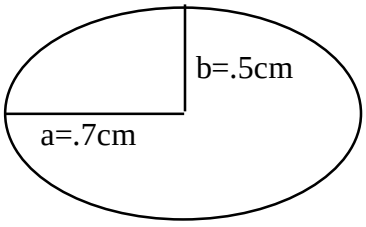

$$p \approx \pi[3(a+b) - \sqrt{(3a+b)(a+3b)}]$$

We then added a 0.3cm tag to the end of the array design with a hole that could be used to fix the array in place with small suture during the surgical process and subsequent experiment.

3.3.A.2 Electrode Constraints

For ongoing recording and stimulation of the spinal cord an electrode array must also be durable through both recording and stimulation. An early attempt at using parylene-C microelectrodes with gold traces and platinum/iridium showed delamination and electrode failure at currents above 0.5mA. Electrodes used for stimulation and recording in the central nervous system must have higher current thresholds to evoke motor outputs and the ability to maintain higher currents (>1.0mA) throughout the healing, scarring, and chronic use. 90/10 Platinum/Iridium was chosen for all future electrodes with the goal of also designing for future safety with modern MRI imaging techniques (D'Andrea, et al. 2014). Target impedance was 100 kΩ as a goal to balance between low-impedance stimulation and hardware requirements and high-impedance electrode recording goals. Before implantation the impedance of each trace was measured on the arrays. Trace impedance was measured at 1 kHz using an IMP-2A Metal Electrode Impedance Tester (Bak Electronics, Inc. Umatilla FL). Trace impedance was 107 ±38 kΩ.

3.3.B Surgical Protocol

All protocols were approved by the University of Washington Institutional Animal Care and Use Committee. Both animals used in this experiment were adult female *Macaca nemestrina* from the Washington National Primate Research Center colony tissue program weighing 7.0 and

7.4 kg. The surgical protocol for both animals was identical. Animals were sedated using ketamine and maintained under isoflurane anesthesia by WANPRC anesthesiology staff throughout the experiment. Experiments lasted the maximum three hours including surgery and electrophysiology, limiting the complexity of stimulation and recording paradigms possible.

Animals were positioned prone in a stereotaxic frame using earbar, mouth roof, and orbit stabilization. We targeted cervical segments C5/6/7 in the first animal and C7/8/T1 in the second animal to understand the spectrum of motor outputs from hand-related cervical spinal cord. The area from C2-T2 was identified using palpation, overlying hair was shaved, and the area was sterilized using surgical antiseptic. A stepwise illustration of the surgical protocol is found in Figure 3.3.3.

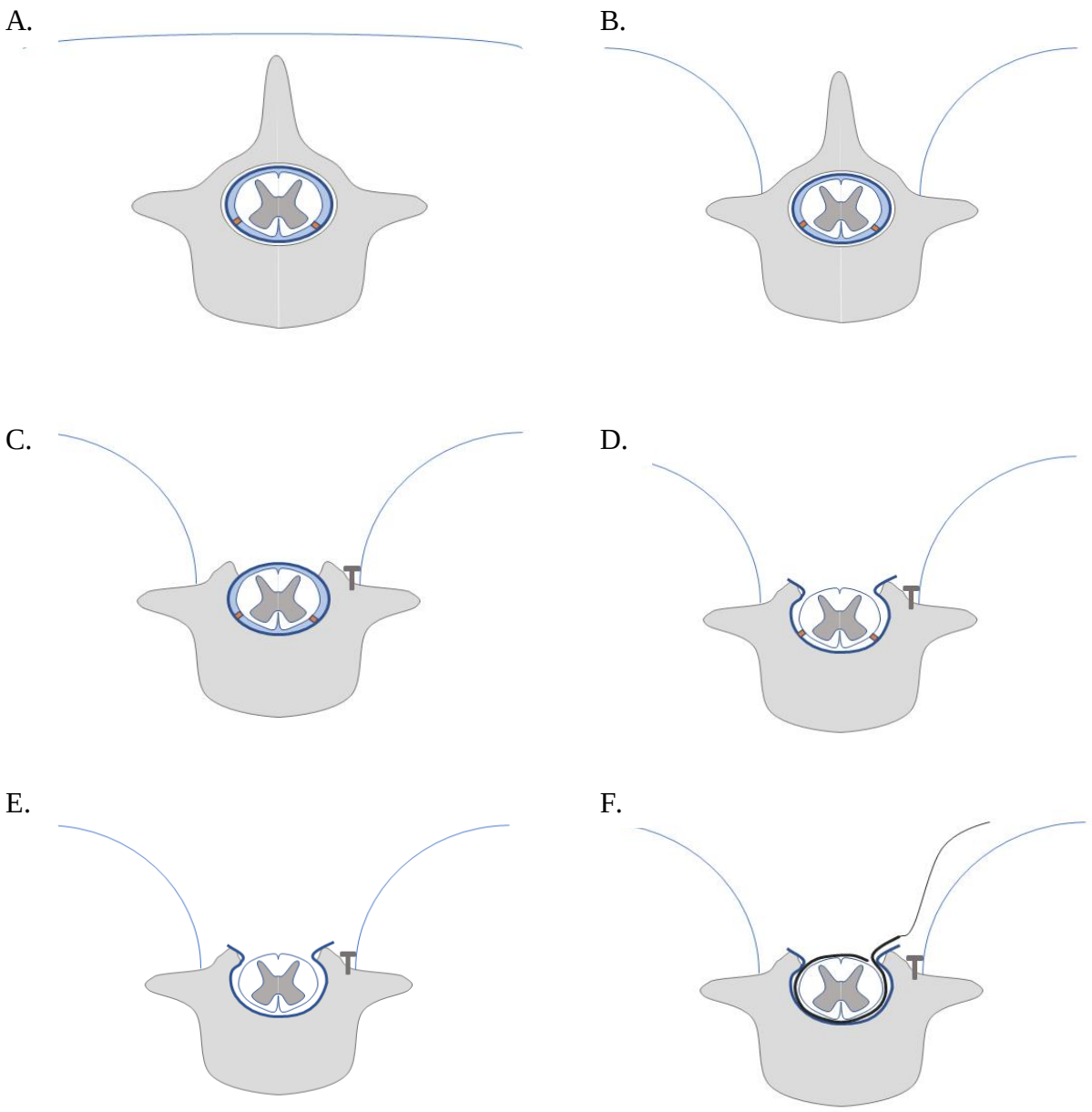

Figure 3.3.3. Cross Section Illustration of Surgical Protocol for Array Design 1.0 outlined in 3.3.B. **A**. The animals were positioned prone on the operating table. **B**. A midline incision exposed dorsal aspect of the target vertebrae. **C.** The dorsal process was removed exposing the dura (dark blue), underlying CSF (light blue), and a ground screw was placed. **D.** The dura was opened and retracted at midline. **E.** The dentate ligament (orange) was cut bilaterally. **F.** The flexible array (black) was inserted under the cord in the subdural space and pushed around the cord. The tag end of the array was loosely sutured to the dura on the insertion side to hold the array in contact with cord throughout the experiment.

We visually identified the muscular midline and used the electro-cautery surgical knife

(Bovie Specialist Pro, Bovie Medical Corporation, Purchase NY) to dissect down to the tips of

the spinal processes of the target vertebrae (C5/6/7 and C7/8/T1 in respective animals). The Bovie tip was swapped from a standard blade electrode to a small ball tip for fine dissection down the lateral masses of the vertebrae. Bovie current was lowered to avoid currents activating the spinal cord during surgery. The dorsal aspect of the target vertebrae were exposed to the lamina and articular processes bilaterally. Rongeurs and a Kerrison punch were used to remove the dorsal process and both laminae, exposing the dura. Electrical ground screws were pre-drilled and inserted into the lateral mass of target vertebrae using the angled method described by Perlmutter, et al. (1998). The dura was pierced and opened along the midline one segment anterior and posterior to target segments. Using blunt instruments the spinal cord was slowly pushed to the side between target segments to expose the dentate ligament on the ventrolateral aspect of the cord. The dentate ligament was cut, freeing the ventral cord from the dura and the process was repeated for the other side.

The array was passed under the cord on one side at the desired segment, between dorsal and ventral root pairs. The cord was gently moved aside again so the array could be grabbed with forceps and pulled entirely around the spinal cord. The array was finally secured in place using 6-0 sutures to connect the tag end of the array to the dura. The entire process was repeated for the second array at the neighboring segment. Ground wires were secured around the ground screws previously placed to complete the surgical process. Only 4 of the 7 electrodes were in contact with the cord at each segment. The dura was left open for the duration of the experiment and moisture was maintained periodically with surgical saline solution. Animals were sacrificed by WANPRC staff at the conclusion of the experiment. Two arrays were placed in each animal in adjacent spinal segments.

3.3.C Experimental Methods

Once electrodes were implanted, we used the remaining surgical time to stimulate as many combinations of electrode pairs as possible and observe motor responses in the surgical suite. Stimulation was delivered as short trains, using 3 constant-current pulses (anodal first square waves 200us per phase) at 300Hz, delivered at 0.5 Hz intervals (STG4008, Multichannel Systems, Reutlingen Germany) between pairs of electrodes (bipolar) or an electrode and the distant ground screw (unipolar). The amplitude of the stimulation began with 250μA and was manually adjusted in 250 μA increments on the fly with a maximum stimulus of 2.0mA. An audible tone was played at stimulation onset to help identify timing of motor responses. The non-stimulated channels were connected to a recording amplifier (g-USB Amplifier, Guger Technologies, Graz Austria) controlled by a custom-written software GUI (Matlab, Mathworks, Natick MA). Neural signals and stimulation triggers were sampled at 4800Hz and saved to file for offline analysis. Line noise was considerable in the surgical suite and only a few representative traces were captured when surgical heating equipment was briefly turned off.

Motor responses were monitored by visual inspection alongside the auditory cue and categorized by arm. Specific muscles were not identifiable, but the movements were categorized into finger (including thumb), forearm (including wrist), and proximal. Movements were also graded coarsely on size, from no response through twitch, and large movement as determined by observing personnel. There was insufficient time during the procedure for a detailed exploration of motor thresholds.

3.3.D Stimulation Results

Motor responses were evoked from the vast majority of electrodes around the cord. Most notably, all 4 ventral electrodes produced bilateral movements. We covered four spinal segments in two animals (C5-T1) and 14/16 electrodes produced motor outputs at from the stimulation sites and all 10 bipolar pairs tested produced motor outputs. Summary results are shown in Figure 3.3.4. Midline dorsal and ventral electrodes produced predominantly bilateral movements while the seven of eight lateral electrodes produced ipsilateral movement. One lateral site unexpectedly produced contralateral movement in the opposite forearm. Of the bipolar stimulation sites 87% (27/31 movements) were subsets of movements evoked at either unipolar site. In four cases the bipolar stimulation added unique movements not found at either stimulation site.

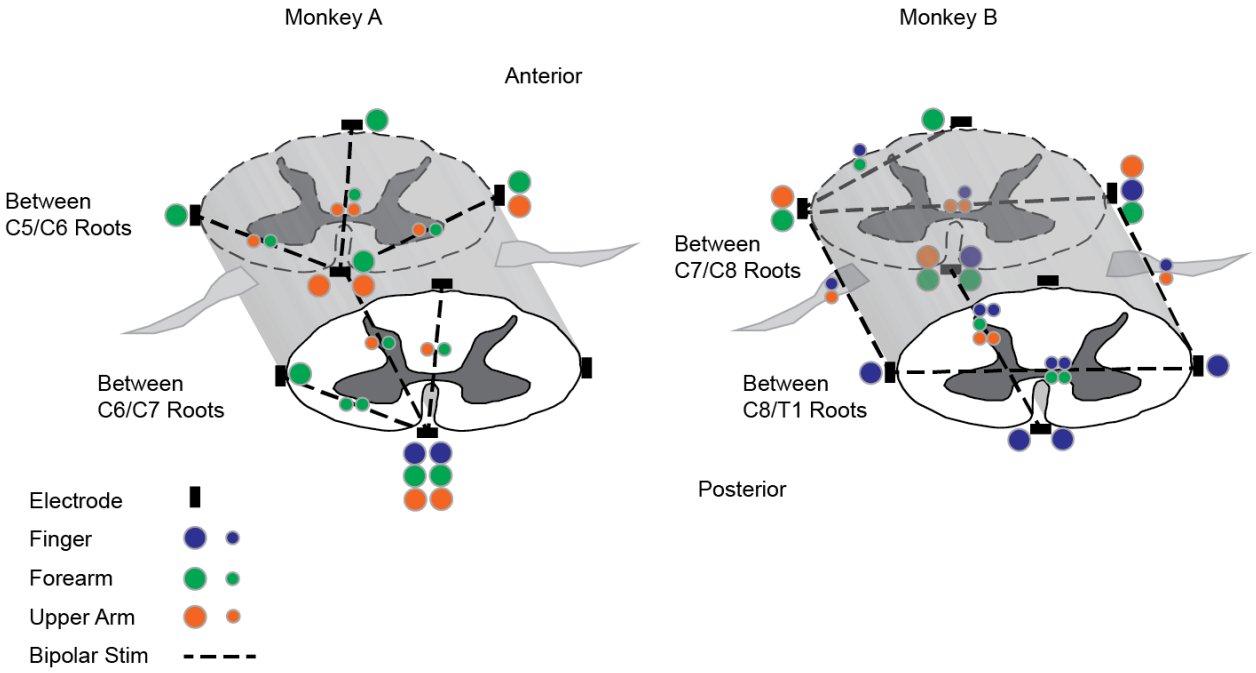

Figure 3.3.4. Summary of movements evoked by spinal stimulation. Bipolar stimulation (dashed lines) generally yielded a subset of the motor outputs from the corresponding unipolar stimulation sites (black symbols). Laterality of movements is indicated by position of the marker relative to the stimulation symbol and size of the symbol corresponds to the relative strength of the movement.

The movements evoked by stimulation of the spinal cord were very naturalistic grossly somatotopically organized by spinal segment. Figure 3.3.5 shows gross categorical somatotopy. While not documented explicitly, the movements encompassed all aspects of arm and hand movement necessary to encompass functional reanimation. We observed synergistic reaching, and grasping movements consistent with intraspinal stimulation results grossly organized by spinal segment (Moritz, et al. 2007, Sharpe and Jackson 2014). We also observed activation of flexor and extensor muscle groups moving the forearm about the elbow as well as the hand about the wrist. Finger movements observed included thumb and forefinger opposition and finger flexion. Finger extension was not observed.

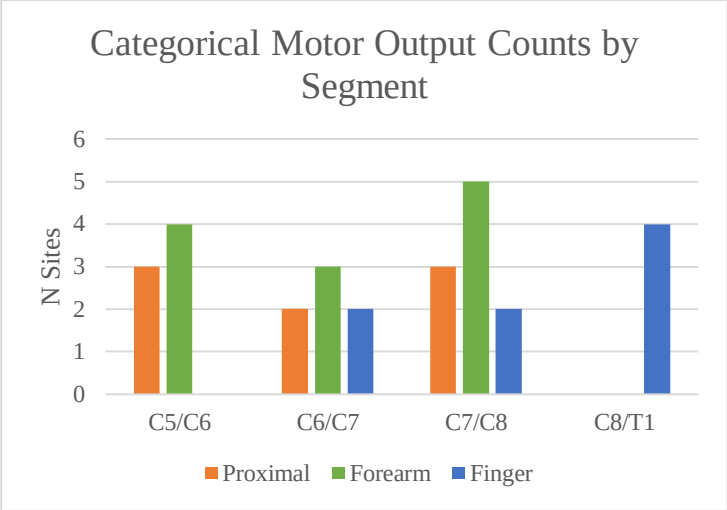

Figure 3.3.5. Summary of the gross somatotopic organization of motor outputs in two animals from unipolar stimulation. Consistent with previous mapping the proximal outputs were seen anterior to distal outputs

The stimulation test current of 250µA was able to elicit movement in 23 of 28 unipolar and bipolar stimulation sites. Three of 28 sites tested required 500uA stimulation, and two sites produced no movement up to 2.0mA.

Electrophysiological recordings were limited due to line noise in the surgical theater. We were able to make one set of recordings in Monkey A with surgical equipment briefly disconnected. Example evoked potentials are shown in Figure 3.3.6. Bipolar stimulation trains (n=25) across the anterior spinal cord produced several spinal evoked potentials when visualized post-hoc and showed electrophysiological phenomena at short (>10ms) latencies likely caused

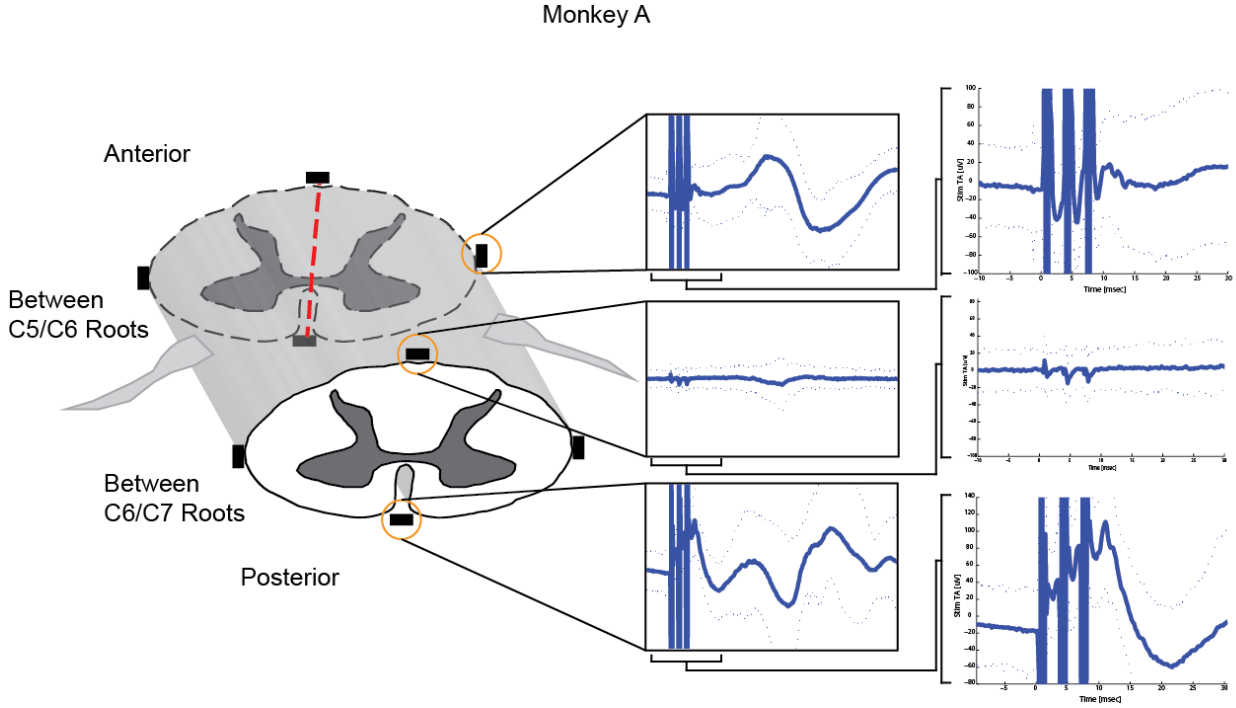

Figure 3.3.6. Example spinal evoked potentials in response to bipolar surface spinal stimulation across Spinal Segment C6. Red line connects electrodes for bipolar stimulation. Insets show stimulation-triggered averages recorded from non-stimulated sites (mean +/- 2 standard deviations, n=25 stimulations). Long timescale responses are shown first with insets to highlight short-latency phenomena.

by direct activation of underlying fibers, as well as longer latencies (>30ms). One ventral site showed evidence of temporal summation in response to train stimulation, potentially indicating that the response comprised aspects of both direct fiber activation as well as trans-synaptic contributions. The amplitudes and thresholds of the evoked potentials were likely lower and higher, respectively than would be expected in an awake animal. Isoflurane anesthesia is known

to reduce excitability, as evidenced by reduced motor evoked potentials as well as ascending F-wave potentials converging on the cervical spinal cord in humans (Zhou and Zhu 2000).

3.3.E Design Feedback

The initial results from Design 1.0 were very promising. Short stimulation trains delivered to the spinal cord surface on the dorsal, ventral, and lateral subdural aspects of the spinal cord produced motor outputs with general somatotopy covering the range of movements necessary for functional reanimation. The data were consistent in two animals. Early electrophysiology showed that electrical potentials could be recorded from the surface of the cord in response to electrical stimulation, validating choices in material design, electrode impedance targets, and stimulation currents.

The main issue for optimization for future iterations was the size and shape of the electrodes. The array was too long to properly fit around the cord. Several electrodes did not contact the cord and were unusable for stimulation. Future generations adapted electrode spacing and array length. Additionally, the geometry of the array led to connector leads running out the back of the animal perpendicular to the cord which is not optimal for chronic implantation and accommodating spinal cord translation within the column. Future revisions adjusted the sizing and spacing of the electrodes to target the leads at the ventral aspect of the cord.

3.4 DESIGN 2.0

Design 2.0 was built to evaluate chronic implantation of the electrode. The chronic experiments carry a much greater risk of adverse effects and so we selected animals that had completed other experiments and had existing cortical hardware. Using these animals expanded

the experimental goals of characterizing not only the spinal longevity and motor outputs, but also expanding to explore cortico-spinal connections.

3.4.A Design

Array 2.0 was designed to improve on the number and variety of motor outputs seen in design 1.0 with additional features to accommodate chronic implantation. The overall layout was rotated by 90 degrees so that the leads exiting the array would run parallel to the axis of the spinal cord and reduce the torque present at the implant site while directing leads towards the animal's preexisting cortical electrode connection hardware (Figure 3.4.1). Additional strain relief was incorporated along the axis of the spinal cord through the use of z-bends made with silastic attachments to accommodate movement of the spinal column within the spinal cord. The width of the array in the rostral-caudal dimension (circumferentially wrapping the cord) was

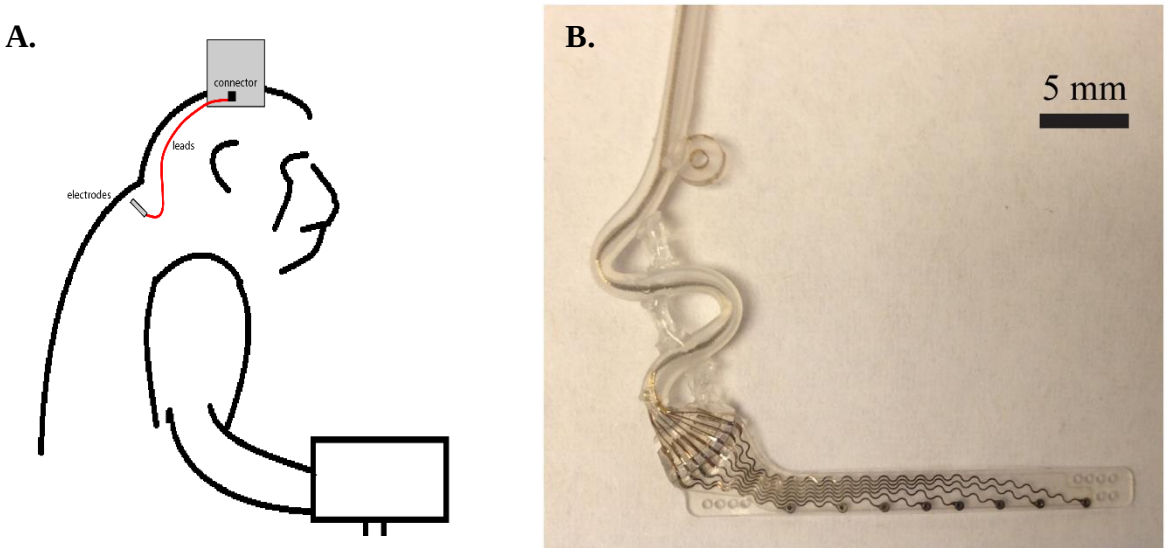

Figure 3.4.1. Overview of Array Design 2.0. A. Schematic of spinal implant electrical routing for array. Electrodes implanted around the spinal cord have leads routed to head caps from previous procedures that can safely house connectors, recording and stimulation hardware, and batteries. **B.** Photograph of Design 2.0. Key features include the 90º turn for leads to improve routing, updated anchor points on the catheter, stress relief in the early catheter, and a variable tie-down pattern of holes for securing around the cord.

reduced to 2.4 mm better fit between dorsal and ventral roots segmentally exiting the cord. In response to array 1.0's oversize length the array was shortened and an adjustable attachment system was implemented using a series of small holes that provided ~5mm of flexibility when attaching the array around the cord. To accommodate the smaller array the eight electrodes were placed closer together to maximize circumferential contact with the cord. Finally a vertebral attachment point was added to the catheter 1.5cm rostral to both the array and the axial strain relief features so the array could be secured to the bone on the dorsal aspect of the cord and prevent significant rotation around the axis of the spinal cord while maintaining rostral-caudal flexibility.

3.4.B Surgical Protocol

The surgical protocol for Design 2.0 was similar to Design 1.0 with additional techniques used for more gently wrapping the array around the spinal cord and rebuilding the mechanical

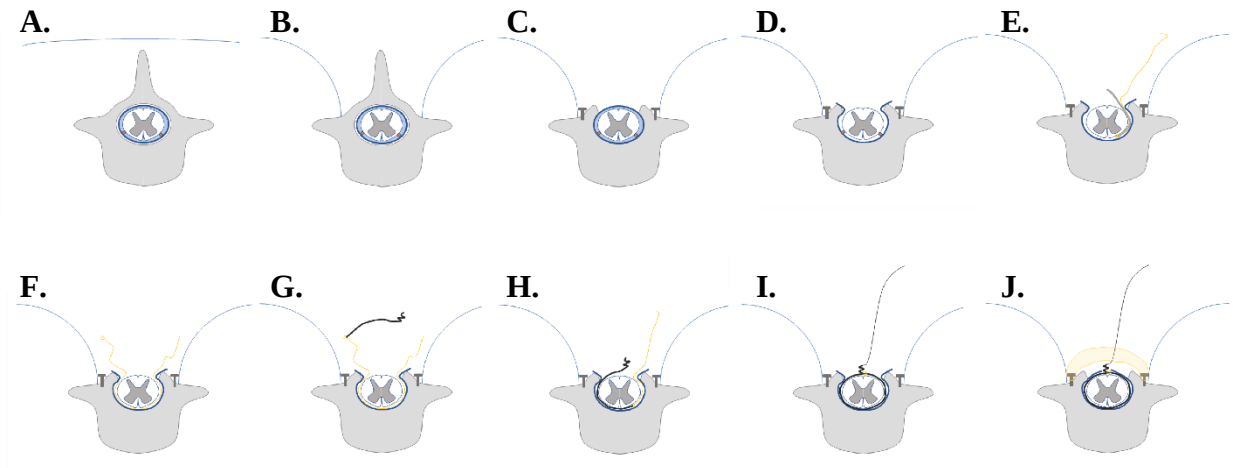

Figure 3.4.2. Design 2.0 Surgical methods. A-D. Bilateral laminectomy as described in 3.3.B **E-F.** A small metal tool (grey) was used to pass suture (yellow) under the spinal cord and tie to the array. **G-H.** The array was gently pulled back around the cord. **I.** The array is fastened to itself using the adjustable fastener holes. **J.** The dorsal aspect of the cord is covered in a layer of gelfoam and covered in acrylic anchored to lateral mass screws.

stability of the cord post-implant. The protocol is outlined in Figure 3.4.2. Steps A-D are the same as detailed in section 3.3.B. A custom spatula tool was fashioned to help pass the arrays under the spinal cord without disturbing the dorsal and ventral roots. Once the spinal cord was separated from the dura and dentate ligaments at the section of interest a 1.5 x 60x.02 mm section of 301 Half Hard stainless steel was bent to match the curvature of the spinal cord during surgery (Figure 3.4.3). A small hole was punched into the end of the thin metal strip and suture

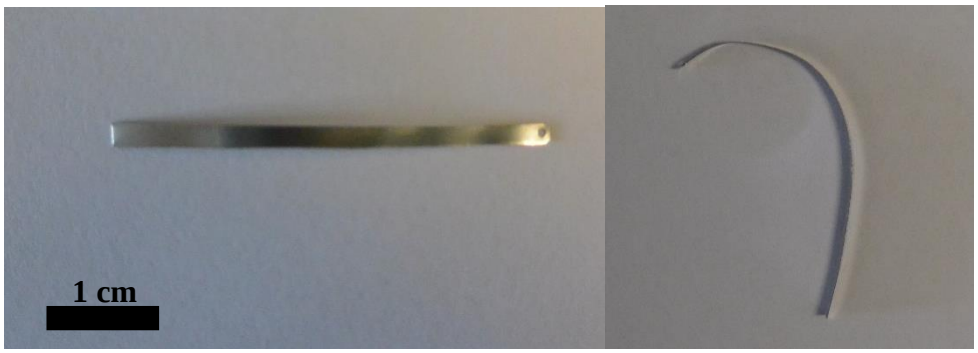

Figure 3.4.3. Custom Array Insertion Tool. A. Front view. **B.** Side View.

lightly tied to the hole. The metal provided enough mechanical strength to pass under the spinal cord. The suture was pulled under the cord, removed from the tool, and the tool was removed from under the spinal cord. The suture was then tied onto the array and used to gently pull the electrode lead end of the array around the spinal cord. The array leads were positioned along the central axis of the cord (Figure 3.4.4) and secured in place. The dura was closed with 5-0 suture, gel foam was placed over the incision, and a dam of acrylic was used to cover the missing dorsal

process space of the exposed segments. The animals were allowed to recover and monitored for signs of discomfort.

3.4.C Experimental Methods

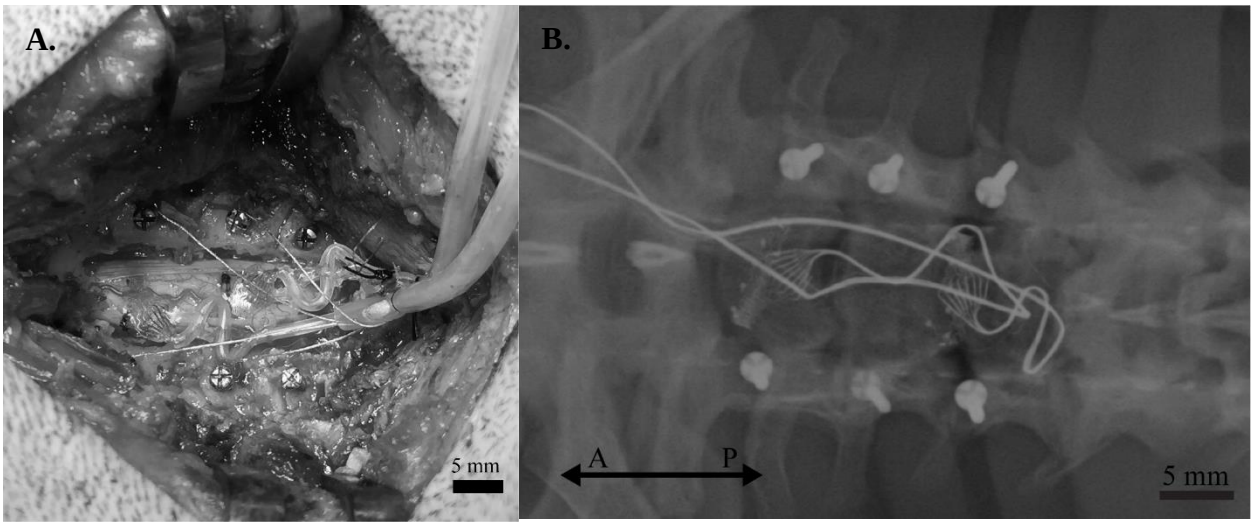

Figure 3.4.4. Post Implantation Position Verification. A. Photograph of electrodes implanted in Animal V. Full laminectomy of vertebrae C5-C7 is visible over electrodes. Bilateral anchoring and electrical ground screws are visible before the acrylic cap is created. **B.** Radiograph of electrodes implanted in Animal T. A-P indicates anterior and posterior of animal. Full laminectomy of vertebrae C5-C7 is visible over electrodes. Bilateral anchoring and electrical ground screws are visible as well. Electrodes are wrapped around the spinal cord in the subdural space. Electrode leads are given slack (posterior side) before being routed up to the head-mounted can for housing connectors to allow translation of the array during normal animal movement.

We conducted tests of 6 electrode arrays, (48 electrodes) in three animals (Monkey O, V, and T) to determine whether Array 2.0 was a suitable platform for producing long term motor outputs in a chronic primate model. Animals were managed by WANPRC veterinary staff between experiment sessions. The animal history, implant locations, and type of motor data collected are listed in Table 3.4.1. We discovered post-mortem that the C5 array in Monkey O was installed in reverse at the C5 segment with the electrode leads facing away from the surface of the cord and insulated from direct contact. The mis-positioned array was tested with the same measures as the

rest of the arrays; however the data from the C5 array is included in the qualitative movement analysis but excluded from the quantitative stimulation threshold analysis as results were significantly greater than all other arrays. In Monkey T an array was implanted at C7 successfully, but the implanted leads running to the animal's head for the array were destroyed shortly after implantation and before any data could be collected. It is excluded from all analyses.

Qualitative movements were noted by visual inspection to an approximate muscle group or movement (i.e. bicep, or wrist flexion), and then bucketed into categories of trunk, proximal (movements about the elbow and shoulder), and distal (finger, thumb, and wrist movements).

Table 3.4.1. Summary of Array 2.0 Implant Durations.

Animal	**Implant Location**	**Total Sessions**	**Motor Output Data Type**	**Medical History**
Monkey T	C5,C7(connector failed)	3	Visual Inspection, EMG	MRSA
Monkey V	C5,C7	1	Visual Inspection	MRSA
Monkey O	C5(incorrectly positioned),C7	5	Visual Inspection,	Cortical Implant Failure, MRSA

For experiments animals were sedated using 10mg/kg ketamine and transported to the lab space. Body temperature was maintained using a circulating warm water pad. Animals were given additional doses of ketamine if their movements became disruptive during data collection, typically after ~1 hour of experimentation time. Experiments lasted less than two hours. Animals were returned to their home cage and monitored for recovery at the conclusion of the experiment.

Stimulation was delivered on multiple days through a Ripple Grapevine Neural Interface Processor unit with a stimulating Micro+Stim headstage (Ripple Systems, Salt Lake City, UT). As in previous designs, stimulation was delivered as a single biphasic pulse (anodal first, 200us/phase, at 1Hz) ramp (n~=25) as described in Chapter 2 with currents ranging from 100-700µA delivered between a target electrode and a distant ground screw anchored to the lateral

mass of a vertebrae. Consistent with previous experiments we categorized threshold as the intensity at which a movement was observed in 100% of the stimulations. These movements could occur in a single muscle (i.e. bicep), a coordinated movement (wrist flexion, where it was difficult to assign an individual muscle), or simultaneous, wherein more than one movement/muscle was observed at a current threshold. We also observed additional supra-threshold movements that occurred when stimulation exceeded threshold and additional groups were activated. In one experiment, wire EMG electrodes were temporarily implanted in four muscles of the distal and proximal arm (biceps, triceps, flexor carpi ulnaris (FCU), and extensor carpi ulnaris (ECU)) using a needle and wire technique and correct placement in the target muscles was verified via trains of low-intensity stimulation. Wires were routed to the headstage for simultaneous recording. Signals were digitized at 30kHz and stored. Post hoc signals were downsampled to 2kHz and high pass filtered over .1 Hz to remove baselines before averaging and rectifying and calculating stimulation triggered averages using data from -25 to +250ms surrounding a stimulation.

3.4.D Results

Evoked Movements

We tested 40 electrodes for evoked movements across three animals and two spinal segments. Unipolar surface stimulation to a distant ground evoked ipsilateral movements at 65.0% of the 40 sites tested. Distal movements occurred in 35.0% of sites, proximal

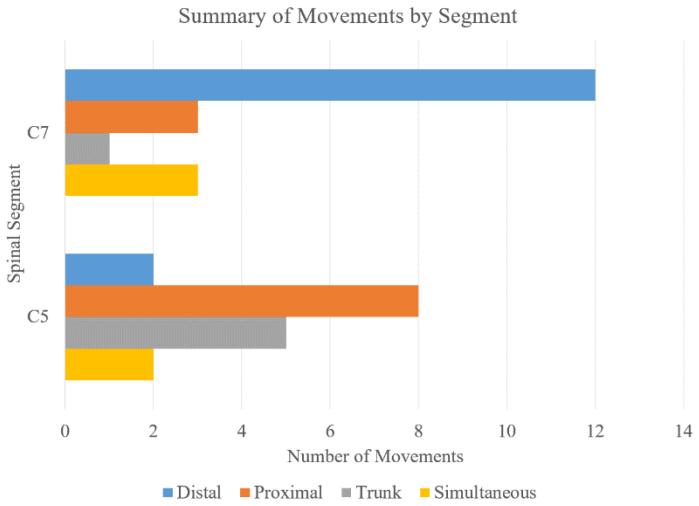

Figure 3.4.5. Categorical Responses by Segment. C5 and C7 electrode arrays exhibited segmentation of responses where C5 elicited more proximal and trunk movements whereas C7 elicited more distal movements across three animals.

movements in 27.5% of sites, and trunk movement in 15.0% of sites. For 13.0% of sites simultaneous movements occurred across multiple movements/muscle groups. The breakdown of C5 and C7 distal, proximal, trunk and simultaneous movements are presented in Figure 3.4.5. We see fairly clearly that there is more proximal and trunk movement from the C5 electrodes compared to the C7, and C7 is weighted towards distal movement. Simultaneous movements were comparable at the two segments.

The stimulation threshold was for eliciting movement was 298 ±177.9µA (The misplaced C5 array not included in the current analyses produced movements at 4 electrodes the threshold was 725±170.8µA) across all sites, which is higher than stimulation currents required for intraspinal microstimulation (Moritz, et al. 2007). We also wanted to understand any circumferential effects electrode position had on threshold. We took the previous mathematical ellipse model described in Section 3.3.1.A and matched the physical dimensions of the manufactured array and electrode

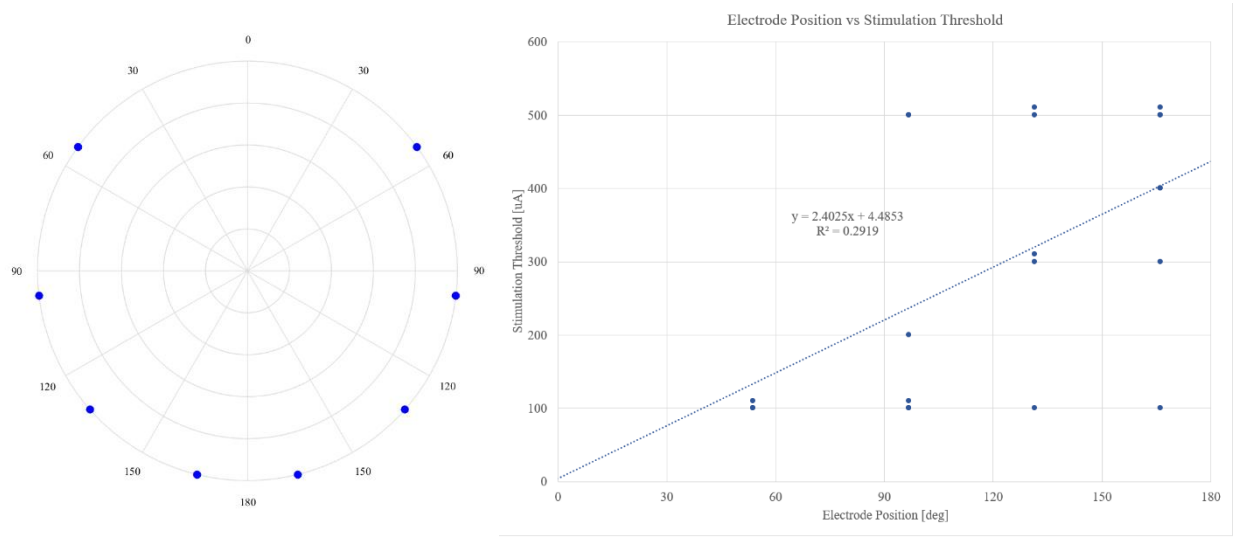

Figure 3.4.6. Circumferential Stimulation Thresholds. A. A circular model of implanted electrodes around the cord **B**. The stimulation response as a function of electrode position shows a trend towards higher ventral thresholds compared to dorsolateral responses.

locations to the perimeter of the ellipse model. From there we normalized back to a circle to compare stimulation threshold by electrode along the dorso-ventral axis as seen in Figure 3.4.6.A

We then collapsed the electrode position along the vertical axis to obtain the comparison of radial electrode position to stimulation intensity seen in Figure 3.4.6.B. Overlapping datapoints due to threshold symmetry were maintained during analysis but separated for visual clarity in the figure. Interestingly we see a slight trend towards higher thresholds at the ventral aspect of the cord for unipolar stimulation.

In addition to unipolar stimulation to a distant ground we also tested bipolar stimulation paradigm across electrodes within an array following the same stimulation ramp protocol. We tested a C7 array in all possible combinations with stimulation up to 700μA. The data are summarized as threshold movement + suprathreshold movements color coded alongside their numerical value in Table 3.4.1. Of note we see that the summary matrix is not symmetrical along the diagonal, indicating there are potentially anodal and cathodal factors of stimulation that affect or change the exact pathway by which movements are evoked. This presentation of C7 data also highlights the great variety of responses present during bipolar stimulation. It has been hypothesized and explored in spinal stimulation EMG data (Sharpe and Jackson 2014) that temporally separated, paired stimulation delivered to two sites generate motor outputs that sum linearly in time. In that framework some data was collected at 0 ms delays from dorsal and ventral paired stimulation. For Sharpe it appeared to trend that responses to paired dorsal stimulation remained a linear combination while a ventral paired stimulation displayed nonlinear behavior. Our dataset allows us to explore these combinations in depth as depicted in Figure 3.4.7. We first broadly categorized movements into flexions or extensions at the distal (hand, wrist, finger) or proximal (bicep and tricep) levels. Using the unipolar stimulation data as a reference we built out the theoretical linear combination hypothesis map. We then compared the data to the hypothetical linear combination and counted both addition (movements that actually

occurred but weren't predicted) and subtraction errors (movements that were expected to occur but didn't). We could then tally the total number of errors as a measure of deviation from linearity. We found that the superposition principle that was touted for combinational EMG did not hold well at the categorical level. We found only 23.21% of sites were correctly predicted with 59 total errors (in a space of 56 bipolar combination pairs).

Table 3.4.1. Array Design 2.0 Monkey O C7 Bipolar Stimulation Summary

Cathode / Anode	E1	E2	E3	E4	E5	E6	E7	E8
E1			R fing flex 500uA	R thumb flex 500	L wrist flex and tri 500 +L fing flex, R tri, wrist flex 600	R tri, wrist flex L tri 600	R tri, wrist flex 500	R tri, wrist flex 500
E2		R tri, wrist flex 500	R fing flex 400	R tri, R wrist flex 500	R tri, wrist flex 400	R fing flex, lat, tri L wrist flex 500	R tri, wrist flex 400	R tri, fing flex 400
E3	R fing flex 400	R thumb and finger flex 400	R tri, wrist flex 500	R fing flex, ulnar dev 300	R finger Flex 300	R fing flex 300 + R wrist flex 400	R hand grasp, wrist ext 400 + tri wrist flex, fing flex 500	R tri, fing flex 400
E4	R thumb flex 400	R thumb ext, tri 500	R fing flex 600					
E5	R thumb 500 + R fing flex, tri, L tri 600	R wrist flex, tri 500	R wrist flex, fing flex, tri 500		L tri 500			
E6	R fing flex, wrist flex, L tri 600	R tri 400 + R wrist flex 500	R tri, wrist flex 500			L tri 600	L tri 400	L tri 400
E7	R wrist flex, tri 400	R wrist flex, tri 400	R wrist flex, tri 400	L tri 600	L tri 600	L wrist flex 600		
E8	R wrist flex, tri 500	R tri, fing flex 400 + Rwrist flex 500	R fing flex 400	L ulnar dev 700	L thumb flex 400 + L ulnar dev 500	L tri, wrist flex 600	L tri 700	

Table 3.4.1 shows a full list of movements evoked by bipolar stimulation across all possible electrode pairs. The diagonal contains unipolar anodal-first stimulation to a distant ground. We may naïvely expect to see a symmetric matrix however there may be anodal and cathodal effects changing the outputs of inverse responses between electrode pairs.

Theoretical	E1	E2	E3	E4	E5	E6	E7	E8
E1	0	R PE, R DF	R PE, R DF	0	L PE	L PE	0	0
E2	R PE, R DF	R PE, R DF	R PE, R DF	R PE, R DF	R PE, R DF, L PE	R PE, R DF, L PE	R PE, R DF	R PE, R DF
E3	R PE, R DF	R PE, R DF	R PE, R DF	R PE, R DF	R PE, R DF, L PE	R PE, R DF, L PE	R PE, R DF	R PE, R DF
E4	0	R PE, R DF	R PE, R DF	0	L PE	L PE	0	0
E5	L PE	R PE, R DF, L PE	R PE, R DF, L PE	L PE	L PE	L PE	L PE	L PE
E6	L PE	R PE, R DF, L PE	R PE, R DF, L PE	L PE	L PE	L PE	L PE	L PE
E7	0	R PE, R DF	R PE, R DF	0	L PE	L PE	0	0
E8	0	R PE, R DF	R PE, R DF	0	L PE	L PE	0	0
Actual	**E1**	**E2**	**E3**	**E4**	**E5**	**E6**	**E7**	**E8**
E1	0	0	R DF	R DF	L DF	R DF, R PE, L PE	R DF, R PE	R PE, R DF
E2	0	R PE, R DF	R DF	R DF, R PE	R DF, R PE	R DF, R PE, L DF	R PE, R DF	R PE, R DF
E3	R DF	R DF	R PE, R DF	R DF	R DF	R DF	R DE	R PE, R DF
E4	R DF	R DF	R DF	0	0	0	0	0
E5	R DF	R DF, R PE	R DF, R PE	0	L PE	0	0	0
E6	R DF, L PE	R DF, R PE	R DF, R PE	0	0	L PE	L PE	L PE
E7	R DF, R PE	R DF, R PE	R DF, R PE	L PE	L PE	L DF	0	0
E8	R DF, R PE	R DF, R PE	R DF	L DE	L DF	L PE, L DF	L PE	0
Additions	**E1**	**E2**	**E3**	**E4**	**E5**	**E6**	**E7**	**E8**
E1	0	0	0	1	1	2	2	2
E2	0	0	0	0	0	1	0	0
E3	0	0	0	0	0	0	1	0
E4	1	0	0	0	0	0	0	0
E5	1	0	0	0	0	0	0	0
E6	1	0	0	0	0	0	0	0
E7	2	0	0	1	0	1	0	0
E8	2	0	0	1	1	1	1	0
Subtractions	**E1**	**E2**	**E3**	**E4**	**E5**	**E6**	**E7**	**E8**
E1	0	2	1	0	1	0	0	0
E2	2	0	1	0	1	1	0	0
E3	1	1	0	1	2	2	2	0
E4	0	1	1	0	1	1	0	0
E5	1	1	1	1	0	1	1	1
E6	0	1	1	1	1	0	0	0
E7	0	0	0	0	0	1	0	0
E8	0	0	1	0	1	0	0	0
Total Errors	**E1**	**E2**	**E3**	**E4**	**E5**	**E6**	**E7**	**E8**
E1	0	2	1	1	2	2	2	2
E2	2	0	1	0	1	2	0	0
E3	1	1	0	1	2	2	3	0
E4	1	1	1	0	1	1	0	0
E5	2	1	1	1	0	1	1	1
E6	1	1	1	1	1	0	0	0
E7	2	0	0	1	0	2	0	0
E8	2	0	1	1	2	1	1	0

Figure 3.4.7. Linearity Analysis of Bipolar Stimulation at C7. From the top down a Theoretical map of superpositions was created by adding the responses to unipolar stimulations across pairs. The data was lateralized and categorized by movement type for ease of comparison (L PE = Left Proximal Extension (Triceps), R DF = Right Distal Flexion (finger or wrist)).

EMG Responses

In another experiment we were able to capture EMG from 4 ispilateral muscles during a small subset of unipolar and bipolar stimulation ramp sets. The stimulation-triggered averages (N=25) are presented in Figure 3.4.8.

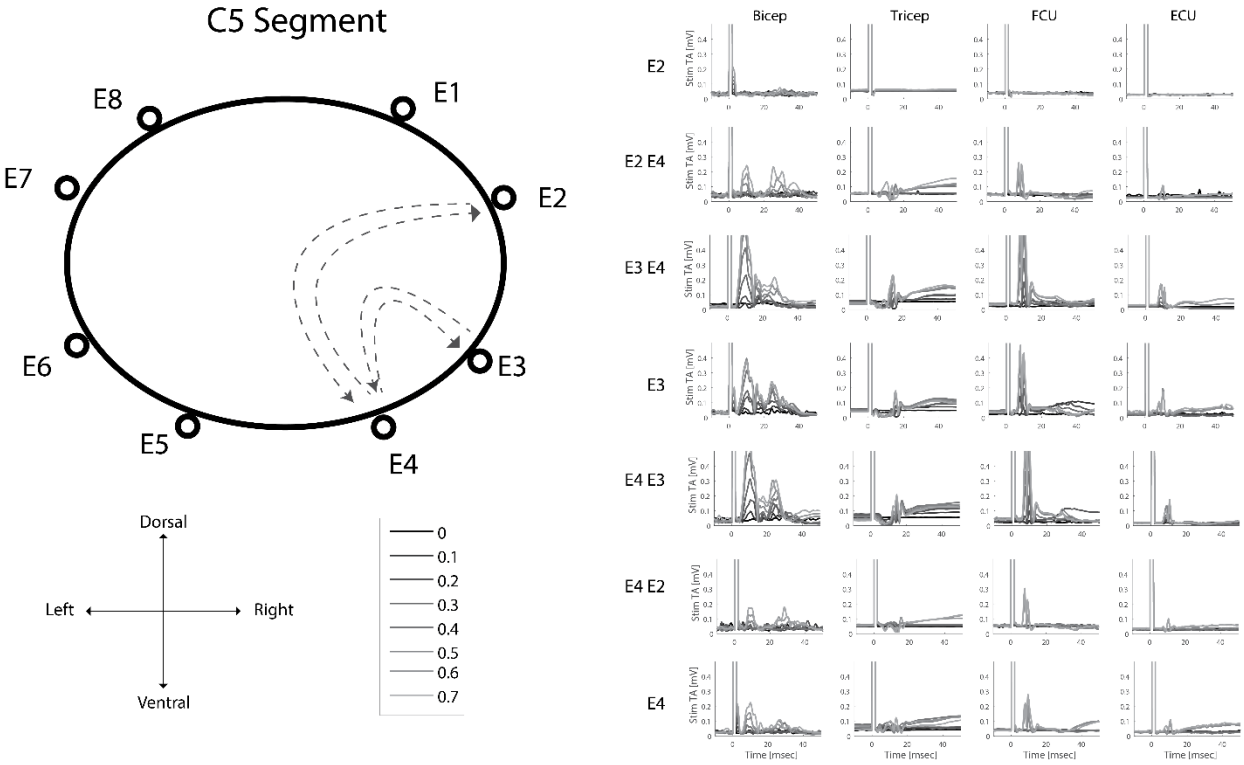

Figure 3.4.8. Ipsilateral EMG Responses to Unipolar and Bipolar Stimulation. Electrodes 2-4 were stimulated with single pulse stimulations from 100-700uA using a ramp stimulation protocol while Monkey T was sedated. EMG recordings were taken from four dominant and oppositional arm muscles. Bipolar stimulation produced higher amplitude outputs than either unipolar stimulation site. Altering the polarity of the stimulation (E3/E4 vs E4/E3) produced slightly different responses.

3.4.E Design Feedback

A variety of mechanisms contributed to failure of the chronic implants. Table 3.4.2 summarizes experiment duration and endpoints. Only one of the three failures was directly

related to the flexible array technology; the remainder were related to connectors, perioperative management, and preexisting health concerns.

Pain management appears to be a major limitation in working with non-human primate models of reanimation. We noted during the recovery period post-surgery for all animals that there was a fine line to balance between ensuring the animals' post-surgical pain is dulled and not causing undue stress and over treating pain. Pain management is already a multifactor problem in veterinary medicine where ordinal scales and physician conversation can't take place (Di Vicenti 2013). Confounding that with destabilizing spinal surgery adds yet another layer of complexity to the care process. With extensive spinal cord surgery the animal is at risk of severe spinal cord injury in response to hyper flexion or hyperextension of the spine post-surgery. There are not standard bracing systems in place for behaving primates and the bone fusion process to recover from a spinal surgery is expected to take more than 8 weeks (Boden 2002). This long recovery is a large risk window for overuse injuries. In one animal we observed an acute SCI as a result of hyperextension against the bracing material on the dorsal aspect of the vertebrae. The second animal was observed with a slightly ruptured C7 disc on X-ray which was shortly followed by a constriction of the spinal column likely caused by electrode migration following increased mobility of the spinal column. We hypothesize that both of these failure mechanisms were caused by poor control over the spinal fixation and forces produced by the adult primates. The third animal was put down due to complications from a previous procedure that affected

Table 3.4.2. Array 2.0 Implant Durations and Failure Mechanisms.

Animal	Implant Location	Implant Duration [days]	Failure Mechanism
Monkey T	C5, C7	23	Electrode Translation
Monkey V	C5, C7	9	Unrelated
Monkey O	C5, C7	3	Induced Cervical SCI

cortical function and likely incurred a spinal cord injury during a seizure unrelated to the surgical protocol.

The promising early results seen with subdural flexible arrays were compromised by mechanical problems in the chronic setting that ultimately led to premature electrode failure in several tests. The motor responses were very encouraging and the concentration of response on the ventral aspect of the cord encourages more design on approaches for accessing that new territory. Future designs look towards integrating more robust fixation techniques while maintaining flexibility in stimulation layout. Our linearity analysis calls into question the prevailing thought that motor outputs to paired stimulation acts linearly. While poor linearity is undesirable from an engineering systems perspective, the fact that we can create wholly new subsets of movements that are not necessarily bounded by the original electrode placement is a potential advantage for the future of spinal stimulation as a restorative paradigm.

3.5 DESIGN 3.0

Design 3.0 prompted rethinking access to the ventral aspect of the spinal column. Discussions with spinal neurosurgeons including Drs. Christoph Hofstetter, Trent Treadway, and Jeffery Roh around the failure mechanisms seen in chronic implantation of Design 2.0 all moved towards existing, well-tolerated spinal instrumentation. Our initial designs were predicated on a dorsal surgical approach mirroring existing spinal stimulation, fixation hardware, and electrode placement techniques. Design 3.0 altered this paradigm by separating the dorsal and ventral electrodes and adapting a ventral approach and mirroring the orthopedic safety profile of well-established cervical total disk replacement technologies. By combining the established protocols of dorsal epidural stimulation with paddle electrodes and ventral epidural stimulation using adapted cervical replacement disks instrumented with electrodes we hoped to improve the safety

profile of the electrodes while maintaining the variety of motor outputs seen with earlier design revisions. We tested the ventral aspect of the protocol in acute preparation but were unable to test them in concert.

3.5.A Design

For Design 3.0 we proposed a two part implant that separates dorsal and ventral electrodes, minimizes structural damage during implantation, and maintains access to the ventral stimulation targets accessed by the previous generations of electrodes.

The ventral electrodes are integrated into existing styles of tolerated disk replacement implants. A variety of commercially-available designs exist including static polymer, static metal alloy, and articulated designs (Cincu 2014) are available which are used to alleviate pain and motor symptoms caused by disk herniation. Importantly, multiple disk segments can be surgically replaced using this technique as illustrated in Figure 3.5.1. In traditional disk replacement surgeries the dorsal aspect of the replacement disk is in close proximity to the ventral aspect of the spinal canal. Surgical consultation with collaborating neurosurgeons confirmed that the procedure could easily be adapted to place a modified disk on the subdural space of the spinal cord.

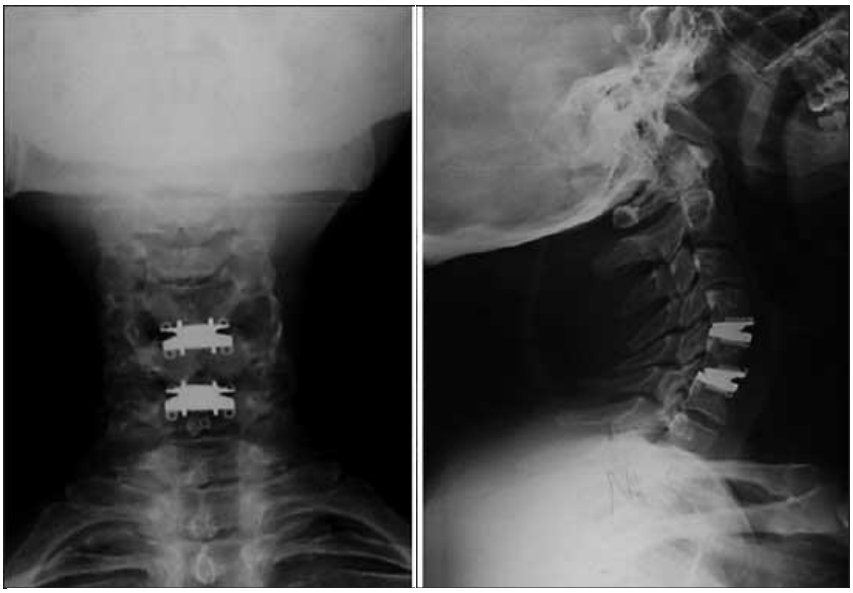

Figure 3.5.1. Radiograph of adjacent articulated cervical replacement disks in a human subject while maintaining range of motion. Adapted from Cincu 2014.

The other half of the array design could be addressed using existing clinical dorsal epidural techniques. Flexible paddle electrodes, either commercially available for dorso-medial coverage or as designed in Array 2 for dorsolateral coverage could be inserted in the same procedure with much less invasive protocols compared to array Designs 1 and 2 standard protocols.

Two electrodes sets were manufactured to test the feasibility of the technique. First, a set of four plug-style electrodes were hand made using the same methods as outlined in Chapter 2 with only one contact per site. These insulated plugs were ~1mm in diameter when insulated and designed to slip into pre-drilled holes directly though the vertebral body and rest on the ventral epidural aspect of the spinal cord. A second electrode was manufactured in the style of existing cervical disc replacements using biocompatible polyether ether ketone (PEEK) (Sigma Aldrich, St. Louis MO), Figure 3.5.2. A small piece of PEEK was machined into a 5x4x2mm block and five Pt/Ir electrode wires were inserted through .5 mm holes drilled longitudinally through the block and secured with silastic. The wires were soldered to connector leads within a silicone catheter alongside a low-impedance ground wire and again sealed with silastic. Trace impedances for the replacement disc array were 10.4 ±4 kΩ and the plug array was 25.5±8 kΩ at 1kHz.

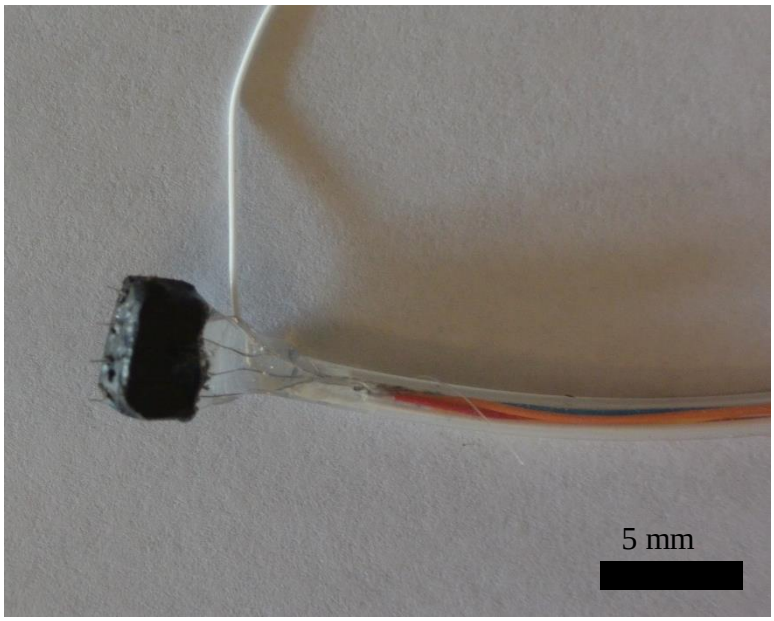

Figure 3.5.2. Modified Replacement Disc Electrode used for Array 3.0

3.5.B Surgical Protocol

The ventral approach required a novel surgical procedure very different from previous strategies and took place in two parts. A procedural schematic of the implant protocol can be seen in Figure 3.5.3.

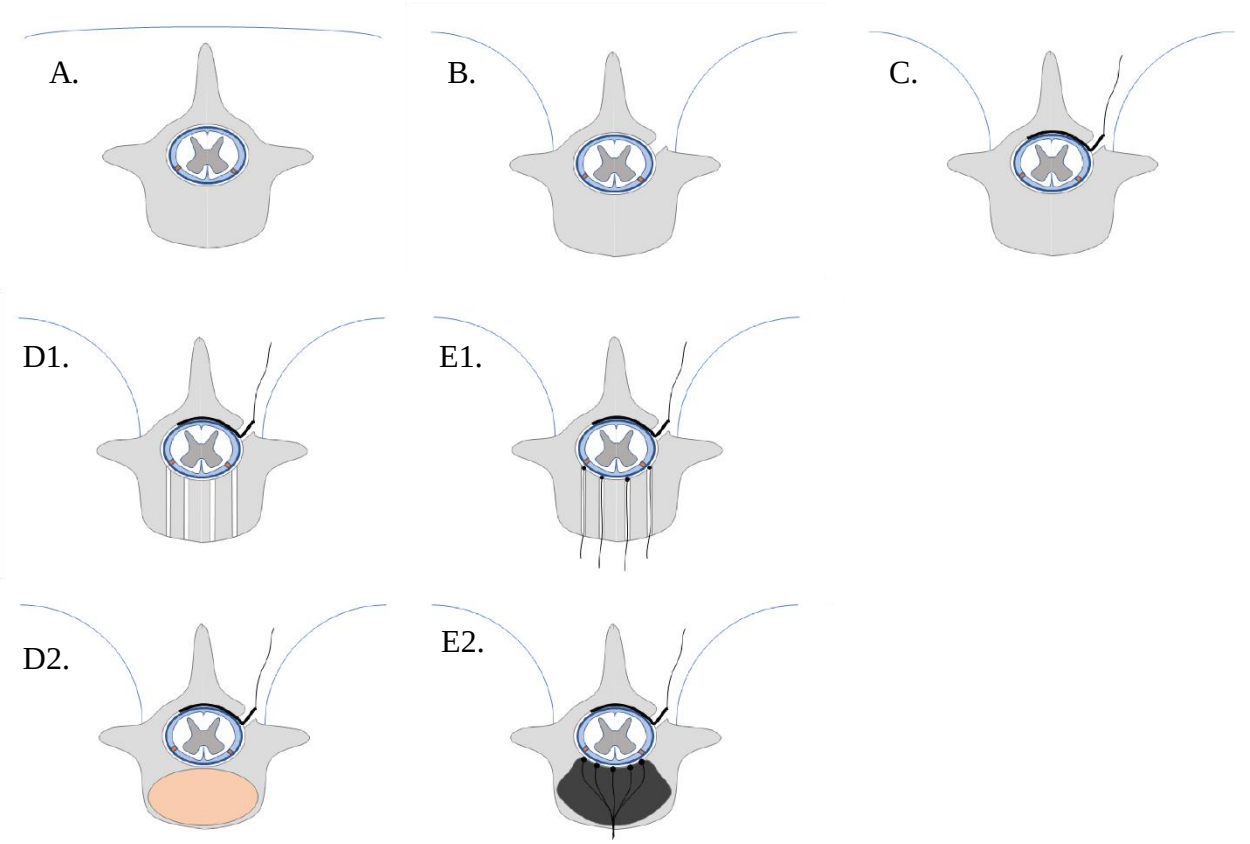

Figure 3.5.3. Cross Section Illustration of Surgical Protocol for Array Design 3.0. **A**. The animal is positioned prone on the operating table. **B**. Soft tissue is resected and a small hemilaminectomy gives access to the dorsal epidural aspect of the cord. **C.** The dorsal array is placed. **D1.** For the ventral plug design the animal is flipped supine, a midline incision is made and vertebrae exposed. A series of holes is drilled through the vertebral body. **E1.** Electrodes leads are placed into the holes and secured with methyl methacrylate. **D2.** For the disk replacement design the intervertebral disk is removed (orange). **E2.** A pre-sized replacement disk is slid into place and the two adjacent vertebrae are fixed at the vertebral body with standard fixation hardware.

The surgical process was assisted via intraoperative fluoroscopy to verify ventral vertebrae positions. The animal (Female, *M. nemestrina*, 6.8kg) was sedated under isoflurane anesthesia and placed supine on an air support bag to cradle the head and neck. Electrocautery was used to open 8cm M/L in the mid-cervical region. Blunt dissection using fingers was used to gently part the underlying air sacks and fascia away from C4-C7 vertebrae and expose the vertebral bodies. Connective tissue on the vertebrae was removed and a needle inserted into the disc between two arbitrary vertebrae as a landmark for in-surgery imaging.

A fluoroscopic image was used with the needle as reference to identify exposed vertebrae. The plug electrodes were inserted first. We located C5 and C7 vertebrae and used a small bore drill bit (1mm) to drill 2 holes per vertebrae spaced ~2mm evenly from midline in the M/L plane. We initially intended to insert electrodes in the holes until the pressure of the ventral dura was felt. A small needle ground wire was placed under the skin at the dorsal midline of the animal. Figure 3.5.4 shows fluoroscopic images of the implantation procedure.

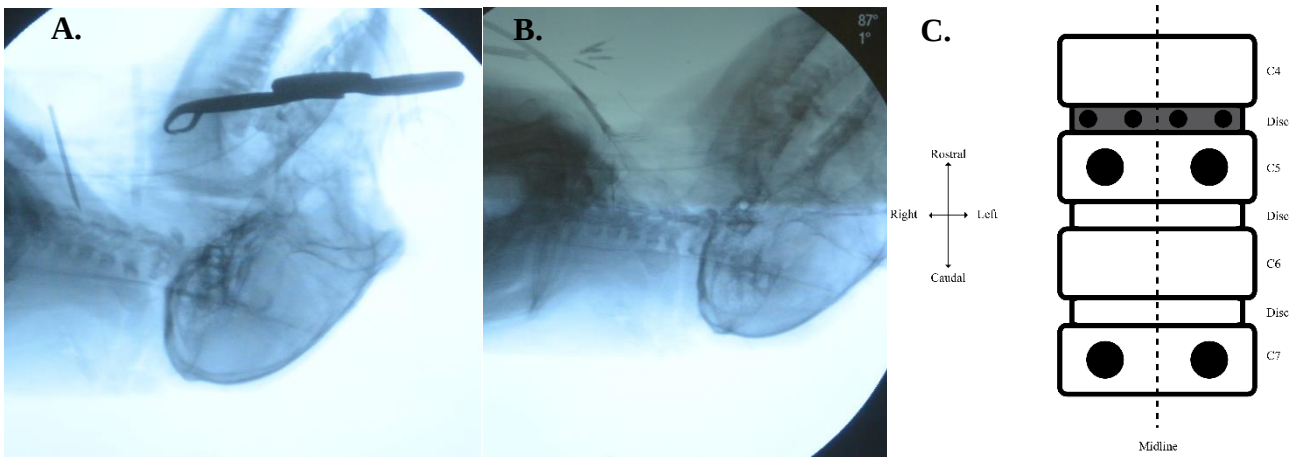

Figure 3.5.4. Fluoroscopic images obtained during the Array 3 experiment. **A** A reference needle was used for identifying vertebrae from the ventral approach. **B**. Two plug electrode arrays inserted in C5 and C7 vertebral bodies. C. Schematic of idealized implant locations from the ventral view perspective.

The modified replacement disk electrodes were then placed following traditional disk replacement protocols. Briefly the C4/C5 disc was removed using a kerrison punch, scalpel, and small curette and the bone faces were cleaned and smoothed using a 2mm burr bit to expand and shape the disk replacement opening. We chose the C4/C5 disc for two reasons, first to explore a previously unmapped location, and second to not interfere with the existing plug electrode placements. The modified disk was then press fit into the matching space and ground wires were attached to the dorsal lead.

The surgical protocol for chronic implantation was designed to take place in two phases, separated by a week of recovery and monitoring. In the first surgery a cortical housing would be installed to house connectors and any cortical implants. Second, the dorsal electrode array would be implanted and leads would be routed up to the cortical housing. The animal would be overturned in surgery and the dorsal electrodes would be placed. The animal was sacrificed following the experiment per WaNPRC Tissue Program protocols for organ harvesting.

3.5.C Experimental Methods

We were able to test one acute ventral preparation. In this proof-of-concept experiment we stimulated each of the electrodes and electrode pairs within the plug array and replacement disc while the animal remained under isoflurane anesthesia post-implant. At each site a stimulation ramp as previously described and accompanying auditory tick was used to probe stimulation thresholds at all sites matching stimulation techniques for Design 2.0. Bipolar pairs of electrodes were tested using biphasic, anodal first single pulse stimuli. The animal was visually inspected for signs of hand and arm movement. Threshold was determined as the current (in 50µA) steps which elicited a movement 100% of the time. When threshold was found to be less than 100µA

we found the lower threshold to the nearest 5µA. We also tested the motor responses to a paradigm of 40Hz trains of stimuli delivered for 500ms at .5Hz intervals.

3.5.D Stimulation Results

We tested the stimulation responses to four individual plug electrodes placed on the left and right ventral aspect of C5 and C7 vertebral bodies, as well as a custom 6-lead instrumented replacement intervertebral disc placed between C4 and C5 vertebrae. Motor threshold for the plug electrodes were 366±28µA with a standout low threshold response of 45 µA at C5-R which was likely caused by advancing the electrode through the dura during insertion.

The stimulation results from Design 3.0 were very comparable to the Array 2.0 results with a full spectrum of movements seen in response to stimulation through each all of the 4 electrode plugs placed in C5 and C7. Bilateral movements including proximal and distal flexion and extension were seen. We also tested each stimulation pair with trains of stimulation at 40 Hz, which produced strong, robust movements for the duration of the .5s stimulation duty phase and did not appear to fatigue through multiple stimulations. Full summary datasets are reported below for completeness:

Summary responses to single stimuli

Site	Stim Type	Current [uA]	Threshold [u	L Motor Outputs	R Motor Outputs
C5-L	single	400	350	BR, delt	
C5-L	single	700	350	BR,delt, Bi	
C5-R	single	45	45		delt
C5-R	single	60	45		Bi, delt,
C5-R	single	90	45		Bi, Delt, BR
C7-R	single	350	350		FDS, ulnar, thumb flex, thumb adduction
C7-R - C5-R	single	50	50		BR, supinator, Bi
C7-L	single	400	400	Tri	
C7-L	single	450	400	Tri, Fing Flex	
C7-L	single	800	400	Tri, Fing Flex, Thumb flex	
C7-L - C5-L	single	350	350	delt	
C7-L - C5-L	single	500	350	delt, tri	
C5-R - C7-L	Single	60	60		Bi
C5-R - C7-L	Single	300	60	lat	Bi
C5-R - C7-L	Single	500	60	Fing Flex, Lat	Bi
C5-L - C7-R	single	350	350	delt	fing flex, thumb flex
C5-L - C7-R	single	700	350	bi, delt	fing flex, thumb flex
C5-R - C5-L	single	60	60		delt
C5-R - C5-L	single	200	60	delt	BR
C5-R - C5-L	single	600	60	delt	BR
C7-L - C7-R	single	300	300	tri	Fing Flex
C7-L - C7-R	single	350	300	Fing Flex, thumb flex, tri	Fing Flex
C7-L - C7-R	single	700	300	Fing Flex, thumb flex, tri	Fing Flex

Summary Responses to 40 Hz trains

Site	Stim Type	Current [uA]	Threshold [u	L Motor Outputs	R Motor Outputs
C5-L	train	350	350	BR, delt	
C5-L	train	700	350	BR, delt, Bi	
C5-R	train	45	45		Bi, Delt
C7-R	train	300	300		strong grip, finger flex, Bi, FCU
C7-R - C5-R	train	350	350		BR, supinator, Bi
C7-L	train	450	450	Tri	
C7-L	train	500	450	Tri, Fing Flex, Thumb flex	
C7-L - C5-L	train	350	350	delt	
C7-L - C5-L	train	700	350	delt, tri, bi, pec, finger flex	
C5-R - C7-L	train	40	40		Bi
C5-R - C7-L	train	300	40	lat	Pec, Bi
C5-R - C7-L	train	500	40	Fing Flex, Lat	Pec, Bi
C5-L - C7-R	train	300	300	delt	fing flex
C5-L - C7-R	train	600	300	delt,bi,tri,wrist ext	fing flex, thumb flex
C5-R - C5-L	train	60	60		delt, BR
C5-R - C5-L	train	400	60	delt	delt, BR
C7-L - C7-R	train	300	300	thumb flex	Fing Flex
C7-L - C7-R	train	600	300	Fing Flex, thumb flex, pronator	Fing Flex, thumb flex, pronator
C7-L - C7-R	train	700	300	Fing Flex, thumb flex, wrist flex	Fing Flex, thumb flex, pronator

The single replacement disc array we tested similarly easy to place and secure, however verification of positioning was difficult even with the aid of in-surgery fluoroscopy. We were forced by the placement of the earlier plug electrodes to move the disc array rostrally to the C4/C5 segment where we expected to have responses dominated by proximal movements. Biceps contraction was the only response we saw and thresholds were much higher than all the other designs we had tested (1012 ±125µA). Biceps responses were lateralized on the right side

of the array but bilateral responses appeared throughout midline and left side electrodes failed to produce a motor response even with up to several milliamps of current, leading us to believe there was a fault in the manufacture and current was not reaching the electrodes.

Summary Replacement Disc responses:

Site	Stimulation	Current [uA]	Threshold	L Motor Output	R Motor Output
Site 1	Single	950	950		Bi
Site 2	Single	950	950		Bi
Site 3	Single	1200	950	Bi	Bi
Site 4	Single	1200	1200	Bi	Bi
Site 5	Single	3000	N/A		
Site 6	Single	4000	N/A		

3.5.E Design Feedback

The surgical protocol for the ventral approach was significantly easier than the previous array designs. Insertion took less than 30 minutes for all arrays and the amount of bone structure removed was minimal. Even when coupling this protocol with a hemi-laminectomy to place a dorsal array in tandem the subject will lose almost no structural bone support. Adapting a protocol that is already in human practice is a much more robust framework for experimental longevity.

The stimulation results from the quick design test also were encouraging in the that we could reproduce a full range of movements encompassing both hands, anti-gravity biceps movements as well as proximal deltoid with just 4 electrodes. Combining these four stable electrodes with even a standard small dorsal column stimulating array could be valuable for patients with mobility impairments. There are two suggested next steps in the tests that should be pursued based on discussions with practicing neurosurgeons. First, we should adapt existing, well-tolerated human implant hardware currently used for spinal stabilization and disc replacement. Commercially-available, pediatric-sized replacement discs offer the manufacturing precision and

physical sizes necessary for long-term primate experimentation. Simple aftermarket modifications can allow the addition of electrodes and possibly even embedded stimulation electronics. Second, we should expand the adapted hardware platform to acute testing in human subjects with existing conditions requiring disc replacement in cervical region. It is a viable path to perform acute tests in-surgery using modified versions of the same hardware that the patient is receiving permanently. Current surgical protocols allow for multiple implant fittings during surgery and by opening up the experimental protocol to otherwise healthy individuals with a minor skeletal issue we could greatly expand the population available for implant testing and validation while maintaining the current low-risk profile of replacement disc implants.

3.5.F Summary Discussion

This is the first set of experiments to investigate a novel platform for interfacing the cervical spinal cord to induce upper limb movement, in primates. Overall we found that these arrays are capable of producing the necessary spectrum of naturalistic movements for use in functional neurorecovery. Serious challenges were encountered in the longevity of early designs. Balancing post-operative pain, animal movement, and surgical risk are highly complex in the non-human primate model. The lack of primate-specific braces, and self-managed medication regiments, as are present in human protocols, underscores the difficulty in working with this model organism. The robust movements elicited using the paradigms of design 3.0 are encouraging steps towards spinal BMI platforms with maximized motor outputs and specificity alongside minimal surgical risk.

MECHANISMS OF ACTION

We did not explicitly address the exact mechanisms by which movement was produced. Several factors may contribute to the variety of motor responses observed. Activation areas in

response to electrical stimulation are expected to fall off with distance squared and the low stimulation currents at threshold (<250μA) suggest that direct neuronal activation is likely not the main activation pathway. Previous work and simulation of cortical neuronal tissue suggests that fibers of passage have lower stimulation thresholds than cell bodies (Gustafasson 1976, Histed 2009). Computational models of electrical stimulation for hindlimb stepping in rats (Cappograsso 2013) also suggest that trans-synaptic activation is the predominant mechanism in response to intraspinal microstimulation, which in theory should be activating tissue even closer to spinal motoneurons.

Our observations that most stimulation sites produce multiple movements also suggests that the path is not directly tied to ventral motoneuron activation and is likely mediated by stimulating fibers from interneurons and intraspinal tracts. We also observed no occurrences of purely oppositional movement, indicating that the stimulated systems likely were mediated via interneurons or fibers rather than directly stimulating efferent motoneurons which would be more likely to produce a more random pattern of muscle activation. The latencies we observed (all >5ms) also provide evidence that the mechanisms is polysynaptic since it is much later than the ~2.6ms activation time we would expect from a direct activation model.

Trans-synaptic and interneuron-mediated interactions may indeed be an advantage of spinal stimulation for motor reanimation. We observed robust, synergistic movements that aligned with natural behaviors across all implant designs. We also know that spinal stimulation produces a more natural recruitment order than nerve stimulation in the muscle fibers carrying out those movements, which decreases fatigue and may increase strength (Mushahwar and Horch 2000, Bamford 2005). Finally, we know that circuits in the spinal cord remain functional after injuries that alter descending commands. The post-injury stability of ISMS motor function observed in

rats (Sunshine 2013) may not be exactly consistent in primates and humans due to disparity on descending command loss; however there are cases of injured primates controlling spinal stimulation paradigms for functional recovery (Nishimura 2013b). Likely many mechanisms of action converge to produce robust movements and additional experiments will be required to tease out the contribution of each.

BMI APPLICATIONS

The ultimate goal of this work is to further the tools available to BMI researchers, technologists, and clinicians as we strive to deliver the most intuitive and capable rehabilitative paradigms for people suffering from spinal cord injury. Pioneering work by Moritz (2008), Pohlmeyer (2009), Bouton (2016), and Ajiboye (2017) have shown that the brain can drive control signals that restore some level of natural function to the upper limb with functional electrical stimulation of the forearm muscles. Computationally this can be a difficult problem with 32 muscles of the hand, arm and forelimb (most not easily accessible through surface stimulation) working in concert to produce movements. Recruitment order and fatigue concerns aside, surface spinal stimulation appears to provide a natural range of movements from a lower set of dimensions that can be more easily encoded in stimulation to produce movement, and likely a more intuitive control paradigm for BMI applications. In the case of prolonged use it is likely that both learning and plasticity may be present in spared pathways that will further increase control and function (Nishimura 2013b).

While robotic systems may allow completion of pre-programmed tasks (Hochberg 2012), the psychological agency of a patient is removed. Based on previous surveys of patient desires we maintain that the spinal cord is the optimal level for reanimation to restore fine motor skills. Foundational tools for interfacing with the spinal cord are a platform on which advances in

cortical decoding (Branco 2017), new control algorithms (Lebedev 2017), and closed-loop feedback (Bensmaia 2014, Zimmerman 2014) can be built just as in the development of many cortical brain computer interfaces (Moran 2010). Challenges remain around longevity which may be mitigated by combining spinal stimulation with established orthopedic technologies as preliminarily reported in our Array Design 3.0. Moving forward with the project we would suggest changing the design of Array 3.0 to retrofit existing, commercially available pediatric replacement disk technology, either articulated or solid, with electrodes so that all established hardware technology can be used. A solid spinal base implant using a ventral approach could then be coupled with a minimally invasive dorsal epidural electrode to give almost circumferential coverage at any level. Ideally as miniaturization technology advances the ventral hardware could physically house implanted electronics controlling stimulation and recording electronics (Shadoost 2018).

3.6 Conclusions

Spinal implants in primates are notoriously challenging and this project was no exception. The motor outputs from acute tests and the early phases of chronic testing in primates were very promising. Cervical epidural stimulation produced motor outputs to the hand and arm that were consistent across subjects and followed expected rostral-caudal organization. Surgically, the ventral aspect of the spinal cord in the cervical region is an accessible target motor pool that holds distinct promise for future restorative technologies. Early tests of motor function produced strong motor outputs in all three design revisions. Chronic implantation of electrodes around the spinal cord produced mixed results. Initial implant recovery timelines were promising but second generation designs did not provide adequate movement with the spinal cord and led to premature failure for both electrode-related and other reasons. The third revision of the device was most

promising. Ventral spinal stimulation offers much promise for motor recovery of hand and arm function. Robust, differentiated, bilateral movements were seen throughout testing and adapting existing surgical techniques for a new purpose could solve the remaining design issues and bring the technique to many patients currently without therapeutic options for treatment.

3.7 REFERENCES

Ajiboye AB, Willett FR, Young DR, Member WD, Murphy BA, Miller JP, Walter BL, Sweet JA, Hoyen HA, Keith MW, Peckham PH, Simeral JD, Donoghue JP, Hochberg LR, Kirsh RF. 2017. Restoration of reaching and grasping movements through brain-controlled muscle stimulation in a person with tetraplegia: a proof-of-concept demonstration. Lancet. 389(10081):1821-1830.

Bamford, J. A., Putman, C. T., & Mushahwar, V. K. (2005). Intraspinal microstimulation preferentially recruits fatigue-resistant muscle fibres and generates gradual force in rat. The Journal of Physiology, 569(3), 873-884.

Barola G, Singh-Sahni K, Staas Jr. W, E, Shatin D, Ketcik B, Allen K. 1995. Epidural Spinal Cord Stimulation in the Management of Spasms in Spinal Cord Injury: A Prospective Study. Stereotact Funct Neurosurg; 64:153-164.

Bensmaia SJ, Miller LE. 2014. Restoring sensorimotor function through intracortical interfaces: progress and looming challenges. Nat Rev Neurosci. 15:313-325.

Boden, S. D., Kang, J., Sandhu, H., & Heller, J. G. (2002). Use of recombinant human bone morphogenetic protein-2 to achieve posterolateral lumbar spine fusion in humans: a prospective, randomized clinical pilot trial 2002 volvo award in clinical studies. Spine, 27(23), 2662-2673.

Bouton CE, Shaikhouni A, Annetta NV, Bockbrader MA, Friedenberg DA, Nielson DM, Sharma G, Sederberg PB, Glenn BC, Mysiw WJ, Morgan AG, Deogaonkar M, Rezai AR. 2016. Restoring cortical control of functional movement in a human with quadriplegia. Nature 553:247-250.

Branco MP, Freudenburg ZV, Aarnoutse EJ, Bleichner MG, Vansteensel MJ, Ramsey NF. 2017. Decoding hand gestures from primary somatosensory cortex using high-density ECoG. Neuroimage. 15(147): 130-142.

Capogrosso M, Wenger N, Paspopovic S, Musienko P, Beuparlant J, Bassi Luciani L, Courtine G, Micera S. 2013. A Computational Model for Epidural Electrical Stimulation of Spinal Sensorimotor Circuits. J Neurosci 33(49):19326-19340.

Cincu R, Lorent FdA, Gomez J, Eiras J, Agrwal A. 2014. Long term presercation of motion with artificial cervical disc implants; A comparison between cervical disc replacement and rigid fusion with cage. Asian J Neurosury. 9(4): 213-217.

Courtine G, Bunge MB, Fawcett JW, Grossman RG, Kass JH, Lemon RN, Maier I, Martin J, Nudo RJ, Ramon-Cueto A, Rouiller EM, Schnell L, Wannier T, Schwab ME, Edgerton VR. 2007. Can experiments in nonhuman primates expedite the translation of treatments for spinal cord injury in humans? Nat. Med. 13:561–66

.

Danner SM, Krenn M, Hofstoetter US, Toth A, Mayr W, et al. 2016. Body Position Influences Which Neural Structures Are Recruited by Lumbar Transcutaneous Spinal Cord Stimulation. PLOS ONE 11(1): e0147479

D'Andrea G, Angelini A, Familiari P, Caroli E, Frati A. 2014. Platinum-iridium subdermal magnetic resonance imaging-compatible needle electrodes are suitable for intraoperative monitoring during image-guided surgery with high-field magnetic resonance imaging: an experimental study. Neurosurg. 10(3)387-392.

DiVincenti, L. (2013). Analgesic Use in Nonhuman Primates Undergoing Neurosurgical Procedures. Journal of the American Association for Laboratory Animal Science : JAALAS, 52(1), 10–16.

Fong AJ, Roy RR, Ichiyama RM, Lavrov I, Courtine G, Gerasimenko Y, Tai YC, Burdick J, Edgerton VR. 2009. Recovery of control of posture and locomotion after spinal cord injury: solutions staring us in the face. Prog Brain Res. 175:3953-418.

French JS, Anderson-Erisman KD, Sutter M. 2010. What do spinal cord injury consumers want? A review of spinal cord injury consumer priorities and neuroprothesis from the 2008 neural interfaces conference. Neuromodulation. 13:229-231.

Fuentes R, Petersson P, Siesser WB, Caron MG, Nicolelis MA. 2009. Spinal cord stimulation restores locomotion in animal models of Parkinson's disease. Science. 323:1578-1582.

Giszter SF. 2015. Spinal primitives and intra-spinal micro-stimulation (ISMS) based prostheses: a neurobiological perspective on the "known unknowns" in ISMS and future prostpects. Front Neurosci. 9(72); 1-16.

Grahn PJ, Lavrov IA, Sayenko DG, Van Straaten MG, Gill ML, Strommen JA, Calvert JS, Drubach DI, Beck LA, Linde MB, Thoreson AR, Lopez C, Mendez AA, Gad PN, Gerasimenko YP, Edgerton VR, Zhao KD, Lee KH. 2017. Enabling Task-Specific Volitional Motor Functions via Spinal Cord Neuromodulation in a Human with Paraplegia. Mayo Clin. Proc. 92(4): 544-554.

Gustafsson B, Jankowska E. 1976. Direct and indirect activation of nerve cells by electrical pulses applied extracellularly. J Physiolo. 258:33-61.

Histed MH, Bonin V, Reid RC. 2009. Direct activation of sparse, distributed populations of cortical neurons by electrical stimulation. Neuron. 63: 508-522.

Hochberg LR, Bacher D, Jarosiewicz B, Masse NY, Simeral JD, Vogel J, Haddadin S, Liu J, Cash SS, van der Smagt P, Donoghue JP. 2012. Reach and grasp by people with tetraplegia using a neutrally controlled robotic arm. Nature. 485:372-375.

Jankowska, E., & Edgely, S. A. 2006. How Can Corticospinal Tract Neurons Contribute to Ipsilateral Movements? A Question With Implications for Recovery of Motor Functions. The Neuroscientist : A Review Journal Bringing Neurobiology, Neurology and Psychiatry, 12(1), 67–79.

Lebedev, MA, Nicolelis MAL. 2017. Brain-Machine Interfaces: From Basic Science to Neuroprostheses and Neurorehabilitation. Physiol Revs. 97(2) 767-837.

Lemon, RN. 2008. Descending Pathways in Motor Control. Annu. Rev. Neurosci. 31:195-218.

Melzack, R, Wall, PD. 1965. Pain Mechanisms: A New Theory. Science. 150(3699) 971-979

Moran D. 2010. Evolution of brain-computer interface: action potentials, local field potentials, and electrocorticograms. Curr Opin Neurobiol. 20:741-745.

Moritz CT, Lucas TH, Permutter SI, Fetz EE. 2007. Forelimb Movements and Muscle Responses Evoked by Microstimulation of Cervical Spinal Cord in Sedated Monkeys. J Neuophysiol. 97:110-120.

Moritz CT, Perlmutter SI, Fetz EE. 2008. Direct control of paralyzed muscles by cortical neurons. Nature. 456 639-642.

Mushahwar V. K., Horch K. W. 2000.Selective activation of muscle groups in the feline hindlimb through electrical microstimulation of the ventral lumbo-sacral spinal cord. IEEE Trans. Rehabil. Eng.8: 11–21.

Nishimura Y, Perlmutter SI, Eaton RW, Fetz EE. 2013a. Spike-Timing-Dependent Plasticity in Primate Corticospinal Connections Induced during Free Behavior. Neuron 80: 1301-1309.

Nishimura Y, Perlmutter SI, Fetz EE. 2013b. Restoration of upper limb movement via artificial corticospinal and musculospinal connections in a monkey with spinal cord injury. Front Neural Circuits. 7(57): 1-9.

NSCISN. Spinal Cord Injury Facts and Figures at a Glance. Birmingham: AL; Alabama national Spinal Cord Injury Statistical Center, 2016.

Perlmutter, SI, Maier, MA, Fetz, EE. 1998. Activity of Spinal Interneurons and Their Effects on Forearm Muscles During Voluntary Wrist Movements in the Monkey. J Neurophysiology. 80(5): 2475-2494.

Pohlmeyer EA, Oby ER, Perreault EJ, Stolla SA, Kilgore KL, Kirsh, RF, Miller LE. 2009. Toward restoration of hand use to a paralyzed monkey: brain-controlled functional electrical stimulation of forearm muscles. PLoS ONE 4 e5924.

Shahdoost S, Frost SB, Guggenmos DJ, Borrell JA, Dunham C, Barbay S, Nudo RJ, Mohseni P. 2018. A brain-spinal interface (BSI) system-on-chip (SOC) for closed-loop cortically-controlled intraspinal microstimulation. Analog Integr Circ Sig Process (e-pub ahead) https://doi.org/10.1007/s10470-017-1093-1.

Sharpe AN, Jackson A. 2014. Upper-limb muscle responses to epidural, subdural and intraspinal stimulation of the cervical spinal cord. J. Neural Eng. 11:1-16

Shealy NC, Mortimer, JT, Reswick, JB. 1967. Electrical Inhibition of Pain by Stimulation of the Dorsal Columns: Preliminary Clinical Report. Anesthesia & Analgesia. 46(4): 489-491.

Silva, Nuno A, Sousa, Nuno, Reis, Rui L, Salgado, Antonio J. 2014. From basics to clinical: A comprehensive review on spinal cord injury. Progress in Neurobiology, 114:25-57.

Sunshine MD, Cho FS, Lockwood DR, Fechko AS, Kasten MR, Mortiz CT. 2013. Cervical intraspinal microstimulation evokes robust forelimb movements before and after injury. J Neural Eng. 10(3): 1-10.

Thevathasan W, Mazzone P, Jha A Djamshidian A, Dileone, V, Di Lazzaro V , Brown P.. 2010. Spinal cord stimulation failed to relieve akinesia or restore locomotion in Parkinson disease. Neurology, 74:1325-1327

Varma AK, Das A, Wallace G, Barry J, Vertegel AA, Ray SK, Banik NL. 2013. Spinal Cord Injury: A Review of Current Therapy, Future Treatments, and Basic Science Frontiers. Neurochem Res. 38(5): 895-905.

Vismara, I, Papa, S, Rossi, F, Forloni G, Veglianese P. 2017. Current Options for Cell Therapy in Spinal Cord Injury. Trends Molecular Med. 23(9): 831-849.

Watson C, Paxinos G, Kayalioglu G (eds). 2009. The Spinal Cord. Academic Press, San Diego, pp 1-7.

Zhou HH, Zhu C. 2000. Comparison of isoflurane effects on motor evoked potentials and F-wave. Anesthesiology. 93(1)32-38.

Zimmerman JB, Seki K, Jackson A. 2011. Reanimating the arm and hand with intraspinal microstimulation. J Neural Eng. 8(5):1-14.

Zimmerman JB, Jackson A. 2014. Closed-loop control of spinal cord stimulation to restore hand function after paralysis. Front. Neurosci. 8(87): 1-8.

Chapter 4. vHAB: A Gamified Therapy and Assessment Platform for Recovery After Neuromuscular Trauma

Build and test a novel platform for closed-loop rehabilitation of hand and arm function in patients undergoing physical therapy for stroke and spinal cord injury.

SUMMARY OF CONTRIBUTIONS

This chapter was first published in part as Chapter 4 of Tyler Libey's Ph.D. Thesis titled: *Restoring function after neuromuscular trauma: novel paradigms and tools for volitional control of neural activity in untethered environments and vHAB: a gamified therapy intervention tool for post-injury rehabilitation*. This engineering and clinical work involved many researchers and clinicians and wouldn't have been possible without a team effort. Tyler Libey, PhD and I conceived of the system and made system-level implementation decisions. I architected the therapist/patient workflow, designed the therapeutic activities, and recruited therapists and patients. I also designed the hardware specifications, making many versions of the original EMG recording system and sensor positioning system. I designed the clinical study, wrote and received the IRB approval. Together we performed pilot testing, collated subject data, and analyzed subject data.

A clinical case study is in preparation for publication and the full patent citation (included in section 4.10) follows:

Libey et al. System and methods for automated administration and evaluation of physical therapy exercises. Patent Application 15/154,382. 13 May. 2016.

4.1 BACKGROUND

4.1.A *Introduction*

Injuries affecting the upper extremity, from the shoulder down through the hand have a disproportionate impact on overall quality of life and long-term independence. These injuries encompass direct trauma to the limb, cases of bone fracture, dislocation, and soft tissue damage as well as higher-order injuries to neural control of limb movement for a variety of conditions including stroke, spinal cord injury and neuro-degenerative conditions. The clinical practice of rehabilitation is one of the most important aspects of long-term recovery from these injuries. This is especially true for neurological trauma like stroke and spinal cord injury which require the re-learning of skills after loss of function. Repetitive practice, broadly through the forms of physical and occupational therapy, can lead to neural plasticity allowing patients to regain function over time. For a complete review see Duncan and Lai 1997 [1], Richards and Pohl 1999 [2], and van Der Lee 2001 [3]. Compared to lower limb dysfunction, regaining upper limb function may be more difficult to achieve [4] but brings significant improvements in quality of life. For patients suffering from paralysis after stroke, recovery is highly dependent on the severity of injury. Stroke has significant heterogeneity and there is much ongoing research on what levels of treatment bring the optimal outcomes for varying levels of injury. Motor loss localized to one side of the body, or hemiplegia, and general limb weakness affects approximately 80% of patients following stroke, creating a huge annual population of patients with clinical need for rehabilitation.

Rehabilitation comes in a variety of specific techniques, most of them involving repetition of specific activities with different types of feedback and sensory support. Traditional upper extremity interventions include neurodevelopmental techniques, bilateral arm training,

strength training, task-specific training, trunk restraint, sensorimotor stimulation and training, mental practice, splinting, constraint-induced movement therapy, and mirror therapy. The major categories are detailed below. Recent technology developments and a health system-wide focus on evidence-based care have also fueled innovation in the robotic and digital health delivery of therapy as detailed below. Full context is important for understanding the design choices, parameter space, and long-term goals of developing new technology-based interventions for functional recovery post-injury. These techniques have been clinically tested against each other in a variety of registered clinical trials; however a great deal of diversity exists in clinical practice. This diversity mirrors the heterogeneity of stroke and the lack of understanding of motor learning and functional output reorganization after an individual's unique disease presentation.

4.1.B *Traditional Rehabilitation*

4.1.B.1 Neurodevelopmental Techniques:

Neurodevelopmental techniques focus on inhibiting abnormal muscle patterns and highlighting correct activation patterns in patients. Three main varieties have been adopted in clinical practice over the years. Brunnstom's Movement Therapy [5] promotes synergies of flexors and extensors during recovery, hoping that natural processes will allow specialization later in recovery. Proprioceptive Neuromuscular Facilitation combines manual movement with a focus on the patient's strongest existing movement and verbal coaching to drive functional gains [6]. The Bobath approach puts patients in postures opposed to their developing synergies and relies on autonomic and reflexive responses to drive correct behavior [7]. These treatments have

been found to not be significantly different from each other in patient outcomes [8]. These techniques are the basis for many exercises currently performed in clinic.

4.1.B.2 Task-specific Training:

Specific task practice and performance is required for motor learning to occur and has been established in the rehab space [9]. The intensity of this training does not directly relate to the improvement of function [10]. High intensity, short time programs (3 weeks, 45 min/day) of upper limb training periods have shown improvements in limb function and dexterity [11]. Low intensity, longer span interventions have reported similar improvements in function [12, 13]. The key to this therapy is the task-specific nature of the activities in driving functional outcomes.

4.1.B.3 Constraint-Induced Movement Therapy (CIMT)

CIMT is a slight departure from traditional therapy techniques. To force the patient to use the affected limb in more daily scenarios and increase the focus on repetitive use of the injured limb therapists bind the unaffected limb, constraining it, and preventing the patient from using their good limb for compensatory strategies [14]. Meta-analyses of the technique have shown an improvement across a variety of clinical functional assessments, including Wolf Motor Function Test, Action Research Arm Test, and the Fugl Meyer Assessment [15]. In most cases patients were required to self-administer restraints targeting hours per day and six of seven trials included in the review tracked self-reported adherence and compliance; however the one study that actually tracked adherence found that patients were averaging less than 50% adherence [16]. This underscores an overarching need for compliance monitoring and motivation in rehab to maximize patient outcomes as well as building techniques for allowing the patient to focus use on the affected limb.

4.1.B.4 Mirror Therapy

Mirror therapy relies on visual feedback to improve outcomes. The technique was originally adopted from the field of phantom limb pain treatment. Patients hide their affected limb behind a large mirror and perform rehabilitation tasks with both limbs while doubling visual feedback only from the unaffected limb. A review of mirror therapy applications has shown improvements in daily function, pain, and neglect [17]. This underscores the importance of dynamic positive visual feedback during stroke recovery for neuroplastic and motivational purposes.

4.1.C *Emerging Techniques*

4.1.C.1 Robotic Therapies

One factor in retraining function for weak or hemiparetic arm function is adding support and guiding movement through the use of robotic systems, both active and passive, that can support or move the arm through therapeutic movements. These systems benefit from not requiring any implicit ability in the disabled hand and have shown significant recovery potential in the clinical setting. The first and most notable of these systems is the MIT Manus Robot. The Manus and most others allow patients with very limited function to begin motor rehab at the earliest stages of recovery. Several studies documenting the use of the Manus over the course of a decade have shown definite and sustained patient improvement both in the earliest [18] and later stages of stroke progression [19]. There are a variety of robotic devices currently on the market. However cost remains a significant barrier to clinical adoption at scale, with robots costing between $80k and $1.5M, depending on the model.

4.1.C.2 Digital Therapies

Advances in computer, sensor, and gaming technology have created a new opportunity for delivering and quantifying rehabilitation. Gaming technology has driven the lion's share of the growth of digital rehab. The most relevant platforms thus far have been based on the Nintendo Wii [20] and Microsoft Kinect [21]. Preliminary studies listed previously indicate that this type of gaming technology provides similar outcomes to traditional therapy techniques, but has the added benefit of automatic quantification of therapies and decreased in-person costs. While the manufacturer's platform games have been used in a therapy setting alongside traditional techniques, a number of companies are emerging to create novel content using the respective sensors. These platforms have the ability to emulate most of the types of therapy listed above. These platforms leverage motion capture through specialized infrared cameras and skeleton tracking algorithms as well as handheld controllers that transmit accelerometry data to a computer to control on-screen actions. The scope and scale of these products allow for capture of low-resolution (~10cm) motion capture of normal postures including large arm and shoulder movements as well as balance and posture tracking.

Table 4.1.1 Kinect-Based Therapy Platforms Currently Available

Company	**Product**
Jintronix	JRS-Jintronix Rehabilitation System [22]
Reflexion Health	VERA – Virtual Rehabilitation Assistant [23]
Rehabtics	Rehabtics [24]
Mira	MIRA [25]
RespondWell	Respondwell [26]
5Plus	MFAsT [27]
SPECS Laboratory	RGS – Rehabilitation Gaming System [28]
GES Therapy	GesBalance, GesArcade,GesAircraft [29]

While these systems may be able to address large motor deficits in patients post-stroke, the technical limitations of the systems and sensors are not applicable directly to hand function

recovery. None of the existing Kinect-based systems provide fine resolution for hand motion capture or any additional physiological data streams.

4.1.C.3 Hand-Specific Digital Tools

There are several digitally-equipped glove sensors that use cloth capacitance sensors to detect finger tapping with the Flint Rehab MusicGlove [30] and the digital exoskeleton from Neofect , the RAPAEL [31]. Additional exoskeleton-like passive systems for assistance with flexion and extension of the fingers can be purchased from the Saebo Company. Each of these glove-based systems brings advantages to the rehabilitation process, from quantifying single degrees of freedom in the fingers to providing mechanical support for flexion and extension during movement. Gloveless motion capture for hand function has recently been possible at low latency and low cost following the release of the commercial Leap Motion sensor. There are a few companies with commercially available beta-stage Leap-Motion-based rehab devices including Virtualware based in Europe and VirtualTouchTherapy based in the US.

4.1.D *Tools for Clinical Assessment of Motor Function*

One of the key factors driving clinical excitement about the digital revolution of rehabilitation is the ability to bring rapid, automated quantification into the clinical workflow. Traditional measures include a host of standard questionnaires and rating scales as well as a few basic tasks with primitive outcome measures. A full review of relevant hand and arm qualitative questionnaires for documenting hand and arm function are summarized by Baker et. al [32]. Few of these tests incorporate physiological data into determining a patient's status or progress. Quantified assessments are more vague, including the Box and Blocks task, a numerical count of the number of small blocks a patient can move across a partition in a minute [33] and the 9-Hole

Peg Task, a timed dexterity task requiring patients to remove and replace 9 pegs from holes in a board [34]. While they both provide a quantifiable number outputs, neither of these standardized tests is based on physiological function or data. Other techniques for assessing recovery include surface electromyography and grip dynamometry. Surface EMG is rarely used clinically because of the time and effort required by clinical staff to prep skin, apply electrodes, and analyze data. Grip dynamometry is also used occasionally to track progress during recovery [35]. Advances in digital sensing technology can be leveraged to improve the speed and consistency with which complex measurements of the hand and arm are captured and reported.

4.1.E *Factors in Clinical Adoption*

There are many confounding factors in the adoption of new methods in rehabilitation that impact the quality, length, and intensity of rehabilitation. The American healthcare system places an enormous burden on the speed and efficiency of care delivered through most channels. Proper documentation and billing practices in hospitals, inpatient rehabilitation facilities, skilled nursing facilities, and outpatient centers push therapists to deliver care with very little down time. As a result of these factors innovation and novel techniques are slow to reach the rehab space because there is typically a long delay between innovation and payer acceptance of methods and changes in the federal and private payer structures. Consequently, cost and workflow integration are two of the biggest challenges when creating solutions for long-term rehabilitation.

4.1.F *The Advantages of Digital Health Solutions for UE Rehabilitation*

Digital solutions for quantifying and delivering engaging, focused rehabilitation for the upper extremity have the opportunity for enhancing the current standard of care and extending traditional therapy outside the standard clinical channels. The evolution of low-cost consumer

sensors and ubiquitous computing with laptops, desktop computers, mobile phones and tablets offers a set of platforms from which rehab can be delivered and quantified in the clinic, in post-acute settings, and long-term in the home. The continuity of care across the long-term recovery allows clinicians and patients the ability to understand small changes in function and manage long-term goals to improve recovery potential. Using remote technologies for care management lowers costs of healthcare delivery and improves adherence to care when barriers such as travel and time, are reduced. The digital world also offers the ability to create engaging simulations and repetitive exercises that keep patient's attention and provide tools and content for educating them during recovery while providing task-specific training and repetitions to drive functional outcomes. By providing digital solutions that emulate the key drivers of current therapy standards we can provide care more consistently and deliver treatment more cost effectively to a larger number of patients while tracking detailed data on biometric progress everywhere therapy is delivered.

4.2 SYSTEM SUMMARY AND DRIVING PRINCIPLES

vHAB is a gamified therapy and assessment platform designed to assist patients in upper extremity rehabilitation after an injury such as stroke, spinal cord injury, or trauma. vHAB uses custom software and commodity sensors to deliver fun and engaging games that emulate real therapy tasks (Figure 4.2.1). Therapists can use vHAB with their patients to increase engagement in traditional therapy while simultaneously recording fine details of biometric improvement. This is all accomplished using a motion capture camera to track a patient's hand to control custom games tailored to specific movements. The patient places their hand approximately six inches above the sensor and performs simple movements, such as wrist flexion and extension, which controls various in-game objects. We pair the motion capture camera with a muscle activity armband to provide further insight into the patient's arm function. Combining muscle activity sensing with the kinematic recordings allows us to provide an unprecedented view of a patient's hand and arm during therapy. Data recorded with the system is automatically analyzed to provide detailed measurements to the patient and therapist.

vHAB combines this ability to view detailed progress with the engaging games to enhance adherence to therapy and drive care decisions. vHAB is designed to be used in clinics, such as skilled nursing facilities, outpatient centers, and inpatient facilities, as well as the patient's home after they have left the clinic. This continuity of care allows patients to go home fully understanding the therapy tasks they should perform to enhance their recovery. The software and hardware that comprise the vHAB system are described in detail in sections 4.3, 4.4 and 4.5. In sections 4.6, 4.7, and 4.8 we will discuss the use of vHAB in various pilots and studies, both at home and in the clinic. In the remainder of this section we will discuss the path and design choices made to reach this final system.

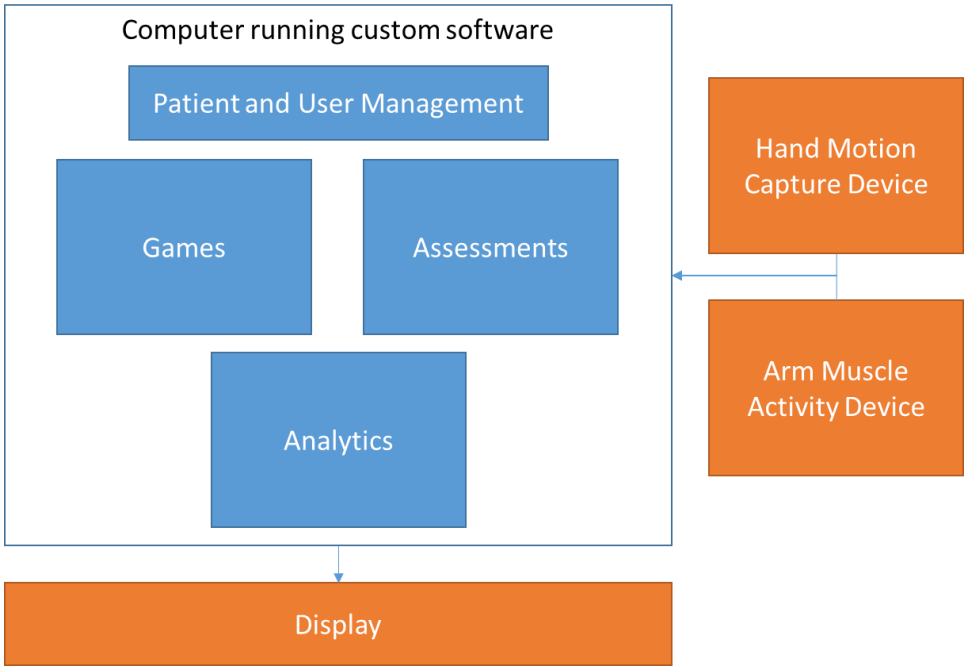

Figure 4.2.1: vHAB components block diagram. The vHAB system uses commodity hardware (orange) and custom software modules (blue) to deliver engaging and cost effective therapy to patients recovering from neuromuscular injuries.

4.2.A *vHAB Design Principles*

vHAB did not start out as the system it is today. The first iteration of vHAB was created with little thought to the end user. We were designing a game platform partially inspired by the Neurogame system created by Moritz et al [52]. The Neurogame system utilized muscle activity of the forearm to control a few actions in a commercially available game. Early conversations with the system's creators revealed that patients were able to get much better at the muscle activity control aspect of the game itself, but that the improved control did not directly translate into functional improvement outside the game environment (C. Moritz, personal communication,

March, 2014). We knew then that we had to develop more effective games, and we established a few key principles of the vHAB system:

1) **The games are simple to understand, only containing 1 task and 1 goal per game module.**
2) **The games are based on existing therapy tasks.**

Our main hypothesis relied on the idea that therapy tasks performed in the clinic are the current best standard for recovery. We believe that having patients perform those exact movements with our system would at the very least be equivalent to the care they were previously receiving, and that then we would not fall victim to the same challenges of the Neurogame system. With those key principles established, we could then attempt to enhance the therapy experience. These advancements were as follows:

3) **Provide feedback to the patient to drive the correct actions**
4) **Make therapy engaging to drive adherence in both the home and clinic**
5) **Present biometric insight to drive quantified, evidence-based care**

These three principals are clearly evident in existing gamified therapy systems, but have yet to be incorporated into a system built from the ground up containing the first two principles. Finally, we fully understood that the system needs to be cost effective and easy to use to reach patients we set out to help. This first prototype of the vHAB system included a $20,000 clinical EMG recording system and a virtual reality headset. This prototype was too expensive, and difficult to set up in practice. This led us to our final development principle:

6) **Use commodity hardware that is accessible to a general population.**

The word accessible refers not only to the cost, but to the usability. We will expand this concept further in the sections below.

Over the course of this project, we have iterated through 4 main versions of the vHAB system to attain these 6 principles. Below we detail some of the major design choices that went into building the system. Changes were informed through interviews and focus groups with end-users and field experts, as well as general user testing of the system with patients and therapists.

4.2.B *Game Design*

As discussed previously, we were strongly inspired by the works of Moritz, among other gamified therapy systems previously described. Many of these systems use commercial consumer games (AAA games) and pass-through software that translates external sensor data into mouse movement or key presses. These systems suffer from three major flaws: 1) learned behavior in the game does not always transfer to physiological recovery or performance in daily tasks, 2) changes in the AAA game, for either security reasons or game improvement may lead to incompatibility with the therapy system, and 3) the game's inherent design does not reflect the therapeutic exercise and may require additional abstraction and training to be effective. We determined early in the design process that to address these flaws as well as meet principles 1 and 2, we needed to create our own therapy games from the ground up. However his brought to light a new problem: we were not therapy experts or game developers.

4.2.B.1 Task Design through Shadowing and Interviews

Early in the development process we established ongoing relationships with occupational therapists, rehab medicine professors, and other field experts. Common themes were present across all of the shadowing and interviews, such as the importance of feedback and functional relevance in a task. During a meeting with Dr. Jared Olson at the University of Washington we came up with most of our early game concepts and some of our design principles. From this

meeting we began development on the first iteration of a reach and grab game and a pinch movement game.

Through a set of meetings with Dr. Janet Powell and one of her Ph.D. students we discussed the importance of accounting for compensation during therapy tasks. Patients will often shrug their shoulders to move their hand higher or move their trunk to reach further forward. In a normal clinical setting this can be accounted for with an attentive therapist's feedback, but at home the patients have no such restrictions or feedback. In our development, we strove to strike a balance between ease of use and preventing unwanted compensation. We also discussed the importance of time sensitivity for clinicians and therapists. They need simple systems that do not interrupt their workflow. Alternatively the system has to be a significant time saver in the long run to be of clinical value. Our system attempts to address this issue through the automatic documentation and assessments, while also providing increased accountability of the therapists.

We had the opportunity to shadow therapists in practice at Harborview Medical Center in Seattle, Washington. In addition to seeing firsthand the antiquated tools they used, we saw the importance of individual finger dexterity and range of motion. One of the most striking examples, however, was a therapist playing a "patty-cake" style game with their patient. The patient was hemiparetic and suffered from spatial neglect. She struggled to keep her right arm in sync with the therapist, but was mostly unaware of her poor performance. The therapist had to continuously remind the patient to watch her right hand, and each time she was given that feedback she was able to perform slightly better. This showed the importance of using both hands concurrently after a hemiparetic injury, and also reinforced the need for audio and visual feedback during task performance. After this experience, we began the development of a two-handed game in which the patient was rewarded for moving both hands simultaneously while we

provide immediate visual feedback that addresses some of the difficulties associated with spatial neglect. It is also important to note that this task was one of the most complex performed in that facility. Most of the other tasks consisted of much simpler movements and instructions, further reinforcing our first design principle.

One of the most important concepts that we are unable to currently address is the use of physical objects during tasks. A significant amount of in-clinic therapy uses putties, paper clips, playing cards, and pencils that the patient is tasked with manipulating in a variety of ways. We knew at the start of our development that we would not be able to view the hand while it is holding an unknown object. These objects are not used as often in the home, usually due to the complexity of the setup. If a patient struggles to pick up a paper clip from the table, they will also likely struggle with getting the paper clip from the packaging or drawer. Additionally, if the paperclip falls to the floor they may not be able to retrieve it. This component of the use experience was particularly striking. We may not be able to use objects, but we can still design an interface and game set that are playable and navigable by the patients.

Many additional games were developed over the course of two years with similar shadowing and interview experiences. We have had the great opportunity to continuously test our developing games with these groups, gaining invaluable feedback and ideas for new games and assessments. Game development during this time was also supplemented with outside knowledge.

4.2.B.2 Game Mechanics and Graphics

We knew we were never going to be able to design a AAA game so we began deriving inspiration from smaller game development studios who use Unity. Unity is a game development platform that uses C# as its main scripting engine and a 3D viewpoint within its IDE to view the

game in real time as it is developed. Developing games within this environment was a clear learning process that shows through our game development history (Figure 4.2.2). Increased familiarity with the software led to clear improvements with the game functionality, leading to fewer bugs and better usability. However, we were still limited in our game design skills, and the games were often clunky and visually unappealing. We were aiming to develop a system that not only utilized principles 1 and 2, but were engaging and fun (principle 4) so that people wanted to do their therapy. To help us meet these goals we reached out to a few experts in the gaming field.

Figure 4.2.2. Comparison of the Reach and Grab game over time. **Left**. Initial working prototype from April 2014. The patient's hand was a brown cube that changed height and width to represent an open vs closed hand. The task of the game was to move the white cubes into the trashcan at the bottom left. UI elements were placed randomly throughout the environment. **Right**. Modern version from May 2016. The icon of the patient's hand opens and closes with the patient's hand. The task is functional, in that the patient moves fruit into a bowl. UI elements are offset from the environment.

4.2.B.3 Difficulty

We knew the importance in designing games that are playable by patients with differing degrees of impairment, but we were unsure how to accomplish this. In our case, our adjustable

parameters were primarily related to the mapping of real world movement to in game movement. By increasing and decreasing the "Sensitivity" values we can make a game easier or harder respectively. Increasing difficulty of a standard game can be done automatically as long as it is seamless, but in our implementation we are also dealing with issues of fatigue and pain. We met with an expert in game difficulty design with experience in designing adaptive educational games (Yun-En Liu, personal communication, November, 2014). We discussed these main issues and began prototyping multiple systems for handling difficulty control. While we created automatically adjusting settings algorithms based on performance or time, we concluded that in the early iterations of the system, simple is better. In the current instance of the system, the therapist has full control of the settings while the patient is in the clinic. The home version, however, has preset easy, medium, and hard settings. This was a difficult engineering choice, where the game design principles were overwritten by the ease of use principles presented from the therapists. While changing settings may take more time, they provide direct control to the therapist and do not require increased learning to understand what the system is doing. Difficulties are set to the easiest settings for each patient at the start of their therapy. Increasing the difficulty is optional at this point, which ensures that the therapists and patients do not become frustrated with the automatic-style systems. These automatically adjusting systems will be further explored later as we continue to learn more about our system's use in practice.

4.2.B.4 Engagement

Throughout the design process we discussed game design principles with Dave Roberts from PopCap Games and Peter Anderson from both Bigfish Games and DoubleDown Entertainment. These three companies represent a combination of commercial casual, AAA, and gambling games. Showing our system to these individuals brought about two main concepts that we

incorporated into the development of vHAB and the fulfillment of principle 3. Firstly, our graphic design and game modeling abilities are limited from both a skill and cost perspective. If this is the case in other fledgling game companies, traditional practice stresses that it is more important to focus on game mechanics and usability rather than trying to improve the visuals of a game. Further, steps should be taken to future proof the games so that improvements can easily be made. Following this advice, we began modifying existing games to have a plug and play visual style. This has allowed graphical transitions as shown in Figure 4.2.2 to happen swiftly without slowing down usability of the system.

Secondly, while addictive is a word we tend to avoid in the medical space, we surely want our games to keep people coming back to their therapy on a daily basis. In the casual gaming space, this is accomplished primarily with engagement "wrappers" that tie the game's individual mini-games together. A popular example is PopCap's Peggle which uses Unicorns and other animals as mascots throughout the experience, despite the game having nothing to do with these fantasy creatures. This concept resonated well with vHAB since each of our games has a different theme (or no theme at all). As in the models discussed above, however we did not have the expertise to design a theme around our system. To accomplish this we sought an additional collaboration with the Digital Future Lab (DFL) at UW Bothell to create our garden wrapper. Over the course of 12 weeks, we partnered with the DFL to design the wrapper and modify our overall user interface (Section 4.2B). This included the creation of art assets and diagrams suggesting the proper use of these assets. For the wrapper DFL did some initial demographic focus group testing of the persons that would fit the skilled nursing facility market. For this testing, they proposed both a travel metaphor and a garden metaphor. While the testing was not substantive due to time constraints, evidence suggested that the garden metaphor would have the

most traction with this market. Again, as in the 3D modeling, we have built the wrapper in a way that could be easily extended into a travel, or other themed, metaphor. The garden wrapper sits as a separate set of UI elements in the Game Select Screen (Section 4.4.A.7-8) and within the games themselves (Section 4.4.B). Within those sections we fully describe the individual aspects of the garden wrapper. Overall, we believe the use of the garden wrapper will aid in the patient's desire to return to the system over the course of their recovery.

4.2.B.5 Instructions and Tutorials

As previously discussed, we set out to design simple games, with only one task and one movement. While we succeeded fairly well in this game design, we struggled with the patient experience with the system. Users were verbally instructed to start with their hand about 6" above the sensor, but for nearly all first-time users (patients and otherwise), patients would place their hand directly on the sensor, sometimes even picking it up and waving it around. Solving this design problem was two-fold: we slightly modified the hardware, which we discuss in Section 4.2.D.2 below, and we began creating tutorials within the games.

Early tutorials consisted of in-game video overlays (Figure 4.2.3 (Top Left)), which were often obtrusive and barely helpful, or a series of looping images in the top left corner of the game (Figure 4.2.3 (Top Right)) which were time-intensive to create and had limited success in helping patients understand the game. These systems were steps in the right direction but did not quite reach the level of instruction we needed. With the help of DFL, we designed non-blocking tutorials that led a new user through each game (Figure 4.2.3 (Bottom)). A non-blocking tutorial provides information to the user while allowing them to perform the same actions they could normally. For example, in *Reach and Grab*, a user is instructed to reach out and grab virtual fruit and place them in a bowl. The tutorial starts with a text popup saying "Place your hand 6" above

the sensor." As soon as we detect their hand over the sensor, we show them their virtual hand and the text changes to say "Move your hand towards the fruit." As their virtual hand moves towards the fruit we then present them with the next prompt. These tutorials are designed to be ignored by experienced users, but helpful for first time users. They allow for general exploration of the virtual space and are only presented during the patient's first play through of the game. Any tutorial can be retriggered through a button in the user interface.

Figure 4.2.3. Tutorials for the Ball Roll game throughout vHAB development. Top Left. A quickly abandoned tutorial method. Clicking the small "?" button in the top left corner would popup a video showing the system in use which would block the user's view of the game. **Top Right**. A less blocking, but inefficient tutorial method. The image on the top left would cycle through 6-10 frames showing how to play the game. These were effectively carefully controlled videos with additional information overlaid, but were not viewed as very helpful in our pilot studies. **Bottom**. The current tutorial method. Our current method has less information that either

of the previous versions, but has been viewed as much more helpful. We still include video tutorials, but they are in the game select screens before the game is loaded (Figure 4.2.5 (Bottom)).

Through our work with Digital Futures Lab we also determined that our potential offering of 17 games would be too many for any therapist to start with given our current UI system. We noticed this as well during one of our first pilot studies (Section 4.6), where we tried to explain how just 10 games worked over their short 1-hour lunch period. Our current system has more than 10 games built into the system, but only 7-10 are presented at any given time. Further, we have developed training documentation and one-sheet summaries that we leave behind with the therapists for further reference.

4.2.B.6 Game Audio and Visual Feedback

Early versions of the vHAB system did not include any audio feedback. Additionally, the visual feedback only related to either a "score" event or the movement of the patient's hand. This made the games relatively mundane over longer playthroughs. Adding sound effects to contact events made a huge difference in the games, while also making many of the games easier to understand. Many people who played *Reach and Grab* would move their hands into the fruit and try to make a fist, which led to a very unnatural experience (Figure 4.2.4 (Left)). Further, the fruit would be held in odd positions with the virtual hand or they wouldn't know whether they had successfully grabbed the fruit before moving away. With the assistance of the Digital Futures Lab, we designed and implemented a "magnetization" system (Figure 4.2.4 (Right)). The magnetization system works by quickly moving the target virtual object to the correct position under the patient's virtual hand as soon as the hand is nearby. During this movement we provide

a “zip” sound that informs the patient that they have successfully moved towards the object. While the object is in position, the patient can make a fist to “grab” the object which is signified by both the change in hand shape and a “ding” sound. The patient can move the magnetized object around while in a small area without grabbing but if they move out of that range the object will move back to its starting position. This change to the visual feedback, with the addition of task related sounds, made the games much easier to play and understand.

Figure 4.2.4. Reach and Grab grabbing control techniques. Left. Initial control system. In this version the virtual hand could intercept the fruit before a grabbing motion was made, causing an unnatural experience for the user. **Right**. Current magnetization control system. This version may feature floating fruit, but it allows for the user to know they are in the correct position to then make a fist to grab the fruit.

4.2.B.7 Assessments vs Games

All of our games make measurements related to that game’s task and associated functional movements. These measurements include individual joint range of motions, reaction times, tremor, and many others. Over time we have refined these measurements, making them faster to compute and more robust to missing data or short sessions. Each game, however only computes a few task related measurements. We set out to design a system that allowed for a full workup of arm function that could be performed periodically throughout a patient’s recovery. This would

allow a therapist to identify weaknesses in the patient's progress and adjust care accordingly, while simultaneously providing a reliable and consistent measure. Our first attempt was the creation of vAssess, a preloaded set of tasks that led a patient through making a fist and squeezing, reaching range of motion, and wrist range of motion measurements. vAssess was well received with outpatient clinics who did not necessarily perform therapy in clinic, but wanted a consistent way to measure progress. However, most of these clinics are very time-restricted with their patients and vAssess took anywhere from 3-5 minutes to complete. Further, the clinicians only cared about 2 or 3 of the 10 measurements we were presenting. We incorporated this feedback into the creation of a modular assessment system that allows for custom sets of tasks to be created for specific uses (Section 4.4.C). Now a clinician can create an assessment that only performs the wrist angle range of motion measurements, saving time and making the presented results easier to understand.

4.2.C *UI Design*

The user interface for the vHAB system has undergone nearly as many changes as all of the games combined. First we needed a way to manage navigating between all of the games, then we needed a way to change the settings for each game. Next we needed a way for patients to have their own settings, so that when a therapist started using a system with a patient they didn't need to reset all of the settings. Finally we needed a way for a therapist to create new patients and identify them easily, which required a login and therapist management system. This base functionality then allowed us to add items such as patient notes, data viewers, and patient dashboards. All of these systems are described in detail in Section 4.4.B. In the following text we describe a few of the design changes that led us to that final system.

4.2.C.1 Aesthetics

One of the important changes throughout all of our user interface screens was color and UI element consistency. This was not one of the strongest pieces of early feedback from healthy users, patients or therapists. These groups certainly cared more about system functionality than aesthetics, but as became apparent in early user testing, the system would see easier adoption with a cleaner and more consistent UI. Users would often miss some functionality because it was hidden behind some off-color button that they thought was just a label. As an example, for many months during an early pilot, no one knew they could take notes on their patient because the "User Profile" tab (Figure 4.2.5 (Top Right)) was the same color as the currently visible level navigation panel. We have made substantial efforts to make UI elements consistent in our development since this feedback.

4.2.C.2 Level Navigation

We tested multiple level navigation and level organization methods throughout the course of development. We started with just numbering each scene and using keyboard shortcuts to navigate. This clearly would not last in a clinic, as even the developers has difficulty remembering which game was assigned to each number. We then moved to a UI button system where each game had a static button on the screen that loaded the game (Figure 4.2.5 (Top Left)). This quickly became a problem as we started swapping games in and out. We then moved to a dynamic button list that was generated based on all the levels in the system (Figure 4.2.5 (Top Right)). This worked much better and was great for use by the therapist; however many patients had difficulty pressing the smaller buttons. As we added the garden wrapper and moved to a unified patient experience color theme, we settled on the current game select screen (Figure 4.2.5 (Bottom)). The therapists can then limit the games displayed on this screen through a

separate Game Settings screen (Section 4.4.A.4). Our next challenge with the level navigation comes alongside the addition of more games. One of our long-term goals is to categorize the games based on functional movements or associated activities of daily living. This will require yet another level navigation redesign to ensure the system works well with both patients and therapists.

Figure 4.2.5. Level navigation screens throughout vHAB development. Top Left. First button focused level navigation menu from version 0.1.4. This menu was easy to use, but was limited in the information provided about each game. **Top Right**. A more organized level navigation menu from version 0.3.9. Here we provided more information for the therapist, and were closer to the correct solution. The "User Profile" tab was eventually moved into the patient dashboard screen (Section 4.4.A.3). **Bottom**. Final level navigation screen. With the addition of the garden wrapper, the layout in 0.3.9 was not sufficient for the amount of information

provided. Further, we wanted to scale back the number of games presented at any time to enhance the user experience.

4.2.C.3 Settings Controls

Modifying settings within the vHAB system is crucially important for not only ensuring that a patient can play a game at the beginning of their therapy, but that the game can become harder as the patient recovers. The very first iteration of settings controls required a complex pressing of buttons while in a game that resulted in unclear functionality while simultaneously blocking the gameplay (Figure 4.2.6 (Top Left)). This was quickly discarded in favor of an intermediate screen that sat between the level navigation and the start of the game (Figure 4.2.6 (Top right)). This still provided a confusing experience for the therapists, especially when they did not want to modify any settings. The current iteration allows settings to be changed in two ways, both of which are easy to do, but fully optional. The first is with a special Game Settings screen (Figure 4.2.6 (Bottom Right), Section 4.4.A.4) and the second is with an in-game popup accessible in the in-game UI (Figure 4.2.6 (Bottom Left), Section 4.4.B). These two complementary methods allow for session planning before a patient is present and for real time changes in response to the patient's performance. Additionally, we have made many changes to the names and values associated with the settings. In the game functionality a value may range from 0.3 to 5.3 and be named "fingerAngleGain", but we remap this to a 1-10 slider named "Sensitivity". Finally, all settings are paired with detailed descriptions and usage suggestions that can assist a naïve therapist.

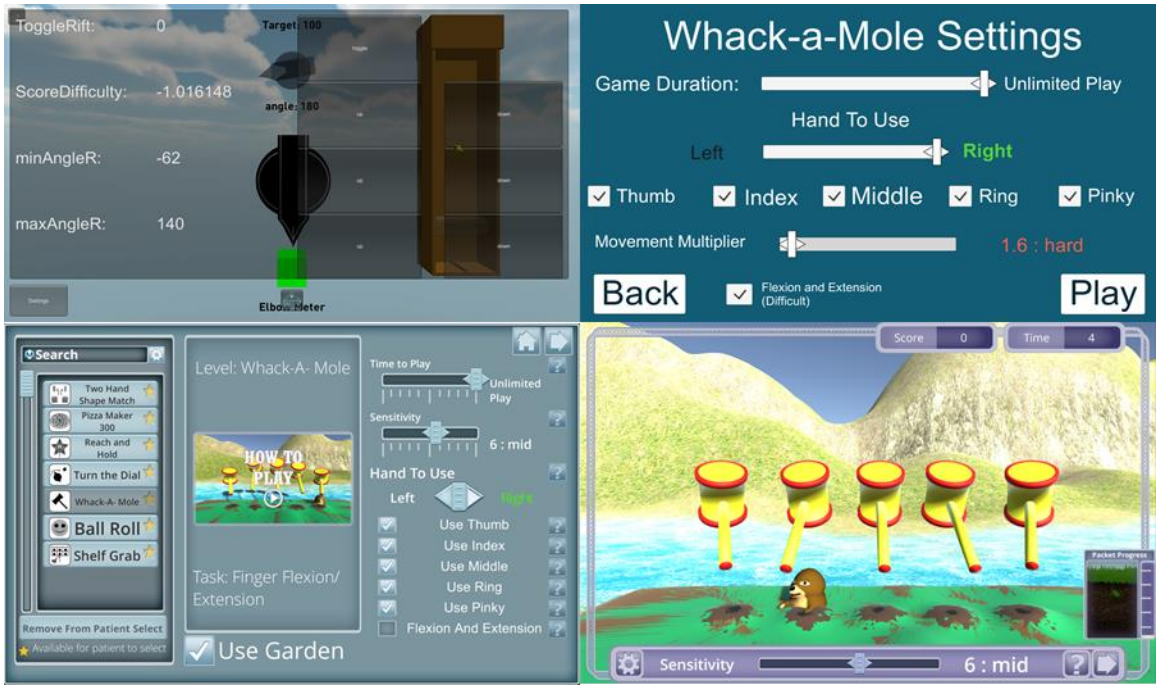

Figure 4.2.6. Game settings throughout vHAB development. **Top Left**. Early settings management system in the dial turn game (v 0.1.4). Here we used the Dial Turn game settings as the example since it had the most settings at the time. This system allowed for changes within the game, but blocked gameplay and was difficult to understand. A score Difficulty of -1.016148 was an irrelevant number for both us as developers and the therapist. **Top Right**. The settings management system from version 0.3.8. Here we started getting better at describing the settings, but having a separate screen in between game select and the game did not work with therapist workflow**. Bottom Lef**t. The Game settings screen of the current version. Here a therapist can control the settings for each game before the game select screen is loaded. **Bottom Right**. In-Game Settings in the current version. Alternatively, the therapist can change the settings in game without hindering the patient's ability to play the task.

4.2.C.4 User Interface Flow

The user interface flow underwent extensive changes throughout the development process as we iterated on making the experience seamless for therapists and patients. In early builds, the level navigation system, like one shown in Figure 4.2.5 (Top Left), was the first screen the therapist saw. The patient management and therapist management were added at the point when we needed a way to load patient specific settings. After this point we had 4 distinct UI screen types: therapist login, patient select/management, game settings, and game select. Integrating with therapist workflow is one of the greatest challenges in ensuring the system's ability to help patients. We attempted to minimize the number of button presses a therapist would need to perform to start using the system. This is balanced, however, with system security and clarity of use. We eventually made the game settings screen an optional screen supplemented by in-game settings, but getting to this settings screen was not straight-forward and the system was overly circular. Therapists would find that they had accidentally logged out a patient in the process of changing settings and were then unsure if the changes had stayed the same. For the most recent version we added a patient dashboard screen. This screen comes directly after a patient is logged in and acts as a patient "home" screen. Four simple options are presented in the dashboard that categorize the actions a therapist can take: Games, Assessments, Settings, and Data Viewer. Each of these screens has home buttons that take the patient straight back to the dashboard.

4.2.C.5 Data Presentation

A core feature of the vHAB system is the automatic measurements that occur while a patient is playing a game or doing an assessment. While calculating these measurements is relatively straightforward (Section 4.5), presenting them was an entirely different matter. To accomplish principle 5 we needed to be able to inform the therapists how their patients were

performing within any given game session. We attempted to do this in real time with the first few iterations of the system (Figure 4.2.7 (Left)), but this was obtrusive and was not very useful for tracking progress. We then moved to a small graph present in the Game Select screen (Figure 4.2.7 (Right Top)). This graph created points for each instance of the game that occurred and plotted them each on the graph. This method was flawed for two main reasons: 1) the data was presented linearly, but not collected that way. A session 4 days ago had the same spacing as two sessions within the same day, which made the data difficult to interpret. 2) The graph was quite small and we had lots of different variables to present. A toggle system allowed therapists to turn on and off the displayed variables, but it wasn't quite enough to present the data clearly. We ended up creating a completely separate screen for viewing patient data and modified the x-axis to be calendar based (Figure 4.2.7 (Right Bottom)). Therapists can view data based on day, week, or month, allowing for easy comparison of values over time. The toggle system still exists, but as a larger UI Element. In future iterations we will modify the toggle system further by presenting the most useful variables at the top of the list for easy access.

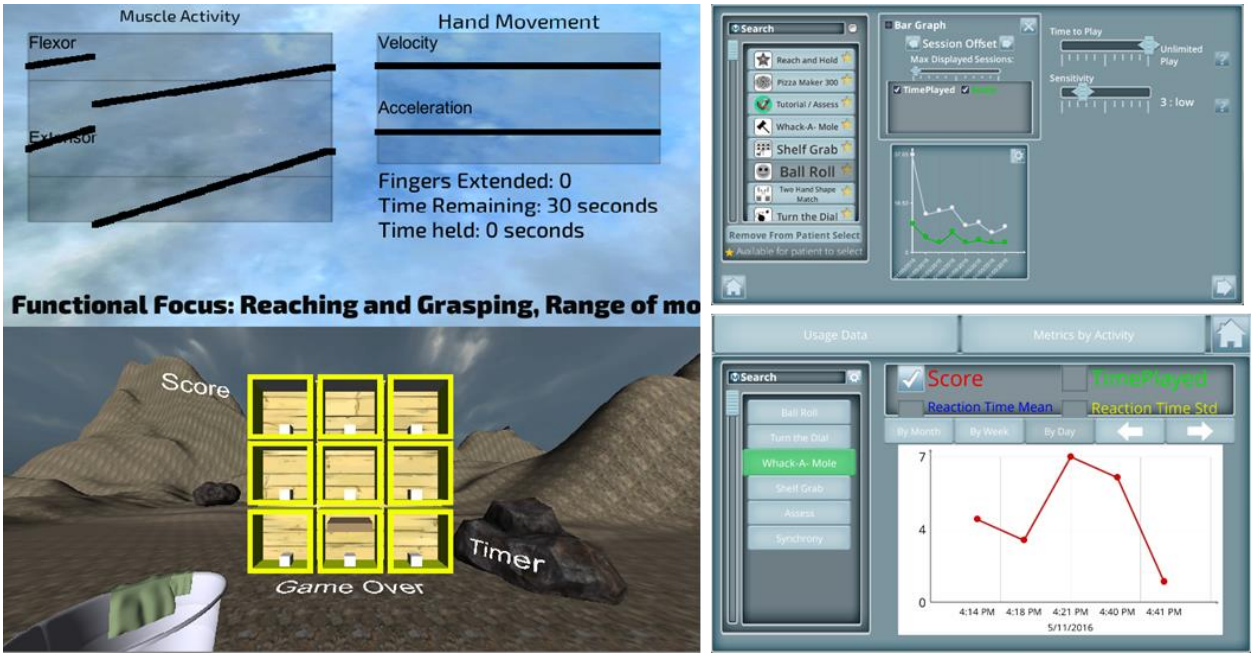

Figure 4.2.7. Data presentation methods throughout vHAB development. Left. Full data presentation framework for *Reach and Grab* in version 0.1.2. This full panel was viewable on the system screen showing muscle activity and key metrics updated in real time as the patient played the game. Aside from taking up half of the screen, the data wasn't useful for the average therapist. **Top Right**. Data presentation framework for version 0.4.7. Data was presented alongside game settings in a small panel in the center-middle. Options to control the graph were available as a popup immediately above the graph. Presenting data here was succinct and allowed for a one-screen therapist planning portal, but ended up being too small to be useful. **Top Left.** Current data presentation framework. This full screen viewer contains much of the same information as that in 0.4.7 but is larger and presents the data by time, not session.

4.2.D *Hardware design*

While vHAB is primarily a software platform, the therapy we deliver would not be possible without the sensors and systems we use. By bundling the hardware with a pre-loaded computer

we ensure that the system is easy to use out of the box. This is a key component of what we have developed. Early feedback and research into other therapy devices showed clearly that having a software download that required external peripherals would never make it to the patients. Jintronix, for example, attempted to sell a Microsoft Kinect based therapy platform into facilities but required the therapists or patients (for home use) to purchase and set up the Kinect on their own (P. Goodrich, Madrona Principal, Personal Communication May 2014). This delivery model was not successful and now Jintronix bundles all of their hardware together with pre-installed software. In following this model, alongside principle 6, we set out to create a bundle of hardware that is still easy to use and robust to user error. A full description of the final included hardware along with its specifications, capabilities, and connections is provided in Section 4.3.

4.2.D.1 Display and Computation

The first version of the vHAB system was designed to use a virtual reality (VR) headset (Figure 4.2.8). Immersive VR offers many benefits to the vHAB system that are difficult to describe to a naïve VR user. Using VR with the vHAB system allows the users to feel as if they are directly controlling the game object as opposed to moving their hand which in turn controls a virtual object. Further, VR removes a patient's affected limb from their view. This allows the vHAB system to display function that may be greater than their actual ability to drive progress. These benefits, however, are not fully explored as the use of VR currently violates our 6th design principle. VR headsets are expensive, even two years after we first prototyped a VR system. This makes delivering the full bundled system to a care facility very difficult and a home user nearly impossible. Further, VR headsets are difficult to put on by a healthy user, let alone a patient suffering from a neuromuscular disability. Even if a patient has help to put on the system, they

may reject it for cosmetic reasons. One early piece of feedback we received when testing our VR prototype was “I’m not putting that thing on my head” from a user who didn’t want to mess up her hair. VR is a hardware display technology we are actively following for future improvements to the vHAB system, but for the current version does not represent a good design decision. Using a tablet system or desktop screen provides a great experience for users that is more cost conscious and accessible.

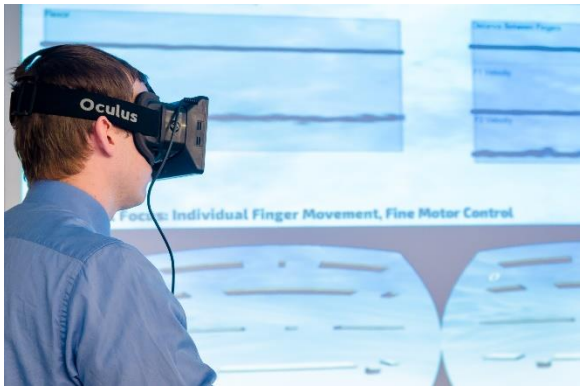

Figure 4.2.8. VR Headset used in prototype version of the vHAB system. In this example, the user is playing an early version of a pinching game using the VR headset.

The choice of computers for the vHAB system is primarily driven by the availability of USB ports for our peripherals. Significant testing was performed on multiple tablets to determine the most cost effective option for the end-users. Many tablets do not have USB ports and others use processors that are not fast enough to provide enough data for our analysis or a smooth game experience. This led to a tradeoff between cost of the hardware and user experience. The most expensive tablets would provide the best experience, but a lower cost tablet may lead to lags in the game controls or sparse data. In the end we decided to utilize the middle end Surface Pro tablets from Microsoft, but are continuously evaluating new technology as it becomes available.

4.2.D.2 Peripherals

The peripherals are the leading drivers in vHAB's hardware functionality. Traditional computer peripherals (ex. Mouse, keyboard, game controller) are efficient and ergonomic input modalities, but they do not capture the actual movement of the hand that is driving the control. Input modalities that more closely mimic physiological function have become more prevalent alongside the adoption of commercial virtual reality and gaming systems. For example, the Microsoft Kinect has seen widespread use in therapy [25] due to its ability to accurately track body posture and limb positions.

For our system, we needed an accurate representation of the hand's movement, which large camera-based systems such as the Kinect do not provide. From the beginning of the system's development we have used the Leap Motion controller to track the hand kinematics. Hardware changes relating to the Leap primarily revolved around placement and use of the sensor as opposed to its cost or capabilities. This hand movement tracking provides the "what" of the movement, but does not provide the how. The relationship between hand movement and muscle activity becomes more difficult to predict with neuromuscular traumas. One common complication after a stroke, for example, leads to decreased muscle control complexity, as patients work to compensate for spasticity with over-exerted movements [36]. Measuring the muscle activity of a patient throughout their recovery provides insight into "how" a patient is moving. By combining the muscle activity with kinematics, we can immediately verify the movements the patient is making without supervision. This allows us to make comparisons of muscle activity across activities based on the precise movements as opposed to second hand therapist records. Our muscle activity recording systems, however, have changed dramatically along the way.

Hand Motion Sensor – Leap Motion

The main challenge we've had in the use of the Leap Motion sensor came from its inherent novelty to our target end-user. Very few people have used optical motion trackers, such as the Kinect, outside of gaming enthusiasts and those few who have undergone new therapy sessions using these systems. Further, people are used to interacting with a computer with their hands, but always through touch. The Leap requires people to hold their hand about six inches above two stereoscopic cameras embedded within the sensor. In many cases, however, people would either place their hand directly on the sensor, like they would for a computer mouse, or they would pick it up and wave it around. To address this, we designed a plastic holder for the Leap to make it seem more permanently grounded. This holder extends the Leap's physical footprint on the table, while making it more cumbersome to hold. Our current 3D printed prototypes seem to have helped account for these user errors, but significant testing is still underway.

An additional problem we saw in development was that therapists often placed the sensor too close to the display screen. This would prevent patients from being able to reach forward far enough to reach targets in any reaching style game. To assist therapists in the setup of the system, we designed a custom mousepad with outlines of the ideal peripheral and tablet placements.

Muscle Activity Sensor

The first vHAB prototype used the Biometrics Muscle Activity Sensing platform, a $20,000 clinical-grade system that could record precise muscle activity at a high data rate (1-2 kHz). This system required sticking electrodes onto the patient's forearm where the electrodes were attached to a bulky wireless battery pack that would sit awkwardly on the table. Aside from the cost and obtrusive physical qualities of the system, the system required that the electrodes be

placed in the same orientation and position for each use in order to compare data across sessions. While this may have been possible to achieve in a development setting with careful planning, it was not going to possible at wide scale use by untrained therapists. This system clearly violated principle 6, so we set out to find an alternative.

At first, we set out to create our own muscle activity sensing sleeve. Fair progress was made towards this goal, but part of the way through the development a commercial alternative named the Myo Armband, by Thalmic Labs, was released at a $200 price point. The Myo records 8 channels of bipolar muscle activity using equally spaced electrodes set within a plastic armband. The armband transmits data wirelessly through Bluetooth Smart and contains a rechargeable battery. However, the data recorded by the Myo only has 8 byte resolution and updates between 50 and 100 Hz, depending on the required transmission distance. This is a significant downgrade from the clinical system used in our prototype, but represents a good tradeoff in cost and ease of use. The cost, however, still may be prohibitive for some of our end-users and is not normally included in the home version of vHAB. We decided, based on customer feedback and internal analysis, that having muscle activity data for the average home user was not as important as the standard range of motion data gathered by the Leap alone, and therefore did not justify the increased cost.

4.3 System Description: Hardware Components

The hardware systems used to support the vHAB software consist of several parts that encompass both the computation hardware and physical sensors as well as the peripheral hardware accessories that provide enhanced usability and clarity for system setup in the clinic and at home (Figure 4.3.1). Each of the components contribute to system data requirements or clinical usability.

Figure 4.3.1. Block diagram of vHAB hardware components and image of assembled Home system. Individual hardware pieces are connected through a combination of wired and wireless methods while accessories aid in system setup and use.

4.3.A *Tablet Computer Hardware*

The vHAB system runs on the Microsoft Surface Pro line of tablets. Tablet computers are an important design choice for use in the clinical rehabilitation setting. Therapy gyms are crowded and often therapy is provided in a variety of settings including standing in gym, sitting in gym, and bedside for patients who are unable to travel to the therapy gym. Tablets combine the

necessary portability and small size factor while not sacrificing computational power. The Surface tablets run full Windows Operating Systems, have touch screen input, support Intel i5 processors, and have a dedicated USB 3.0 port for connecting to peripheral sensors. For device implementation all standard software is removed from the tablet prior to use to create a clean slate for the vHAB installation.

4.3.B *Leap Motion Kinematic Sensor*

The Leap Motion is a commodity camera system designed to use hand gestures to control objects while engaged in a Virtual Reality Headset environment. The system uses stereoscopic visual and infrared time-of-flight cameras with proprietary low-resource overhead to output computational estimations of up to 2 hand positions over the hemispherical sensor capture area. The outputs of these hand positions are noted in figure 4.3.2. The positional accuracy of these outputs has been documented at .2mm [37]. The positional data is output at 120Hz over a USB 2.0 or greater connection. Because of the nature of the stereoscopic infrared illumination there are some limitations to device performance that could potentially affect system use in certain environments. In the presence of direct sunlight or

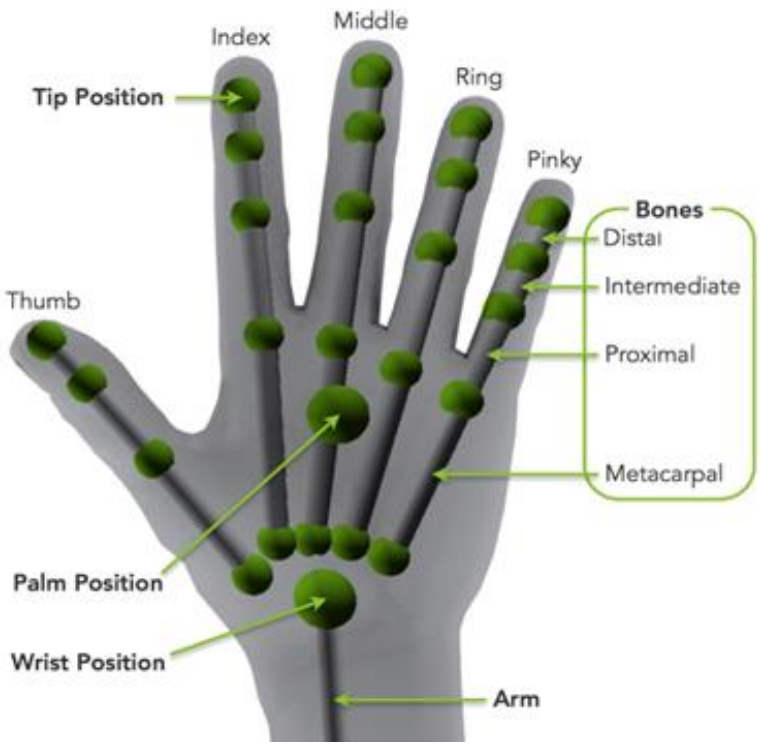

Figure 4.3.2. Example kinematic output from Leap Sensor API [38]. The Leap sensor provides direct access to individual joint positions (green spheres) as well as direction vectors (grey bars) of up to two hands at a time.

4.3.C *Leap Motion Holder*

The Leap Motion camera is a symmetrical device with a USB output cable. Early patient and clinical beta testing exposed the need for a carrier device to properly orient the Leap Motion for naïve clinical users and patients alike. We designed a case for the sensor that properly oriented the sensor in front of the user and provided additional information on hand positioning over the sensor (Figure 4.3.3). A 3D model of the holder was created in the Blender development environment (blender.org), exported to the CatalystEX 3D printing software, and printed to size using a uPrintSE laminar 3D printer (Stratsys, Eden Prairie, MN).

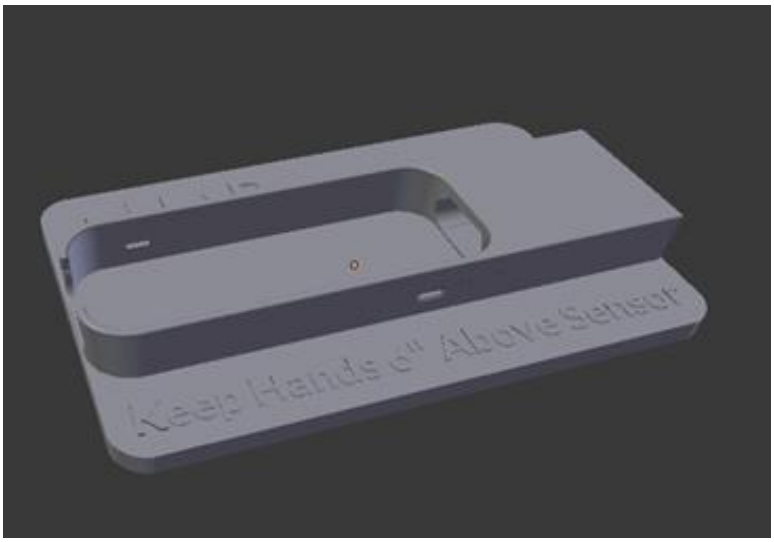

Figure 4.3.3. 3D Rendering of computer model used for holding Leap Motion Sensor in the correct orientation. The holder assists in device placement and prevents patients from picking up the sensor.

4.3.D *Myo Armband*

One of the fundamental barriers to technology adoption in the rehab space is complexity and time spent in preparation. The Myo EMG Armband is a commodity 8 channel dry, bipolar surface EMG system equipped with simultaneous gyroscopic and accelerometry-based data streams (Figure 4.3.4). The primary function in commercial applications is the gesture-based control of assigned functions that plug into existing software modules to provide a new input modality to computing devices. The device communicates over the Bluetooth Low Energy (BLE) protocol. The data from the Myo consists of 8 raw EMG channels sampled at 200Hz, accelerometer and gyroscopic data sampled at 50Hz, and pre-classified pose data. Our application centers around the EMG data acquisition so all other data is disabled during acquisition. The primary design consideration in choosing the Myo as a data acquisition device is

the user friendly and adjustable armband which can be easily cleaned between patients while providing high fidelity EMG data. We have developed algorithms that provide a rotational normalization of electrodes to account for inconsistent placement between sessions. This information will be detailed elsewhere.

Figure 4.3.4. Myo armband with exposed sEMG contacts. The design of the band allows for use on arms with circumference between 7.5 and 13.4 inches.

4.3.E *Setup Placemat*

The vHAB environment facilitates full reaching and grasping motions. To facilitate the correct placement of the sensor to capture the full (~16") arm extension from a neutral position we created a setup placemat that specifies the correct orientation and spacing of the hand sensor. The design includes placement instructions for the screen or monitor as well as the hand sensor. It also includes written instructions for interacting with the hand sensor and directions to a web site for any technical issues. The design was created in Adobe Illustrator and realized on a custom-printed 11x17x1/16" foam mouse pad.

4.4 System Description: Software Components

4.4.A *User Interface and User Experience*

A key component of the vHAB system is a seamless user experience for both the patient and the therapist. Early in the development a large emphasis was put on creating games that were intuitive to start playing, but as we kept adding new features and additional settings it was clear that we needed a UI to wrap it all together. Further, as we shadowed therapists and gathered early product feedback we began to see the importance of patient-specific data, which led to the need for a therapist-specific patient management system. In the following sections we describe the functionality of the user interface and the design choices made to reach the final version.

The front end user interface for facility use consists of 7 screens: A1: Therapist Management, A2: Patient Management, A3: Patient Dashboard, A4: Settings Management, A5: Data Viewer, A6: Assessment Select and A7: Game Select (Figure 4.4.1). The Game Select also contains an optional engagement Wrapper (A8). The interface is organized to account for multiple system use cases. For security and privacy reasons we hide a majority of the patient specific information behind both a therapist login in A1 and a patient select in A2. Further, if a therapist primarily uses Assessment modules, but rarely the Games, the dashboard will allow them to see the information most relevant to them. The home version of vHAB consists only of screen A7 and the Wrapper. This slimmed down version provides a much simpler interface for patients to navigate at home, even if their movement is impaired.

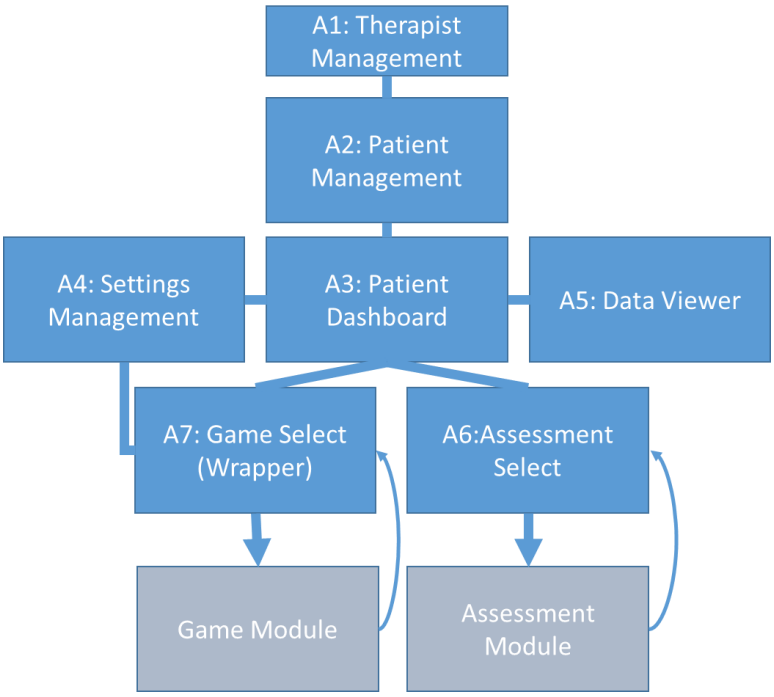

Figure 4.4.1. Screen flow for vHAB User interface. Blue boxes represent individual user interface screens used for managing user information and settings prior to using a game or assessment (Grey boxes). Lines between flows represent a bidirectional option to change screens, whereas the arrows represent a one way flow.

The 2D assets for the user interface were primarily designed through a collaboration with the Digital Futures Lab at University of Washington Bothell. During this design phase we took our initial user interface concepts and molded them into the final version seen below. This process created a few overall design guidelines such as color, element positioning, and margin styles. Asset creation was handled primarily in Adobe Photoshop and Balsamic. Photoshop was used in the image creation, while Balsamic was used for prototyping the organization of the individual components (Figure 4.4.2). Further image editing was performed in GIMP, an open source editing program, or Adobe Illustrator.

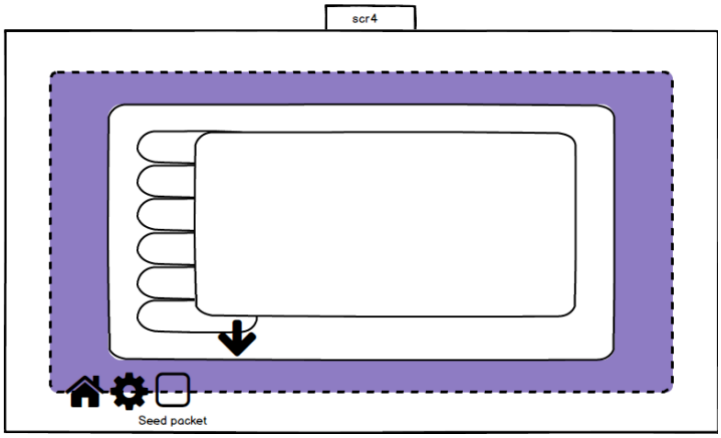

Figure 4.4.2. Early Balsamic markup of the Game Select Screen. Balsamic was useful in prototyping what a UI screen might look like early on in the design process.

The creation of each screen was accomplished by assembling the 2D assets alongside scripting components in the Unity game engine. The Unity engine contains prebuilt UI functions through a set of Canvas elements. Each element contained functions such as “OnClick” handles for “Buttons” and “On Value Changed” handles for input fields. These prebuild functions were useful for creating basic functionality, but custom scripts were required in each screen to build a working interface. Navigating between screens was accomplished through a set of custom “screen navigation” functions and Unity’s built-in scene manager. These screen navigation functions also handled information between screens by either saving variables to local or system memory.

The vHAB UI is also built for multiple screen resolutions. While we currently are deploying primarily on the Surface Pro line of tablets, other use cases may demand support for more resolutions. Within the Unity Canvas framework, all UI elements can be set to scale their widths or heights up or down in relation to a base resolution. When each UI element is placed on the screen in Unity, we also set a set of scaling parameters that dictate how it will scale. This

solution is far from perfect. Some elements scale better than others, mainly based on how they were created, which results in empty space on the screen, or oddly pixelated items. It does however, ensure that all of the information is available to the user, regardless of their screen resolution.

Key Concepts

Patient User Name (pUN): The pUN is a display handle used in screen A2 to select the correct patient to work with. We recommend that the pUN is not the patient's real name to limit the PHI we are storing.

Patient Identification String (pID): The pID is an additional step in securing the patient's PHI. The pID is created when the patient is created using the "New Patient" functionality in screen A2 and is a unique random MD5 hash string value consisting of 25 character values. After a patient is selected, all data is stored in a folder tied to the pID. Further, all global usage data and summary statistics are stored with the pID as a tag. This security step prevents someone from accessing the root directory of the system and gathering a patient's data by name or other identifying factors.

Patient lists. Each therapist has a list of patients that they are currently working with. This list contains a mapping between the pUN and their pID. This list also contains any additional PHI for that patient such as demographic or injury information. This list is encrypted at rest and can only be decrypted using the specific therapist's login information.

4.4.A.1 Therapist Management

The therapist management screen is the entry point for all use of the vHAB system. Early on we decided that we wanted each therapist to have their own list of patients. If the system housed a shared list across an entire therapy facility, the patient list would quickly become

overwhelming and there would be increased chances for duplicate patient User Names (pUN). Therefore, the first thing we wanted a therapist to do was access their unique patient list and set up the system to show only those patients. Further, as we begin looking forward towards the secure storage of PHI, we knew this list of patient information needed to be secure. This led to the need for both therapist User Names and associated login credentials. The therapist management screen consists of 5 distinct features: i. Therapist Registration, ii. Therapist Login, iii. Password Reset, iv. System Feedback, and v. Exit (Figure 4.4.3).

Figure 4.4.3. Therapist Management screen A1. This screen has five main buttons that serve the functions described below. The "Suite" text on the top of the screen represents the version of the system (to be distinguished from a "Home" build).

i. **Therapist Registration.** New therapists must first register an account so that we have a place to store their patient lists. Here we ask for their intended user name, password, and email. Upon pressing the Register button a popup will appear asking for these values and lead them through the registration process. This information is hashed and stored on the local system for future lookup. The system also checks that the user name does not already exist for that facility and that it does not contain any special characters.

ii. **Therapist Login.** To get the patient list for the therapist, the therapist must enter the user name and password they used during registration. These values are then rehashed and compared to the stored values on the local system. Upon successful login the therapist's patient list is loaded into memory and screen A2 is loaded.

iii. **Password Reset.** In order to recover a lost password the therapist must enter the email and user name they used during registration. Upon pressing the Password Reset button a popup will appear asking for these values and leading them through the reset process. These values are rehashed and compared to the stored values on the system. If the email and username are found then a temporary 8 character key is generated and sent to the email. This key is valid for 15 minutes during which the therapist must enter the key into the local system. If the keys match, the therapist has an opportunity to overwrite the stored password with a new password. If 15 minutes have expired, the key is removed from local memory and the process must be restarted. This security procedure aligns with industry standard protocols.

iv. **System Feedback**. Using this feature, a therapist can directly send feedback and comments to the developers of the vHAB system. Upon pressing the Feedback button a popup will appear leading them through the feedback process. We use an SMTP email client setup through a special email to automatically send an email containing the information entered into the text fields. Further, we send the device name, IP address, and facility name if available so that we can send a response if requested and identify potential issues with a group of systems.

v. **Exit.** This is the main way to close the system. Exit functionality is crucial in ensuring all processes have properly exited and specific variables are reset. In some use cases, we disable the exit button since the computer will only be used to run the vHAB software.

4.4.A.2 Patient Management

When a therapist logs in correctly, their list of patients is loaded into memory. This list then populates the patient list panel with a button for each patient. If a therapist is logging in for the first time, or has not yet created a patient, this panel will be empty. Simple patient management functions are available in this screen to create and delete patients. In this screen we attempt to limit the amount of PHI displayed at any given time. Simple information, such as pUN is available in list format, but a patient's name must be clicked in order to view the basic demographic information. We made this design choice to accommodate multiple workflows. In an ideal world, a therapist would have set up a patient, with the appropriate game settings and activities prior to seeing the patient. However, in the case where a therapist session changes and they decide to use vHAB, there needs to be a strong emphasis on UI efficiency and PHI security. Thus, this screen has six main functions i. Create new patient, ii. Select a patient, iii. Delete selected patient, iv. Load selected patient, v. sort patients, and vi. Logout therapist (Figure 4.4.4). Additionally, the therapist name is displayed in the top right corner as a verification that the therapist login process was successful.

Figure 4.4.4. Patient Management screen A2. This screen has six main buttons that serve the functions described below. The "Select a patient" text on the right of the screen represents the currently selected patient information. If no patient is selected it will display as above.

i. **Create new patient**. Upon clicking the "New Patient" button, the therapist will be presented with a popup that will lead them through the creation of a new Patient. In this popup, the therapist will be prompted for the pUN, as well as optional demographic information such as age, gender, and handedness. Finally, the therapist will be prompted to enter any additional notes on the patient. These notes are available in the Patient Dashboard (A3) screen. When the prompts are completed, the system takes the information and appends it to the therapist's patient list and then creates a patient select button in the patient select panel. Specific checks are made on the pUN upon creation to ensure the pUN is unique for the therapist and that it contains no special characters.

ii. **Select patient.** A button is added to the patient select panel for each patient in the therapist's patient list. When clicked, the screen will be updated with that patient's information and the "Continue" button (iv) and "Delete" button (iii) will become interactable.

iii. **Delete selected patient.** At times, a therapist may create a test patient or they may simply have too many patients in their list. The delete functionality removes the patient's pUN and pID from the therapist's patient list; however it does not delete the de-identified data behind the pID folder. Saving this data provides the possibility of undoing a delete operation and allows for the global usage data of a system to maintain accuracy. Upon clicking the "Delete" button, the therapist is prompted with "Are you sure you would like to delete (pUN)?" before the operation is complete.

iv. **Load selected patient.** This button becomes interactable when a patient is selected (ii). When clicked all of that patient's information will be loaded into memory from their pID folder. When the information is loaded, the therapist is taken to the Patient Dashboard (A3) screen.

v. **Sort patients.** The small cogwheel icon and the "search" input field allow for sorting of the patient list. Searching moves the best string matched pUN to the top of the patient select panel. Clicking the

cogwheel icon allows for alphabetic sorting (A-Z or Z-A) and by the time created. Patients are initially sorted by time created, with newest patients being pushed to the top.

vi. **Logout therapist**. This button returns the therapist to the Therapist Management Screen (A1). Additionally, all patient information is cleared from program's memory. At the end of each session the therapist should logout to ensure system security.

4.4.A.3 Patient Dashboard

The patient dashboard is the landing page for the patient. Here, the therapist loads the next screen based on what they would like to do in their therapy session. In the development of the system, we decided to split the system between Assessments and Games. This dashboard allows a therapist to clearly know whether they are doing a game or assessment with their patient. The patient dashboard is also the home for a patient's notes and contains functionality for adding new notes to the ones already created in the "New patient" functionality. Loading the patient dashboard screen officially starts a "Session" which is a key component for the data saving structures discussed below in D. Data Management. The Patient dashboard screen consists of 6 main functions: i. Load Assessments, ii. Load Games, iii. Load Settings Management, iv. Load Data Viewer, v. Add new notes, and vi. End Session (Figure 4.4.5).

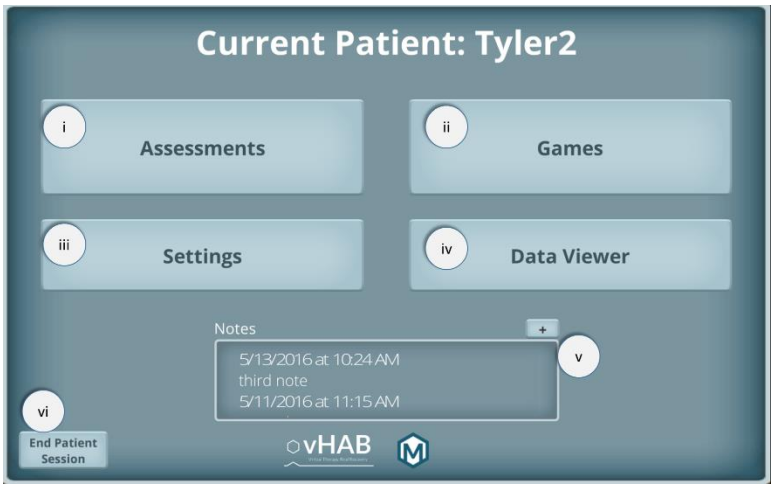

Figure 4.4.5. Patient Dashboard screen A3. This screen has six main buttons that serve the functions described below. The "Current Patient" text on the top of the screen represents the currently selected patient. This text serves as a verification that the proper patient was loaded into memory from the patient management screen.

i. **Load Assessments.** Loads Assessment Select screen (A6).

ii. **Load Games.** Loads Game Select screen (A7).

iii. **Load Settings Management.** Loads Settings Management screen (A4).

iv. **Load Data Viewer.** Loads Data Viewer screen (A5).

v. **Add new notes.** Clicking the '+' icon in the notes section creates a popup for the entry of a new note. Notes are stored as a text document in the pID folder and contain both a date-time string and the notes string. Notes are added to the notes panel with the most recent notes at the top. Notes are loaded into this panel when this screen is loaded. The notes panel is scrollable to view past notes.

vi. **End Session.** Pressing this button ends the current patient session and returns the therapist to the patient management screen (A2). This also removes all of the current patient's information from the program's memory.

4.4.A.4 Settings Management

Each game activity has multiple settings that affect how the game is played in terms of difficulty, length of play and required movements. These settings can all be modified in this screen before a game is loaded. This allows a therapist to pre-plan a therapy session with specific settings for that patient. It is important to note that settings for all games are patient specific and stored as a key-value pair text file in the pID folder. When a new patient is created, they are assigned a default set of settings from a *GlobalSettings.txt* file. Each time settings are changed the key-value pair in the patient's folder is modified. This screen also contains information on each game and the ability to add or remove a game from the game select screen (A7). This screen contains 3 distinct panels each with multiple functions as well as basic screen navigation functions (Figure 4.4.6).

Figure 4.4.6: Settings Management screen A4. This screen has three main panels, two buttons and a toggle that serve the functions described below.

i. **Game Select Panel.** This panel contains all of the game activities available to the therapist. While we currently have more than 10 games, we may choose to present less games to a therapist based on their functional focus. In this panel each game with a filled in star is made available in the Game Select

screen (A7). Removing games from the patient's view was requested from early system feedback. Therapists were concerned that a patient may be distracted by too many games, or may want to play a finger movement related game based on its name, when they are supposed to work on wrist movement. Clicking any of these buttons updates the Game Information Panel (ii) and Game Settings Panel (iii) with that games information and settings.

ii. **Game Information Panel.** This panel displays the name of currently selected level along with a tutorial video and task specifications. The tutorial videos are aimed at the therapist and show how to use the system with a patient. The task specifications relate the functional tasks associated with the game, such as the movement types and body parts used in the game.

iii. **Game Settings Panel.** Each Game has many different settings, described in full in 4.4.B. Games below. In this screen all of the settings can be modified before a game is played. This is useful for the therapist if they would like to pre-plan an entire therapy session without having to change settings in game. Settings in this panel are presented as sliders, toggles, and Boolean buttons. Sliders represent integer or float value settings, whereas both the toggles and Boolean buttons represent 0 or 1 values. Boolean buttons are used where there may be only two choices (such as left or right hand) but a traditional toggle option does not make sense.

    Each setting is also populated alongside a '?' icon. Pressing these icons produces a popup panel describing the setting and its functionality. We also provide suggestions on how to use the setting appropriately with different patients.

iv. **Wrapper Toggle**. This toggle turns on and off the wrapper component of the game select menu. The wrapper is useful for patients using the system over multiple sessions, but may be a hindrance if the patient isn't using it.

v. **Screen Navigation Buttons.** The Home icon returns the therapist to the Patient Dashboard screen (A4) while the arrow button takes the therapist directly to the Game Select screen (A7). If the Game Select screen is loaded this way and a game was selected in the Game Select Panel (i) that game will be preselected in the Game Select screen.

4.4.A.5 Data Viewer

One of the major advantages of vHAB over other rehab systems is the inclusion of detailed metrics and analytics that are calculated automatically during each game or assessment. These metrics are detailed further in Section 4.4.D below, but here we overview the presentation methods for these metrics. The Data Viewer screen has two main panels, a Usage Data panel (Figure 4.4.7 (Top)) where activities are organized by time, and a Metrics By Activity (Figure 4.4.7 (Bottom)) where metrics are organized by the game or assessment activity. Having these two different panels allows the therapist to start with the information that is interesting to them. For example, an outpatient therapist who only sees a patient once every few weeks may be interested in seeing what activities were done last time the patient visited and would use the Usage Data Panel. On the other hand, an inpatient facility may do the same activities every day and is more interested in documenting the progress a patient is making in wrist range of motion from *Ball Roll*. Presenting data at multiple levels is an ongoing design decision.

As discussed previously, the vHAB system has many different end users, both from their actual role in therapy and their level of interest in the data coming from the system. Simply documenting how often a patient performed an activity may be enough for many users, but completely mundane information for others. The current version was the product of many focus groups and general discussion with experts in the field. Addition of other sorting methods, such as a By Function panel, will likely be added in the future to allow for users to see all information related to metrics such as “Speed” or “Endurance”. These “rolled-up” metrics would contain metadata from all calculations of related data such as “Time to trial” or “reaction times over a

session". Additional steps on the data analytics side will need to be taken on this data to create these metrics.

When the data viewer screen is loaded, a data parser goes through all of the data stored under the pID folder and converts each data point into a graphablePoint class. A data point can be simple usage data such as time played, or complicated metrics such as wrist range of motion. These graphablePoints are stored in local memory in lists for quick access. These lists can be sorted and applied to the User Interface when the appropriate buttons are clicked. This method is very quick, but may become problematic with large amounts of data. Other data management options are being explored, such as only loading the most recent 5 days' worth of data, or storing the most access data in different structures in the pID folder.

The Data viewer screen consists of the two main panels as discussed above. Each panel has various functionality as discussed below (Figure 4.4.7).

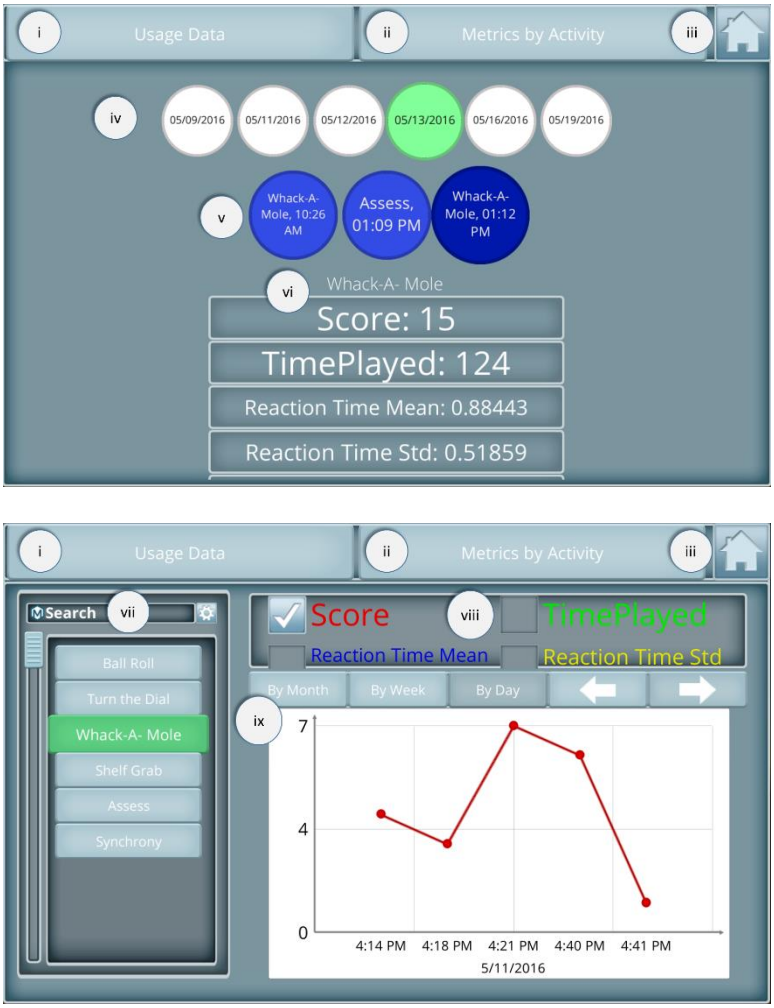

Figure 4.4.7: Data Viewer screen A5. **Top. Usage Data Panel.** This panel contains usage data and metrics sorted by time played. The system uses a node-like functionality, allowing additional information to be displayed when a given node is clicked. **Bottom. Metrics by Activity Panel.** This panel contains individual metrics sorted by game. In this example, the therapist has selected the "*Whack-a-Mole*" activity and is viewing the score over multiple sessions occurring on May 11, 2016.

i. **Usage Data Navigation Button.** Clicking this button will load the Usage Data panel. This will also reset the currently selected nodes, providing a blank slate for the therapist to navigate.

ii. **Metrics by Activity Navigation Button.** Clicking this button will load the Metrics by Activity panel. This will also reset the main graph and currently selected metrics.

iii. **Home Button.** Clicking this button will take the therapist back to the Patient Dashboard screen.

--- Usage Data Panel Only

iv. **Date Nodes.** These nodes are populated based on a sorted and condensed "graphablePoint" list. Each unique date is given a node button that, when clicked, generates activity nodes (v) that occurred on that date.

v. **Activity Nodes.** These nodes are populated based on a sub list from the Date Nodes' list. Each activity on a given date is given its own node, even if that activity occurred multiple times in that date. Activities are sorted by time, with the most recent activities being the rightmost nodes. Clicking an activity node populates the Activity panel (vi) with all of that activity's information.

vi. **Activity Panel.** This panel is populated by all of the "graphablePoints" found for the currently selected activity. Each "graphablePoint" is given a small panel displaying the metric name and the value. Each of these panels is clickable and, when clicked, will preselect that activity type (vii) and metric toggle (viii) in the Metrics by Function panel (Figure 4.4.7 (Bottom)).

--- Metrics by Function Panel Only

vii. **Activity Select Panel.** This panel contains a list of all of the activities that the patient has done. If the activity is not visible on this graph it means that either the activity has not been played, or that no metrics were available for that activity. This functionality primarily comes into play if someone selects an activity, but for one reason or other cannot complete the activity. Clicking an activity in the panel will create a list of all of the "graphablePoints" that came from that activity and generate the metric toggles (viii) for all metric types found for that activity.

It is important to note that not all instances of that activity will be guaranteed to contain every metric type. Some metrics require minimum number of trials to compute, and therefore will not exist for all instances. This is handled by skipping the plotting of that point in the main graph panel.

Clicking a new activity will also clear all of the currently graphed points on the main graph, but will not reset the time offsets or date sorting methods. Activities can be sorted by most recently played or can be searched through with the sort options at the top of the panel.

viii. **Metric Toggles.** These toggles are generated when an activity button is clicked in the Activity Select Panel (vii). Each toggle controls whether or not that metric is displayed on the main graph. Some activities contain more than 10 different metrics, which can get very crowded on a single plot. Each toggle is color coded to the line color of its corresponding metric on the main graph.

ix. **Main Graph.** The main graph displays the metric data for every checked Metric Toggle. The main graph has three main display modes: "By Month", "By Week", and "By Day". Each of these modes changes the x-axis values of the graph to the appropriate time span. The design of this view came after seeing the challenges most therapists had interpreting an early version of the data viewer that plotted data "as-available". The old method simply labeled each point with the date and time it came from, but this resulted in a non-linear data set.

The challenge with the current method is that it does not allow for multiple data points to exist for a given day in the "By Month" or "By Week" views. To fix this, we average all of these points and display a slightly darkened data point to convey that the point is averaged. Clicking these darkened points will load that day in the "By Day" view, where multiple points can be displayed.

Time navigation arrows (top right of the main graph) allow the therapist to go backward and forward in time. These arrows only allow the therapist to go back in time to the first date where data exists. However, if data does not exist for a given week, this empty week will still be displayed in the "By Week" view. This design choice was made for navigation consistency, but may be revisited in the future.

Graph assets were developed with GraphMaker [37], a third-party Unity asset. GraphMaker provides a framework for placing data points in the proper locations on a screen of varying sizes and allowed greater flexibility when designing the system.

4.4.A.6 Assessment Select

In early builds of the system we had a single game called vAssess. This game contained about five minutes of preset activities that were designed to assess hand function in one simple test. We learned, however, that many users (both therapists and physicians) were not interested in all of the activities included within vAssess. Instead of creating multiple games that addressed each of these user's desired activity sets, we created a modular assessment platform that allows the user to customize their vAssess experience by selecting only the measurements that are relevant to that specific patient and combining them into a seamless game session. To date, we have created ten different modules consisting of range of motion tests, strength/fatigue tests, and questionnaires. These modules are described in detail in Section 4.4.C below.

Managing this customization, however, required a special screen to create, load and save these custom lists (Figure 4.4.8). The Assessment Select screen contains multiple features and is currently undergoing major changes to the framework to make it easier to use. The current system prompts the user to create their custom list by dragging and dropping modules into a list. The user can also load preset or saved lists for speed. The current system, however, is not optimized for therapist workflow, especially as we continue to add modules. Future iterations of the system will include better sorting methods for the modules (such as by type, or by functional relevance), and will likely start the user at a load module set screen to make starting an assessment faster.

Figure 4.4.8. Assessment Select screen A6. This screen allows for the creation and loading of custom lists of assessment modules. Users can drag and drop modules from the left column listing all the modules to their custom list on the right. In this example, a user is dragging a module over to their custom list. The hand-cursor represents the user's interaction point (either a mouse click or a screen touch). The green box shows where the module would be placed if the user let go of the BubblePopper60 module.

i. **Module List Panel.** This panel lists all of the available assessment modules that can be added to a user's custom list. To add a module to the list, the user clicks (or touches) and drags the module to the Selected Module Panel (ii). When the module is halfway across the screen, the target module slot will turn green. To add the module to that slot, the user releases the mouse (or touch) and the module will snap into place. Releasing a module before a slot has turned green will not add it to the custom list. Dropping a new module on a slot that already contains a module will remove the old module from the list and replace it with the new one.

   Each module button also has an inset help button ('?'). Clicking this button will show a popup panel for that specific game. Each popup panel contains a tutorial video for that module and a brief description of the module (Figure 4.4.9 (Top)).

This module list is also sortable with either string matching through the search function or alphabetically by pressing the cogwheel button.

ii. **Selected Module Panel**. This panel lists the user's current module list. When the user starts the assessment, these modules will be presented to the patient in the order they are displayed in this list. New slots can be added by clicking the "Add Slot" button at the bottom of the list. Slots can be removed by clicking an "X" button within the slot. This "X" button is only viewable when the user is not dragging a module. An empty slot will be ignored when generating the module list.

The list can contain multiple instances of the same module, in which case each module is treated as a separate instance of the activity for data analysis purposes. This allows for the comparison of a module before and after some other module. For example, a user may be interested in fatigue before and after a range of motion exercise.

Each module in this panel can also be clicked and dragged to rearrange the order of the list. Here, if a module is dropped on a slot that already contains a module, the old module is placed in the selected module's previous slot. This previous slot is indicated by a yellow tint on the slot while the module is being dragged. To remove a module from the list the user must move it to the opposite side of the screen.

iii. **Load Functions**. There are two options for loading preset lists into the Selected Module Panel. When a module list is loaded with either method, it can still be modified and then resaved.

The "Load from List" button will generate a popup (Figure 4.4.9 (bottom right)) prompting the user to select from a list of module sets. This list of module sets contains both pre-generated lists that we have created (designated with a star in the button) and custom lists that the user has generated and saved (iv). Clicking one of these module sets will display that modules set's individual modules to the left of the panel. The user can then load that module set or return to the main Assessment Select screen.

The load recent method will load the module set that was most recently used. Currently, this is user independent and relies only on a program memory variable. However, if a facility often uses the same module set this may be a quicker way to load their list. This feature will likely be replaced with a “Favorites” list that is the first thing the user sees to further increase workflow efficiency.

iv. **Save Function.** After a user has created a module set in the Selected Module Panel (ii) they can save their list to a local file for future use. Clicking this “Save” button will generate a popup (Figure 4.4.9 (bottom left)) that prompts the user to name their custom list. This popup also displays the modules they have selected as a verification step.

v. **Clear Function.** This button will clear the list in the Selected Module Panel (ii) allowing the user to start from scratch when designing a custom module list.

vi. **Start Button.** This button will load the vAssess activity scene with the modules in the Selected Module Panel preloaded.

vii. **Home Button.** Clicking this button will return the user to the Patient Dashboard screen (A3).

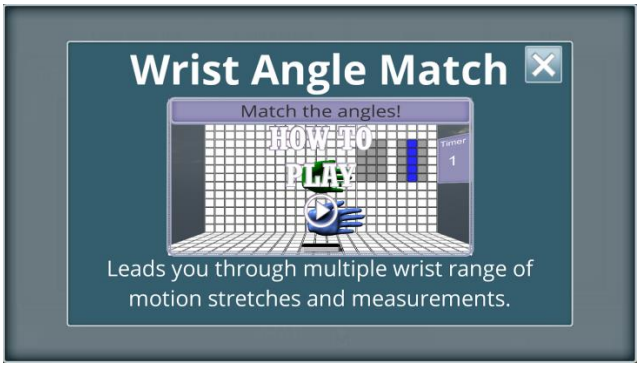

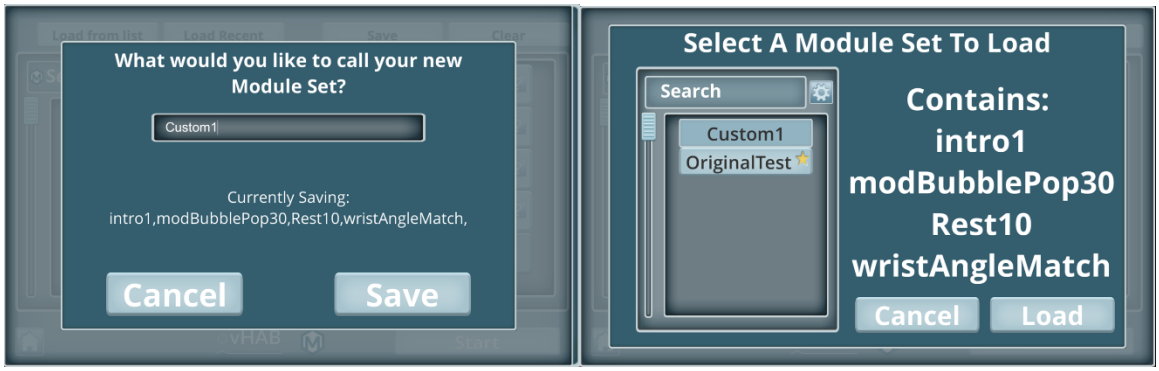

Figure 4.4.9. Additional Assessment Select screen A6 popup functions. Top: Help panel popup. This popup is generated when an Assessment Module button's inset "?" help button is pressed. It contains a module-specific tutorial video and description. **Bottom Left**: Save module list popup. This popup is generated when a user clicks the save button. This popup allows the user to save a custom list of modules for viewing in the load module list popup. **Bottom Right**: Load module list popup. This popup is generated when the user clicks the "load from list" button. This popup allows the user to load preset lists of modules as opposed to custom creating a list.

4.4.A.7 Game Select

The Game Select screen contains a list of the available games, a video tutorial, and a "Play" button (Figure 4.4.10). This screen is designed to be presentable to the patient as well as the therapist. An ideal therapy session would involve the therapist selecting the patient, modifying all settings, and loading this screen before they have started working with the patient. In this way, the patient only sees basic information about the available therapy activities and can even interact with the UI in a useful way. This screen and the UI within each game have a different set of UI elements than previous screens, with different theme colors and styles. This is to convey the difference to the therapist, but also creates a more unified experience for the

patient. This screen is also the home of the Garden Wrapper which is described further in section 4.4.A.8.

Figure 4.4.10. Game Select Screen A7. This screen allows the therapist and the patient to select the game activity they would like to do. After a game is played, the users are returned to this screen to select another game.

i. **Game Select List.** This list is populated with all of the games that are within the patient's list as defined in the Game Settings screen (Figure 4.4.6.i). Clicking each button will load the appropriate tutorial video in ii and allow that game to be loaded.

ii. **Tutorial Video.** Each game has a tutorial video used to instruct a naïve patient on how to play the game. While most of the introduction and training will be provided by the therapist, we found, through various user testing experiences, that a short video can be a great starting point for both users. By watching a video before launching the game, the patient's focus is on learning the task as opposed to trying the task incorrectly. In viewing early patient – therapist interactions, many patients would ignore the therapist when the game started, likely because they assumed they could automatically figure out how to play. Since our paradigm is unlike what most patients would have seen before, these initial training steps are very important.

iii. **Play Button.** This button will load the currently selected game. Before loading the game, the backend software will load the appropriate variables for that game to ensure a smooth experience.

iv. **Navigation and Wrapper Buttons.** The home button returns the therapist to the Patient Dashboard screen (A3). The cogwheel button returns the therapist to the Game Settings screen (A4). The tree button shows the garden for the wrapper (Figure 4.4.11) while the seed button loads the seed select menu for the wrapper (Figure 4.4.12). Both of the wrapper functions are described further below.

v. **Current Seed Display.** This text element shows the patient what seed packet they are working towards within the wrapper. Showing this element here reminds the patient that they are working towards a goal, while also providing information to the patient if they would like to change their target goal.

4.4.A.8 Wrapper

The vHAB game engagement wrapper was a product of the collaboration with the Digital Futures Lab at University of Washington-Bothell (UWB). The wrapper is designed to tie all of the games together with a unified theme, despite the fact that all of the games are very different in both activity and art assets. The wrapper also provides a global scoring system which allows for motivation to be sustained across games and between therapy sessions. The wrapper is only available in the game activities and not the assessment activities. This was designed to drive use towards the games as exercises and assessments as one time check-ins of function and progress. The wrapper can be turned off or back on at any time in the Game Settings screen (A4). Turning off the wrapper may be useful in short-term use cases where a patient may only be exposed to the system for a short time and the long-term engagement is not an important factor in using the system.

Wrapper Mechanics

Before starting a game for the first time, the user is prompted to select the goal they would like to work towards and all points scored within a game go towards this goal. In our wrapper, there are 18 distinct goals that the patient works toward. At the completion of each goal, the patient is rewarded by viewing progress in the wrapper's home screen in the form of animations and sound. Completing all 18 goals will unlock a button that allows the patient to view all of these animations in sequence.

To complete a goal, the patient must accumulate 100 progress points. In game points are mapped to progress points based on an estimated eight week use of the system, though this timespan can be modified based on the system's use case. The mapping between progress points and in-game points is not constant, and is instead designed to change over time. Over time, more in-game points will be required to accumulate the same number of progress points. This is designed to engage patients early on while driving them to increased use and better performance over time. To create the current mapping model we made a few basic assumptions:

1) The amount of time played each day would increase over time
    a. Patient recovery and increased endurance will allow for slow, yet sustained increases over time.
    b. Working towards a goal may increase the amount of time they play if they are close to completing a goal.
2) The number of points scored within each minute would increase over time
    a. Patient familiarity with the game's rules will provide early increases
    b. Patient recovery will allow for sustained increases assuming game difficulty settings are not changed

Further, we wanted progress to feel linear over time, so that putting in a day's work on day 36 felt as rewarding as day 1. To this effect, we build the model around finishing 25% of the total progress every 2 weeks. We also assumed the patient was only using the system 4 days a week and that they could start with a 1:1 mapping. The current model can be represented by:

Eq 4.4.1. $y = -0.0011x + 1$

where y = points/progress point and x is cumulative minutes played. Currently, y is clamped to not be less than 0.1 which works well in this model, but may need to be adjusted for longer time frames. This model does not take into account the variability of points scored in different games. It is also likely that this model does not optimize patient motivation over time. Further research will need to be performed to reach this optimization point for all different use cases of the system.

Wrapper Theme

Based on user acceptance testing performed by UWB, we decided to use a Garden metaphor for the wrapper. In this metaphor, the patient is growing a garden with their progress towards recovery. The garden contains 6 distinct plants with 3 stages of growth. Each stage of growth represents a goal and upon completion shows a brief animation of the plant growing. When a plant is completed, the patient is also rewarded with a new animal in their garden near the completed plant. A patient starts with an empty garden but over time can grow a full garden with 6 plants and 6 moving animals (Figure 4.4.11).

Figure 4.4.11. The Garden View of the Wrapper within the Game Select screen (A7). Left. An early stage garden with only stage 1 of the Hydrangea goal complete. **Right**. A completed garden with all six plants visible. Clicking the continue button here will take the user back to the main game select screen.

When selecting a plant (target goal) the user is presented with a set of seed packets to choose from (Figure 4.4.12). Selecting that seed will update the user's goal, but will not reset progress previously made towards a goal. Progress towards a goal is monitored within the Game's UI by showing a meter that fills with each progress point made. For each 20 progress points, the user is rewarded by a brief seed growth animation within the Game UI's progress panel. Upon completing a game, the patient is presented with a popup of summary stats (Figure 4.4.13). After a few seconds, this popup will move to the top right of the screen and show the patient their garden. If a goal was completed (i.e. 100 progress points were achieved) the animation and sound effects for the new plant will be displayed.

Figure 4.4.12. Seed select popup for the wrapper. This popup occurs within the Game Select screen (A7) when the seed button is selected from the navigation panel. The navigation panel (i) changes based on what popup is displayed. In the seed select popup the user can return home, go to settings, view their garden, or load the game select popup. Seed packets are displayed (ii) in a fanned out format. They can be navigated through by clicking on a given packet, which will bring that packet to the center, or by clicking the arrows in the lower panel (iii). Clicking the center packet or the check box will select that packet for the patient's goal.

Figure 4.4.13. The game summary popup for the wrapper. This popup panel will appear after each game if the wrapper is enabled. This popup displays the basic stats from the recently played game alongside the progress made towards the current packet.

Wrapper Use Prompts

At multiple points, a patient may not have a goal selected. This can happen with new patients and after a goal is completed. In both these cases, we prompt the users with a popup asking if they would like to select a seed packed. The popup can be dismissed and the game select view is shown, or they can accept and the seed packet select popup can be shown. Upon five successive dismissals with no goal selected the wrapper will be disabled. The wrapper can be re-enabled at any time through the Game Settings screen (A3).

4.4.B *Games*

Games are the primary activity within the vHAB system. In our system a game is an activity in which the patient moves their hand or arm above the main kinematic sensor to control various digital objects on the screen. These objects can be direct representations of their hand with a three dimensional hand model, or more abstract representations such as a paddle or a dial. When the patient moves their hand above the sensor, the mapped game object seems to move immediately due to the low latency of the sensor (<33ms) [38]. In all games we only represent a subset of the hand's full movement in the control of game objects. For example, we may only look at the rightmost hand's palm normal angle relative to a preset plane to control the angle of a game object. Lowering the dimensionality of this control space makes games much easier to learn for the patient and allows us to design carefully controlled experiences that are optimized for the sensor's abilities.

For the main vHAB system we have created over 15 games, with about 8 of them finished and the other games in various states of user testing and development. The process of creating games was a very iterative process, involving shadowing therapists, in-person interviews with field experts, user testing, and creative discussions with experts in user experience design. We have previously detailed the design process (Section 4.2), but it is important to reiterate that many games have changed drastically since the first version and many of the current games will continue to change. In the sections below, we describe the games in their current form.

Each game was created using the Unity game engine which provided a framework for placing 3D models, in game 2D UI elements, and assigning scripts to control the movement of these objects. 3D models were created primarily using Blender, a 3D modeling tool. Skinning the 3D models was accomplished using 2D image editors such as Adobe Illustrator and GIMP. 2D elements were created in the same way the main UI (Section 4.4.A) was created with the help of the Digital Futures Lab at University of Washington Bothell (DFL UWB). DFL also assisted in user experience design of some of the games. Audio elements for the games were acquired through a third-party Unity asset [39].

Each game possesses its own unique control, target generation, and trial structures. However, multiple threads are common throughout each game. Audio feedback is used both as a reward signal at the completion of a trial and as a cue element within a trial to show the patient they are making the correct movements. In addition to the main control elements, particle effect visual cues are used in varying circumstances to show in-trial feedback. These visual elements may draw a patient's attention to a given game object or signify the completion of an in-trial

step. These audio and visual reward elements add a layer of fun and engagement that users expect from traditional games, while also providing crucial performance feedback.

Games consist of a set of trials over a set amount of time. A trial consists of presenting the patient with a target or objective and the patient performing the appropriate movement to match or move towards the target. Completing a trial gives the patient in game points which are then mapped to "progress points" as described above. This trial structure comes into play with the analytics structure we've created in section 4.5: Analytics Description.

Each game has multiple settings that are specific to that game's difficulty or control options. These settings allow patients of multiple ability levels to play the same games. For example, a patient with limited mobility in their wrist can still play *Ball Roll* at a high sensitivity setting. The sensitivity setting provides a multiplier for the movement of the game object. With a high sensitivity, a small movement of the wrist will move the paddle as much as a large wrist movement with a low sensitivity. We provide preset minimums and maximums for most settings to prevent the games from being unresponsive, but for the most part our settings ranges cover all levels of function. Some settings are more Boolean, simply turning on or off a given feature or game target requirement. Settings are also patient specific, stored within their pID folder, so that the therapist does not need discover the correct settings for a patient on each use. Future changes to the settings structures will allow for automatic starting settings based on a first-use assessment. Additionally, we have explored multiple options for automatically adjusting settings as we see increased or decreased performance. At this time, however, most therapists requested that they have direct control over the settings as they are learning how to use the system. Settings for all games are summarized in Table 4.4.1.

Table 4.4.1. Settings for all games.

Setting	Function	Games used
Time to play	Controls how long the game is played. If set to the maximum value the game is in "Unlimited" play mode.	All Games
Sensitivity	Controls how much real world movement is needed to move an in game object. This value modifies preset remapping functions discussed below.	Ball Roll, Reach and Grab, Reach and Dwell, Pizza, Whack-A-Mole, Two Hand Shape Match, Pill Box
Min and Max Values	Dictates a range of values from which a game can generate targets	Turn the Dial
Toggles	Toggles have varying functionality such as specifying which fingers can be used, whether a patient is able to make a fist, or what types of targets are generated	Reach and Grab, Pizza, Whack-A-Mole, Two Hand Shape Match,
Thresholds	Dictates at what level of a value does a specific action occur, such as when in a grasp is the patient officially making a fist	Reach and Grab, Pizza, Two Hand Shape Match, Finger Position Match, Giant's Teeth

Each game has a common game UI (Figure 4.4.14) created in the same theme as the Game Select screen (4.4.A.7). This UI serves multiple functions such as changing game parameters and navigating between screens. The UI also displays relevant information about the game state, such as score, elapsed time, and garden progress. This UI was designed to be unobtrusive while still being easy to use on multiple hardware systems. One of the key components of the in-game UI is the ability to modify settings while a patient is playing a game. A therapist can make a game easier or harder based on a patient's ability without having to return to the Game Settings screen (4.4.A.4). Each setting for the currently loaded game is dynamically populated in a small popup at the bottom of the screen (Figure 4.4.14 right). A therapist experienced with the vHAB system can utilize this function to modify the game's difficulty while a patient is playing the game to subtly increase the difficulty and push for better performance. Each setting is also accompanied by a help "?" button that creates a small descriptive popup just above the settings panel.

Each game also contains built in pop-up tutorials (Figure 4.4.15). These popups show up the first time a patient is playing a game or anytime the '?' button is pressed in the in-game UI. These tutorials consist of a set of text prompts that are displayed within the game space. Specific requirements must be met to advance the tutorial. Some prompts are advanced with time, but others require specific in-game actions. For example, we want to continuously remind patients to keep their hand at least 6" above the sensor. The prompt reads "Place your hand 6" above the sensor" and an in-game tracker looks for a hand above the sensor before advancing the prompt. This interactive tutorial provides a good first experience for patients, while not limited experienced patients from exploring the space on their own.

Figure 4.4.14. In game user interface. Left. The standard starting UI using *Whack-a-Mole* as an example. **Right**. In-game UI with the settings panel enabled.

i. **Game state display.** These panels show the current score and elapsed time of the game. The score value is updated at the completion of each trial. The time value counts up in the "Unlimited" play mode and counts down if a game time is set.

ii. **Game Control Panel.** These four buttons control multiple in-game functions. The circular arrow restarts the game. Restarting a game resets the game score and timer, but progress points are saved and all analytics are still calculated. The "?" button generates the in game tutorial popup (Figure

4.4.15). The cogwheel button generates the in-game settings popup (iv). The forward arrow finishes the game and loads the wrapper congratulations screen (4.4.A.8).

iii. **Goal progress.** This panel shows the accumulated progress points towards the currently selected goal. The meter on the right fills with each progress point earned. At each 20% fill mark, the seed image "grows" with an animation to signify a mark in progress.

iv. **Settings Popup.** This popup allows for the modification of settings within the game. Each setting can be modified by interacting with the slider or toggle element in the center of the popup. Clicking the inset "?" button generates a help panel describing the setting. Clicking the arrow button will show the next available setting.

Figure 4.4.15. In game tutorial popup. This popup shows up when a patient plays a game for the first time or when the "?" button is pressed. These tutorials are designed to help the patient learn to play the game in an interactive way.

Game Summaries

The sections below describe each game with its corresponding movements, control paradigms, and therapeutic relevance. We have selected 10 games that represent the wide range of tasks our system is capable of. Additional games are briefly referenced in B11. Other Games below, and are removed as they represent either an incomplete experience or utilize the same movements and control schemes but use a different visual. The games below are ordered in level

of movement complexity. All games can be played with either hand automatically unless otherwise indicated.

Key Terms.

Sensor zero. A neutral position above the sensor (Figure 4.4.16) where x = z = 0, and y = a detectable distance (ideally >6").

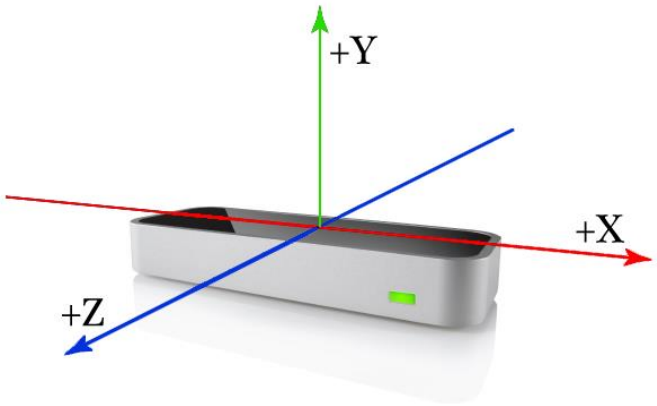

Figure 4.4.16. Leap coordinate system. The Leap motion reports measurements in three dimensions (x,y,z) as displayed above. Positive X axis is normally to the right of the user, positive Z towards the user, and positive Y, up. Figure reproduced under fair use from [38].

Remapping. We use a set of remapping functions to move between the patient's real position and game object positions on the screen. These set of remapping equations utilize preset values within the control scripts that translate a volume of real space to a volume of 3D game space. These remapping equations follow a similar pattern:

Eq. 4.4.2. $$\text{game}_{new} = \frac{(\text{leap}_{new} - \text{leap}_{min}) * (\text{game}_{max} - \text{game}_{min})}{(\text{l}_{max} - \text{l}_{min})} + \text{game}_{min}$$

Leap minimums and maximums are set using the leap's sensor zero as well as estimated ranges, while the game minimums and maximums are set based on the game's design and required operating space. This function primarily applies to positioning, such as translating the

x,y, and z position of the patient's real hand to their virtual hand in game. This remapping can be adjusted using a sensitivity 's' that decreases the measured range of the leap sensor without adjusting the game boundaries. By moving both leap_{min} and leap_{max} in Eq. 4.4.2 closer to sensor zero, a given leap_{new} will produce a larger game_{new} value.

Eq 4.4.3. $$\text{leap}_{min} = \text{leap}_{min} * \frac{s}{10}$$

Lerp. A game development term used to smooth two values over time. The lerp functionality allows for incremental movement towards a target value to be automatically adjusted each frame. For example, if we want a game object to eventually end up at position (1,1,1) and it is currently at (0,0,0). We would not want to just change the position in a single frame since it would result in a visually choppy jump instead of a smooth movement. We can't just move a set amount each frame since we are using a variable frame rate. With a properly setup Lerp function, we can move a variable amount each frame based on the "delta time" or the time since the last frame. This results in a smoother movement while also ensuring game objects interact with each other. The speed at which a value Lerps can be adjusted depends on the desired effect. Most Lerps are recursive, incrementing the current value towards the target value based on the frame rate.

Collisions. Each 3D game object has an invisible mesh around it to control interactions with other objects. When two meshes overlap, we can call preset functions that handle what each object does when it collides with another. Collisions are used for picking up objects, as well as detecting when a moving object has reached a target position. Some collisions are handled with a physics model and simply prevent objects from passing through each other.

Magnetization. The use of magnetization with introduced in Section 4.2.B.6. An object becomes magnetized to the patient's virtual hand when the hand collides with a specially set

collision mesh surrounding the virtual object. An object will stay magnetized as long as its center position is within that collision mesh. The object will snap back to its original position if it leaves the collision mesh and the patient has not yet met the exit criteria, such as making a fist.

Symbols. Multiple symbols are used below in the equations representing game control paradigms (Table 4.4.2). For any $\dot{\square}$ box, an uppercase letter represents a real world value, such as the Hand Position ($\dot{H}$), while a lowercase letter represents an in-game object or a remapped value.

Table 4.4.2. List of symbols for game control paradigms.

Symbols	Meaning
$\tilde{\square}$	rotation as a quaternion
$\dot{\square}$	Position as a 3 dimensional vector
$\vec{\square}$	Direction between two positions as a 3 dimensional vector
$\wr\wr a \rightarrow b, t$	Lerp from vector, float, or quaternion 'a' to a new value 'b' consisting over time t
Δt	Time between frames

4.4.B.1 Ball Roll

Functional Movements: Wrist flexion and extension.

Objective: Move the paddle left and right to push the ball off of the table.

Movement Control Paradigm: The angle of the paddle is mapped to the direction of the hand as a distance from the YZ plane. The direction of the hand $\vec{H}$ is calculated by extracting the x component of the directional vector between the center of the palm $\dot{P}$ and the center of the wrist $\dot{W}$ (Eq. 4.4.4). This value is multiplied by the sensitivity setting value's' and remapped to game space (Eq. 4.4.5). This final value controls the angle $\tilde{h}$ of the paddle anchored closest to the patient with a fast Lerp function (Eq. 4.4.6).

Eq. 4.4.4. $\overrightarrow{H} = \angle \dot{P} x \dot{W}$

Eq. 4.4.5. $h = \overrightarrow{H}(x) * \frac{180}{\pi} * S$ $\quad$ -80°< h <80°

Eq. 4.4.6. $\tilde{h} = \wr\tilde{h} \rightarrow (0, h, 0), 20 * \Delta t$

Game Control Paradigm: The speed at which the ball travels along the table is dictated by the average of the speed v of the paddle when the two game objects first collide (Eq. 4.4.7). The ball will reset every 20 seconds to prevent it getting stuck or travelling too slowly to score. When a ball leaves the table it collides with the troughs at the end of the table. The patient is rewarded with particle effects, auditory feedback and a game point for a completed trial. A new ball is then dropped from the ball dispenser in the center of the screen.

Eq. 4.4.7. $v = \frac{\Delta h}{\Delta t}$ $\quad$ 1< v

Summary: This game is one of the simplest games we have created, but works on a fundamental functional movement. Overcoming muscle spasticity after injury is one of the more difficult problems early on in a patient's recovery. This game can be adjusted to require small changes in angle to move the paddle which can allow individuals with spastic flexion to still play the game, slowing working towards increasing their range of motion. Further, this game does not require any timing or sustained movements. This allows patients to take their time completing a trial or even rest part of the way through.

Figure 4.4.17. Ball Roll Game. In this game the patient moves their hand left and right at the wrist to control a panel (i) to push the yellow ball towards the trough (ii). When the ball reaches the trough a new ball drops from the dispenser (iii).

4.4.B.2 Turn the Dial

Functional Movements: Forearm pronation and supination.

Objective: Rotate the "player" dial to match the target dial while keeping the elbow stable. When matched, the patient must hold that rotation for a set amount of time.

Movement Control Paradigm: The angle of the player dial $\tilde{d}$ is controlled by the x and y components of a normal vector coming from the center of the patient's palm $\vec{N}$ adjusted for handedness (Eq. 4.4.8). The normal vector is orthogonal to an idealized "flat" palm, but functions as if the hand was flat even if a fist is made. Handedness is calculated by preset leap functionality that determines if the viewed hand shapes best represent a left or right hand. This is primarily determined by the indent of the palm and relative position of the thumb and pinky. The rotation of the dial is handled with a Lerp function to enhance the smoothing of the game (Eq. 4.4.9). The patient's relative elbow position $\dot{E}_p$ (calculated as the difference of x positions of the

center of the palm and the elbow) is remapped (Eq. 4.4.2-3) to an elbow meter game object $\dot{e}$ on the screen.

Eq. 4.4.8. $d = \tan^{-1}\left(\frac{\vec{N}.x}{\vec{N}.y}\right) * \frac{180}{\pi}$ $\quad d = d + 180 \;\; iff \; \vec{N}.x < 0$

$\quad d = d - 180 \;\; iff \; Handedness = Right$

Eq. 4.4.9. $\tilde{d} = \wr\tilde{d} \rightarrow (0, d, 0), 15 * \Delta t$

Game Control Paradigm: Sample target angles are generated at the start of the game from a pool defined by the min and max angle game settings 'a_{min}' and $'a_{max}'$. If the player dial angle is within a preset tolerance (10 degrees) and the elbow meter is within its maximum bounds $\pm\, 'e_{max}'$ from center ($\dot{E_p}$ = 0), then a timer begins. A trial is complete if the timer value exceeds the hold time setting value $'t'$. If the player dial angle or elbow position leaves the tolerated range the timer is reset. The timer value is mapped to a UI element on the screen that fills as the patient meets the trial criteria.

Summary: *Turn the Dial* focuses on pronation and supination of the forearm by having the patient control the knob of a radio to match a target knob. Further, the patient must keep their elbow in line with their hand while matching the angle for the timer to increment. This is done to ensure that the patient is rotating their forearm and not compensating by rotating at the elbow. By directly adjusting a_{min} and a_{max} a therapist can hone in on a patient's problem areas. Finally, the hold time setting t can be reduced to a minimum to work on range of motion, or increased to higher levels to work on stretching and strength.

Figure 4.4.18: Turn the Dial Game. The patient controls the rotation of the right dial (ii) to match the target dial (i). The patient's relative elbow position is also tracked (iii) to ensure proper form during the movement. If the elbow and hand angle are in the proper position, a timer begins, filling a UI meter (iv).

4.4.B.3 Reach and Hold

Functional Movements: Arm range of motion and trunk stability.

Objective: Move the in-game hand towards the floating shapes and hold the position for a set amount of time.

Movement Control Paradigm: The position of a virtual game hand is directly remapped to the patient's palm position in all three dimensions based on preset game boundaries (Eq. 4.4.2-3). The virtual hand's x-y and x-z position is projected to two dimensional grids at the bottom and back of the game space to assist in visualizing the patient's current position.

Game Control Paradigm: The patient must move the virtual hand into a randomly generated target object within the three-dimensional game space. If the virtual hand's collider is in contact with these targets a timer will begin counting. While the timer is counting, the color of the target will being to change. A trial is complete when the timer meets or exceeds the hold time

setting *'t'*. The timer will reset if the virtual hand is no longer in contact with the target object. The target's position is mapped to the same two dimensional grids as the virtual hand as an additional feedback element for the patient.

Summary: *Reach and Hold* takes advantage of the Leap Motion sensor's ability to track hand position in three dimensions. The patient can reach out in front of them within the Leap's interaction space to touch virtual targets with their virtual hand. Using higher hold times a patient can work their trunk stability and arm strength while in a static position. Moving between targets also works on a patient's accuracy and reaction time to presented stimuli. Adjusting this game's sensitivity setting requires the patient to produce smaller or larger real movements to reach the targets. Gradually decreasing the sensitivity setting may lead to the patient increasing their range of motion over time. Projecting the hand and target to a two-dimensional space allows the patients to learn how to move a virtual hand in three dimensions more easily.

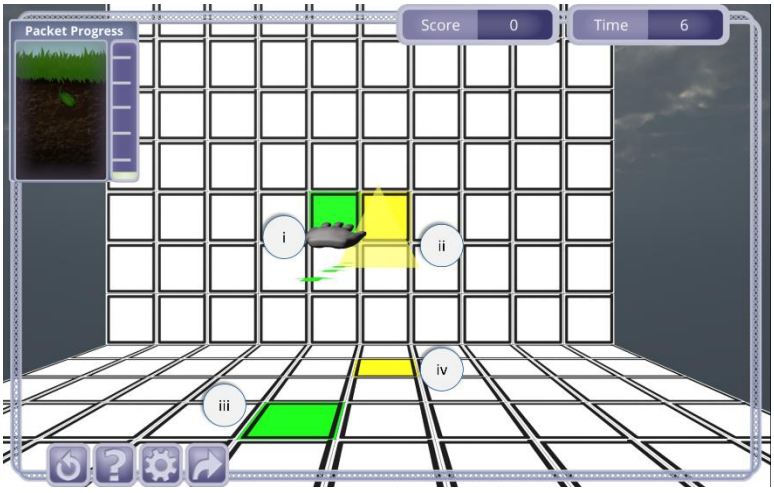

Figure 4.4.19. Reach and Dwell Game. In this game, the patient moves their virtual hand (i) in three dimensions to reach towards target game objects (ii, yellow triangle). The virtual hand's

position and target position are projected onto two-dimensional grids (iii, green and iv, yellow respectively).

4.4.B.4 Reach and Grab

Functional Movements: Arm range of motion and grip.

Objective: Grab virtual fruit off a shelf and move it to the bowl on the counter.

Movement Control Paradigm: The patient's virtual hand is controlled in the same way as in *Reach and Dwell*. In this module however, we've added the ability to open and close the virtual hand. The virtual hand can either be opened or closed depending on whether the patient's "grasp strength" is above (closed) or below (open) a preset threshold. "Grasp strength" is a value provided by the leap motion system that reflects how close all of the visible fingers are to the center of the patient's palm and ranges from 0 (flat palm) to 1 (fist).

Game Control Paradigm: Six fruit are randomly generated and placed in six preset spots on the game shelf. When the player's virtual hand is near the fruit, the fruit will magnetize to the patient's hand. The patient can then make a fist to grab the fruit. While grabbed the fruit can be moved around the game space. The fruit will be dropped if the patient opens the virtual hand. Dropping fruit so that it collides with the bowl will result in a completed trial. Dropping fruit anywhere else will cause the fruit to snap back to its starting position. When all six fruit have been dropped into the bowl, six new fruit will be generated in the game shelf.

Summary: *Reach and Grab* works on coordinated movements in a wide three dimensional space. Patients must reach out in front of them towards the shelved fruit. After magnetization, the patient must make a fist to grab the fruit and then move back towards the bowl. When they are over the bowl they can open their hand to release the fruit and drop it in the bowl to complete a trial. If a patient cannot open and close their hand, this game can be adjusted

to automatically grab the object after magnetization with a “Make Fist” setting. This, however, requires the patient move the fruit so it collides with the bowl directly to complete a trial. One of the strong benefits this game offers is the ability to have an easily repeatable grasp and move task that is not readily available in a true physical space. To emulate this game’s setup, a therapist would need to replace the target objects on the shelf each time a patient completed a trial. In the home it would require the patient to reset the shelf each time, which may be impossible for the patient to complete.

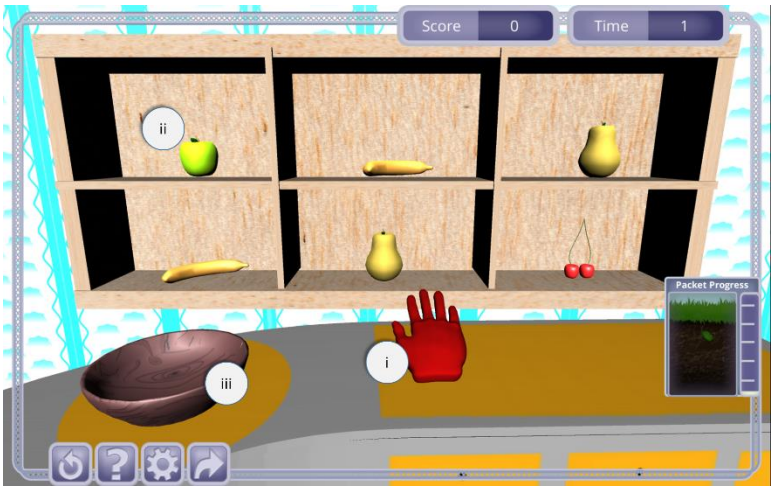

Figure 4.4.20. Reach and Grab Game. In this game, the patient moves their virtual hand (i) in three dimensions to reach towards fruit on a shelf (ii). The patient can then grab the fruit and drop it into a bowl (iii).

4.4.B.5 Pizza

Functional Movements: Arm range of motion, hand grip, and pattern matching.

Objective: Grab the virtual pizza ingredients in the correct order and place them on the pizza.

Movement Control Paradigm: The control paradigm for this game is the same as in *Reach and Grab*. However, the game boundaries for remapping (Eq. 4.4.2) are restricted to the x-y plane so that patient movement is only required left-right and up-down.

Game Control Paradigm: The game mechanics are fairly similar to *Reach and Grab* where pizza ingredients are magnetized and need to be "grabbed" to be moved to the pizza crust. In this game, however, the pizza ingredients need to be added in a specific order (sauce -> cheese -> toppings). The correct object to grab is highlighted with a particle effect for feedback. Patients can grab the wrong objects, but if they try to drop them on the pizza crust the ingredient will snap back to its starting position. Adding all 5 ingredients to the pizza will cause the scene to reset.

Summary: The *Pizza* game is a functional re-skin of *Reach and Grab* with a slight pattern matching twist. Additionally, while *Reach and Grab* focuses on reaching forward and back with slight deviations to the left and right, this game focuses on left and right movements. A patient is rewarded for a completed trial when each ingredient is added to the pizza, but receives an additional visual and audio feedback reward when the pizza is completed. Settings for this game are the same as in *Reach and Grab*, allowing patient's with limited mobility to play with higher sensitivity settings.

Figure 4.4.21. Pizza Game. In this game, the patient moves their virtual hand (i) in primarily 2 dimensions to make a pizza. Patients must grab ingredients in the correct order (sauce (iii) -> cheese (iv) -> toppings (v)) and drop them on the pizza crust (ii).

4.4.B.6 Giant's Teeth

Functional Movements: Quick velocity changes (as in brushing your teeth)

Objective: Move the toothbrush quickly back and forth to remove the plaque from the giant's teeth.

Movement Control Paradigm: The patient's palm position $\dot{P}$ is remapped to a virtual toothbrush (Eq. 4.4.2). The leap boundaries are similar to those in the *Pizza* game, leading to movements primarily in the x-y plane.

Game Control Paradigm: Each auto-generated plaque object contains a collider mesh. When the running, rectified average of the toothbrush velocity $||v||_{n...}$ exceeds a set value 'v' the plaque touching the toothbrush will disappear (Eq. 4.4.10). The target velocity 'v' can be adjusted with a game setting. The running average value is only counted when the toothbrush bristles are within the plaque's collider mesh, meaning the patient must make quick and small movements to remove the plaque. Running average is calculated over n = 10 samples or about

500ms, with variations occurring due to varying framerates. Specifying horizontal or vertical requirements in the settings menu allows for only the velocity components of the target direction to count. This is akin to substituting $\dot{\dot{P}}_t$ for $P.\dot{x}_t$ *or* $P.\dot{y}_t$ in Eq. 4.4.10. After each of the eight plaques have been removed, they will all respawn in their original positions.

Eq. 4.4.10. $$|v||_{n\ldots} = \frac{(||v||_{n-1} + ||v||_{n-2} + \cdots + ||v||_1) + \frac{\|\dot{P}_t - \dot{P}_{t-1}\|}{\Delta t}}{n}$$

Summary: *Giant's Teeth* has the most straightforward mapping to real world function. The acceleration of the hand as it changes from one direction to the opposite direction is necessary for a lot of movements, especially brushing teeth. By modifying the required velocity value 'v' a therapist can start their patient at easier difficulties, often allowing the patient to clear an entire row of plaque in one good movement. Increasing this value requires the patient to carefully control their movements while still moving quickly. Allowing the therapist to specify between horizontal or vertical movement further allows for patients to work on their specific problem areas.

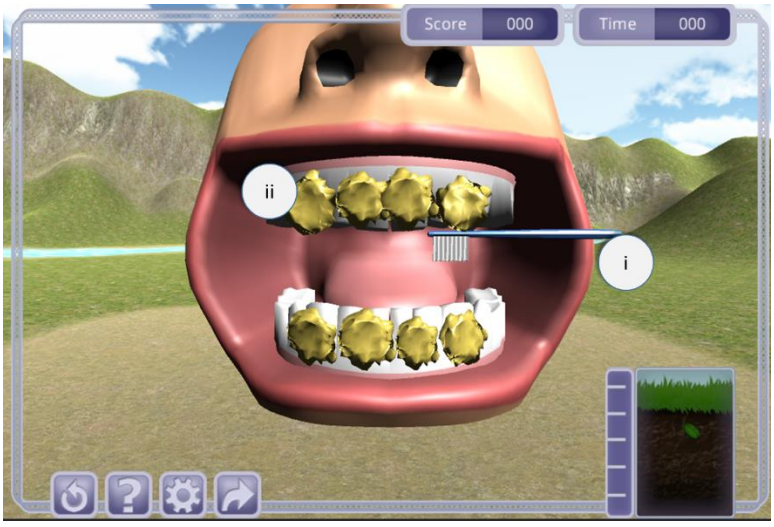

Figure 4.4.22. Giant's Teeth Game. In this game, the patient moves a virtual toothbrush (i) to remove plaque (ii) from the giant's teeth. Patients maintain contact with the bristles of the brush and the plaque while rapidly moving left and right or up and down to remove it.

4.4.B.7 Whack-A-Mole

Functional Movements: Finger Flexion and Extension.

Objective: Move the hammers up and down to hit the moles as they pop up.

Movement Control Paradigm: The relative position of each of the patient's finger tips controls the angle $'\tilde{h}'$ of five corresponding hammers pivoted around the base of the hammer's handle '$\dot{h}$'. Both the angle and height of the hammer are adjusted to induce a smooth controlled motion that doesn't accidentally hit a mole when it is at rest. First the fingertip position '$\dot{F}$' is remapped to game space $\dot{f}$ (Eq. 4.4.2). The y position '$\dot{f}.y$' of each finger is used to calculate an average position '$\dot{f}.y_{avg}$' (Eq. 4.4.11). We calculate hammer position using this average value along with an additional compensation that adjusts for pronation and supination of the wrist using a remapped palm position '$\dot{p}$' and the palm normal '$\vec{N}$' (Eq. 4.4.12). Hammer rotation is directly mapped to rotation along the x axis using the height value and a few preset values (Eq. 4.4.13). Further, this mapping is directly adjustable by a sensitivity setting *'s'*.

Eq. 4.4.11. $\dot{f}.y_{avg} = \dot{f}.y_{thumb} + \dot{f}.y_{index} + \dot{f}.y_{middle} + \dot{f}.y_{ring} + \dot{f}.y_{pinky}$

Eq. 4.4.12. $\dot{h}.y = ((\dot{f}.y_{avg} - \dot{f}.y) - (\dot{p}.x - \dot{f}.x) * \vec{N}.x) * s$

Eq. 4.4.13. $\tilde{h} = (90 - \frac{60 * \dot{h}.y}{4}, -25, 0)$

Game Control Paradigm: Each hammer has a collision mesh on the hammer's head and the mole is surrounded by one collision mesh. Mole positions are randomly selected from 5 pre-determined positions immediately beneath the hammers. A trial is completed when a collision

between the hammer and mole occurs and the mole respawns in a new location. The mole's position cannot be the same two trials in a row. A further option for this game allows for moles to appear above the hammers as well. In this case, the mole's position is randomly selected between all 10 positions but cannot occur at the same height twice. Additional settings prevent the mole from showing up beneath specified fingers. These settings also directly affect Eq. 4.4.11 where that removed position is removed from the calculation of the average. If only one finger is used the average position defaults to the remapped palm position. A one finger setting, however, is only useful if the mole appears above the hammers as well.

Summary: *Whack-A-Mole* works on the flexibility of individual fingers. Each finger must move independently to reach the mole as any concurrent movement will adjust the average value (Eq. 4.4.11) and hinder the movement of the hammer. The sensitivity on this game works in a similar manner as the others, but has a much larger impact on the game's requirements. Healthy individuals may even have a hard time reaching pinky targets on the lowest sensitivity without practice since the ring finger tends to move alongside the pinky finger. This game does require patients to be able to spread their fingers slightly as the Leap camera has difficulty identifying fingers if they are too close together.

Figure 4.4.23. Whack-A-Mole Game. In this game patients must move individual fingers to control the position of hammers (i). The patient must move individual hammers to hit a randomly appearing mole (ii).

4.4.B.8 Two Hand Shape Match

Functional Movements: Bilateral hand movement, forearm pronation and supination, and grip.

Objective: Move both hands to match both the height and shape of target hands. When matched, the patient must hold the position for a set amount of time.

Movement Control Paradigm: Both of the patient's hands are remapped to game space (Eq. 4.4.2) in the y direction only. Each hand can be in three distinct states: 'chop', 'slap', and 'fist' determined by the hand's grab strength 'G' and palm normal '$\vec{N}$ ' (Figure 4.4.24). A chop shows the hand flat in the y-z plane, a slap shows it flat in the x-z plane, and a fist shows the hand closed.

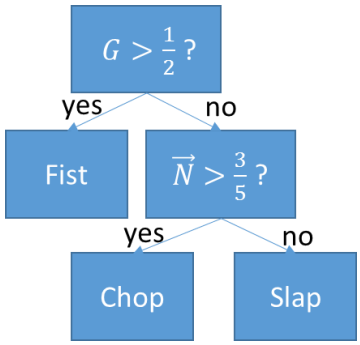

Figure 4.4.24. State diagram for Two Hand Shape Match Game. To determine which of the three states the hand could be in we first look at the grab strength and then the palm normal.

Game Control Paradigm: The patient must move their hands to match both the shape and height of two mirrored target hands. The mirrored hands can either be high or low and can be in any of the three hand states (‘chop’, ’slap’, or ‘fist’). A ‘Same Shape’ toggle setting forces both hands to be the same shape. A ‘Match Height’ toggle setting places both hands in the top position and removes the matched height requirement. When the states are matched, a timer will start that fills a center feedback meter. A trial is completed when the timer exceeds the hold time setting value. If the state becomes unmatched either from height or shape, the timer will reset. Additional height feedback elements are shown next to the timer meter. The two blocks nearest the meter show the target hand height, while the outer blocks show the patient’s current hand height.

Summary: *Two Hand Shape Match* requires a considerable amount of coordination with both hands. While the states can be matched in any order (left or right first, height or shape first), a high score comes from moving all pieces together in a coordinated manner. Moving between slap and shop states works on pronation and supination, while making a fist works on grip. Having the target shapes be different requires additional cognitive skills to view the mirrored hands and translate that to the correct patient hand movements. Modifying the sensitivity (or

even turning off "Match Height") can allow the patient to focus more on shape matching if they have difficulty in keeping their arms at a certain height. Alternatively, a low hold time can allow a patient to make quick movements up and down to reach higher scores.

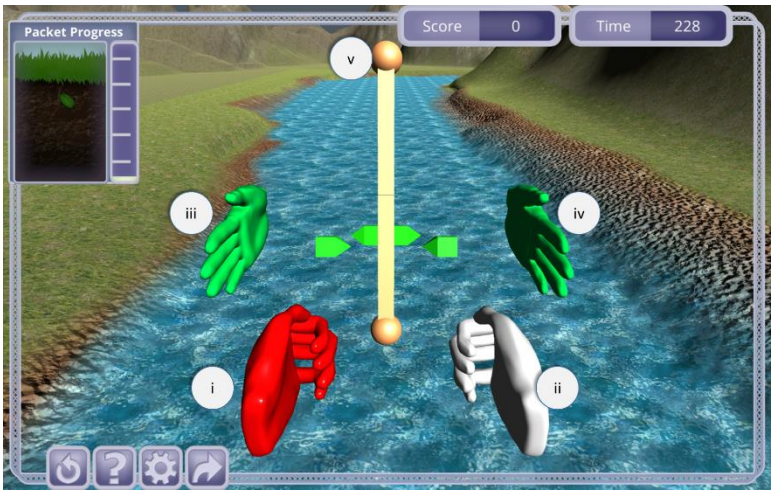

Figure 4.4.25. Two Hand Shape Match Game. In this game patients must move both left (i) and right (ii) virtual hands to match both the height and shape of corresponding target hands (iii and iv). A hold time meter with attached height indicators (v) provide additional visual feedback for the task.

4.4.B.9 Finger Position Match

Functional Movements: Finger adduction and abduction, pattern matching

Objective: Match the finger orientation of the target hand

Movement Control Paradigm: The tips of each of the patient's fingers and their relative locations to each other create a set of four touch states. These states estimate whether the fingers are or are not touching each other for the following combinations 1) thumb-index, 2) index-middle, 3) middle-ring, and 4) ring-pinky. A state is true if the tip positions, projected on a line perpendicular to the hand direction, are within a set threshold of each other. This threshold can

be modified by a sensitivity value, but is primarily set based on the Leap's ability to detect the width of a finger. A virtual hand on the screen represents the patient's current state by modifying the relative angles of the fingers at the metacarpophalangeal joints. There are not intermediate states within this model.

Game Control Paradigm: A randomized set of touch states are generated for the target hand. The target hand is then positioned in a similar manner as the patient's virtual hand. A trial is complete if this set of states matches the patient's states after which a new set of states is generated.

Summary: *Finger Position Match* utilizes a simple matching paradigm to work on a patient's ability to spread and compress their fingers. This game has not yet had a theme treatment like the other games, but has already shown popularity amongst some therapists. It is important to note that some patients cannot produce all touch states. Using the right hand as an example, (false, true, false true) represents a hand position that is impossible for some individuals. In the current version, such a state can be skipped, but future work may exclude these entirely. Further, this game requires the patient to make a relatively flat hand, which may be difficult for some patients who otherwise need this type of exercise.

Figure 4.4.26. Finger Position Match Game. In this game, patients must adjust the positions of their fingers to control a virtual hand (ii) and match a target hand (i). Finger positions are represented in a set of finger touch states that indicate whether or not two fingers are touching each other. The above state is 1) true, 2) false, 3) true, 4) false.

4.4.B.10 Pillbox

Functional Movements: Pinch grip, pattern matching

Objective: Move pills from the bottles to the correct slot in the pillbox.

Movement Control Paradigm: Patients control a set of chopstick-like objects that can either be opened or closed. Similar to the virtual hands described in previous games, these chopsticks are remapped to the patient's palm position (Eq. 4.4.2). Opening and closing the chopsticks is controlled by another native Leap parameter 'pinch strength'. Pinch strength is related to how much of a pinch movement the patient is making controlled by how close the thumb tip position is to any other finger. The thumb touching another fingertip produces a value of 1, whereas the thumb being as far away as possible produces a value of 0. If the patient's pinch strength is above a preset threshold the chopsticks will be closed, otherwise they will be open.

Game Control Paradigm: Patients must first open one of the lids on the pillbox by tapping the bottom of their closed chopsticks (the location of a collision mesh) to the target lid. The lid will stay open for a set amount of time depending on a customizable game setting. Patients must then move the chopsticks so that they collide with one of three pill bottles. Each pill bottle has a label stating which corresponding pillbox slots it can fit into. When the chopsticks collide with the pill bottle they must be in an open state. The patient can then close the chopsticks to grab a pill from that bottle. When this action occurs the game creates a pill of the correct color and places it between the end tips of the chopsticks. Finally the patient must move the chopsticks so that the pill is above the target slot in the pillbox and then open the chopsticks to drop the pill. A trial is complete when the pill collision mesh collides with the appropriate pillbox slot. If the pill is dropped in an incorrect slot it will disappear and no points will be given.

Summary: *Pill Box* is by far the most challenging game we have developed. Patients have limited time after opening a lid to grab the correct pill from the bottle and return it to the slot. This game has a direct translation to a patient's activities of daily living, but is limited in its current scope. As an already challenging game, we have limited the pill bottles to static labels (the left bottle is always 'M, T, W' for example). A true ADL task would require us to modify the labels to show that in addition to being able to make the movements, the patient knows how to sort pills from bottles into the correct day in the pill box. Additionally, the task would work best with a limited number of pills per day. In the current iteration, a patient can continuously move pills from the Monday bottle to the Monday slot and still receive points. This is fine for task simplicity but would need to change to make the task more functionally relevant. The chopstick visualization was chosen to more closely resemble a pinch action, but future iterations

may attempt to show a real hand making a pinch movement. Finally, the game is limited in its representation of a pinch. Pinch strength represents the proximity of the thumb to any finger and thus can reach a ‘closed’ value even in non-pinch hand postures (such as a fist).

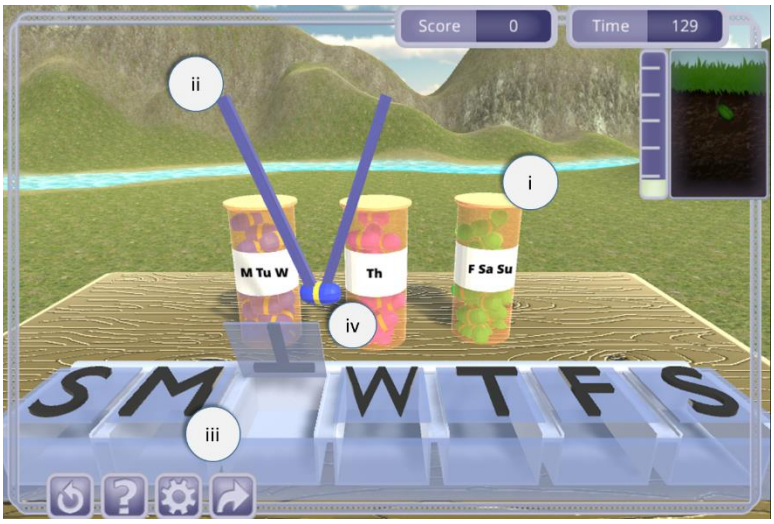

Figure 4.4.27. Pillbox Game. In this game patients must move the chopsticks (ii) to various pill bottles (i) to grab pills (iv). Patients must then drop the pills in the corresponding pill box slots (iii) to complete the trial.

4.4.B.11 Other Games Not Described Here

There are a few games that are not described in the sections above. These are primarily reskins of existing games, such as a boat game that uses the same control paradigm as *Ball Roll* to steer a boat down a river, or games that have not yet been tested thoroughly with our pilot sites, such as a two hand tai-chi type game. Other games are ones we have developed but scrapped due to poor performance in the field. One such example is a pinching game that mapped the thumb and one other finger to balls in space. Spikes would fall from the sky that the patient could dodge by navigating through strategically placed holes. While the game idea itself worked well, we found that too many patients had a difficult time orienting their hands such that

both fingers would be detected properly. This led to frustration from the patient and the therapist and has led us to put the game on the back-burner for future reevaluation.

We also have developed a few sandbox modules that have no direct goals or trial structure, but allow patients to either destroy block-based cities or move items around freely in a kitchen. These modules are interesting as a concept since they allow the therapist to direct patient action by saying things like “put the peanut butter next to the banana”. This, however, makes providing analytics and performance measurements very difficult since we have no time markers of when target actions may have occurred.

4.4.C *Assessments*

The vHAB assessment framework was created out of the vAssess concept game described in Section 4.2. We wanted to be able to streamline our measurement and feedback capabilities from the games so therapists could obtain quick and accurate representations of a patient’s hand and arm function. This streamlining involved removing some of the thematic elements of the games while also sacrificing the repetition inherent in gameplay. Assessments are meant to be performed in the clinic with both the therapist and patient present, and may function best as intermediate check-ins along a patient’s progression. We intend the assessment modules to function as part of the entire vHAB system such that these assessments are done periodically, but the primary therapy is performed within the games. The assessment user interface framework described in section 4.4.A.6, allows therapists to customize an assessment with various modules that specialize in one particular movement or measurement. This list is continuously growing based on recommendations from therapists and clinicians. In the sections below we describe the modules that are currently available for therapists to use.

Assessment Environment

All Modules have the same game scene and environment (Figure 4.4.28). This environment has a few distinct features. First, text prompts appear at the top of the screen describing the current module and the required actions. These prompts function similarly to the tutorial prompts discussed previously, advancing either by time or met physical requirement from the patient. The environment also contains various feedback elements such as a timer panel and a mock virtual Leap Motion controller. Most modules utilize a virtual hand that functions the same way as the hand in *Reach and Dwell*. The patient's real hand is remapped to the virtual hand (Eq. 4.4.2) and the game hand is projected onto front and back grids to assist the patient in locating their hand. In the assessment environment, however, we also trail this projection for a few frames so that the patient has an understanding of their hand's position history. A patient can also make a fist with their hand as in *Reach and Grab* by passing a similar grab strength threshold. In some modules the hand position and ability to make a fist is locked for simplicity.

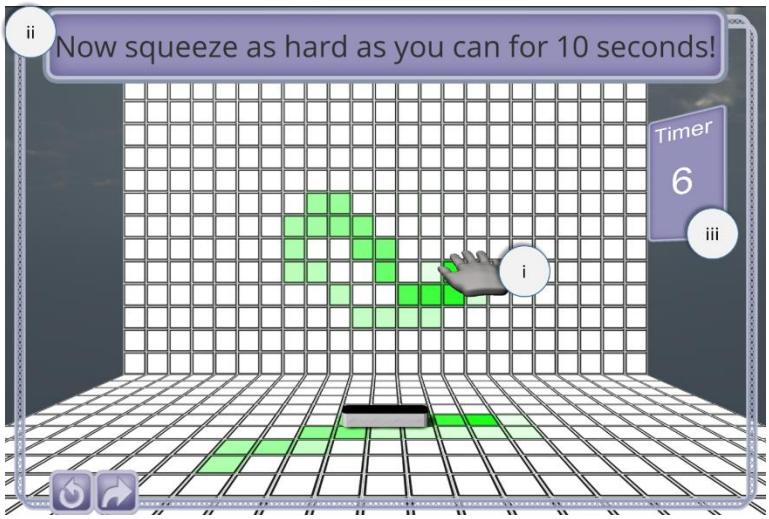

Figure 4.4.28. Assessment environment. The assessment environment is static across most of the assessment modules. In all modules, prompts are displayed at the top of the screen (i) to lead

patients through the exercise. Modules can use a virtual hand (ii) to represent the patient's real hand position and a timer (iii) to assist the patient in the task.

4.4.C.1 Introductory Module

This module introduces a patient to the assessment environment. As previously discussed, many patients have a difficult time interacting with our system at first since they are not physically interacting with anything. This module explicitly addresses this by introducing the system in a piece-wise method. First the prompts describe the purpose of the system then ask the patient to place their hand 6" above the sensor. When a hand is detected, the prompts ask the patient to move their hand around, noticing the projections on the front and back grids. It then introduces the concept of a "home box", a virtual box located at sensor zero, and requests they return to the home box. This module is only intended to be used by the patient one time as an introduction, but may be returned to in special cases such as patients with dementia or after a long break from using the system.

4.4.C.2 Hand OpenCloseOpen

This module asks the patient to place their hand flat above the sensor. Next they are asked to make a fist and squeeze tightly for 10 seconds. Finally they are asked to open their hand again. This module is very simple, but provides great insight into the patient's ability. By having a patient squeeze their fist for 10 seconds, we receive a long profile of their muscle activity and how it changes over time. A single instance can measure a patient's maximum voluntary contraction (MVC), but performing this activity before and after a game or therapy session can provide insights into endurance and strength.

4.4.C.3 Arm Range of Motion

We provide three separate modules for measuring arm range of motion, a 30 second and 60 second bubble popping module and a 60 second painting module. For the bubble popping modules we present the patient with a set of procedurally generated bubbles, starting in the center around the home box. Each time the patient's virtual hand collides with a bubble, we show a popping animation, and generate a new bubble slightly further from the home box up to a maximum volume. As the patient continues to hit more bubbles the required range of motion steadily increases. By starting toward the middle we ensure that all patients can at least hit some of the bubbles. Further each bubble is a discrete object and each popped bubble can be viewed as the completion of a single trial for analytics purposes. From this we can attempt to measure things like path deviations and reaction times alongside the volumetric ranges of motion. The 30 second bubble popping module is for individuals experienced in the 60 second bubble popping module. The main challenge with the bubble popping modules is the visibility of the bubble's depth in the three dimensional environment. Experienced users are able to map where their hand is relative to a given bubble, but a naïve patient will have greater difficulty in performing the task.

The painting range of motion module takes advantage of the projection capabilities of the assessment environment. Instead of trailing a history of projections we simple keep the projection grid filled in wherever the patient's virtual hand has been. The patient is tasked with filling in as many grid panels as they can within the 60 second time period. This version of the range of motion measurement does not have the same discrete task goals, but doesn't suffer from the same depth visualization problems as the bubble popping games.

4.4.C.4 Wrist Range of Motion

In this module we present patients with both their virtual hand and a target hand. The target hand will proceed through a series of orientations designed to test wrist range of motion, such as flexion/extension, pronation/supination, and radial/ulnar deviation. The patient is tasked with matching these angles and then holding the position for 2 seconds. As an assessment we cannot make any assumptions of the patient's true abilities. To account for this we assume a patient is "matching" the target angle if their angle along the current axis of rotation becomes closer to the target angle by a set threshold. For example, in wrist pronation and supination we first display a hand that is flat in the x-z plane and then rotate it around its center along the z-axis. We rotate the target hand 180 degrees as an ideal maximum that the patient could achieve. To advance the prompt, however, a patient only needs to make a 10 degree delta along the z axis. This method can sometimes cause patients to not reach their full range of motion potential, especially if it is their first time through the module. We have noticed, however, that very few patients watch their virtual hand. Instead most attention is focused on the target hand and they work to reach the target angles even if they cannot actually match the true angle.

4.4.C.5 Rest Modules

These modules prompts the user to rest for 5, 10, or 20 seconds depending on the module selected. At the start of the associated rest prompt we start a timer for the corresponding time. At the end of the time we ask the patient to return to the home box. The module is finished when they return to the box, indicating they are ready to begin the next module.

4.4.C.6 Questionnaires

Questionnaires were some of the most requested features within the vHAB system. While we provide new and improved methodologies for delivering therapy, there are still many

supplementary methods that can be used in tandem with our system. Further, questionnaires can be custom designed for facility studies where they may want to correlate our measurements with patient responses or other, more manual, measurements. Providing questionnaires ensures all this data is placed in the same location for easy analysis. The answers to the questions can also be viewed within the data viewer for easy comparisons over time. A questionnaire consists of a set of multiple choice, number line, or input field questions. Currently we have prototyped questionnaires for pain scales, angle verification inputs, and multiple patient hand, wrist, and arm measurement forms that exist as the current standard of care such as QuickDASH [40] and the Patient Rated Wrist Evaluation [41]. The prompt format for a question is much different from a normal module since we do not require a virtual hand or other objects. For the interface we present a touch-based user interface that can be quickly navigated by the therapist or the patient (Figure 4.4.29).

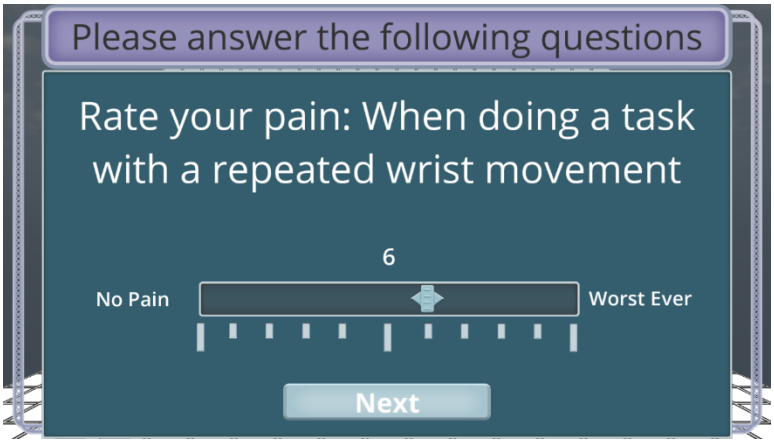

Figure 4.4.29. Sample questionnaire module interface. This sample asks the patient a single question about their pain experienced during a specific situation. This question exists within a set of questions from the Patient Rated Wrist Evaluation questionnaire. To advance, the therapist or patient must click or touch the scale to select their pain and then press next.

4.4.C.7 Combination of Modules

The true power in the assessment framework is the ability to combine a custom set of modules. For example, a sample set may consist of C1. Introduction -> C6.Pain Scale -> C2. Hand Open Close Open -> C3. Bubble Popper 60 -> C2. Hand Open Close Open -> C6.Pain Scale. In this manner fatigue can be viewed as a measure of the difference in MVC between the first and second C2 modules since the patient was tasked with performing a potentially tiring task in between. Impact of therapy on pain can be directly measured by comparing the responses to C6. Comparing this consistent module set over time further allows therapists to make informed decisions about their patient's care.

4.4.D *Data Management*

With the vHAB system we collect hundreds of streams of physiological and gameplay data for each game and assessment. We also track usage data for the games, assessments, and even the menus. Patient specific data is all stored on the local system under the patient's pID while usage data tracked across multiple patients and therapists is stored in a separate global directory. This data needs to be available for both the analysis framework (Section 4.5) and for general validation and testing purposes. In the sections below we describe how the data is collected and stored within the vHAB system.

4.4.D.1 Directory Structure

At the top of the directory structure is a folder named "Data" sitting within the root directory of the vHAB installation. This Data folder holds all of the pID folders alongside basic usage data files and some other operating files, such as an *unlockedLevelList.txt* that hosts an encrypted list of what levels are available for the therapist to use out of the 10+ total. In the home

version, only one pID folder exists for that specific patient. Each pID folder is structured with a series of tiered folders. The top level of the pID folder holds a set of date folders containing all of the game and assessment data for that date, alongside some patient-specific information such as the *patientLevelList.txt* that holds an encrypted list of the games patients see on their game select screen. Within each date folder is set of session folders. A session is any contiguous set of games or assessments that occur without the therapist logging the patient out of the system. Multiple sessions most often occur when a patient is staying in a facility and does morning and afternoon therapy. Within each session folder is a set of folders for each game they played during that session. If a game was played more than once the folder name has a counter added that increments by 1. Each game folder contains all of the raw gameplay and physiological data collected during the game, alongside a results folder produced by the analytics in Section 4.5. A full path to the results folder and the main scalar values may look like:

"./Data/pID/05302016/Session2/BallRoll3/Results/scalar_stats.csv".

Handles to all of the specific portions of the directory are handled with a carefully kept script with public functions for all the other data scripts. This ensures that all of the data is put in a consistent location for a session despite multiple scripts handling the various data saving functions. This overall directory structure allows for easy offline navigation during development but does present data integrity risks. If a therapist navigates to a random patient's folder they could modify specific information about a game or a session, though we expect this to be unlikely to happen in practice.

4.4.D.2 Raw Data

The vHAB system records 4 main streams of raw data during each game and assessment module: leap data, muscle activity data, settings data and metric data. Each of these streams has

its own controller script that saves new data each frame. As mentioned previously, the Leap device updates at up to 120 Hz, and the Myo can record at up to 50 Hz. From these speeds, however, we only sample at the frame rate of the games (about 50Hz). Settings data is updated whenever the settings are changed within the game, while metric data is updated within every each frame. This frame limited approach can be modified to save missed data if it is available, but thus far has not been necessary for game control or analytics. All raw data is saved in separate comma separated value (CSV) format with headers for each data column. Each row of data is time-stamped based on the elapsed game time and the system time. These values are useful in correlating data across data streams.

For leap data we save multiple positional points on the arm, hand and fingers, as well as hand and arm directions, grip and pinch strength, and confidence values. Most games only save one hand's worth of data for the leap (often the rightmost hand in the scene), however other games, like *Two Hand Shape Match*, save data for both hands. For muscle activity data, we save all eight streams of bipolar muscle activity data in its raw form. Settings data contains the current settings values at the start of a game, and all settings modifications. Metric data contains information about the game or assessment that is being played, such as whether the hand is holding a virtual object, when the patient completes a trial, or where a target object has been placed. Each game has a unique list of metric values that are saved.

All of the raw data is processed with a set of algorithms described in Section 4.5. These algorithms produce a set of analytics that are stored within the game directory that the raw data came from. This structure exists as a separate key-value pair file that can be quickly read into the data viewer screens.

4.4.D.3 Usage Data and Long-term Data

vHAB also saves summary data from each time a module is used. Usage data consists of the name of the module or menu, the time of day, the date, and how long the module or menu was opened. This usage data allows us as developers to understand how the systems are used to enhance therapist workflow. Further, this data can be used to identify popular games or assessments for future expansion and targeted updates. Long-term data is patient specific and contains a list of each game or assessment alongside the achieved score and time played. The long-term data is used for quickly graphing simple analytics and metrics in the data viewer screens and for determining if the patient has played the game before in the tutorials systems.

4.5 System Description: Analytics

4.5.A *Foreword: A Note on Contribution*

The following section contains work heavily attributed to Dimitrios C. Gklezakos. Conception, design, and testing were performed by Libey, Mogen and Gklezakos. Coding and implementation were primarily performed by Gklezakos. As such, in the sections below, we will focus primarily on summarizing the values and their use in relation to the vHAB system as a whole, rather than on the equations and accuracy of the measurements.

4.5.B *Introduction*

Integrated and automated analytics are a key component of the vHAB system. Engaging patients with fun games and a score wrapper is only half of the solution to solving low therapy adherence at home. With detailed analytics, patients can see small increases in function to stay motivated in ways they can't do with traditional home therapy. For example, a patient may not be able to see a 5 degree increase in wrist range of motion from day to day, but with the vHAB system they can. Further, therapists can use analytics to better treat their patients. Monitoring multiple analytics over the course of a patient's treatment, allows therapists to identify weak spots and target their therapy to accommodate that patient.

The vHAB analytics platform is created primarily in Python. Each system contains a local installation of the Python framework alongside all of the required packages. At the end of each game or assessment module, raw data is saved to the local system in the specified directory (Section 4.4.D), and then a startup Python script is called to begin the analytics process. This startup script is provided with the most recent module's name and the location of the raw data, which it uses to call the appropriate analytics scripts for that module.

The current set of analytics contains a variety of measurements rooted within traditional therapy paradigms, such as range of motion and reaction times, but also contains some measurements that were previously impossible to record in real time in the therapy facility. These new values present a challenge for both us as developers and for the therapy field in validation and defining appropriate use. Along these lines, we primarily present metrics therapists are familiar with as we continue to validate and collect examples of these new measures.

Throughout the vHAB system there are a few common measurements that are recorded. These values have similar names, but are not necessarily comparable across modules. In the sections below we will describe these analytics and provide examples for some of the games and assessments. A full list of the analytics calculated can be found in table 4.5.1.

4.5.C *Gameplay Analytics*

Game play statistics are the most straightforward of the analytics, but potentially the least useful on their own. To create the gameplay statistics we utilize the raw metric data streams that consist of timestamps for when a trial is completed and additional trial metadata such as target location. From this data, we create “Score”, “Time Played”, and “Reaction Time” statistics that represent how well a patient did in the game. Score is simply the number of completed trials in a session. Time Played is the length of that session. Reaction time is generally target based and is the mean and standard deviation of the time from the start of a trial to the trial’s completion. For example, in *Whack-A-Mole*, a ring finger reaction time of 1.5 seconds means that on average, the patient took 1.5 seconds to hit the 4^{th} position mole with their ring finger, after it appeared.

In addition to these basic analytics for each game, some games provide the opportunity to extract specific meta-analytics. In *Two Hand Shape Match*, for example, we can compare trial

completion steps between hands. If a patient has a slower reaction time in raising their left hand than the right we can present that as a normalized ratio, with 1 representing both hands moving together, and zero meaning that one hand is in position before the next hand moves. This coordination value doesn't have an analog in traditional therapy practice but may be very useful for patients with hemispatial neglect. In other games, such as the *Pizza* game or Pillbox game, we can derive a basic cognitive metric from incorrect trials. If the patient drops a Monday pill in the Tuesday pill box slot it will be measured as an incorrect trial to be compared against the total score the patient achieves. This value may be difficult to interpret since a failure could be caused by a cognitive challenge or by a physical inability to reach the correct target. Thus this value is best utilized alongside other physical analytics such as range of motion or tremor. Finally, we can measure analogs of endurance by examining reaction time changes over a given session. Decreasing reaction times may be a sign of fatigue and we would expect this endurance measure to increase over time. Deriving the scale of the endurance value requires comparison against a norm value. Our current model is being built on the healthy patient data collection described in Section 4.7.

Comparing gameplay metrics becomes very difficult as settings within the game change. A score of 20 with a low sensitivity represents a greater level of performance than a score of 20 with high sensitivity. Further, these metrics cannot be compared across games as the trial structures are very different. In the current version we do not make concessions on presenting these data points, however a future iteration may see setting adjusted scores that use sensitivity values as multipliers for a base scoring system. Overall, the score and time played analytics are meant to be basic summary statistics to enhance engagement, not to drive clinical care. Reaction time values are similarly affected by game settings, but provide interesting within-game session

comparisons. Varied reaction times between fingers in *Whack-A-Mole* may indicate poor performance with specific fingers. This variance should decrease over time as patients recover.

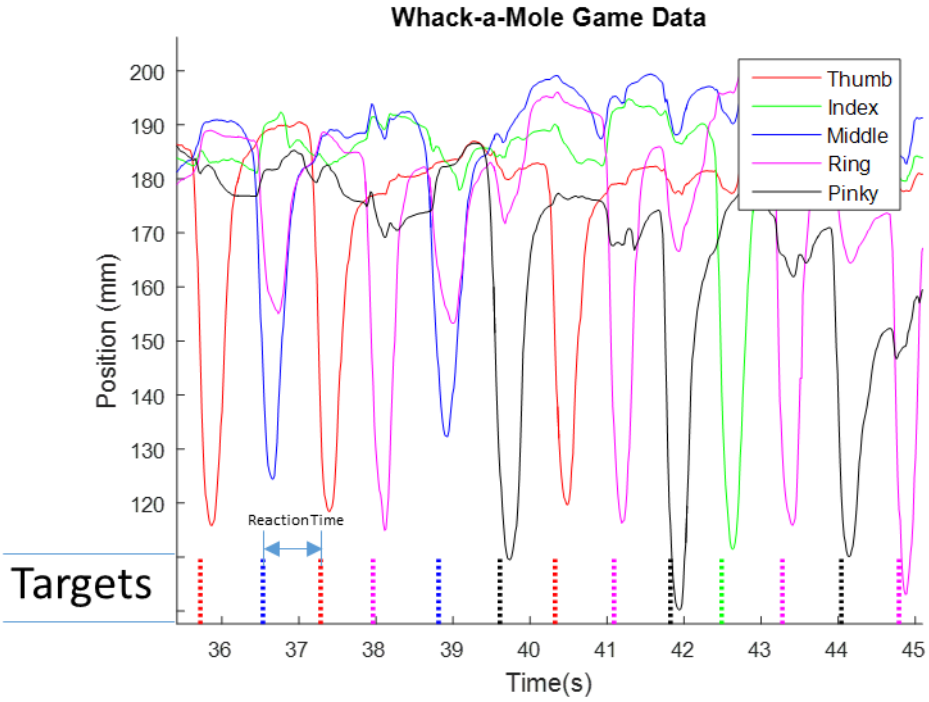

Figure 4.5.1. Gameplay analytics example for Whack-A-Mole Game. Generated targets are shown at the bottom of the plot (dashed lines) alongside the vertical component of the fingertip position in this idealized example. Fingertip height is not directly used to hit the targets, rather a relative position calculation is performed in the game time (Section 4.4.B.5). In this example, extra care to keep the palm flat and finger movements isolated to illustrate the game data components of the data analytics. Reaction time is calculated as the time between trials, averaged over the course of the game on a per-finger basis. In the above example, the reaction time of approximately 0.8s would be attributed to the thumb.

4.5.D *Range of Motion*

Range of motion analytics describe an approximate distance or rotation around a given degree of freedom. Increases in range of motion generally track over time with a patient's

recovery, but are not often measured in the clinic due to the complexity of taking measurements. In a traditional therapy setting range of motion is measured with goniometers. While digital, strain-gauge goniometers can be found on most medical product websites, the most used type consists of a set of plastic protractors. These goniometers present several challenges to use: they only have a specificity of +- 5 degrees, the measurements can vary drastically if the angle is being measured over bony surfaces, and they require that the patient maintain a static position during the measurement.

Our methods of calculating range of motion mimic that of the goniometer. We specifically look at three distinct points on the hand, arm or finger and calculate the angles along the specific axis. For example, in *Ball Roll*, we look at the palm, wrist, and elbow positions to measure angle deviations along the y axis. Some instances of our range of motion measures utilize relative distance measures. This is common amongst the finger motion games where specifying which degree of freedom along the finger to measure is related to the game play. For example, in *Whack-A-Mole* we use the relative position of the finger tips to the center of the palm and other fingers to control the hammer. For this range of motion measure we present the range of vertical distance traveled by each finger. Inverse kinematic models can be applied to these values to estimate the actual angles made by the finger, but these values are not likely accurate in patients recovering from injury. The final type of range of motion we measure is a volumetric arm range of motion. This value varies from 0 to 1 and represents the total three dimensional space the patient moved their hand in out of the total possible space defined by the game and leap boundaries. The validity of this value is determined by the module's ability to ask the patient to perform all possible movements in the three dimensional space, and therefore takes a while to perform. However, no such measurement currently exists and we believe it could be a

very valuable piece of information in determining a patient's ability to reach objects in front of them.

For all range of motion measures we present the mean value and standard deviation of the measurements across all trials in that module. In some user testing and pilot studies, however, these values are not easily translated into the same space as traditional goniometer measures. As mentioned previously, goniometers require that the patient hold a static position during the measurement. Our measurements are taken over more fluid motions and may end up being slightly higher than a held position. Further, a lot of the value of our measurements is in the repetition and continuous nature of the values. A full representation of a range of motion and how it is calculated is shown in the full set of data (Figure 4.5.2). This presentation does not fit into a therapists workflow and summary statistics are difficult to create that represent all of the information in just 20 seconds of data. Further, the standard deviation value or even a decay coefficient value better represent performance over time, but education and detailed documentation are required to provide therapists with the knowledge to interpret these values.

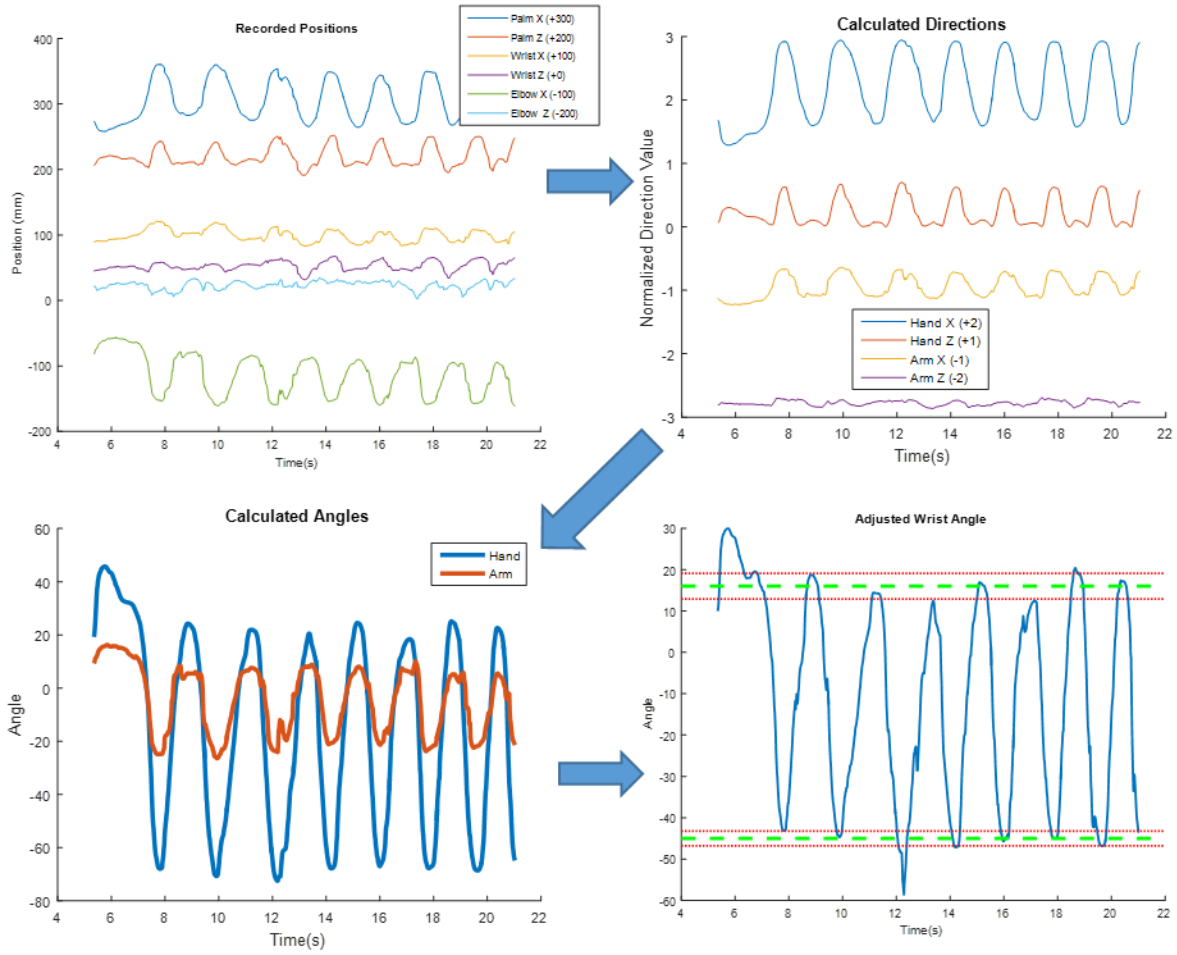

Figure 4.5.2. Sample range of motion plots for the Ball Roll Game. We start with the position of the palm, wrist, and elbow of the patient (Top Left). We use this data to calculate the normalized direction vectors for the hand and arm (Top Right) and then the angles of the hand and arm (Bottom Left). Subtracting these two angles produces our final angle value. Providing a relative value allows us to account for lateral movement of the arm that may occur during gameplay. Minimum (-45+-1.8) and maximum (16+-3.1) angles are displayed in the dashed red and green lines. It is important to note that this may not represent the true maximum or minimum the patient is capable of, but is instead the patient's ability to perform the actions we required of them.

4.5.E *Muscle Complexity*

The muscle activity underlying hand and arm movements can showcase critical aspects of recovery from a variety of conditions. In the case of stroke there are typically several different presentations on the road to recovery including: flaccid paralysis (almost no EMG activity), increasing muscle tone, and spasticity [43]. There are a variety of techniques for processing surface EMG data to extract relevant clinical information from the complex signals. To create the most clinically-digestible numerical value we adapt the Non-Negative Matrix Factorization approach introduced by Seung and Lee in 1999 [44].

The NNMF technique attempts to build a representation of a complex data stream using a linear set of small set of basis vectors. These synergies represent common activation patterns in the muscle activity channels. Figure 4.5.3 shows an example of the NNMF algorithm applied to *Ball Roll* in a healthy patient. Previous research has shown that these synergies are relevant and stable in healthy patient upper extremity muscle activity patterns during isometric force tasks [45]. The technique also shows that synergies remain consistent across patients and change over the course of stroke recovery [46] These synergies can be linearly combined and compared to original sEMG data to understand the impact of the first more variance accounted for by few synergies, the less able the patient. To date this has been shown to be true with lower limb synergies and gait in patients with Cerebral Palsy [36]. Figure 4.5.3 shows an example of the NNMF algorithm deconstructing simple wrist flexion and extension during *Ball Roll*.

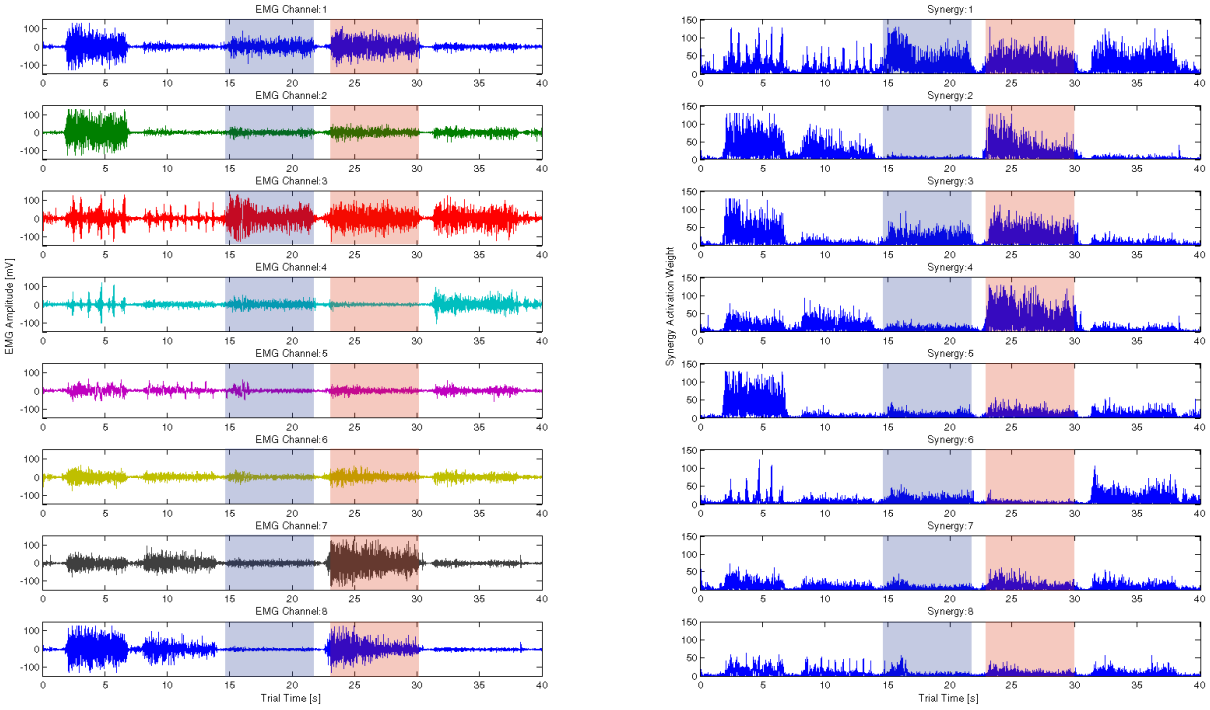

Figure 4.5.3. Example EMG Decomposition from Ball Roll Game. The left panel shows a snapshot of EMG data collected during *Ball Roll*. A sample extension epoch is highlighted in blue and a sample flexion epoch is highlighted in red. In the left panel of raw, randomly ordered EMG traces there are several channels that there are selectively active for flexion (Channels 7 and 8) compared to extension. Synergy activations plotted on the right are ordered by magnitude from 1 to 8. It is important to note that synergy 1 captures both flexion and extension activation patterns and has the greatest magnitude throughout, reflecting the contribution from all contributing electrodes. Subsequent synergies capture extension or flexion more dominantly.

4.5.F *Tremor Characterization*

The fine kinematic tracking of hand position in relation to game object positions and timing allows us to explore quantifying and subtyping the status of different tremors as well. This will be detailed in cowriter's theses.

Table 4.5.1. All analytics for each module.

Module	Section	Analytics
Ball Roll	4.4.B.1	Wrist Flexion/Extension Range of Motion, Reaction Time, Muscle Complexity
Turn the Dial	4.4.B.2	Forearm Pronation/Supination Range of Motion, Reaction Time, Muscle Complexity
Reach and Hold	4.4.B.3	Arm Volume Range of Motion (3D), Reaction Time, Tremor
Reach and Grab	4.4.B.4	Arm Volume Range of Motion (3D), Reaction Time, Tremor
Pizza	4.4.B.5	Arm Volume Range of Motion (x-y plane), Reaction Time, Tremor, Failed Trial Ratio
Giant's Teeth	4.4B.6	Reaction Time,
Whack-a-Mole	4.4.B.7	Finger Flexion/Extension Range of Motion, Reaction Time,
Two Hand Shape Match	4.4.B.8	Reaction Time, Comparative Tremor, Coordination
Finger Position Match	4.4.B.9	Reaction Time, Finger Adduction/Abduction Range of Motion
Pillbox	4.4B.10	Reaction Time, Arm Volume Range of Motion, Failed Trial Ratio
Hand OpenCloseOpen	4.4.C.2	Maximum Voluntary Contraction, Muscle Complexity
BubblePopper	4.4.C.3	Arm Volume Range of Motion, Reaction Time
Painting ROM	4.4.C.3	Arm Volume Range of Motion
Wrist Range of Motion	4.4.C.4	Multiple Wrist Range of Motion

4.6 USE CASE: PILOTS AND EARLY FEEDBACK

4.6.A *Introduction*

We began testing the vHAB with patients and therapists early in the development of the system. This initially took the form of one-on-one sessions with therapists and professionals in the rehab medicine space as described in Section 4.2, but this type of feedback was not enough to finish development of the system. From these sessions we received conflicting reports of healthcare regulations, needs of the therapists, and patient ability in relation to the system. While all of this information was useful, it made it very clear that we had to see the system in use to prioritize development milestones. To accomplish this, we set up partnerships with a commercial entity, the local science center, a hospital in-patient facility, and a skilled nursing facility. These pilots were not focused on collecting or validating data, but were highly organized use-case studies setup to collect usage statistics and end-user feedback. In the sections below we describe the genesis of each pilot, the state the vHAB system was in at the time, and the end results from the pilot, both in terms of system changes and end-user workflow.

4.6.B *Pilot 1: Skyline Retirement Community*

4.6.B.1 Introduction and Methods

Skyline Retirement Community (SRC) in Seattle, Washington is a skilled nursing facility where we conducted our first pilot test of the vHAB system. Skilled nursing facilities present an interesting challenge in end user workflow integration, and our first pilot study elucidated many issues with our early user interfaces and system capabilities. For this pilot we used an early vHAB system without a muscle activity sensor. One system was deployed for a three month

period after a one hour training session with the therapists. Multiple follow up visits were scheduled during the course of the pilot to collect feedback and deliver updated software builds. The vHAB system was set up in SRC's therapy gym where a majority of their therapy was performed. Patients consisted of geriatric patients recovering from a variety of injuries, but no specific demographic information was collected.

4.6.B.2 Outcomes

As a first pilot, we received invaluable feedback relating to the use of vHAB in a skilled nursing facility. In retrospect, it is clear that the system was not yet ready for this level of testing and deployment, both in terms of software and system education. The system was used for three months and then reclaimed to collect and analyze the data; however due to a poorly implemented patient management structure we were unable to analyze patient specific data. The pilot officially ran from January 2015 until we reclaimed the system in September 2015, but the system was not heavily used during any time period. The reasons for this low usage became clear through the follow up sessions with their therapists.

Primarily, we had created a system that was too complex to use, containing too many modules and options. The therapists found the user interface difficult to navigate and the game objective too unclear. Our training protocol at the time consisted of one training session over lunch before leaving the system in the hands of the therapists. During this hour, we demoed the system, but provided no formal training, hands-on experiences, or leave behind documentation. Further, this system did not have built-in tutorials or settings descriptions. These small design changes were fixed over time, but still left the primary issue of training and education. The therapists continued to use a patient account named "Test" instead of creating individual patients

because it was easier to do in their workflow, and, to their knowledge, individual patient accounts did not provide a clear benefit. The in-game settings were confusing and there were too many games to choose from. In a given day, they may have remembered how to use one of the games, but it may not have been useful for that specific patient. It was clear from this experience that training and continued education of the system are just as important as creating a useful system. Each subsequent pilot and experiment has contained a stronger focus on this aspect and has led to better experiences.

4.6.C *Pilot 2: Tacoma Lutheran Retirement Community*

4.6.C.1 Introduction and Methods

The Tacoma Lutheran Retirement Community (TLCR) in Tacoma, Washington is a similar facility to SRC in both patient population and therapist composition. This pilot began a few months after the SRC pilot, which allowed us to refine both the training protocols and the actual vHAB software. For training on the system, we began with a 1 hour lunch training, but scaled back the amount of information we tried to cover and only overviewed three games. We then shadowed the therapists throughout the afternoon as they used vHAB with their patients. We answered questions and received feedback from all users. We also tested a few new software features, such as system auto-start, where vHAB would automatically launch if the system ever shut down. We returned to TLRC multiple times over a six month period to gather additional feedback and update their system with new features.

4.6.C.2 Outcomes

This pilot lasted from July 2015 to December 2015. The versions of the system utilized in this pilot were more sophisticated than that of the first pilot, but the success of the pilot came

from the modified training protocols. Limiting the scope of training to just a few games made the therapists feel comfortable with the system and allowed them to focus on what patients in their case-load could benefit from using vHAB. This pilot led to the creation of the Pillbox game and the Finger Position Match game through personal conversations and iterative feedback. Difficulties in this pilot primarily arose from the distance of the facility from the system's developers. Updates were slow to deliver and it was difficult to troubleshoot the system over the phone with the therapists when something went wrong. These issues are inherent in a developing system and as such we sought a closer partner for our final pilot study.

4.6.D *Pilot 3: Harborview Medical Center*

4.6.D.1 Introduction and Methods

Harborview Medical Center (HMC) in Seattle, Washington hosts an inpatient therapy center that sees primarily stroke, spinal cord injury, and traumatic brain injury patients of varying demographics. This pilot saw quite a different set of users than the previous, skilled nursing facility, pilots and provided new opportunities in testing the limitations of the system. We initiated this pilot as a precursor for an at-home study (Section 4.8) to familiarize the therapists with the system so they could feel comfortable referring their patients to the study. Additionally, it allowed us to validate our previous changes made through the first two pilots for both our training protocols and system deployment. For this pilot, we deployed two systems to approximately 20 therapists over two separate training sessions. We followed a similar, limited game set model, as in the TLRC pilot, but we further supplemented training with scheduled hands-on experience for the therapists. We paired up the therapists and had them use the system together, with one acting as the therapist and the other acting as the patient. This method drove

them to ask usage questions we hadn't heard before and expanded the types of conversations we could have during the pilot.

4.6.D.2 Results and Outcomes

This pilot lasted approximately 4 months (December 2015 to March 2016) and saw over 30 patients of varying injury presentations. Though the system was used significantly more than in the previous pilots, the numbers were not as high as we expected from a high capacity facility. During the first few months, low usage was driven by the system setup in the facility. Due to security reasons, the therapists locked up the tablets overnight. This meant that in order to use the system, they needed to take it out of the locker, wait for the computer to start, plug in the peripherals, and then start the vHAB software. This increased the chance of human error in the setup, and, more importantly, took too long to easily include in a normal workflow. For the last month of the pilot we added a tablet lock to the system and worked with the therapists to establish a dedicated space for the system in their therapy gym. This increased visibility of the system and reduced the workflow burden in using the system, leading to increased use during the last month of the pilot.

4.6.E *User Experience: Pacific Science Center*

4.6.E.1 Introduction and Methods

In July 2015 we were approached by the Pacific Science Center (PSC) in Seattle, WA to assist in the creation of an educational exhibit demonstrating new technologies from the University of Washington. We created a special build of the system consisting of a modified user interface that allowed users to select and play 1 of three games (*Shelf Grab, Whack-A-Mole,* and *Reach and Hold*). The primary purpose was to demonstrate how science and engineering can be

used to help people in need, but we were able to collect general feedback from users to influence system design. We deployed one system in September 2015 and the exhibit ran until March 2016. Working with the PSC we designed a set of questions designed to help us collect feedback. For each game we asked “Tell us how much you did or did not enjoy each game” as a multiple choice and then “What can we do to improve the games?” as a freeform answer. We also asked for demographic information and “Do you have any other feedback?” to capture things we may have missed.

4.6.E.2 Outcomes

For these questions we collected the demographic information and general system satisfaction of 14 users (Figure 4.6.1). The system was used more than 14 times, but feedback was not a required component of the exhibit. There was not a measurable correlation between any of the demographic and user satisfaction, but this is likely due to the low user count.

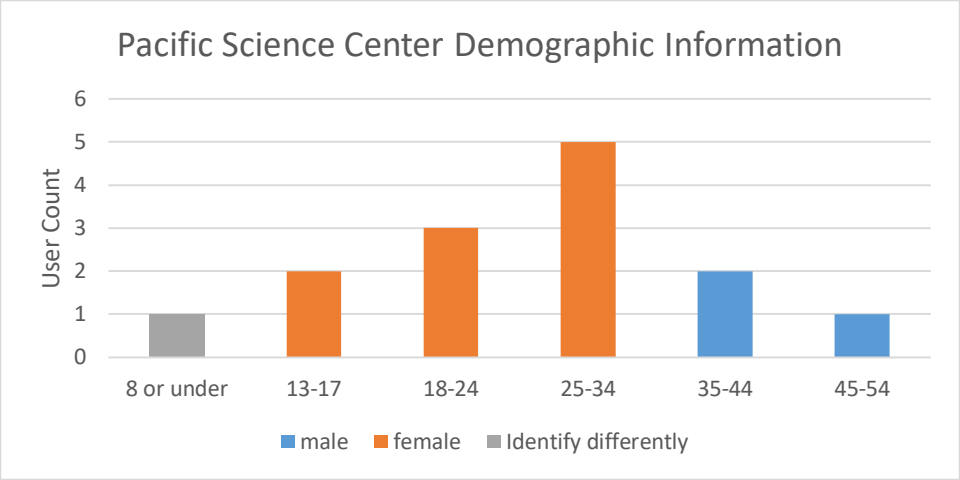

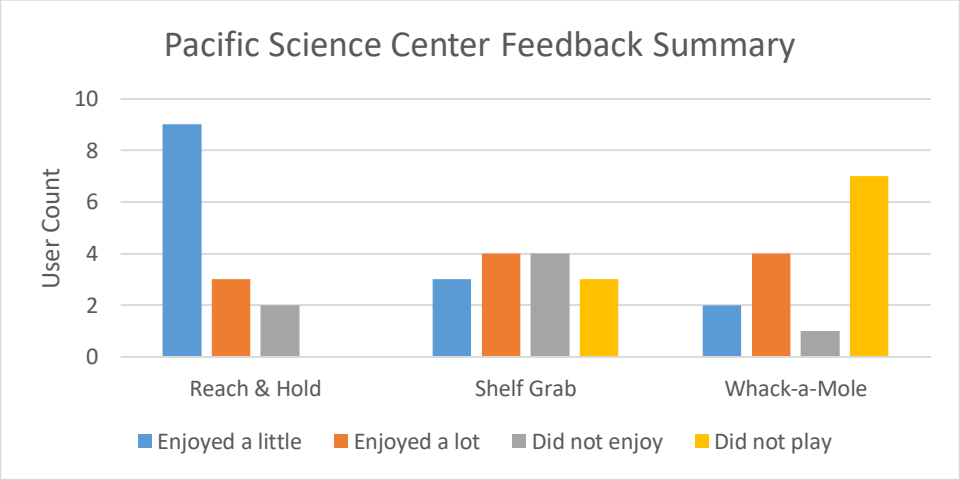

Figure 4.6.1. Pacific Science Center Feedback. Survey information was collected from 14 users over the course of 8 months of system deployment in an exhibit at the Pacific Science Center. Top. Demographic information from PSC survey. Bottom. Feedback summary information from PSC survey.

The special user interface did not contain tutorials nor did any user undergo training for the games. Brief descriptions of the games were provided in the exhibit, but there is no data as to how many people read the descriptions before attempting to play. Of the 14 surveys we received the feedback was primarily positive for each game, and complaints of the system were in the same vein as what we learned in the pilots with users stating:

"Instructions or rename. I had no idea what to do at first. I am used to touching things quickly in computer games."

"More explanation of how you're supposed to place your hand - this is for fingers, right?"

"Didn't explain what you needed to do, I didn't get it."

This feedback reinforced the need for robust instructions within the game. On the other end, however, some users were able to immediately understand the system and even develop strategies. This positive feedback was validating, but did not overshadow the need for system education.

4.7 USE CASE: HEALTHY SUBJECTS

4.7.A *Introduction*

The vHAB system aims to deliver therapy in an alternative way to traditional methods. Through vHAB's ability to automatically track hand kinematics and muscle activity we can create complex analytics (Section 4.5) that fully describe hand and arm function. Therapists, however, are not accustomed to seeing these types of measures, which presents a challenge in implementing the system in therapy facilities. One method of addressing this is by validating the measurements we take against traditional therapy measurements. For example, we could attempt to claim that the wrist angle minimums and maximums in *Ball Roll* are analogous to goniometer measures. This is quite difficult as *Ball Roll* provides the patient multiple attempts to reach this range of motion in a continuous fashion, while goniometer measures are performed under statically held conditions. Further, some analytics we've created, such as endurance curves, muscle complexity, and tremor do not have traditional analogs. To combat these challenges we set out to create a database of healthy user data.

This healthy user database (HUD) will eventually consist of age, gender, and handedness matched measures for most, if not all, of our analytics. Building this database will take considerable time and effort, but is the only reliable way to build maximum value benchmarks for recovery. Creating minimum values for the database is not likely possible as a zero value is possible in most analytics, but does not necessarily represent zero function. It is likely that through the analysis of recovery data we may be able to build models that future patients could be compared against. For initial deployments of the system, we can assume a linear model between zero and the average values in the HUD.

In this section, we describe preliminary attempts at building this healthy user database. Healthy subjects played multiple games in the vHAB system and demographic information and summary analytics were recorded. This work is by no means comprehensive and will require grander scale to fully implement. Further, some analytics, such as muscle complexity and tremor were not adequately collected in these initial results and had to be discarded from the HUD. Finally, it should be noted, that improvements to the system and the analytics were made in response to the collections of these values. This does not necessarily exclude them from the HUD, but instead will weight them less in the averages as we bring in newer data.

4.7.B *Methods*

All recruitment, data collection, and data storage methods were approved by the University of Washington Institutional Review Board prior to study onset.

4.7.B.1 Subject Recruitment

Subjects were recruited through public workplaces at the University of Washington campus in Seattle, WA. No exclusion criteria were used in this study, though subjects needed to be able to lift their hand above the sensor to collect the data. Subjects were recruited with a standard recruitment script explaining the purpose, risks, and benefits of the study and were consented before beginning the study.

4.7.B.2 Data Collection

Age, gender and handedness were collected prior to using the vHAB system. Subjects were seated in a chair and asked to adjust their position so that they were comfortable holding both of their hands six inches above the Leap sensor. Subjects performed all exercises below

with both hands, the order of which was chosen at random. Settings were consistent across all subjects.

First, subjects were led through an early version of our assessment platform that contained the 60 second Bubble Popper Module and the Wrist Range of Motion module. Subjects were then led through three separate games: *Whack-A-Mole* and two others chosen at random. Subjects were given the ability to become familiar with the game mechanics and hand movements in an unrestricted practice mode during which the researchers would provide instruction and answer questions from the subject. Practice was completed when the subject indicated they were comfortable with the game's mechanics and objectives with both their dominant and non-dominant hand. Practice mode was not repeated during the second hand play through. Data was then collected for 60 seconds of gameplay during which subjects were instructed to perform at maximum effort. This procedure was repeated for each of the three games. Subjects were allowed to rest as long as they wished in between each 60-second recording.

4.7.B.3 Data storage

Data was stored in a slightly modified version of the pID structure previously described. As one time users of the system there was no need to store their pIDs in a patient list for a specific therapist. Instead, all healthy subject demographic data was stored alongside a temporary healthy patient ID. No identifiable information was stored for these subjects.

4.7.B.4 Data Analysis

All raw data was processed in the methods described in Section 4.5 when the appropriate data was available to complete the analysis. Analytics were discarded if not enough trials were

completed or if the analytic method changed significantly during the course of subject recordings. No muscle activity data was recorded due to technical issues at the time of recording. This primarily left range of motion, reaction time, and other gameplay related analytics. Standard deviations are used within the analytics to define a subject's trial-to-trial variance. These are either utilized to trim or smooth the values, as in range of motion measures, or are presented as is next to the mean value. Standard errors were used when comparing subject to subject variability in the measurements.

Comparisons of performance between which hand was used (left or right, dominant or non-dominant) and practice vs performance gameplay are calculated using a two sample t-test. Comparisons between left and right hands split the performance metrics based on the hand used during the module. Hand dominance compares performance metrics between dominant and non-dominant hands. Practice-Performance compares all practice values to performance values during the 60-second tests. Practice mode could be completed with either hand. Therefore the comparison between some metrics is excluded as time could be spend switching hands.

4.7.C *Results*

4.7.C.1 Demographics

Data was collected from 17 subjects (11 Female; 14 right handed; Age 42.53±14.4). Subjects played 12 different modules at unequal frequencies. Aside from challenges with our randomization methods, some games, like the Trace Game, were removed from the game pool due to difficulties in system performance. The intersectionality of demographics and game types prevents any significant analysis comparing precise subject groups partially due to all male subjects being right handed. Handedness was utilized to define whether the patient was using

their dominant or non-dominant hand. Additional patient populations will be required to build a HUD that can truly be age, gender and handedness matched.

4.7.C.2 Gameplay Analytics

Data was collected across all 17 patients to produce 31 different gameplay analytics (Table 4.7.1). Population means were not significantly different across either of the three comparisons (hand dominance, play order, or practice) in 30 of the 31 analytics, though it is important to note that some statistics could not be computed due to missing information or low trial numbers. The one analytic that showed a significant difference was *Reach and Hold reaction time* comparing practice to performance ($p= 0.021$). Across all gameplay analytics, standard errors were relatively low, indicating that these values are a good benchmark for the creation of an early version of the HUD.

4.7.C.3 Range of Motion Summary

Range of motion analytics were only performed on four modules (Table 4.7.2), primarily due to changes in data saving and analytics structures that occurred during or after this study that significantly changed the collected values. Measurements were similar across patients, with relatively low standard errors, indicating that these values represent a basis for comparison with the HUD. However, a number of the angles from the wrist ROM were either lower or higher than literature reported goniometer values [42]. As previously discussed, this could be caused by the differences in measurement techniques, but either way warrants further investigation. Statistically significant differences were apparent in both the left-right hand and dominant-non dominant hand comparisons for the Thumb range of motion measurements ($p = 0.025$ and $p= 0.035$ respectively).

Table 4.7.1. Gameplay Analytics for Healthy Subjects. All presented values for reaction times are in seconds and all other values are unitless.

				p-values (Two Sample t-test)		
Game	**Gameplay Metric**	**Mean ± ste**	**Total Count**	**Left-Right**	**Hand Dominance**	**Practice-Performance**
BallRoll	ReactionTimeMean	3.7 ± 0.3	10	0.590	0.669	0.606
	ReactionTimeStd	1.5 ± 0.3	10	0.318	0.426	0.738
	Score/Minute	16.7 ± 1.3	10	0.591	0.684	-
Turn the Dial	ReactionTimeMean	5 ± 0.8	6	0.250	0.250	0.877
	ReactionTimeStd	4.2 ± 1.6	6	0.478	0.478	0.959
	Score/Minute	17.2 ± 2.9	8	0.216	0.216	-
Pizza	ReactionTimeMean	10.7 ± 1.9	6	0.860	0.860	0.116
	ReactionTimeStd	7.7 ± 3.2	6	0.757	0.757	0.893
	Score/Minute	5.4 ± 0.9	6	0.641	0.641	-
Reach and Hold	ReactionTimeMean	3.8 ± 0.2	4	0.147	0.147	**0.021***
	ReactionTimeStd	1.8 ± 0.4	4	0.179	0.179	0.103
	Score/Minute	15.7 ± 0.9	4	0.162	0.162	-
Whack-A-Mole	IndexReactionMean	0.3 ± 0	30	0.863	0.679	0.861
	IndexReactionStd	0.4 ± 0	30	0.880	0.782	0.547
	MiddleReactionMean	0.4 ± 0	30	0.630	0.550	0.742
	MiddleReactionStd	0.4 ± 0	30	0.236	0.266	0.950
	PinkyReactionMean	0.3 ± 0.1	27	0.673	0.435	0.383
	PinkyReactionStd	0.3 ± 0.1	27	0.481	0.285	0.257
	RingReactionMean	0.4 ± 0	29	0.529	0.390	0.086
	RingReactionStd	0.5 ± 0.1	29	0.434	0.171	0.098
	ThumbReactionMean	0.4 ± 0.1	27	0.148	0.176	0.730
	ThumbReactionStd	0.5 ± 0.1	27	0.613	0.523	0.109
	Score/Minute	52.3 ± 3	34	0.203	0.561	-
Two Hand Shape Match	ReactionTimeMean	3.9 ± 0.4	8	0.327	0.369	0.697
	ReactionTimeStd	2.3 ± 0.6	8	0.301	0.375	0.971
	Score/Minute	16.4 ± 1.3	8	0.439	0.557	-
Bubble Popper	BubblesPopped	30.8 ± 2.6	18	-	-	-
Giant's Teeth	Score/Minute	55.6 ± 10.5	10	0.876	0.876	-
Trace Game	Score/Minute	3.9 ± 1.2	4	0.764	0.764	-

Pinch Fall	Score/Minute	16.1 ± 0	2	-	-	-
Reach and Grab	Score/Minute	5.7 ± 0.8	14	0.929	0.929	-

Table 4.7.2. Range of Motion analytics for healthy subjects.

				p-values (Two Sample t-test)		
Module	**Gameplay Metric**	**Mean ± ste**	**Total Count**	**Left-Right**	**Hand Dominance**	**Practice-Performance**
BallRoll	'MaxAngle'	54.4 ± 3.6	10	0.157	0.979	0.649
	'MinAngle'	-50.9 ± 5.4	10	0.970	0.828	0.851
Whack-A-Mole	'IndexRom'	126.8 ± 5.6	30	0.478	0.332	0.628
	'MiddleRom'	134.8 ± 5.3	30	0.520	0.158	0.411
	'PinkyRom'	108 ± 5.2	30	0.261	0.423	0.596
	'RingRom'	127.6 ± 5.7	30	0.120	0.077	0.232
	'ThumbRom'	107.1 ± 5.4	30	**0.025***	**0.035***	0.222
Wrist ROM	'HorizontalExtensionMax'	58.4 ± 3.2	17	-	-	-
	'HorizontalFlexionMin'	-62.3 ± 3.5	17	-	-	-
	'SupinationMax'	74.9 ± 9.5	17	-	-	-
	'SupinationMin'	-61.6 ± 9.1	17	-	-	-
	'VerticalExtensionMax'	55.1 ± 3.9	17	-	-	-
	'VerticalFlexionMin'	-79.9 ± 2.4	17	-	-	-
	'UlnarMax'	42.3 ± 2.8	17	-	-	-
	'RadialMin'	-38.5 ± 2.2	17	-	-	-
Bubble Popper	'ReachVolumeFraction'	0.6 ± 0.1	17	-	-	-

4.7.C.4 Other Measurements

During *Two Hand Shape Match*, we were also able to measure tremor (Table 4.7.3). These values had a much higher standard error than the other measures indicating that the analysis metrics may need to be refined before including these values in the HUD. Further the

actual standard deviation measures with a subject are higher than the mean values, indicating that the variability in the measure is too high to be of use in a clinical setting. Adjustments to these values have been made since this test to improve these measurements for future tests.

Table 4.7.3. Tremor Analytics from healthy subjects.

				p-values (Two Sample t-test)		
Game	**Gameplay Metric**	**Mean ± ste**	**Total Count**	**Left-Right**	**Hand Dominance**	**Practice-Performance**
Two Hand Shape Match	'LeftHandTremorMean'	26.9 ± 10	8	0.403	0.633	1.000
	'LeftHandTremorStd'	31.8 ± 15.8	8	0.368	0.375	0.906
	'RightHandTremorMean'	21.8 ± 7	8	0.233	0.797	0.259
	'RightHandTremorStd'	29 ± 9.6	8	0.216	0.956	0.167

4.7.D *Discussion*

4.7.D.1 Standard deviations vs standard errors

Most of the gameplay and tremor analytics contain both a subject mean and standard deviation and a population mean and standard error. This population does not represent the true population in a traditionally statistical sense, but is the current standard to build against for the HUD. While standard errors across subjects tended to be low, this does not mean that there is not significant variability within a subject over the course a game or assessment. In fact, many of the standard deviations we recorded were within close range of the value means. This variability is to be expected in many of the games for first-time users and is likely to decrease with continued play. Models may need to be adjusted to account for amount of time each game has been played to build accurate models of learning vs recovery of the system.

4.7.D.2 Value comparisons

Most of the values collected did not show significant differences in any of our three test conditions. Of the two analytics that did show significance, it is unclear what may have caused this difference. Low trial numbers put the *Reach and Hold reaction time* value into question, but the difference does make sense in terms of overall game difficulty compared to the other games. *Reach and Hold* is the only included game that requires three-dimensional hand movement, and as mentioned previously, learning how to map hand depth to the virtual space is one of the most challenging aspects of the system to learn. The *Whack-A-Mole thumb range of motion* analytic is a more curious case as it was significant for both the right-left and the dominance comparisons. This may be influenced by the fact that 14 of the patients were right handed, but p – values for the other metrics do not show a direct relationship between the two comparisons. Slight differences between reaction times and ability are likely to occur between hands, but these variations would require much further testing to determine. Instead, these differences could be caused by positioning of the hands above the sensor during the gameplay and the thumb moving in a different plane from the other fingers. This could be verified by systematically testing these values with the hand at varying points over the sensor.

4.7.D.3 Building model of healthy patient data

The above data represent a significant start towards collecting comparative data to use within the vHAB system to help therapists and clinicians interpret vHAB data. As our first implementation of many of these analytics at a large scale it became clear that many of them did not perform as expected, causing system crashes and lags. This experiment also exposed a flaw in the muscle activity recording system, which was good for system development, but bad for building a HUD. Regardless of these missteps, we were still able to collect data for 51 different

analytics over 17 subjects. Many of these values had low standard errors, leading us to feel confident in the creation of an early version of the HUD. This set of data only represent one set of vHAB settings which will impact all comparisons of the gameplay analytics. While it may not be feasible to test all settings for all games, a few additional settings need to be tested to finalize an accurate model.

Our population was inherently biased and not immediately relatable to all of our end-user demographics. Our mean age of 42 does not represent the traditional age of a stroke (66% > 65) [43] nor does it match users in a traditional skilled nursing facility. Further, individuals were recruited from workspaces around a university, which may have produced individuals more familiar with technology than the average population. These biases and the issues mentioned above need to be accounted for in building the full model. While we are still far from implementing the HUD within the vHAB system, this early version can be used to perform internal testing and validation.

4.8 USE CASE: HOME ADHERENCE STUDY

4.8.A *Introduction*

Adherence to a therapy regime after an injury drops off significantly when the patients are sent home [44]. Traditionally, they are sent home with sheets of paper instructions that provide pictures and diagrams of their therapy exercises. In addition to this format lacking any form of enjoyment, patients are not given any feedback as to whether they are performing the exercises correctly or if they are getting any better [45, 46]. In a set of key surveys many patients indicated that they would be more likely to complete their therapy if alternative, engaging, exercises were available [44].

vHAB was created to solve this problem, but there are a few key questions left to answer. First, does vHAB provide access to engaging exercises at home, or are they as boring as traditional methods? Second, does vHAB actually increase adherence to therapy? Finally, does using vHAB improve outcomes for these patients? This question is much more difficult to answer, as developing proper population sizes for outcome studies after injury is a time intensive and expensive task.

Our main driving hypothesis is that **increased adherence through engaging home exercises will lead to better outcomes** simply because patients are performing exercises that would otherwise be skipped. Since vHAB was built directly from existing therapy exercises, it is likely that using vHAB will be equivalent to patients performing these exercises on their own. It is possible that vHAB will lead to better outcomes in the home setting since the system provides immediate feedback and measures of progress in real time, further enhancing the patient's ability to target problem areas of their movement. However, proving that vHAB is better than traditional

exercises is not a line of inquiry we intend to pursue due to the challenges listed above. Instead, we have created a home adherence study that primarily looks at utilization data of the vHAB system and relies on patient feedback to measure system engagement.

In this study, patients who recently suffered a neurological trauma, such as stroke or spinal cord injury, received a vHAB system to use at home over an 8 week period. During this time, we collected usage data, a set of analytics on gameplay and function, and verbal feedback relating to their use of the system. vHAB system use was then compared to how long the patients performed traditional therapy over the same length of time using a custom designed tablet log system. This study is still ongoing at the time of this writing, but below we present the preliminary results for two patients who have completed key milestones within the study.

4.8.B *Methods*

4.8.B.1 Study Criteria

Study participants had a recent injury causing upper extremity impairment and were within 6 months of being discharged from an inpatient facility at the start of the study. Patients were referred directly through their physician, therapist, or other official caregiver, who believed the patient could be a good candidate for extended therapy with the vHAB system. Patients could not participate in the study if they 1) had contraindications for using the muscle activity armband, such as implantable devices (pacemaker, Baclofen shunt) or skin lesions or rash on the forearm, 2) had cognitive deficits as a result of their injury, demonstrated by scoring 5 or more errors on the Pfeiffer Short Portable Mental Status Questionnaire, or 3) vision or hearing impairment. The following study was approved by the University of Washington Institutional Review Board prior to subject recruitment.

4.8.B.2 Tablet Log System

The study was designed to compare usage data between the vHAB system and traditional therapy. In addition to asking patients to recount the duration and time of day of their exercises we designed a custom therapy logging system (Figure 4.8.1) that could be sent home with the patient. This tablet log consisted of a tablet computer and custom software that allowed patients to track how often, and how long they performed their therapy exercises. The software emulated a simple stop watch, where patients would press "Start" when they began their therapy, and "Stop" when they were finished. The amount of elapsed time was then saved to a log file on the local system for future analysis. Patients could also "Pause" the timer if they were temporarily stopping their therapy exercises but intended to continue.

Figure 4.8.1 Tablet Log software. This software was sent home with patients during the Table Log phase of the home adherence study. Patients could use the timer function of the software to track when and how long they performed their therapy exercises.

4.8.B.3 Study Design

The study utilized a delay cross-over method to maximize potential results with smaller patient numbers (Figure 4.8.2). In this method, patients were divided into two groups. In the first 8 weeks Group 1 received the vHAB system and Group 2 received a tablet log. After 8 weeks Group 1 received the tablet log system, while Group 2 received a vHAB system. Each group used these systems for 8 weeks. In this method, usage data can be compared both across and within each group. Upper extremity function was assessed periodically during the study using traditional assessment techniques, such as the Wolf-Motor Function Test, the Box and Blocks test, and a dynamometer measurement. Assessments were performed by a therapist trained in each method. In the event that patients could not perform the minimum requirements for the tests, these assessments could be skipped. In addition to these motor measurements, the Assessment phases included a verbal questionnaire relating to the use of the vHAB system and general function.

4.8.B.4 vHAB Customization

The vHAB software was modified slightly for this study to allow for easier level navigation. Patient and therapist management user interface screens were removed so that when launched, the patient was presented with the game select screen (Figure 4.4.10). A smaller, simplified version of the data visualization screen was added to the game select screen so that patients could easily view any collected analytics. Settings were set during the first Assessment period (A1) and adjusted at each based on the patients current ability. The garden wrapper was utilized with the game point to progress point ratios set to optimally grow the garden over 8 weeks to align with the study length. Finally, patients were presented with a limited set of games based on an early assessment of their functional ability. For example, we did not include *Whack-*

A-Mole in their game set if they could not move individual fingers. This game list would be reassessed during each of the Assessment periods in the study.

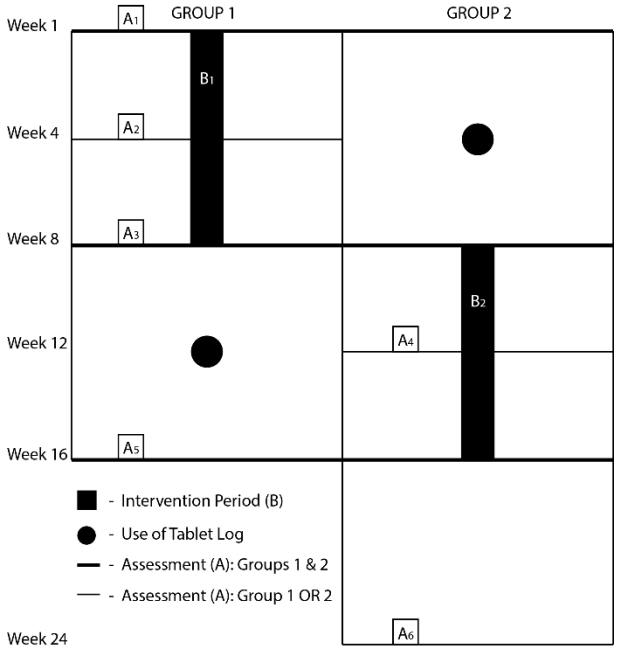

Figure 4.8.2. Home Adherence Study Design Diagram. Patients were divided into two Groups which dictated what system they received first (vHAB/Intervention) or the tablet log. Assessments were performed periodically during the course of the study.

4.8.B.5 Analysis Methods

Usage data consisted of both how long and how often the subjects utilized vHAB or the Tablet Log systems. Cumulative use time for the vHAB system only included time spent within a game module, but did include "rest" periods where the hand was not above the sensor but returned within 5 minutes. Usage of the Tablet Log consisted of all timer log data since patients could pause the system if they were not performing their exercises. vHAB analytics were tracked over the entire 8 week usage period.

4.8.C *Results*

4.8.C.1 Demographics

Two patients with complete spinal cord injuries (C3 and C4) have participated in the study at the time of this writing. While this does not provide enough data to make reliable conclusions regarding system adherence, the data collected so far provides valuable insights into system use. Both patients were unable to perform the physical assessments during the Assessment phase of the study, but game data, analytics, and questionnaire data was still collected.

Both patients were assigned to group 1 and received the vHAB system first. Assessments did not take place at 4 and 8 weeks due to scheduling conflicts. For P01, A2 occurred at day 58, and A3 at day 100. For P02, A2 occurred on day 65 and A3 at day 106. These days are very far outside our study protocol, but may be the norm in trying to schedule visits for individuals with such high levels of injury as it requires high levels of coordination between care staff and the patient.

4.8.C.2 Adherence Data

Both patients utilized the system more before the second assessment (A2) than after (Figure 4.8.3). Reasons for this are further explored in the discussion points below. Early data (Day<50) show increasing usage over time as patients become familiar with the system. Usage days are low (P01:8, P02:14), but each day can contain multiple sessions with different game sessions.

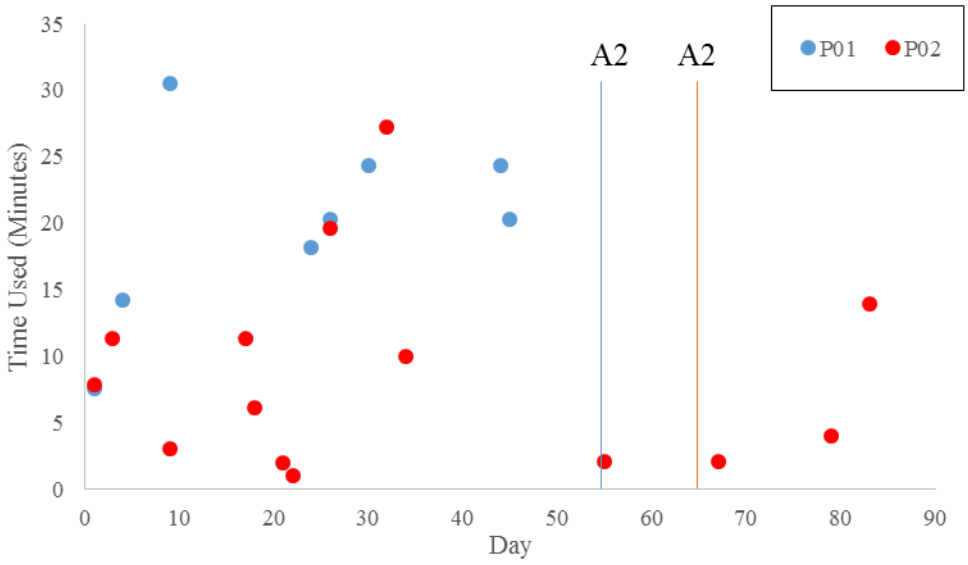

Figure 4.8.3. vHAB usage data in home adherence study. Usage days for P01 (blue) and P02 (orange) were composed of all the individual sessions for that day. Day to day usage was sparse, but some days showed high usage, such as P01 day 9, where the patient used the system 3 separate times playing multiple games each time. Assessment 2 (A2) bars are shown for reference for each patient. It is important to note that P01 did not use the system at all after A2, and P02 barely used the system. P02 preferred *Ball Roll* heavily with 48 play instances, while P01 spilt their time between five different games nearly equally.

4.8.C.3 Analytics Summary

Analytics were performed on most of the sessions for both patients (Table 4.8.1). Some analytics, such as *Ball Roll Max Angle*, could not be calculated for all sessions due to short play times or poor data quality. Other analytics, such as *Turn The Dial* range of motion were not calculated due to an error in the data recordings. The standard deviations of the analytics were relatively high, likely due to both fatigue and eventual learning of the tasks. Most games were not played often enough to extract significant changes over time. Figure 4.8.4 shows *Ball Roll*

angle measurements for P01 (left) and P02 (right) for every play session. Figure 4.8.5 shows the reaction times for those same sessions for P02, who played the game enough times to show decreases in reaction time over time.

Table 4.8.1 Home subject analytics data.

		P01		P02	
Game	**Metric**	**Mean ± Std**	**N**	**Mean ± Std**	**N**
Ball Roll	Max Angle	34.5 ± 14.1	16	56.2 ± 16.8	45
	Min Angle	-45.8 ± 22.5	16	-44.8 ± 15	46
	Reaction Time Mean	9.4 ± 3.9	16	3.4 ± 2.4	48
	Reaction Time Std	10.1 ± 4	16	2.5 ± 3.2	48
Turn The Dial	Reaction Time Mean	9.5 ± 4.2	18	3.4 ± 1.6	4
	Reaction Time Std	11.1 ± 5.6	18	10.4 ± 10.6	4
Reach and Grab	Reaction Time Mean	16.8 ± 10.7	14	10.5 ± 2.8	3
	Reaction Time Std	11.4 ± 11.5	14	5.9 ± 2.7	3
Pizza	Reaction Time Mean	5.4 ± 1.9	14	9.1	1
	Reaction Time Std	5.4 ± 3.9	14	3.9	1
Reach and Hold	Reaction Time Mean	6.1 ± 5.1	15	9.4	1
	Reaction Time Std	6.4 ± 8.7	15	3.0	1
Two Hand Shape Match	Left Tremor Mean	18.6	1	-	-
	Left Tremor Std	34.0	1	-	-
	Reaction Time Mean	4.3	1	-	-
	Reaction Time Std	2.2	1	-	-
	Right Tremor Mean	7.5	1	-	-
	Left Tremor Std	8.0	1	-	-

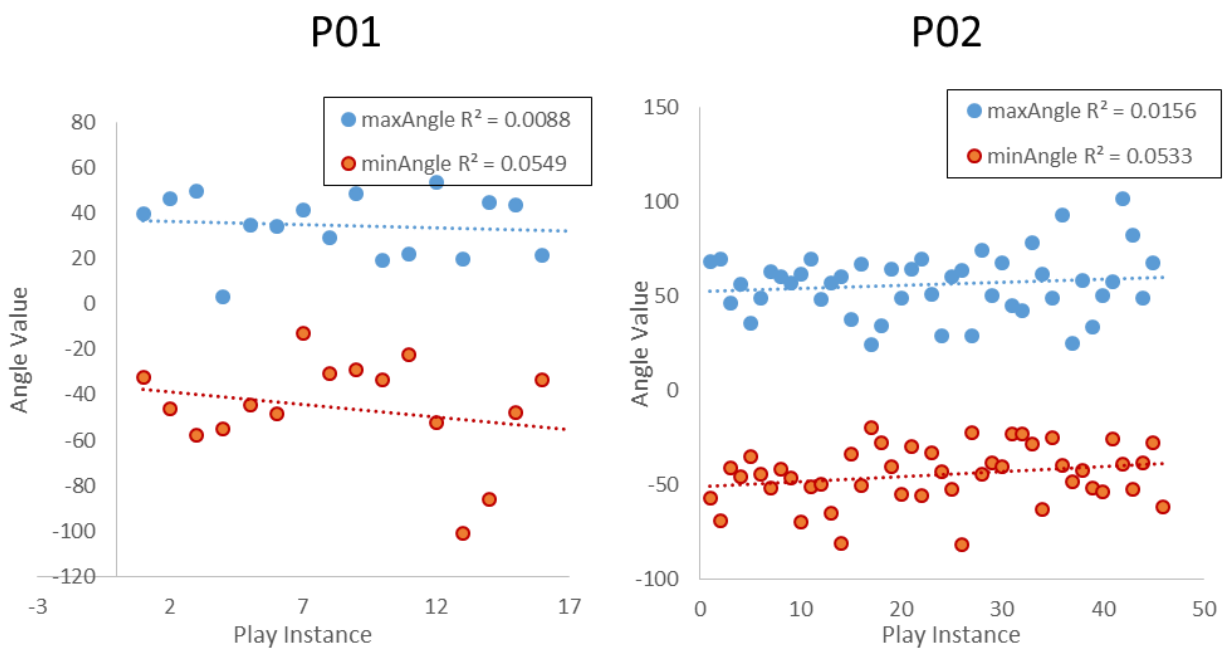

Figure 4.8.4 Ball Roll wrist angle measurements during vHAB home use. Neither the minimum or maximum angles for wrist flexion-extension in *Ball Roll* increased significantly over time for either patient. It is important to note, however, that both patients played the game at the highest sensitivity settings throughout the entire course of the study. Thus, it may have been that they did not need to achieve angles greater than displayed (~50 degrees) to achieve the game's objective.

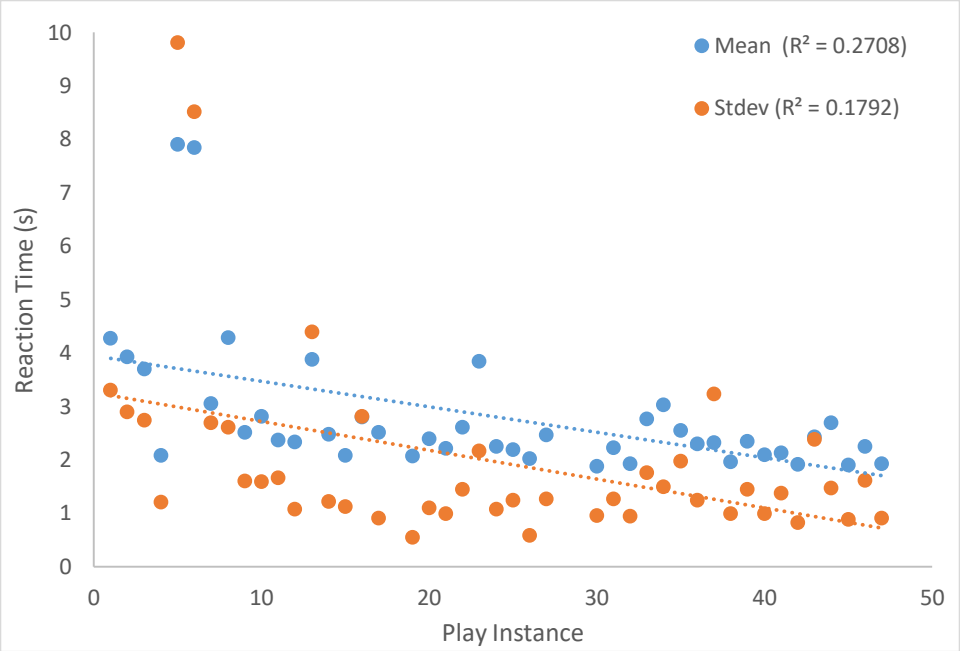

Figure 4.8.5 Ball Roll Reaction Time measurements during vHAB home use. Here we present the only measurable change in game performance. The change in reaction time mean is accompanied by a decreasing change in the standard deviation. This means that the trial-to-trial variability within a given game session decreased as well. It is difficult to tell, with limited data, if this decrease is caused by increasing familiarity with the game or by actual functional improvement.

4.8.C.4 Tablet Log Use

Neither patient utilized the tablet log system during the control portions of the study. This does not mean that they are did not perform therapy during this time.

4.8.C.5 Survey Data

Survey data was collected from both patients regarding their experience with the vHAB system. Table 4.8.2 presents some of the more relevant responses. Questions relating to injury,

demographics, and their perception of gamified therapy were removed as the responses are not relevant at this time. Both patients appeared to have positive experiences with the vHAB system and both would recommend using the vHAB system to others. A common theme among P02, was that the system was great “When it works”. Hardware issues, discussed below, may have influenced this opinion. P01 was very motivated by the garden metaphor, which he found surprising. Multiple suggestions for improvements came from this survey data as well, such as new tutorial and educational components, and assistive control elements.

Table 4.8.2. Survey response questions from vHAB home use

Phase	Question	P01	P02
Before Using vHAB	How often do you engage with your prescribed home therapy tasks?	once a month	no set time, when able
	What is the most difficult part about carrying out your prescribed home therapy tasks?	adding the therapy time into daily routine	frustration about not being able to do things including exercises
	What would make your engagement with your prescribed home therapy tasks easier or more enjoyable?	keep a log, held accountable	faster results, seeing results
After first use	Did you enjoy using the system? Why or why not?	yes - encouraging to do exercise	Yes!
A2	Describe your experience with the vHAB system thus far:	Biggest struggle is daily routine. "Surprisingly motivated by garden metaphor!" Notice getting fatigued during it, depending on time of day. Try not to get frustrated with reach and grab. Run through all games 2x (not two hand shape match), second time through is slower due to fatigue. Get tense and activate other muscles not involved with the task -> has had same issue with different rehab tech.	Great when it works! Can feel it exercising his body, can feel the benefits
	Would you recommend vHAB to someone in a position similar to yourself for their home therapy needs? Why or why not?	Yes, one of the big perks is doing it at home. Time management makes it much easier on the daily routine.	Yes engaging and fun, when it works
A3	Recommendations for improvement	While doing exercises it would be helpful to have someone to consult with to say "remember to activate your shoulder while relaxing your back for movement x". Prompts on the screen could also work.	Voice activated vHAB control. Smooth experience without bugs would make it better.
	Did the vHAB system keep you motivated to do your daily therapy exercises? Why or why not?	More successful when it was set up as a station. Surprised by how motivating the garden aspect was	It is a 2 person project to get started, but great when it works

Would you continue to use the vHAB system once this study has ended for your home therapy needs? Why or why not?	If I could be shown what muscles to work on for the particular exercise it would be more helpful.	I would
Would you recommend vHAB to someone in a position similar to yourself for their home therapy needs? Why or why not?	yes I would, particularly if people are already independent then this would be an even bigger motivating factor	yes, something different and new to do

4.8.D *Discussion*

4.8.D.1 Comparing to model of healthy patient data

Section 7 of this chapter aimed to create a healthy user database of vHAB metric data. This accumulated data is still incomplete, but provides an interesting benchmark to start comparing the two home patients to. *Ball Roll* minimum and maximum angle values for both patients are slightly lower than the healthy user data but still within 1 standard deviation from the healthy users. Reaction time data for the home patients was higher in almost all cases than healthy users. As demonstrated by Figure 4.8.5, however, P02 was able to work to get closer to this norm value. These tools will be very helpful in the continuation of this study and the future use of the vHAB system.

4.8.D.2 Study Populations

Initial protocols for this study called for unilateral injuries and study enrollment within 2 months of being discharged from an inpatient facility. Patient recruitment with these constraints was nearly impossible for our small team. We were interested in these enforcing these limitations since a unilateral injury increases the likelihood that the patient can set up the system on their own. The shorter discharge time was to truly monitor whether they were increasing adherence

significantly with the vHAB system when they would otherwise be likely to do therapy. In our case, both patients were close to 6 months post discharge and were not previously engaged in therapy answering – "When I have time" and "Once a month" – to the pre-study question how often do you do therapy exercises now. We definitely increased the frequency of therapy compared to these answers, but it may have had even more impact if it had been used sooner.

4.8.D.3 Low Usage Data

The two patients we have seen thus far had severely limited function in their hand and arm. They were able to play many of the simpler games at high sensitivity settings; however, we were not able to reliably perform traditional physical assessments throughout the course of the study. This also meant that these patients had a difficult time navigating the vHAB UI on their own. Both patients utilized home health care professionals to help them navigate the vHAB system at home, but this may not be possible for many of our end users. Future iterations of a home-use vHAB system may contain alternative level selection methods, such as voice controls, to assist individuals with more severe impairments.

P01 noted that the system was much easier to use during the first few weeks since it was "setup as a station." At the beginning of the study, our team traveled to his location to set up the system on a table in the living room. For A2, the system was dismantled and brought in for an update and then sent back with P01. Though it is not possible to know for sure, it is likely the system was never set back which explains the lack of usage data. P02 may have had a similar issue post-A2. He reported hardware failures that we attempted to troubleshoot over phone, but were not able to get consistently working. The usage in Figure 4.8.3 does not show multiple 0 score attempts throughout days 60-100, where it is likely the system was not working. This could

have been from poor hardware setup, or from as yet undiagnosed software issues. Either way, hardware assembly processes will be increasingly important in providing a system patients can truly use at home.

4.8.D.4 Tracking traditional adherence

Tracking adherence without a digital system is inherently difficult. It may be weeks in between traditional physician or outpatient visits and relying on a patient's memory of how long and when they did there therapy is not a reliable method for gathering true data. Additionally, patients may not provide accurate results due to various social pressures that accompany injury. These problems presented challenges in designing this study. Providing scientifically accurate values of adherence would require an unbiased observer to watch the patient perform their traditional therapy exercises. It is important to note that the presence of the observer could further influence the patient's adherence to the study. Having the patient fill out pen and paper values can also be unreliable since they may fill them in all at once, just before the study organizers view the data.

Our solution was to implement the Tablet Log system. If patients attempted to rack up multiple sessions immediately prior to an assessment phase, we could examine the time stamps on the data to discount the data. Additional patterns of activity can also be flushed out of the collected data, such as what a "normal" session would look like for that patient. However, this system still has flaws. The presence of the Tablet Log may influence adherence to therapy itself, as the tablet hardware serves as a reminder to perform the therapy. Further, patients may find the timer useful in ensuring they perform 15 minutes of therapy, when they previously may have stopped short at 12 minutes. Finally, if patients truly desired to, they could start the timer while

performing other tasks and set an alarm to remind them to stop the system. It is unlikely that incentives would drive patients to this extreme, but it is nonetheless important when examining the significance of the data.

It may be that outcome measures are the only true way to measure actual adherence, which is contrary to the goals of our central hypothesis. True adherence comparisons may be a good corollary to outcomes, but adherence may prove too difficult to measure with traditional exercises. Alternative methods will continue to be explored as we develop new studies with the vHAB system. One partial solution would be to include a leap motion sensor with the Tablet Log, and have patients perform their traditional exercises over the sensor. This would allow for direct study of the impact of the gamification, movement feedback, and real time analytics on adherence to therapy.

4.8.D.5 Impact of System for Home Use

Based on survey responses, both patients enjoyed using the system at home during the study. Taking this alongside the usage data, indicates that the system needs to be perfected from not only the software and hardware side, but from a setup and accessibility standpoint. With limited data, both from small subject size and low usage data, it is difficult to extract outcomes or any main conclusions regarding adherence.

4.9 FINAL THOUGHTS

Here we have described the creation and testing of vHAB, a gamified therapy and assessment platform designed to enhance rehabilitation after neuromuscular trauma. vHAB consists of both custom software and carefully selected commodity hardware, crafted to meet six design principles aimed at making the system accessible to as many people as possible. Early pilot studies exposed some of the key challenges with implementing any sort of new technology into a health care environment. Multiple iterations of the vHAB design have prepared us to overcome these barriers, allowing vHAB to impact the lives of countless patients. In the following sections, we further examine these barriers and present solutions that may become integral parts of vHAB in the future.

4.9.A *Importance of Commercialization*

Reaching new patients and facilities is a challenge with any new product. From an academic environment, we have reaped many benefits in making new contacts, both from end-users and field experts. This, however, did not necessarily lead to usage of the systems. Anyone can accept a "free" pilot study, but that does not necessarily mean they will use the system. When entities, especially high-efficiency therapy facilities, have to pay for something the incentives become aligned in using the system. It takes more work upfront to justify the use of the system to the facilities, but through the process everyone understands the benefits and limitations of the system. Then, each month of the system's use is carefully monitored for efficiency and benefits to ensure that it is worth paying for. This may be risky early on in a product's development, but would provide more detailed feedback and usage data for continued iterations. It is only through commercialization of vHAB that we will be able to reach this level of engagement with our end-users.

Another key benefit of commercialization of vHAB is the long-term scalability and reach of the system. An academic project cannot manufacture, distribute, and provide the support infrastructure for a system like vHAB. When thinking of vHAB within a corporate infrastructure, however, there are many other key engineering factors that come into play. Cost of the system was always an important consideration, but now the cost models need to be sustainable and accessible. Shipping and system setup become even more important, since we won't be able to personally set up systems as in Section 4.8. Finally, technical support and system updates require additional engineering development to ensure the system's longevity. These topics are not the key focus of this writing, but are worth mentioning to fully describe the future of the system.

4.9.B *Cost and efficiency in healthcare*

We set out to design vHAB to be accessible in price for facilities and end-users at home, but changes in healthcare legislation make this challenge a moving target. For facilities, therapists charge insurance based on skilled therapy reimbursement codes often billed in 15 minute increments. The definition of "skilled" therapy is murky and based more on a facility's experience with reimbursement rejections and documentation practices than an actual true definition. In talking with therapists, it ideally means activity or exercise in which the patient is trying, challenged, and/or engaged. This also means that there is one therapist per patient to monitor the patient and adjust the task when appropriate. Facilities tend to operate at very high efficiencies to maximize profits, meaning 80-90% of the day must be providing skilled therapy for each therapist. Anything that detracts from this time, such as documentation, system setup, or training may not be adopted.

vHAB can be the exercise that the patient is doing during skilled therapy, but current codes do not allow for extra reimbursement to cover the cost of vHAB. Instead, vHAB must

provide additional benefit over traditional therapy to fit into the facilities. These benefits must also outweigh any setup time that may not be present in traditional modalities. Currently, vHAB's main additional benefits come from increased engagement and better insights into recovery. Increased engagement may allow patients to complete their therapy when they otherwise would not perform skilled therapy for a full 15 minutes. Recovery insights through our assessment and analytics systems may allow therapists to better target areas of difficulty or keep patients motivated, but otherwise does not provide direct financial benefit. This, however, is changing.

With recent legislation, many facilities are undergoing dramatic changes in reimbursement processes and resultant therapy practices. The first change comes from the Affordable Care Act's sec. 2706 which established Accountable Care Organizations. We won't go into full detail of the ACA or ACOs here, but it reinforced a growing mantra in the therapy communities of moving from "experience based care" to "evidence based care". Experience based care revolves around established therapists knowing how best to treat patients because they have the experience concerning outcomes resulting from their treatment. This type of care is problematic for multiple reasons, but mostly because it is difficult for insurance companies to establish proper care pathways for their patients that lower risk for re-admittance. Evidence based care aims to solve this in two parts. First, care should be quantifiable with outcomes and incremental progress measures. Second, these measures can be used to define ideal care pathways or ideal outcomes for any given patient. This is a challenging task, given the diversity of patient presentations, but represents a great opportunity for the vHAB system.

The second set of changes comes from the push towards telemedicine. Reimbursement codes for home equipment have existed for a long time, but recent thought-leader shifts may

allow for more healthcare technology to replace traditional splints and bands. In this case, vHAB would be prescribed by the therapist and paid for by the patient's insurance. Therapists and physicians can then use another recently added reimbursement codes to view and analyze the data collected at home. Telemedicine legislation is continuously being presented, which may allow for additional opportunities for facilities to see additional benefits for home use of the vHAB system.

Future improvements to the vHAB system will add more benefits to the facilities to enhance system adoption. Data analytics collected during each module are already helpful for defining a patient's care path. Automated documentation and reporting of these analytics, and even usage statistics, could save therapists time and reduce the risk for declined reimbursements. In the short term, we plan on having exportable text blocks that describe the care that was delivered in the 15 minute session. This text can be copied into a patient's documentation, so the therapist does not need to type out anything. Prototypes of this system have already been created, but defining the ideal information to present still needs user testing and feedback. The long-term vision of this automation will directly integrate this documentation into the patient's electronic medical record. This integration presents additional security and workflow challenges, but should further increase the value of the system to facilities.

4.9.C *Benefits of continuity of care*

In an ideal care model, patients will be exposed to the vHAB system in a facility and then be sent home with their own system. This continuity of care allows patients to be immediately familiar with their home exercise program and provides an unbroken record of their performance. Currently, patient progress is only tracked when they return for follow up outpatient visits. Therapists are under the same pressures described above during these follow-up

visits and may not perform a robust assessment. This leads to sparse data points of a patient's recovery, making evidence based care decisions nearly impossible. With vHAB, measurements are taken during every therapy exercise and assessments can be performed quickly during follow up visits. Not only does this provide more information for the therapist and motivation for the patient, but it represents a huge shift in tracking recovery statistics across patients. Comparing measurements across subjects can help a therapy facility adjust their practices, or help insurance companies identify ideal care pathways that minimize re-admittance. This data may be of additional use to the scientific community for tracking the differences in spontaneous recovery and therapy induced recovery after stroke, or for introducing new biochemical treatments that work alongside traditional therapy practices where adherence data is paramount in validating the treatment's efficacy.

4.9.D *Conclusions*

The vHAB system represents a new opportunity for therapists and end-users to enhance their therapy practices. vHAB can be used in a therapy facility and then be sent home with patients to continue their rehabilitation, enabling an unprecedented monitoring of recovery statistics and adherence. Early pilot studies assisted in the development of the vHAB system and further studies will explore the additional benefits that vHAB can provide. End-user surveys showed that patients enjoyed using the system and provided early evidence that vHAB does improve adherence to therapy at home through its engaging games and wrapper. This writing represents the beginning stages of vHAB. It is our hope that through further development and the commercialization of vHAB that we will be able to establish vHAB as the new de-facto paradigm for upper extremity therapy after neuromuscular trauma.

4.10 vHAB PATENT

The following pages contain the US Patent Application filed for the vHAB platform.

US 20160331304A1

(19) **United States**

(12) **Patent Application Publication** (10) **Pub. No.: US 2016/0331304 A1**

Libey et al. (43) **Pub. Date: Nov. 17, 2016**

(54) **SYSTEM AND METHODS FOR AUTOMATED ADMINISTRATION AND EVALUATION OF PHYSICAL THERAPY EXERCISES**

(71) Applicant: **University of Washington**, Seattle, WA (US)

(72) Inventors: **Tyler Libey**, Seattle, WA (US); **Lars Crawford**, Seattle, WA (US); **Dimitrios C. Gklezakos**, Seattle, WA (US); **Brian Mogen**, Seattle, WA (US)

(73) Assignee: **University of Washington**, Seattle, WA (US)

(21) Appl. No.: **15/154,382**

(22) Filed: **May 13, 2016**

Related U.S. Application Data

(60) Provisional application No. 62/161,100, filed on May 13, 2015.

Publication Classification

(51) **Int. Cl.**

A61B 5/00	(2006.01)
A61B 5/11	(2006.01)
A61B 5/0488	(2006.01)

(52) **U.S. Cl.**

CPC ***A61B 5/486*** (2013.01); ***A61B 5/0488*** (2013.01); ***A61B 5/742*** (2013.01); ***A61B 5/1114*** (2013.01); ***A61B 5/4848*** (2013.01); *A61B 2560/0223* (2013.01); *A61B 2505/09* (2013.01)

(57) **ABSTRACT**

Methods and systems for automated administration and evaluation of physical therapy exercises are provided. A motion prompt is displayed on a display device. Hand position information is generated by a hand position sensing device, and muscular activity information is generated by a muscular activity sensing device, while a user performs the prompted motion. Compliance with the motion prompt is determined by analyzing the hand position information, and muscular activity is evaluated using the muscular activity information. The difficulty of the motion prompts provided by the system is automatically configurable based on the determined compliance with the motion prompt and the muscular activity evaluation.

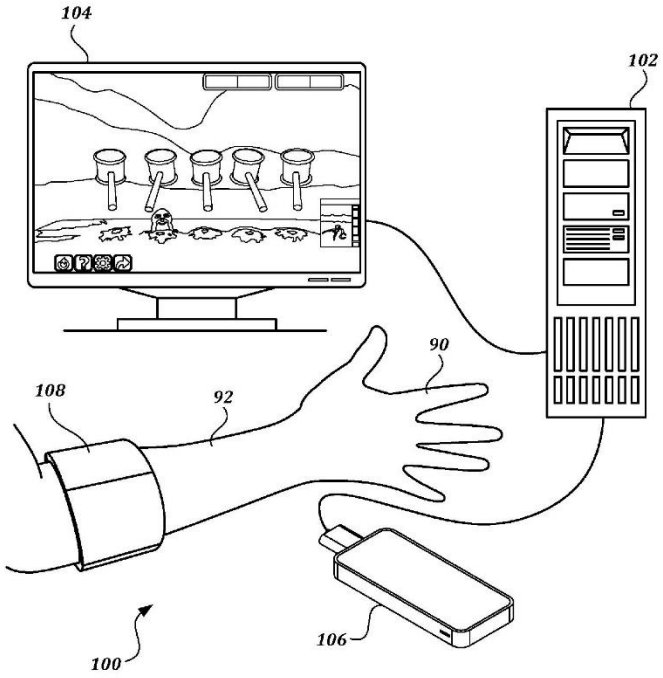

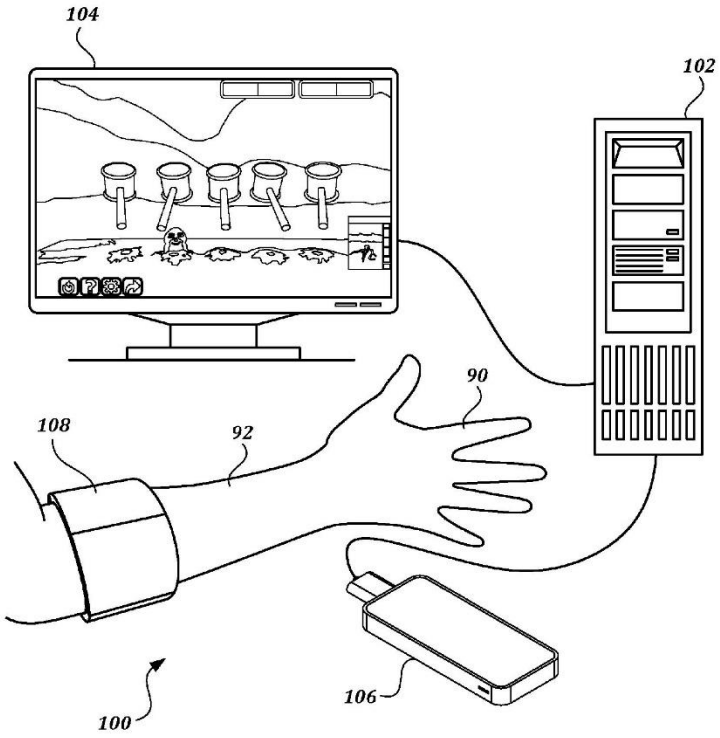

FIG. 1

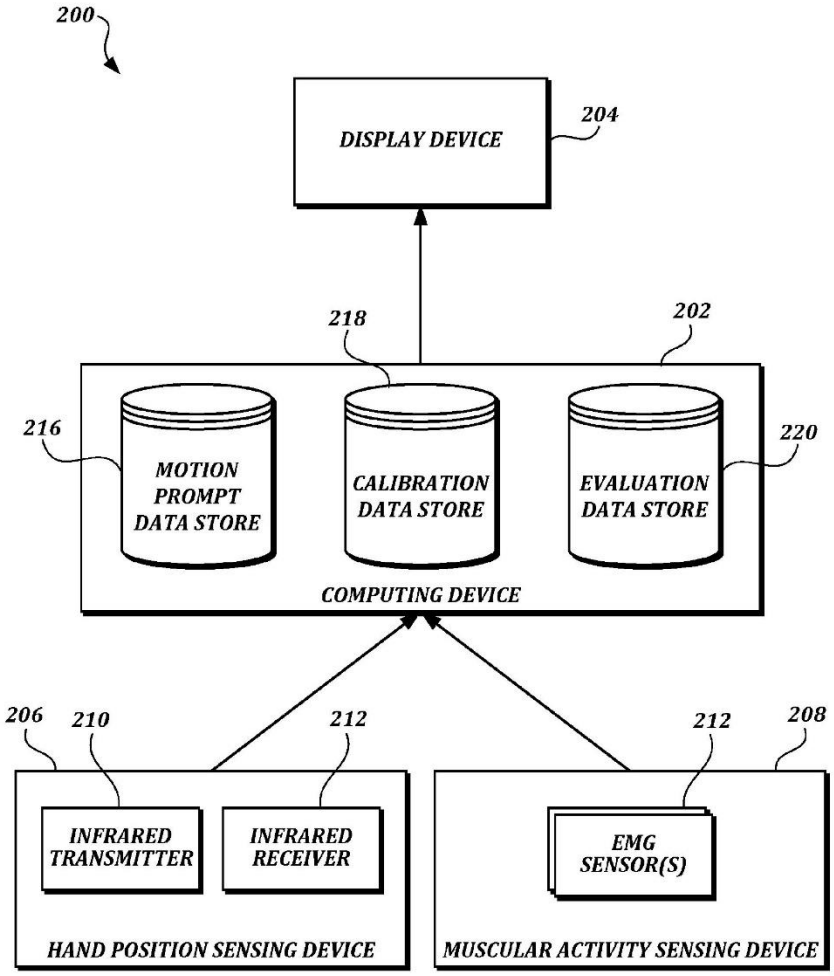
200
DISPLAY DEVICE
204
218
202
216
MOTION PROMPT DATA STORE
CALIBRATION DATA STORE
EVALUATION DATA STORE
220
COMPUTING DEVICE
206
210
212
212
208
INFRARED TRANSMITTER
INFRARED RECEIVER
EMG SENSOR(S)
HAND POSITION SENSING DEVICE
MUSCULAR ACTIVITY SENSING DEVICE

FIG. 2

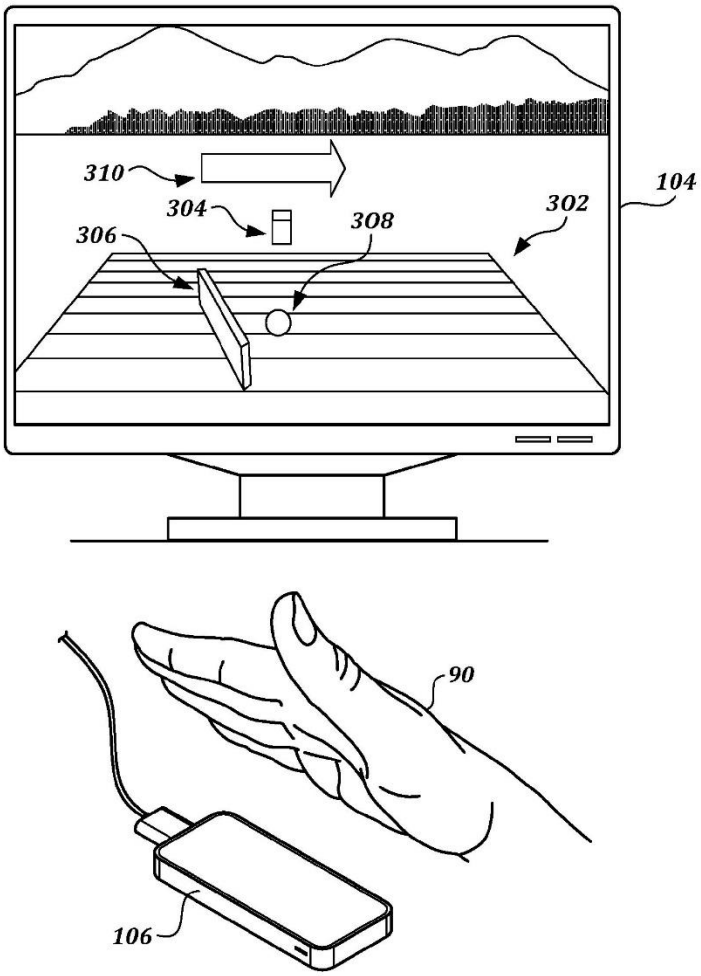

FIG. 3A

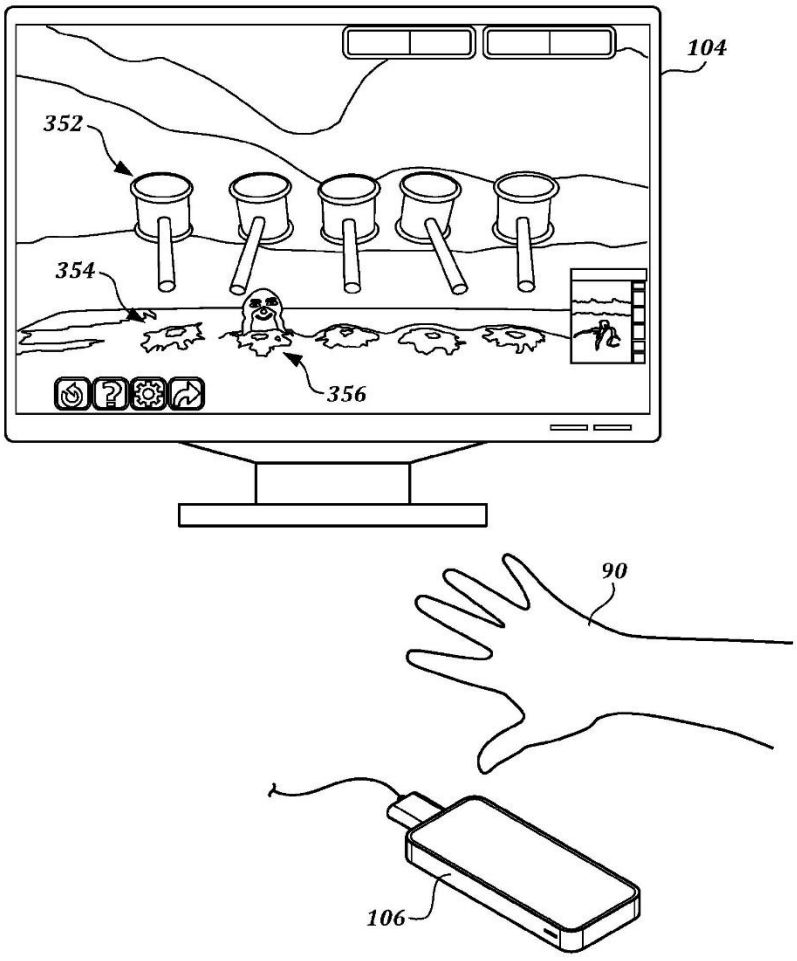

FIG. 3B

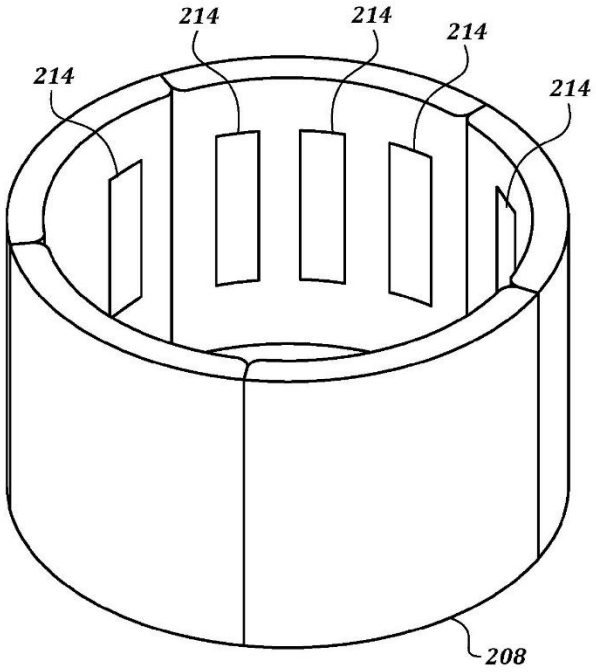

FIG. 4

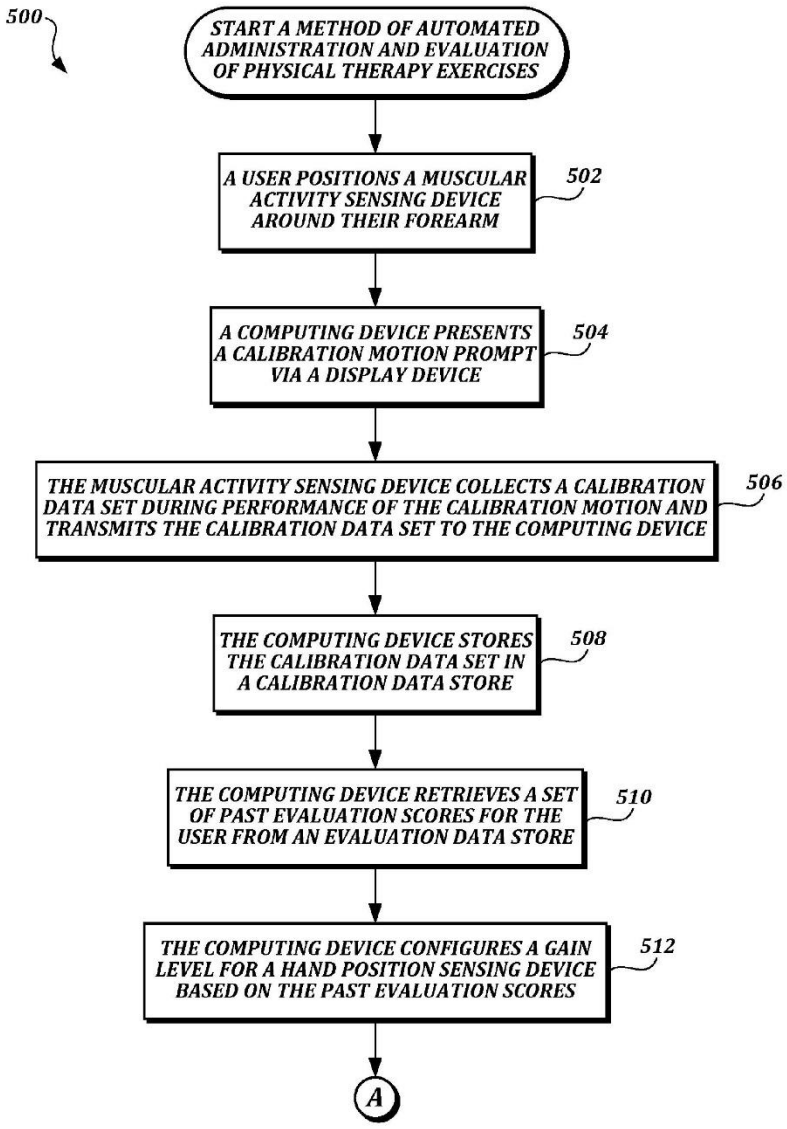
500
START A METHOD OF AUTOMATED ADMINISTRATION AND EVALUATION OF PHYSICAL THERAPY EXERCISES
A USER POSITIONS A MUSCULAR ACTIVITY SENSING DEVICE AROUND THEIR FOREARM
502
A COMPUTING DEVICE PRESENTS A CALIBRATION MOTION PROMPT VIA A DISPLAY DEVICE
504
THE MUSCULAR ACTIVITY SENSING DEVICE COLLECTS A CALIBRATION DATA SET DURING PERFORMANCE OF THE CALIBRATION MOTION AND TRANSMITS THE CALIBRATION DATA SET TO THE COMPUTING DEVICE
506
THE COMPUTING DEVICE STORES THE CALIBRATION DATA SET IN A CALIBRATION DATA STORE
508
THE COMPUTING DEVICE RETRIEVES A SET OF PAST EVALUATION SCORES FOR THE USER FROM AN EVALUATION DATA STORE
510
THE COMPUTING DEVICE CONFIGURES A GAIN LEVEL FOR A HAND POSITION SENSING DEVICE BASED ON THE PAST EVALUATION SCORES
512
A

FIG. 5A

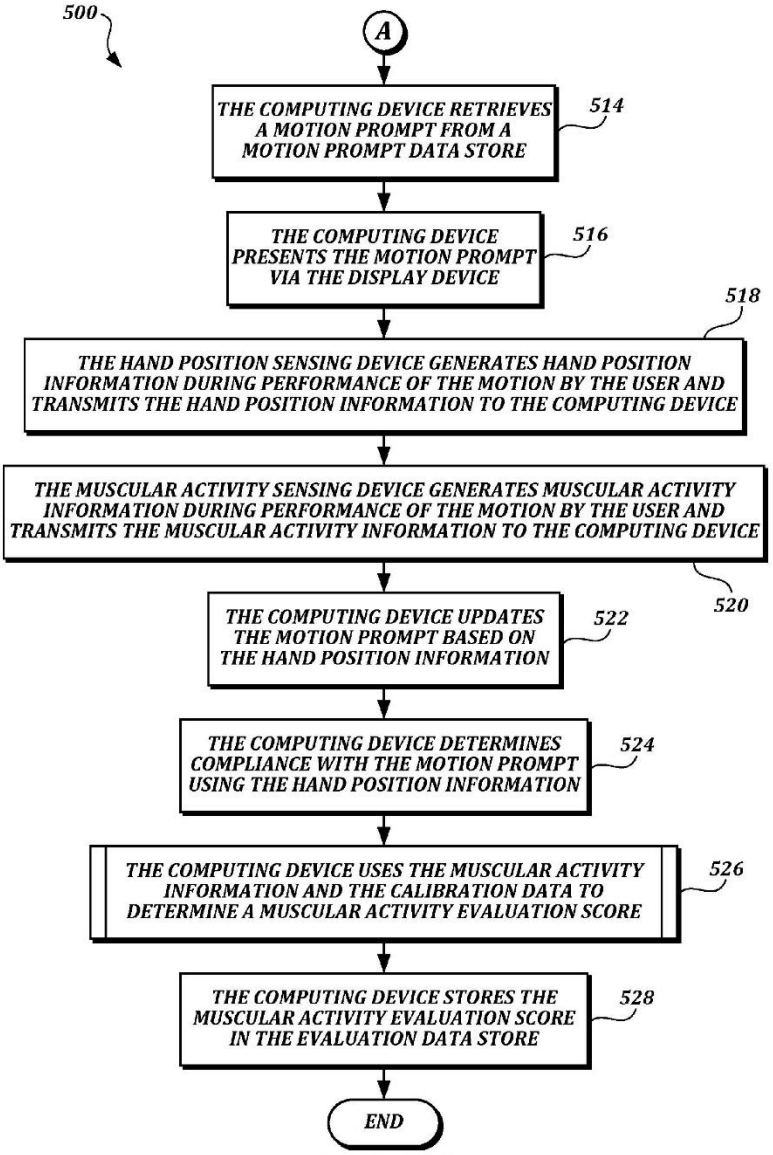
500
A
THE COMPUTING DEVICE RETRIEVES A MOTION PROMPT FROM A MOTION PROMPT DATA STORE
514
THE COMPUTING DEVICE PRESENTS THE MOTION PROMPT VIA THE DISPLAY DEVICE
516
518
THE HAND POSITION SENSING DEVICE GENERATES HAND POSITION INFORMATION DURING PERFORMANCE OF THE MOTION BY THE USER AND TRANSMITS THE HAND POSITION INFORMATION TO THE COMPUTING DEVICE
THE MUSCULAR ACTIVITY SENSING DEVICE GENERATES MUSCULAR ACTIVITY INFORMATION DURING PERFORMANCE OF THE MOTION BY THE USER AND TRANSMITS THE MUSCULAR ACTIVITY INFORMATION TO THE COMPUTING DEVICE
520
THE COMPUTING DEVICE UPDATES THE MOTION PROMPT BASED ON THE HAND POSITION INFORMATION
522
THE COMPUTING DEVICE DETERMINES COMPLIANCE WITH THE MOTION PROMPT USING THE HAND POSITION INFORMATION
524
THE COMPUTING DEVICE USES THE MUSCULAR ACTIVITY INFORMATION AND THE CALIBRATION DATA TO DETERMINE A MUSCULAR ACTIVITY EVALUATION SCORE
526
THE COMPUTING DEVICE STORES THE MUSCULAR ACTIVITY EVALUATION SCORE IN THE EVALUATION DATA STORE
528
END

FIG. 5B

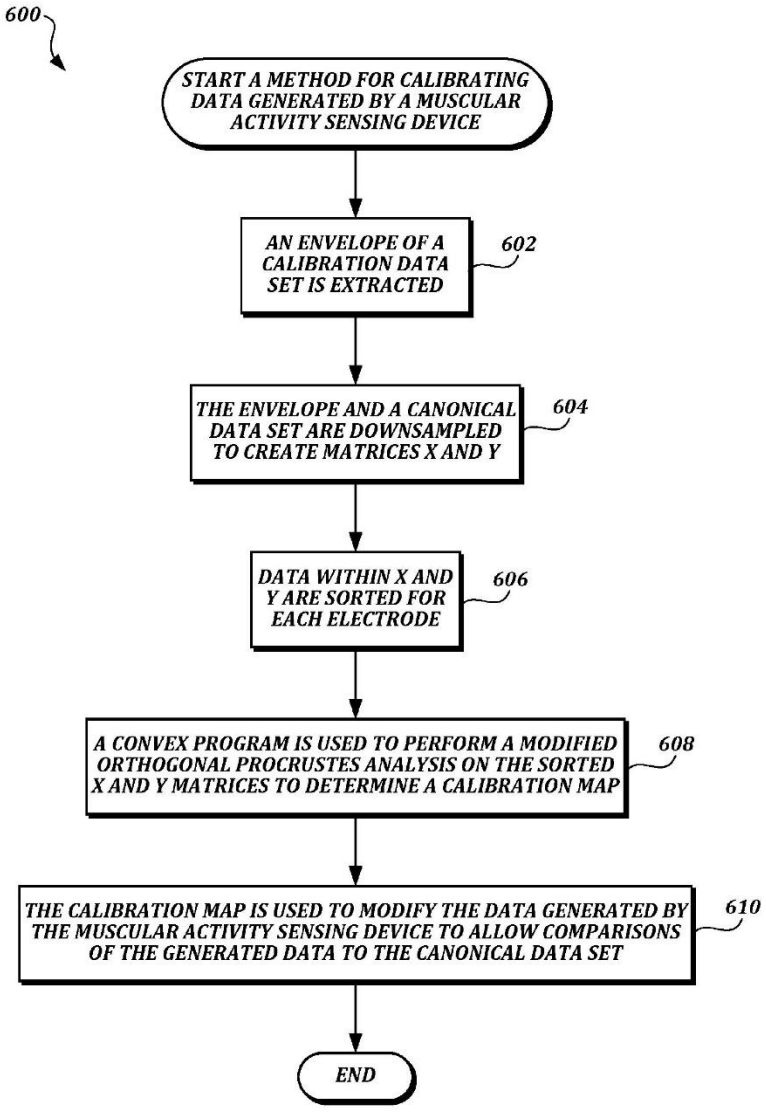
600
START A METHOD FOR CALIBRATING DATA GENERATED BY A MUSCULAR ACTIVITY SENSING DEVICE
AN ENVELOPE OF A CALIBRATION DATA SET IS EXTRACTED
602
THE ENVELOPE AND A CANONICAL DATA SET ARE DOWNSAMPLED TO CREATE MATRICES X AND Y
604
DATA WITHIN X AND Y ARE SORTED FOR EACH ELECTRODE
606
A CONVEX PROGRAM IS USED TO PERFORM A MODIFIED ORTHOGONAL PROCRUSTES ANALYSIS ON THE SORTED X AND Y MATRICES TO DETERMINE A CALIBRATION MAP
608
THE CALIBRATION MAP IS USED TO MODIFY THE DATA GENERATED BY THE MUSCULAR ACTIVITY SENSING DEVICE TO ALLOW COMPARISONS OF THE GENERATED DATA TO THE CANONICAL DATA SET
610
END

FIG. 6

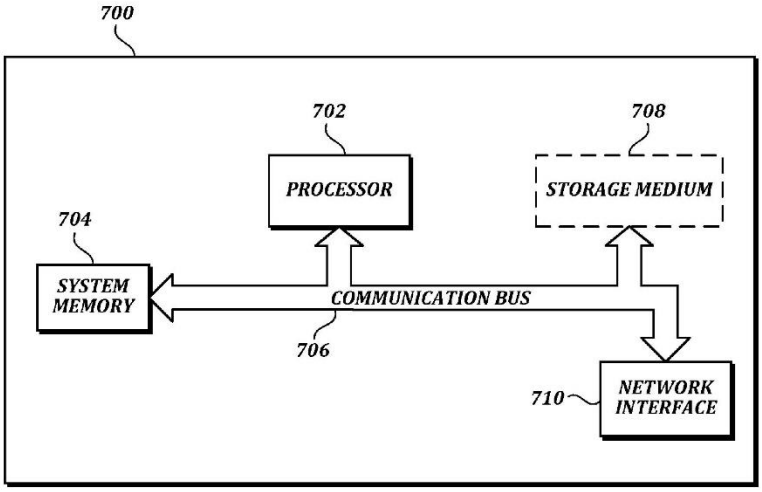
700
702
PROCESSOR
708
STORAGE MEDIUM
704
SYSTEM MEMORY
COMMUNICATION BUS
706
710
NETWORK INTERFACE

FIG. 7

SYSTEM AND METHODS FOR AUTOMATED ADMINISTRATION AND EVALUATION OF PHYSICAL THERAPY EXERCISES

CROSS-REFERENCE TO RELATED APPLICATION

[0001] This application claims the benefit of Provisional Application No. 62/161,100, filed May 13, 2015, the entire disclosure of which is hereby incorporated by reference herein for all purposes.

BACKGROUND

[0002] A large number of patients are currently in hand rehabilitation therapy in the United States as the result of stroke, and this number is projected to grow due to the aging demographic. In 2010, stroke related medical and disability costs totaled $73.3 billion in the United States. Nearly $8 billion of which is spent on hand related rehabilitation alone, as almost 67% of strokes cause forearm motor losses. When a stroke affects a patient's hand function, recovery is slow and gains are incremental and difficult to measure. Patients typically progress through inpatient to outpatient and at-home therapy over the course of six to ten weeks. The slow, immeasurable progress can lead to a premature loss of insurance reimbursement for therapy procedures and low patient motivation and compliance. The almost 17,000 rehab clinics in the United States struggle to provide adequate support for these patients because of the difficulty in tracking improvements and covering the cost of continued outpatient therapy. What are needed are systems and methods that automate the administration of physical and/or occupational therapy procedures, post-surgery assessments, post-operative care, and/or the like (herein collectively referred to as "physical therapy" for ease of discussion) in order to improve compliance rates and reduce the cost of administration. It is also desirable to create systems that can evaluate the performance of physical therapy tasks in a more precise way than is currently available in order to be able to measure and demonstrate small amounts of incremental progress.

SUMMARY

[0003] This summary is provided to introduce a selection of concepts in a simplified form that are further described below in the Detailed Description. This summary is not intended to identify key features of the claimed subject matter, nor is it intended to be used as an aid in determining the scope of the claimed subject matter.

[0004] In some embodiments, a system for automated administration and evaluation of physical therapy exercises is provided. The system comprises a computing device, a display device, a hand position sensing device, and a muscular activity sensing device. The computing device comprises at least one processor and a non-transitory computer readable medium. The display device is communicatively coupled to the computing device. The hand position sensing device is communicatively coupled to the computing device. The muscular activity sensing device is communicatively coupled to the computing device and configured to sense muscular activity in a forearm of a user.

[0005] In some embodiments, a computer-implemented method for automated administration and evaluation of physical therapy exercises is provided. A computing device presents, via a display device, a motion prompt. The computing device receives hand position information from a hand position sensing device. The computing device receives muscular activity information from a muscular activity sensing device. The computing device determines compliance with the motion prompt using the hand position information. The computing device determines a muscular activity evaluation score based on the muscular activity information.

[0006] In some embodiments, a nontransitory computer-readable medium having computer-executable instructions stored thereon is provided. The instructions, in response to execution by one or more processors of a computing device, cause the computing device to perform actions comprising: presenting, by the computing device via a display device, a motion prompt; receiving, by the computing device, hand position information from a hand position sensing device; receiving, by the computing device, muscular activity information from a muscular activity sensing device; determining, by the computing device, compliance with the motion prompt using the hand position information; and determining, by the computing device, a muscular activity evaluation score based on the muscular activity information.

DESCRIPTION OF THE DRAWINGS

[0007] The foregoing aspects and many of the attendant advantages of this invention will become more readily appreciated as the same become better understood by reference to the following detailed description, when taken in conjunction with the accompanying drawings, wherein:

[0008] FIG. **1** is a schematic diagram that illustrates an exemplary embodiment of a system for automated administration and evaluation of physical therapy exercises according to various aspects of the present disclosure;

[0009] FIG. **2** is a block diagram that illustrates details of devices within an exemplary embodiment of a system according to various aspects of the present disclosure;

[0010] FIG. **3**A illustrates an example Ball Roll motion prompt and an associated hand position according to various aspects of the present disclosure;

[0011] FIG. **3**B illustrates an example of a Five Finger Mole motion prompt and an associated hand position according to various aspects of the present disclosure;

[0012] FIG. **4** is a perspective view of an exemplary embodiment of a muscular activity sensing device suitable for use with the system for automated administration and evaluation of physical therapy exercises;

[0013] FIGS. **5**A and **5**B are a flowchart that illustrates an exemplary method of automated administration and evaluation of physical therapy exercises according to various aspects of the present disclosure;

[0014] FIG. **6** is a flowchart that illustrates an exemplary embodiment of a method for calibrating data generated by a muscular activity sensing device according to various aspects of the present disclosure; and

[0015] FIG. **7** is a block diagram that illustrates aspects of an exemplary computing device **700** appropriate for use with embodiments of the present disclosure.

DETAILED DESCRIPTION

[0016] FIG. **1** is a schematic diagram that illustrates an exemplary embodiment of a system for automated administration and evaluation of physical therapy exercises according to various aspects of the present disclosure. The

system **100** includes a computing device **102**, a display device **104**, a hand position sensing device **106**, and a muscular activity sensing device **108**. A user places the muscular activity sensing device **108** on their arm **92**, and moves their hand **90** to be positioned within the sensing range of the hand position sensing device **106**. The computing device **102** causes motion prompts to be displayed on the display device Q**04**, and the user moves their hand **90** and arm **92** as prompted. The hand position sensing device **106** generates data regarding the position of the hand **90** and arm **92** in three-dimensional space, and provides the data to the computing device **102**. The muscular activity sensing device **108** generates data regarding muscular activity within the arm **92**, and provides the data to the computing device **102** as well. The system **100** can thereby guide the user through one or more physical therapy exercises, ensure that the user has performed the exercises as prompted, and evaluate muscular performance and coordination while the exercises are performed. Though a single arm **92** is illustrated, in some embodiments both arms of the user may be used and tracked by the system **100**.

[0017] FIG. **2** is a block diagram that illustrates details of devices within an exemplary embodiment of a system according to various aspects of the present disclosure. As illustrated, the system **200** includes a display device **204**, a computing device **202**, a hand position sensing device **206**, and a muscular activity sensing device **208**.

[0018] The computing device **202** may be any suitable type of computing device, including but not limited to a desktop computing device, a laptop computing device, a tablet computing device, a smartphone computing device, and/or any other suitable type of computing device for storing, receiving, and processing data as described below. Further components common to all computing devices are described below with respect to FIG. **7**. In addition to these components, the computing device **202** is configured to provide (or provide access to) a motion prompt data store **216**, a calibration data store **218**, and an evaluation data store **220**.

[0019] The motion prompt data store **216** is configured to store motion prompt information for a plurality of motion prompts, wherein the motion prompt information defines various factors of how a motion prompt should be presented and how compliance with the motion prompt should be evaluated. Typically, the motion prompts include animated, interactive games that encourage particular types of physical hand motion. Some examples of motion prompts are a Five Finger Mole prompt, a Ball Roll prompt, a Reach and Grab prompt, a Hand Match prompt, and a vAssess prompt.

[0020] FIG. **3**A illustrates an example Ball Roll motion prompt and an associated hand position according to various aspects of the present disclosure. The Ball Roll prompt displays a table **302** with a vertical paddle **306** at or near the middle. The user is prompted to hold their hand **90** vertically, and to flex/extend their wrist to rotate the paddle **306**. As a ball **308** rolls down the table **302** from a launcher **304**, rotating the paddle **306** by flexing/extending the user's wrist causes the ball **308** to be hit to one side of the table or the other as instructed by an arrow **310**. This activity can test flexion and extension of the wrist, among other things.

[0021] FIG. **3**B illustrates an example of a Five Finger Mole motion prompt and an associated hand position according to various aspects of the present disclosure. The Five Finger Mole prompt displays a game field reminiscent of the game "whack-a-mole," having a set of holes **354** from which animated moles **356** may pop up. A set of hammers **352** corresponding to each of the user's fingers is positioned above each of the holes **354**. When a mole **356**, the user moves the associated finger (for example, in the illustrated case, the index finger) vertically in order to move the associated hammer to hit the mole **356**. This activity can test range of motion, coordination, and reaction time for each individual finger of the hand **90**.

[0022] Other prompts are also available: The Reach and Grab prompt displays a grid of cubby holes with balls inside. A virtual hand that mimics the location and orientation of the user's hand is also displayed. The user is prompted to reach out and form fists in order to cause the virtual hand to grab the balls out of the cubby holes. The Hand Match prompt displays a similar virtual hand that mimics the location and orientation of the user's hand, and also displays a prompt hand that changes position and orientation. The user is prompted to move their hand to match the position and orientation of the prompt hand. The Hand Match prompt may test both hands at the same time. The vAssess prompt illustrates the virtual hand, as well as a set of bubbles to be popped by touching them with the virtual hand.

[0023] The calibration data store **218** is configured to store canonical data sets and calibration data that allow data collected by the muscular activity sensing device **208** from multiple different sessions to be compared to each other, regardless of how the muscular activity sensing device **208** is positioned on the user's arm. Further discussion of the creation and use of canonical data sets and calibration data is provided below.

[0024] The evaluation data store **220** is configured to store evaluation scores that represent evaluations of how successfully the user was able to comply with motion prompts. The evaluation scores may then be used to determine rehabilitation progress, to tune the system **200** for future sessions, and/or for any other use. Further discussion of the evaluation scores is provided below.

[0025] As understood by one of ordinary skill in the art, a "data store" as described herein may be any suitable device configured to store data for access by a computing device. One example of a data store suitable for use with the computing device **202** is a highly reliable, high-speed relational database management system (RDBMS) executing on one or more computing devices and accessible over a high-speed network. However, any other suitable storage technique and/or device capable of quickly and reliably providing the stored data in response to queries may be used, such as a key-value store, an object database, and/or the like. Further, the computing device providing the data store may be accessible locally by the computing device **202** instead of over a network, or may be provided by the computing device **202** itself. A data store may also include data stored in an organized manner on a computer-readable storage medium, as described further below. One example of such a data store is a file system or database management system that stores data in files (or records) on a computer readable medium such as flash memory, random access memory (RAM), hard disk drives, and/or the like. One of ordinary skill in the art will recognize that separate data stores described herein may be combined into a single data store, and/or a single data store described herein may be separated into multiple data stores, without departing from the scope of the present disclosure.

[0026] The display device **204** may be any type of display device capable of presenting video and/or audio motion prompts. Typically, the display device **204** is a monitor connected to the computing device via HDMI, FireWire, DisplayPort, VGA, USB, or any other suitable communication technology. In some embodiments, the display device **204** may be incorporated into the computing device **202**, such as in embodiments wherein the computing device **202** is a laptop computing device, a tablet computing device, or a smartphone computing device.

[0027] The figures and description below primarily relate to such embodiments wherein the display device **204** is a monitor. However, in some embodiments, instead of being a monitor the display device **204** may be a virtual reality headset, such as the Rift headset created by Oculus VR, the Vive headset created by HTC Corporation, The PlayStation VR headset by Sony Corporation, the Gear VR headset by Samsung, and/or the like. In some embodiments, the display device **204** may be an augmented reality headset such as the Glass headset created by Google Inc., the HoloLens headset created by Microsoft Corporation, and/or the like. Any technology capable of presenting a motion prompt may be used for the display device **204**.

[0028] The hand position sensing device **206** is any device capable of generating three-dimensional position information that represents the elements of a user's hand or hands. In the illustrated embodiment, the hand position sensing device **206** includes at least one infrared transmitter **210** and at least one infrared receiver **212**. In some embodiments, at least two infrared receivers **212** may be used in order to obtain stereo images and thereby collect three-dimensional position information. One example of a device suitable for use as a hand position sensing device **206** within the system **200** is a Leap Motion controller created by Leap Motion, Inc, though any other suitable device with similar functionality may be used. The hand position sensing device **206** may be communicatively coupled to the computing device **202** using any suitable technique, including but not limited to a USB connection, a FireWire connection, Bluetooth, Bluetooth Low Energy, ZigBee, WiFi, a LAN connection, a WAN connection, and an internet connection.

[0029] The muscular activity sensing device **208** is any device capable of generating data indicating muscular activity within the arm of the user. In the illustrated embodiment, the muscular activity sensing device **208** includes a plurality of surface electromyography (EMG) sensors **214** that are capable of determining muscular activity from the surface above the muscle on the skin. In some embodiments, each of the EMG sensors **214** may include two or more electrodes that are used to measure potential differences between particular locations on the skin. One example of a device suitable for use as a muscular activity sensing device **208** within the system **200** is a Myo armband controller created by Thalmic Labs Inc., though any other suitable device with similar functionality may be used. The muscular activity sensing device **208** may be communicatively coupled to the computing device **202** using any suitable technique, including but not limited to a USB connection, a FireWire connection, Bluetooth, Bluetooth Low Energy, ZigBee, WiFi, a LAN connection, a WAN connection, and an internet connection

[0030] FIG. **4** is a perspective view of an exemplary embodiment of a muscular activity sensing device suitable for use with the system for automated administration and evaluation of physical therapy exercises. The muscular activity sensing device **208** includes a plurality of EMG sensors **214**. As is shown, the muscular activity sensing device **208** exhibits rotational symmetry about the lumen through which the arm is inserted. Because the muscular activity sensing device **208** is a bracelet, there is a distinct possibility that the EMG sensors **214** will be placed in a different rotational position on the arm for each session. Embodiments of the present disclosure compensate for different positions as described below, and may use the rotational symmetry of the muscular activity sensing device **208** to enhance the accuracy of the compensation.

[0031] FIGS. **5**A and **5**B are a flowchart that that illustrates an exemplary method of automated administration and evaluation of physical therapy exercises according to various aspects of the present disclosure. From a start block, the method **500** proceeds to block **502**, where a user positions a muscular activity sensing device **208** around their forearm. As discussed above, the rotational position of the muscular activity sensing device **208** may not matter, but instead will be compensated for during the calibration process discussed below. Next, at block **504**, a computing device **204** presents a calibration motion prompt via a display device **204**. One example of a calibration motion prompt includes animations that prompt the user to perform a sequence such as (1) horizontal flexion; (2) horizontal extension; (3) radial deviation; (4) ulnar deviation; (5) vertical flexion; and (6) vertical extension. Each motion may be prompted to be held for three seconds, and may be followed by a three second rest. In some embodiments, the calibration motion prompt may direct these motions by presenting textual descriptions of the motions. In some embodiments, the calibration motion prompt may direct these motions by presenting animations that depict each desired motion. The calibration movements allow the muscular activity sensing device **208** to gather labeled muscular activity data for each of the movements.

[0032] At block **506**, the muscular activity sensing device **208** collects a calibration data set during performance of the calibration motion and transmits the calibration data set to the computing device **202**. In some embodiments, the hand position sensing device **206** may also transmit hand position information to the computing device **202**. At block **508**, the computing device **202** stores the calibration data set in a calibration data store **218**. In some embodiments, the hand position information may be stored in the calibration data store **218**, as well, while in other embodiments, the hand position information may simply be analyzed by the computing device **202** to determine whether the calibration data set should be considered valid. The calibration data set may be used for analyzing data gathered during later exercises, as discussed further below.

[0033] The method **500** then proceeds to block **510**, where the computing device **202** retrieves a set of past evaluation scores for the user from an evaluation data store **220**. In some embodiments, the past evaluation scores may directly indicate difficulty levels that have been successfully completed or gain levels that have been used by the user for one or more motion prompts. In some embodiments, the past evaluation scores may indicate levels of physical ability, such as range of motion, speed of motion, muscular strength or endurance, and/or the like. At block **512**, the computing device **202** configures a gain level for a hand position sensing device **206** based on the past evaluation scores. If the past evaluation scores indicate that range of motion is

small or the muscular strength is weak, the gain may be set high in order to translate small movements or efforts into large movements on the display. This allows for a feeling of accomplishment to the user, and allows the user to see a demonstration of progress. If the past evaluation scores indicate that the range of motion are large or normal or that the muscular strength is high, the gain may be set low in order to increase the challenge for the user. The past evaluation scores may also be used for other tuning of the system **200**, such as selecting types of motion prompts to be presented, selecting a difficulty of motions to be performed, and/or the like. The method **500** then proceeds to a continuation terminal ("terminal A").

[0034] From terminal A (FIG. **5**B), the method **500** proceeds to block **514**, where the computing device **202** retrieves a motion prompt from a motion prompt data store **216**. As stated above, the motion prompt may be selected from a plurality of motion prompts based on past evaluation scores. At block **516**, the computing device **202** presents the motion prompt via the display device **204**. At block **518**, the hand position sensing device **206** generates hand position information during performance of the motion by the user and transmits the hand position information to the computing device **202**.

[0035] In some embodiments, the hand position information includes three-dimensional location information and orientation information for one or more anatomical elements of a hand. For example, objects representing the three-dimensional location one or more hand bones (such as distal phalanges, intermediate phalanges, proximal phalanges, metacarpals, and so on) may be included in the hand position information. As another example, other information relating to the overall position of the hand, such as a vector orthogonal to the face of the palm, a vector indicating arm position, a vector indicating elbow position, a vector indicating wrist position, and so on, may be provided.

[0036] At block **520**, the muscular activity sensing device **208** generates muscular activity information during performance of the motion by the user and transmits the muscular activity information to the computing device **202**. In some embodiments, the muscular activity information may be provided by the muscular activity sensing device **208** in a raw form as a stream of electrical potential values obtained by each of the EMG sensors **214**.

[0037] At block **522**, the computing device **202** updates the motion prompt based on the hand position information. For example, the computing device **202** may cause an on-screen item, such as a paddle, a hammer, or a representation of a hand, to move to mimic the motion represented by the hand position information. The computing device **202** may also alter other objects within the prompt, such as balls, targets, and/or the like, based on the motion represented by the hand position information. At block **524**, the computing device **202** determines compliance with the motion prompt using the hand position information. For example, the computing device **202** may perform collision detection between objects within the motion prompt to determine if a goal (such as grabbing a ball with a virtual hand, hitting a virtual target, and/or the like) was achieved. As another example, the computing device **202** may perform a measurement of hand/arm position compared to a standard, such as a flexion of at least 30 degrees, and an extension of at least 30 degrees," regardless of the presentation of the motion prompt.

[0038] In some embodiments, particular metrics are computed for each of the motion prompts to evaluate performance. For each of the metrics, the metric may be evaluated in comparison to a predetermined threshold that indicates a successful completion of the motion. The computing device **202** may use the determined compliance to determine game actions, such as advancing to a more difficult level in a game, repeating a current level of difficulty, reducing the level of difficulty (or increasing the gain), and/or the like.

[0039] For the Five Finger Mole prompt, the system **200** may determine individual finger range of vertical motion, finger independence, average trial for each finger in terms of vertical position, and mean and standard deviation of reaction time. Finger independence may be measure in two ways. The first technique is via a correlation matrix of vertical finger movement. The second technique is via the distance covered by other fingers relative to the finger associated with a given trial. For example, for a thumb trial, the distance travelled by each finger is divided by the distance traveled by the thumb.

[0040] For the Ball Roll prompt, the system **200** may determine minimum and maximum angle of the wrist, minimum and maximum wrist angle trimmed by standard deviation, and average flexion and extension in terms of angle. To compute the average flexion and extension in terms of angle, the minimum or maximum wrist angle during a trial is determined and an interval is centered around it. The interval is extended to reach the beginning or the end of the trial window, whichever is closer. If the interval length exceeds a predetermined threshold, the trial is included in the computation of the average trial, otherwise it is rejected. The number of flexions and extensions included for this computation may be saved to get a sense of how accurate it is.

[0041] For the Reach and Grab prompt, multiple "intervals" are measured, wherein an interval is what takes place between putting an item in a bin and the last time the user touched the item. These intervals may be pruned by depth using standard deviation to exclude intervals where the item was dropped and picked up at a later time. The end-points of the intervals in virtual 3D space may be clustered via k-means to figure out where the shelves lie in the real volume sensed by the hand position sensing device **206**. This defines a range-of-motion (ROM) window. The error, defined as the distance from the cluster centroid to which each reach end-point belongs, may be used to measure reach precision. Path accuracy may be computed as the squared distance of the actual path from the straight line between the interval beginning and end. This estimates the quality of path planning. Accuracy may be binned by shelf end-point target (six target). Path tremor may be computed as above, but using a smoothed version of the path instead of a straight line. This estimates how jittery the movement is. Tremor may be binned as above. Each of these measures may be used to evaluate the movement.

[0042] For the Hand Match prompt, if the positions of both hands are measured, then a root-mean-square (RMS) of the left and right hand path tremor may be calculated. A vertical distance between the hands over the whole session and on average over various trials may also be measured. An angle of palm normals during the whole session may also be measured.

[0043] For the vAssess prompt, a volume of the convex hull of points corresponding to popped balloons may be

calculated, which estimates a physical reach. A trimmed max and min angle for radial/ulnar deviation, vertical flexion/extension, horizontal flexion/extension, and supination may also be determined.

[0044] One of ordinary skill in the art will understand that the actions described with respect to blocks **516-524** may be performed concurrently and repeatedly for a period of time.

[0045] At procedure block **526**, the computing device **202** uses the muscular activity information and the calibration data to determine a muscular activity evaluation score. Any suitable technique may be used, and the techniques may be different for different motion prompts. In some embodiments, the muscular activity information may be normalized using the calibration data before using the normalized muscular activity information to determine the muscular activity evaluation score. One example procedure for using the calibration data to normalize the muscular activity data for comparison to previous sessions is illustrated in FIG. **6** and described below.

[0046] For determining the muscular activity evaluation score, one example technique relates to the variance explained by muscle synergies. Muscle synergies are a representation of how the nervous system controls complex hand movements, where multiple muscle groups are activated simultaneously to achieve any given action. Instead of individually controlling the various muscles required to perform a movement, the nervous system can generate a movement pattern by combining a (usually small) set of such synergies. In an injury state where the nervous system is damaged and/or reorganizing it is common for the muscle activation patterns to be less complex. Accordingly, a muscular activity evaluation score can be determined by tracking the explained by a reconstructed signal as a function of muscle synergies employed, as a measure of the overall complexity of the muscle activations of the patient. Monitoring the profile of these muscle synergies over time can provide a measure of progress.

[0047] With respect to the muscular activity information generated by the system **200**, a synergy is represented by an n-dimensional vector that explains the activations of each electrode for each synergy, whereas the synergy activations explain how synergies are employed over time. Specifically, a non-negative matrix factorization of the envelope of the n-dimensional muscular activity information can be performed, wherein n is the number of channels of muscular activity information provided by the muscular activity sensing device **208**. One example embodiment of a muscular activity sensing device **208** includes eight EMG sensors **214**, and so would produce eight-dimensional information. This models the acquired signal as a collection of constant muscle activation patterns (synergies) scaled by a time-varying activation component. The non-negative matrix factorization decomposes the muscular activity information into n n-dimensional muscle synergies and n-dimensional activations of synergies over time. Some other techniques for determining the muscular activity evaluation score may include cluster distance between clusters of data points for given movements, and the like.

[0048] The method **500** then proceeds to block **528**, where the computing device **202** stores the muscular activity evaluation score in the evaluation data store **220**. In some embodiments, the method **500** may at this point return to block **514** and display another prompt, or display the same prompt with different gain or difficulty settings. Otherwise, the method **500** proceeds to an end block and terminates.

[0049] Normalizing the muscular activity data is desirable in order to generate meaningful muscular activity evaluation scores that can be compared to each other from separate sessions, because exact reproduction of EMG electrode placement is inherently hard. This is a significant obstacle for experiments that span sessions between which the user removes the muscular activity sensing device **208**. An inter-session analysis of such information will likely result in inexact comparisons due to differences in positioning. As an example, consider the Ball-Roll prompt. During the session, muscular activity information is captured. A subsequent analysis reveals electrode activations during flexion or extension, correlated with the contraction of the muscles directly below or in the surrounding area of each electrode. An example inter-session comparison would be to compare these electrode activations between sessions, as a proxy to contraction strength of the underlying muscles, related to each of the two movement groups, over time. The goal is to enable such an analysis, without requiring precise placement of the bracelet on the forearm. The solution to this problem is to learn a mapping from the electrode positions of one session to the other, effectively translating data between frames of reference.

[0050] FIG. **6** is a flowchart that illustrates an exemplary embodiment of a method for calibrating data generated by a muscular activity sensing device according to various aspects of the present disclosure. The method **600** is an example of a method suitable for use in procedure block **526** illustrated in FIG. **5**B.

[0051] From a start block, the method **600** proceeds to block **602**, where an envelope of a calibration data set is extracted. As discussed above with respect to blocks **504-508** in FIG. **5**A, the calibration data set may be generated via the performance of a standardized set of movements, and the calibration data set may be stored in the calibration data store **218**. The envelope may be extracted using any suitable technique, such as low-pass/high-pass filtering of the signal or a Hilbert transform.

[0052] Next, at block **604**, the envelope of the calibration data set and an envelope of a canonical data set are downsampled to create matrices X and Y. The canonical data set may be a calibration data set that is stored the first time the system **200** is used by a given user. Alternatively, the canonical data set may be a pre-configured data set that is stored in the system **200** during manufacturing. In some embodiments, the canonical data set may already be in the form of an envelope. In some embodiments, the envelope of the canonical data set may be extracted when needed in a similar manner to the extraction of the envelope of the calibration data set. In some embodiments, the canonical information may be retrieved from the calibration data store **218**. The sampling results in two matrices in $\mathbb{R}^{(N_1+\ldots+N_k)\times d}$, where N_i is the number of data points in movement group i and d is the number of electrodes.

[0053] Next, at block **606**, data within X and Y are sorted for each electrode. This results in matrices X, $Y \in \mathbb{R}^{(N_1+\ldots+N^{(k)})\times d}$, with the property that for each movement group i and electrode j, the vector $X_{N_{ij}}$ is sorted in ascending order. This is done so that each data row of X and Y within the same data group corresponds approximately to the same quantile of the intra-group distribution.

[0054] The method **600** then proceeds to block **608**, where a convex program is used to perform a modified orthogonal Procrustes analysis on the sorted X and Y matrices to determine a calibration map A. Previous attempts at solving similar problems have used an orthogonal Procrustes approach. However, this approach is not suitable for EMG calibration. A rotation matrix $A \neq I$ will surely assign negative coefficients to some of the source electrodes when trying to reconstruct the targets. When the desired analysis depends on non-negative aspects of the signal or the orientation features are non-negative, the translated data obtained from the orthogonal Procrustes will often be negative and therefore unsuitable. Another issue with applying this technique to EMG data is that negative channels do not make sense since we expect the signals to be additive.

[0055] A first approach for a convex program suitable for use in determining a calibration map is to modify the orthogonal Procrustes approach by replacing the orthogonality constraint with the positivity constraint $A \geq 0$. The convex program formulation of this technique is:

$$\min_{A} \|Y - AX\|_F^2$$

[0056] such that $A \geq 0$. The solution can then be obtained via various constrained convex optimization techniques. One approach that works well for this application is to perform gradient descent on the objective and project the solution at each step to the feasible set by setting all negative elements of A to zero.

[0057] Higher quality solutions can be obtained when assumptions can be made regarding the topology of the muscular activity sensing device **208**. For example, when the muscular activity sensing device **208** is a bracelet that exhibits rotational symmetry, one can assume that the various electrode positionings are simply rotations of each other. In this context, the quality of the solution can be improved by imposing additional constraints on the solution. Specifically, one can assume that each electrode of the target positioning can be reconstructed by only a few electrodes of the source. This intuition can be added to the model by requiring that each row of A is sparse. One way of incentivizing the model to favor sparse solutions is penalizing the l_1-norm of A given by:

$$\|A\|_1 = \sum_{i,j} |A_{ij}|$$

[0058] The resulting convex program is:

$$\min_{A} \|Y - AX\|_F^2 + \lambda \|A\|_1$$

[0059] such that $A \geq 0$, wherein λ is the sparsity hyperparameter. Larger values of λ favor sparser solutions at the expense of reconstruction quality. A suitable optimization technique for this program is FISTA modified to project the current solution to the feasible set as described above.

[0060] At block **610**, the calibration map is used to modify the data generated by the muscular activity sensing device **208** to allow comparisons of the generated data to the canonical data set. In some embodiments, the matrix of data generated by the muscular activity sensing device **208** may simply be multiplied by A to normalize the data to match the orientation of the canonical data set. Hence, data generated by any subsequent configuration/position of the muscular activity sensing device **208** could be normalized by A to be in the same position, and therefore be comparable no matter what orientation in which the muscular activity sensing device **208** was placed on the user's arm. The method **600** then proceeds to an end block and terminates.

[0061] FIG. **7** is a block diagram that illustrates aspects of an exemplary computing device **700** appropriate for use with embodiments of the present disclosure. While FIG. **7** is described with reference to a computing device that is implemented as a device on a network, the description below is applicable to servers, personal computers, mobile phones, smart phones, tablet computers, embedded computing devices, and other devices that may be used to implement portions of embodiments of the present disclosure. Moreover, those of ordinary skill in the art and others will recognize that the computing device **700** may be any one of any number of currently available or yet to be developed devices.

[0062] In its most basic configuration, the computing device **700** includes at least one processor **702** and a system memory **704** connected by a communication bus **706**. Depending on the exact configuration and type of device, the system memory **704** may be volatile or nonvolatile memory, such as read only memory ("ROM"), random access memory ("RAM"), EEPROM, flash memory, or similar memory technology. Those of ordinary skill in the art and others will recognize that system memory **704** typically stores data and/or program modules that are immediately accessible to and/or currently being operated on by the processor **702**. In this regard, the processor **702** may serve as a computational center of the computing device **700** by supporting the execution of instructions.

[0063] As further illustrated in FIG. **7**, the computing device **700** may include a network interface **710** comprising one or more components for communicating with other devices over a network. Embodiments of the present disclosure may access basic services that utilize the network interface **710** to perform communications using common network protocols. The network interface **710** may also include a wireless network interface configured to communicate via one or more wireless communication protocols, such as WiFi, 2G, 3G, LTE, WiMAX, Bluetooth, and/or the like.

[0064] In the exemplary embodiment depicted in FIG. **7**, the computing device **700** also includes a storage medium **708**. However, services may be accessed using a computing device that does not include means for persisting data to a local storage medium. Therefore, the storage medium **708** depicted in FIG. **7** is represented with a dashed line to indicate that the storage medium **708** is optional. In any event, the storage medium **708** may be volatile or nonvolatile, removable or nonremovable, implemented using any technology capable of storing information such as, but not limited to, a hard drive, solid state drive, CD ROM, DVD, or other disk storage, magnetic cassettes, magnetic tape, magnetic disk storage, and/or the like.

[0065] As used herein, the term "computer-readable medium" includes volatile and non-volatile and removable

and non-removable media implemented in any method or technology capable of storing information, such as computer readable instructions, data structures, program modules, or other data. In this regard, the system memory **704** and storage medium **708** depicted in FIG. **7** are merely examples of computer-readable media.

[0066] Suitable implementations of computing devices that include a processor **702**, system memory **704**, communication bus **706**, storage medium **708**, and network interface **710** are known and commercially available. For ease of illustration and because it is not important for an understanding of the claimed subject matter, FIG. **7** does not show some of the typical components of many computing devices. In this regard, the computing device **700** may include input devices, such as a keyboard, keypad, mouse, microphone, touch input device, touch screen, tablet, and/or the like. Such input devices may be coupled to the computing device **700** by wired or wireless connections including RF, infrared, serial, parallel, Bluetooth, USB, or other suitable connections protocols using wireless or physical connections. Similarly, the computing device **700** may also include output devices such as a display, speakers, printer, etc. Since these devices are well known in the art, they are not illustrated or described further herein.

[0067] The particulars shown herein are by way of example and for purposes of illustrative discussion of the preferred embodiments of the present disclosure only and are presented in the cause of providing what is believed to be the most useful and readily understood description of the principles and conceptual aspects of various embodiments of the disclosure. In this regard, no attempt is made to show structural details of the invention in more detail than is necessary for the fundamental understanding of the system and methods, the description taken with the drawings and/or examples making apparent to those skilled in the art how the several forms of the disclosure may be embodied in practice.

[0068] As used herein and unless otherwise indicated, the terms "a" and "an" are taken to mean "one," "at least one" or "one or more." Unless otherwise required by context, singular terms used herein shall include pluralities and plural terms shall include the singular.

[0069] Unless the context clearly requires otherwise, throughout the description and the claims, the words "comprise," "comprising," and the like are to be construed in an inclusive sense as opposed to an exclusive or exhaustive sense; that is to say, in the sense of "including, but not limited to." Words using the singular or plural number also include the plural and singular number, respectively. Additionally, the words "herein," "above," and "below" and words of similar import, when used in this application, shall refer to this application as a whole and not to any particular portions of the application.

[0070] The description of embodiments of the disclosure is not intended to be exhaustive or to limit the disclosure to the precise form disclosed. While the specific embodiments of, and examples for, the disclosure are described herein for illustrative purposes, various equivalent modifications are possible within the scope of the disclosure, as those skilled in the relevant art will recognize.

[0071] All of the references cited herein are incorporated by reference. Aspects of the disclosure can be modified, if necessary, to employ the systems, functions, and concepts of the above references and application to provide yet further embodiments of the disclosure. These and other changes can be made to the disclosure in light of the detailed description.

[0072] Specific elements of any foregoing embodiments can be combined or substituted for elements in other embodiments. Moreover, the inclusion of specific elements in at least some of these embodiments may be optional, wherein further embodiments may include one or more embodiments that specifically exclude one or more of these specific elements. Furthermore, while advantages associated with certain embodiments of the disclosure have been described in the context of these embodiments, other embodiments may also exhibit such advantages, and not all embodiments need necessarily exhibit such advantages to fall within the scope of the disclosure.

The embodiments of the invention in which an exclusive property or privilege is claimed are defined as follows:

1. A system for automated administration and evaluation of physical therapy exercises, the system comprising:

a computing device comprising at least one processor and a non-transitory computer readable medium;

a display device communicatively coupled to the computing device;

a hand position sensing device communicatively coupled to the computing device; and

a muscular activity sensing device communicatively coupled to the computing device and configured to sense muscular activity in a forearm of a user.

2. The system of claim **1**, wherein the computer-readable medium of the computing device has computer-executable instructions stored thereon that, in response to execution by the at least one processor, cause the computing device to perform actions that include:

presenting, by the computing device via the display device, a motion prompt;

receiving, by the computing device, hand position information from the hand position sensing device;

receiving, by the computing device, muscular activity information from the muscular activity sensing device;

determining, by the computing device, compliance with the motion prompt using the hand position information; and

determining, by the computing device, a muscular activity evaluation score based on the muscular activity information.

3. The system of claim **2**, wherein the hand position information includes three-dimensional location information and orientation information for one or more anatomical elements of a hand.

4. The system of claim **2**, wherein the muscular activity sensing device includes a plurality of surface electromyography (EMG) sensors.

5. The system of claim **4**, wherein the muscular activity information includes a stream of surface EMG sensor values.

6. The system of claim **5**, wherein determining a muscular activity evaluation score includes determining a calibration map for the muscular activity information using a modified orthogonal Procrustes technique.

7. The system of claim **2**, wherein the actions further include presenting, by the computing device via the display device, an indication of sensed motion based on the received hand position information.

8. The system of claim **2**, wherein the actions further include:

setting, by the computing device, a gain level to be used by the hand position sensing device; and

updating, by the computing device, the gain level to be used by the hand position sensing device based on at least one of the determined compliance with the motion prompt and the determined muscular activity evaluation score.

9. A computer-implemented method for automated administration and evaluation of physical therapy exercises, the method comprising:

presenting, by a computing device via a display device, a motion prompt;

receiving, by the computing device, hand position information from a hand position sensing device;

receiving, by the computing device, muscular activity information from a muscular activity sensing device;

determining, by the computing device, compliance with the motion prompt using the hand position information; and

determining, by the computing device, a muscular activity evaluation score based on the muscular activity information.

10. The method of claim **9**, wherein the hand position information includes three-dimensional location information and orientation information for one or more anatomical elements of a hand.

11. The method of claim **9**, wherein the muscular activity information includes a stream of sensor values from a plurality of surface electromyography (EMG) sensors of the muscular activity sensing device.

12. The method of claim **9**, wherein determining a muscular activity evaluation score includes determining a calibration map for the muscular activity information using a modified orthogonal Procrustes technique.

13. The method of claim **9**, further comprising presenting, by the computing device via the display device, an indication of sensed motion based on the received hand position information.

14. The method of claim **9**, further comprising:

setting, by the computing device, a gain level to be used by the hand position sensing device; and

updating, by the computing device, the gain level to be used by the hand position sensing device based on at least one of the determined compliance with the motion prompt and the determined muscular activity evaluation score.

15. A nontransitory computer-readable medium having computer-executable instructions stored thereon that, in response to execution by one or more processors of a computing device, cause the computing device to perform actions comprising:

presenting, by the computing device via a display device, a motion prompt;

receiving, by the computing device, hand position information from a hand position sensing device;

receiving, by the computing device, muscular activity information from a muscular activity sensing device;

determining, by the computing device, compliance with the motion prompt using the hand position information; and

determining, by the computing device, a muscular activity evaluation score based on the muscular activity information.

16. The computer-readable medium of claim **15**, wherein the hand position information includes three-dimensional location information and orientation information for one or more anatomical elements of a hand.

17. The computer-readable medium of claim **15**, wherein the muscular activity information includes a stream of sensor values from a plurality of surface electromyography (EMG) sensors of the muscular activity sensing device.

18. The computer-readable medium of claim **17**, wherein determining a muscular activity evaluation score includes determining a calibration map for the muscular activity information using a modified orthogonal Procrustes technique.

19. The computer-readable medium of claim **15**, wherein the actions further comprise presenting, by the computing device via the display device, an indication of sensed motion based on the received hand position information.

20. The computer-readable medium of claim **15**, wherein the actions further comprise:

setting, by the computing device, a gain level to be used by the hand position sensing device; and

updating, by the computing device, the gain level to be used by the hand position sensing device based on at least one of the determined compliance with the motion prompt and the determined muscular activity evaluation score.

* * * * *

4.11 REFERENCES

1. Duncan, P.W., & Lai, S. M. , *Stroke Recovery.* Top.Stroke Rehabil, 1997. **4**(3): p. 51-58.
2. Richards, L. and P. Pohl, *Therapeutic interventions to improve upper extremity recovery and function.* Clinics in Geriatric Medicine, 1999. **15**(4): p. 819-+.
3. van der Lee, J.H., et al., *Forced use of the upper extremity in chronic stroke patients - Results from a single-blind randomized clinical trial.* Stroke, 1999. **30**(11): p. 2369-2375.
4. Hiraoka, K., *Rehabilitation effort to improve upper extremity function in post-stroke patients: A meta-analysis.* Journal of Physical Therapy Science, 2001. **13**(1): p. 5-9.
5. Brunnstrom, S., *Motor testing procedures in hemiplegia: based on sequential recovery stages.* Phys Ther, 1966. **46**(4): p. 357-75.
6. Voss, D., Ionta,Mk, Myers,Bj, *Proprioceptive Neuromuscular Facilitation - Patterns and Techniques.* Rehabilitation Literature, 1985. **46**(9-10): p. 296.
7. Bobath, B., *Adult Hemiplegia - Evaluation and Treatment.* Rehabilitation Literature, 1979. **40**(5-6): p. 160-160.
8. Luke, C., K.J. Dodd, and K. Brock, *Outcomes of the Bobath concept on upper limb recovery following stroke.* Clinical Rehabilitation, 2004. **18**(8): p. 888-898.
9. Schmidt, R.A., *Motor learning & performance: From principles to practice*. 1991: Human Kinetics Books.
10. Page, S.J., *Intensity versus task-specificity after stroke: how important is intensity?* Am.J.Phys.Med.Rehabil., 2003. **82**(9): p. 730-732.
11. Galea, M.P., K. J. Miller, and S. L. Kilbreath. *Early task-related training enhances upper limb function following stroke*. in *Annual Meeting of the Society for Neural Control of Movement*. 2001. Sevilla, Spain.
12. Winstein, C.J., et al., *A randomized controlled comparison of upper-extremity rehabilitation strategies in acute stroke: A pilot study of immediate and long-term outcomes.* Arch Phys Med Rehabil, 2004. **85**(4): p. 620-8.
13. Whitall, J., et al., *Bilateral and Unilateral Arm Training Improve Motor Function Through Differing Neuroplastic Mechanisms: A Single-Blinded Randomized Controlled Trial.* Neurorehabilitation and Neural Repair, 2011. **25**(2): p. 118-129.
14. Taub, E., G. Uswatte, and R. Pidikiti, *Constraint-Induced Movement Therapy: a new family of techniques with broad application to physical rehabilitation--a clinical review.* J Rehabil Res Dev, 1999. **36**(3): p. 237-51.
15. Hakkennes, S. and J.L. Keating, *Constraint-induced movement therapy following stroke: A systematic review of randomised controlled trials.* Australian Journal of Physiotherapy, 2005. **51**(4): p. 221-231.
16. Ploughman, M. and D. Corbett, *Can forced-use therapy be clinically applied after stroke? An exploratory randomized controlled trial.* Archives of Physical Medicine and Rehabilitation, 2004. **85**(9): p. 1417-1423.
17. Thieme, H., et al., *Mirror therapy for improving motor function after stroke.* Cochrane Database of Systematic Reviews, 2012(3).
18. Volpe, B.T., et al., *Robot training enhanced motor outcome in patients with stroke maintained over 3 years.* Neurology, 1999. **53**(8): p. 1874-1876.
19. Lum, P., et al., *Robotic devices for movement therapy after stroke: current status and challenges to clinical acceptance.* Top Stroke Rehabil, 2002. **8**(4): p. 40-53.

20. Saposnik, G., et al., *Efficacy and safety of non-immersive virtual reality exercising in stroke rehabilitation (EVREST): a randomised, multicentre, single-blind, controlled trial.* Lancet Neurol, 2016.
21. Haas D., P.S., Yu J., *Kinect Based Physiotherapy System for Home Use.* Current Directions in Biomedical Engineering, 2015. **1**(1): p. 180-183.
22. Archambault P.S., et al., *Towards Establishing Clinical Guidelines for an Arm Rehabilitation Virtual Reality System*, in *Replace, Repair, Restore, Relieve – Bridging Clinical and Engineering Solutions in Neurorehabilitation*. 2014. p. 263-270
23. Shubert TE, B.J., Chokshi A, Barrett M, Komatireddy R, *Are Virtual Rehabilitation Technologies Feasible Models to Scale an Evidence-Based Fall Prevention Program? A Pilot Study Using the Kinect Camera.* JMIR Rehabil Assist Technol 2015. **2**(2).
24. Kang X., *Methods for providing telemedicine services* 2014, Rehabtics LLC.
25. Mousavi Hondori, H. and M. Khademi, *A Review on Technical and Clinical Impact of Microsoft Kinect on Physical Therapy and Rehabilitation.* J Med Eng, 2014. **2014**: p. 846514.
26. *RespondWell Telerehabilitation Software*. 2016; Available from: http://respondwell.com/.
27. Kurillo, G., et al., *Tele-MFAsT: Kinect-Based Tele-Medicine Tool for Remote Motion and Function Assessment.* Stud Health Technol Inform, 2014. **196**: p. 215-21.
28. Cameirao, M.S., et al., *Neurorehabilitation using the virtual reality based Rehabilitation Gaming System: methodology, design, psychometrics, usability and validation.* J Neuroeng Rehabil, 2010. **7**: p. 48.
29. *Ges Therapy*. 2016; Available from: http://gestherapy.com/.
30. Friedman, N., et al., *MusicGlove: motivating and quantifying hand movement rehabilitation by using functional grips to play music.* Conf Proc IEEE Eng Med Biol Soc, 2011. **2011**: p. 2359-63.
31. Song, H. *RAPAEL: Wearable Technology and Serious Game for Rehabilitation*. in *Proceedings of the 2016 CHI Conference Extended Abstracts on Human Factors in Computing Systems*. 2016.
32. Baker, K., S.J. Cano, and E.D. Playford, *Outcome measurement in stroke: a scale selection strategy.* Stroke, 2011. **42**(6): p. 1787-94.
33. Mathiowetz, V., et al., *Adult norms for the Box and Block Test of manual dexterity.* Am J Occup Ther, 1985. **39**(6): p. 386-91.
34. Oxford Grice, K., et al., *Adult norms for a commercially available Nine Hole Peg Test for finger dexterity.* Am J Occup Ther, 2003. **57**(5): p. 570-3.
35. Bohannon, R.W., *Adequacy of hand-grip dynamometry for characterizing upper limb strength after stroke.* Isokinetics and Exercise Science, 2004. **12**(4): p. 263-265.
36. Steele, K.M., A. Rozumalski, and M.H. Schwartz, *Muscle synergies and complexity of neuromuscular control during gait in cerebral palsy.* Dev Med Child Neurol, 2015. **57**(12): p. 1176-82.
37. Weichert, F., et al., *Analysis of the accuracy and robustness of the leap motion controller.* Sensors (Basel), 2013. **13**(5): p. 6380-93.
38. LeapMotion. *Leap Motion SDK and Plugin Documentation*. 2016; Available from: https://developer.leapmotion.com/documentation/.
39. Scott, S., *Graph Maker for Unity®*. 2016.
40. Imphenzia, *Universal Sound FX for Unity®*. 2016.

41. Beaton, D.E., et al., *Development of the QuickDASH: comparison of three item-reduction approaches.* J Bone Joint Surg Am, 2005. **87**(5): p. 1038-46.
42. MacDermid, J.C., et al., *Patient rating of wrist pain and disability: a reliable and valid measurement tool.* J Orthop Trauma, 1998. **12**(8): p. 577-86.
43. O'Dwyer, N.J., L. Ada, and P.D. Neilson, *Spasticity and muscle contracture following stroke.* Brain, 1996. **119 (Pt 5)**: p. 1737-49.
44. Lee, D.D. and H.S. Seung, *Learning the parts of objects by non-negative matrix factorization.* Nature, 1999. **401**(6755): p. 788-91.
45. Roh, J., W.Z. Rymer, and R.F. Beer, *Robustness of muscle synergies underlying three-dimensional force generation at the hand in healthy humans.* J Neurophysiol, 2012. **107**(8): p. 2123-42.
46. Roh, J., et al., *Alterations in upper limb muscle synergy structure in chronic stroke survivors.* J Neurophysiol, 2013. **109**(3): p. 768-81.
47. Delp, S.L.e.a., *Maximumisometric moments generated by the wrist muscles in flexion-extension and radial-ulnar deviation.* Journal of Biomechanics. **29**(10): p. 1371 - 1375.
48. Hall, M.J., S. Levant, and C.J. DeFrances, *Hospitalization for stroke in U.S. hospitals, 1989-2009.* NCHS Data Brief, 2012(95): p. 1-8.
49. Shaughnessy, M., B.M. Resnick, and R.F. Macko, *Testing a model of post-stroke exercise behavior.* Rehabil Nurs, 2006. **31**(1): p. 15-21.
50. C, G., *Issues of parent compliance: what the clinician and researcher should know.* Physical and Occupational Therapy Pediatric 1991. **11**: p. 73-77.
51. Touillet, A., et al., *Assessment of compliance with prescribed activity by hemiplegic stroke patients after an exercise programme and physical activity education.* Ann Phys Rehabil Med, 2010. **53**(4): p. 250-7, 257-65
52. *Rios, D., et al., Neurogame Therapy to improve wrist control in children with cerebral palsy: A case series.* Dev Neurorehabil, 2013.**16**(6): p.398-409.

Chapter 5. Closing Remarks

Final thoughts and a summary of work.

The central nervous system integrates a wide variety of internal and external signals to generate robust motor control. The exact mechanisms of these control mechanisms remain unknown, but damage throughout the system can impair function that causes real hardship for individuals affected. Signals in motor cortical areas may be strengthened and weakened by repeated use or disuse. Direct activation of the spinal column may be a target for activation via motor pools in the ventral horn which directly and reliably activate forelimb muscles in a graded manner. Finally, repetitive activity engaging the full motor system in a directed physical therapy approach may strengthen and retrain spared motor control pathways after injury, leading to increased overall function.

This thesis explored several neural engineering approaches to restoring motor function. Directed cortical reorganization in response to repetitive stimulation was explored using paired stimulation protocols and was found to increase direct connectivity measures in some areas of cortex. A novel approach to spinal cord stimulation was designed, fabricated, and tested in a series of case studies, producing robust movements and steps toward clinical utility. Finally a platform for long-term, data-driven rehabilitation techniques focusing on hand and arm function was built and tested in a cohort of clinical patients. In thinking of long-term translational solutions to central nervous system motor impairment researchers, engineers, physicians, therapists, and patients must all recognize the complexity of the motor system and incorporate techniques and approaches that engage all inputs and outputs to the nervous system to achieve maximal recovery.

CURRICULUM VITAE

Brian Joseph Mogen, Ph.D.

CAREER OBJECTIVES

To combine my engineering understanding alongside the principles of closed-loop brain-computer interfaces and advance medical and commercial applications of technology. My basic science experience has covered applications in microfluidics, both physics and manufacturing, as well as cellular physiology applications. My neuroscience work has broadly covered plastic change mechanisms in primate cortex as well as fundamental motor output device theory and manufacture.

EDUCATION

2011	B.S. Biomedical Engineering	University of Wisconsin
	Certificate, Biology in Engineering	
2018	Ph.D. Bioengineering	University of Washington

PRE-DOCTORAL TRAINING

2010	Hilldale Research Scholar	University of Wisconsin

MOGEN BIBLIOGRAPHY

Publications:

Seeman, S. C., **Mogen, B. J**., Fetz, E. E., & Perlmutter, S. I. (2017). Paired Stimulation for Spike-Timing-Dependent Plasticity in Primate Sensorimotor Cortex. *Journal of Neuroscience*, *37*(7), 1935-1949.

Smith, W. A**., Mogen, B. J**., Fetz, E. E., Sathe, V. S., & Otis, B. P. (2016). Exploiting Electrocorticographic Spectral Characteristics for Optimized Signal Chain Design: A 1.08 Analog Front End with Reduced ADC Resolution Requirements. *IEEE transactions on biomedical circuits and systems*, *10*(6), 1171-1180.

Kerstein, P. C., Jacques-Fricke, B. T., Rengifo, J., **Mogen, B. J**., Williams, J. C., Gottlieb, P. A., ... & Gomez, T. M. (2013). Mechanosensitive TRPC1 channels promote calpain proteolysis of talin to regulate spinal axon outgrowth. *Journal of Neuroscience*, *33*(1), 273-285.
Resto, P. J., **Mogen, B. J**., Berthier, E., & Williams, J. C. (2010). An automated microdroplet passive pumping platform for high-speed and packeted microfluidic flow applications. *Lab on a Chip*, *10*(1), 23-26.
Resto, P. J., **Mogen, B. J**., Wu, F., Berthier, E., Beebe, D., & Williams, J. (2009). High Speed Droplet-based Delivery System for Passive Pumping in Microfluidic Devices. *Journal of Visualized Experiments: JoVE*, (31).

Conference Publications:

1. Smith, W. A., **Mogen, B. J**., Fetz, E. E., Sathe, V. S., & Otis, B. P. (2016). Exploiting Electrocorticographic Spectral Characteristics for Optimized Signal Chain Design: A 1.08 Analog Front End With Reduced ADC Resolution Requirements. *IEEE transactions on biomedical circuits and systems*, *10*(6), 1171-1180.
2. Seeman, S. C., **Mogen, B. J**., Fetz, E. E., & Perlmutter, S. I. (2015, October) Paired stimulation induces spike-timing dependent plasticity of neural connections in primate sensorimotor cortex. *Society for Neuroscience*.
3. Smith, W., **Mogen, B**., Fetz, E.E., & Otis, B. (2014, September). A spectrum-equalizing analog front end for low-power electrocorticography recording. In *European Solid State Circuits Conference (ESSCIRC), ESSCIRC 2014-40th* (pp. 107-110). IEEE.
4. Bonaci, T., Herron, J., Libey, T., **Mogen, B.J**., Chizeck, H. (2014, November). How Susceptible is the Brain to side-channel private information extraction? An experimental analysis using non-invasive brain-computer interfaces. *Society for Neuroscience*.
5. **Mogen, B.J.** (2010, April) Characterization of an automated microdroplet passive pumping platform for high-speed and packeted microfluidic flow applications. National Conference for Undergraduate Research (NCUR).
6. Resto, P.J., **Mogen, B.J.,** Berthier, E., Beebe, D.J, Williams, J.C. (2009, October) An Automated Accessible High-Speed Fluidic Delivery System Using Micro-Droplet Passive Pumping in Microfluidic Devices. Biomedical Engineering Society National Convention.

Conferences Attended:

1. 2017 e3iVR Ethics in Virtual Reality
2. 2015 Society for Neuroscience, Chicago, IL
3. 2015 American Occupational Therapy Association Conference
4. 2015 Consumer Electronics Showcase. Las Vegas, NV January 5-9.
5. 2010 Annual ACP/CMA National Media Convention. Louisville, KY October 27-31.
6. 2010 National Conference on Undergraduate Research, Missoula, MT

Invited Talks

1. Invited Talk, University of Wisconsin – River Falls, Biology 389-Neurobiology, 29 October 2012.
2. Invited Lecture, University of Washington, BioEngineering 503

3. Invited Lecture – REU Summer class
4. Invited Lecture – EMBA Course
5. Design Beyond Video Games: Applications in Healthcare and Beyond, Seattle Arts Institute, 11/7/2016

Patent Applications:

1. **Mogen, Brian** , Libey Tyler, Browd, Samuel, Smith, Melissa, and Gklezakos, Dimitiros. SYSTEM AND METHODS FOR AUTOMATED ADMINISTRATION AND EVALUATION OF HEAD INJURY-RELATED EXERCISES. UW Ref 47966.01US1 3/17/2017
2. Libey, Tyler, Crawford, Lars, Gklezakos, Dimitrios, and **Mogen, Brian**. "SYSTEM AND METHODS FOR AUTOMATED ADMINISTRATION AND EVALUATION OF PHYSICAL THERAPY EXERCISES." U.S. Patent Application 15/154,382, filed November 17, 2016.
3. **Mogen, Brian.,** Libey, Tyler, and Rich, Timothy. A MEASUREMENT AND INTERVENTION TOOL FOR HEMISPATIAL INATTENTION AFTER RIGHT BRAIN STROKE. Provisional Patent Application No. UW: [IP:47383.01US1]. December, 2015